

**Integrating microbial community analyses and
environmental factors for a better understanding of
complex plant material- and bio-based and biodegradable
plastic microbiomes.**

DISSERTATION

Submitted to obtain the academic degree

Doctor rerum naturalium (Dr. rer. nat.)

at the Faculty of Biology, Chemistry and Earth Sciences

of the University of Bayreuth

by

Benjawan Tanunchai

From Chiangmai, Thailand

Bayreuth, 2022

This doctoral thesis was prepared from March 2021 to September 2022 at the Department of Soil Ecology, UFZ-Helmholtz Centre for Environmental Research, Halle (Saale) and Institute of Bioanalysis, Coburg University of Applied Sciences and Arts, Coburg, Germany. Doctoral researcher (Ms. Benjawan Tanunchai) was supervised by Dr. Witoon Purahong at the UFZ and Prof. Dr. Matthias Noll at Coburg University of Applied Sciences and Arts. I sincerely thank my supervisors for their helpful and constructive advice.

Doctoral researcher (Ms. Benjawan Tanunchai) is currently working under supervision of Prof. Dr. Matthias Noll at Institute of Bioanalysis, Coburg University of Applied Sciences and Arts, Coburg, Germany.

This is a full reprint of the thesis submitted to obtain the academic degree of the Doctor of Natural Sciences (Dr. rer. Nat.) and approved by the Faculty of Biology, Chemistry, and Geosciences of the University of Bayreuth.

Date of submission: 26.10.2022

Date of defence: 16.01.2023

Acting dean: Prof. Dr. Benedikt Westermann

Doctoral committee:

Prof. Dr. Matthias Noll (reviewer)

Prof. Dr. Tillmann Lüders (reviewer)

Prof. Dr. Andreas Römpp (chairman)

PD Dr. Alfons Weig

TABLE OF CONTENTS

ABBREVIATIONS	IV
SUMMARY	V–VI
ZUSAMMENFASSUNG	VII–VIII
1. INTRODUCTION	1–16
1.1.1. Decomposition of plant materials (leaf litter and deadwood) and their impact on ecosystems and environments	1–2
1.1.2. Degradation of plastics and their impact on ecosystems and environments	2–4
1.1.3. Bio-based and biodegradable plastics: Threats or opportunities?	4–6
1.1.4. Biodegradability of leaves, deadwood, and bio-based and biodegradable plastics: The importance of microbes and their interactions	6–9
1.1.5. Abiotic factors drive decomposition and degradation of plant material- and bio-based and biodegradable plastics	9–10
1.1.6. Climate change impacts on biotic and abiotic factors	10
1.1.7. Community assembly processes control the microbiome during decomposition and degradation of plant material- and bio-based and biodegradable plastics	10–12
1.2. High resolution molecular techniques and enzyme analysis	12–16
1.2.1. DNA metabarcoding	12–14
1.2.2. Differentiation of active microbial community members by immunocapture technique	14
1.2.3. Quantitative real-time PCR assay	14–15
1.2.4. Fluorimetric enzyme assays	15–16
2. Synopsis	16–44
2.1. Aims and hypotheses	16–19
2.2. Study design and study sites	19–22
2.3. GENERAL DISCUSSION	22–32
2.4. TRANSFERABILITY OF THE KNOWLEDGE	32–35
2.5. CONCLUSION	35–37
2.6. References	38–44

3. DECLARATION OF CONTRIBUTION AND PUBLICATIONS	45–176
3.1. DECLARATION OF CONTRIBUTION	45 – 51
3.2. Litter 1: FungalTraits vs. FUNGuild: Comparison of ecological functional assignments of leaf- and needle-associated fungi across 12 temperate tree species.	52 – 70
3.3. Litter 2: A poisoned apple: First insights into community assembly and networks of the fungal pathobiome of healthy-looking senescing leaves of temperate trees in mixed forest ecosystem.	71 – 87
3.4. Litter 3: More than you can see: Unraveling the ecology and biodiversity of lichenized fungi associated with leaves and needles of 12 temperate tree species using high throughput sequencing.	88 – 105
3.5. Litter 4: Tree mycorrhizal type regulates leaf and needle microbial communities, affects microbial assembly and co-occurrence network patterns, and influences litter decomposition rates in temperate forest.	106 – 120
3.6. Deadwood 1: Cross-kingdom interactions and functional patterns of active microbiota matter in governing deadwood decay.	121 – 131
3.7. Plastic 1: Fate of a biodegradable plastic in forest soil: Dominant tree species and forest types drive changes in microbial community assembly, influence the composition of plastisphere, and affect poly(butylene succinate-co-adipate) degradation.	132 – 147
3.8. Plastic 2: Nitrogen fixing bacteria facilitate microbial biodegradation of a bio-based and biodegradable plastic in soils under ambient and future climatic conditions.	148 – 157
3.9. Plastic 3: Future climate change enhances the complexity of plastisphere microbial co-occurrence networks, but does not significantly affect the community assembly.	158 – 164
3.10. Plastic 4: Interactions between high load of a bio-based and biodegradable plastic and nitrogen fertilizer affect plant biomass and health: A case study with <i>Fusarium solani</i> and mung bean (<i>Vigna radiata</i> L.).	165 – 176
4. List of publications in peer-reviewed journals	177–179
Acknowledgement	180
(Eidesstattliche) Versicherungen und Erklärungen	181

ABBREVIATIONS

Abbreviation	Full name
μm	Micrometer
AM	Arbuscular mycorrhiza
AM_BL	Broadleaved arbuscular mycorrhizal trees
ANOVA	Analysis of variance
bp	Base pair
BrdU	Bromodeoxyuridine
C	Carbon
Ca	Calcium
CNDD	Conspecific negative density dependence
CO ₂	Carbon dioxide
DNA	Deoxyribonucleic acid
DOC	Dissolved organic C
dsDNA	Double-stranded deoxyribonucleic acid
EcM	Ectomycorrhiza
EcM_BL	Broadleaved ectomycorrhizal trees
EcM_C	Coniferous ectomycorrhizal trees
Fe	Iron
GCEF	Global Change Experimental Facility
Gt C	Gigatons of carbon
h	Hour
ITS	Internal Transcribed Spacer
K	Potassium
Mg	Magnesium
mm	Millimeter
N	Nitrogen
N ₂	Atmospheric nitrogen
NGS	Next Generation Sequencing
<i>nifH</i>	Nitrogenase
NMDS	Nonmetric multidimensional scaling
N _{Min}	Mineralized N
N _{Org}	Dissolved organic N
P	Phosphorus
PBAT	Polybutylene adipate terephthalate
PBS	Polybutylene succinate
PBSA	Polybutylene succinate-co-adipate
PCR	Polymerase chain reaction
PHA	Polyhydroxyalkanoate
PLA	Poly(lactic acid)
qPCR	Quantitative real-time polymerase chain reaction
R^2	Goodness-of-fit statistics
RNA	Ribonucleic acid
rRNA	Ribosomal RNA
SA	Salicylic acid
ssDNA	Single-stranded DNA
UV	Ultraviolet

SUMMARY

The decomposition of plant materials is a crucial step in nutrient recycling, such as C, N, and P content, which are important for plant growth and maintenance of ecosystem functioning. The degradation of bio-based and biodegradable plastics is expected to reduce plastic pollutants. Microbial activities are key factors for the decomposition and degradation of plant materials and bio-based and biodegradable plastics. In this dissertation, I employed high-resolution molecular techniques to identify the core microbiome during leaf litter and deadwood decomposition as well as plastic degradation in agricultural and forest ecosystems. Community assembly processes, co-occurrence networks, and responses to environmental factors were analyzed. Overall, the results suggest that saprotrophic fungi, especially *Mycena*, highly dominated the fungal community composition, especially during the late stage of decomposition of both leaf litter and deadwood. For the degradation of polybutylene succinate-co-adipate (PBSA), I detected enrichment of potential plastic degraders, including *Tetracladium*, *Fusarium solani*, *Cladosporium*, and *Exophiala*. Some have been previously reported as plant pathogens for different crops (e.g., citrus and faba bean), raising concerns about economic losses in agriculture. Bacterial groups (*Sphingomonas* and *Allorhizobium-Neorhizobium-Pararhizobium-Rhizobium*) related to N cycling substantially contributed to the bacterial community composition alongside the chemoheterotrophic bacteria. The copy number of the *nifH* gene, which is a key gene for the dinitrogenase reductase of N₂-fixing microorganisms, was quantified in decomposing plant materials and plastic across different ecosystems. Its correlation with the fungal gene copy number indicates direct and indirect relationships between N₂-fixing microorganisms and fungi. The co-occurrence network revealed supporting results for bacterial and fungal interactions, and N₂-fixing microorganisms were the key stone taxa in different habitats. For community assembly, the results were more complex and varied depending on the substrates and the ecosystems in which the substrates

were being decomposed. Stochastic processes are the main processes governing the microbial community composition during plastic degradation. However, during leaf litter decomposition, deterministic processes are increasingly important in governing bacterial community composition. This dissertation is the first large leaf litter decomposition experiment in temperate forest ecosystems and reveals metabolically active deadwood decomposers. This plastic degradation experiment was conducted for the first time in temperate forests and agricultural ecosystems under future climate conditions. Overall, the results of this comprehensive dissertation allowed us to gain a deeper understanding of how the interaction between different microbial kingdoms occurs during plant material and bio-based and biodegradable plastic decomposition processes.

ZUSAMMENFASSUNG

Die Zersetzung von Pflanzenmaterial ist ein entscheidender Schritt in die Nährstoffwiederverwertung wie C-, N- und P-Gehalte, die für das Pflanzenwachstum und die Aufrechterhaltung der Ökosystemfunktion wichtig ist. Inzwischen ist der Abbau von biobasierten und biologisch abbaubaren Kunststoffen die Hoffnung, Plastik-Pollution zu lösen. Der Schlüsselfaktor für die Zersetzung und den Abbau von Pflanzenmaterialien und biobasiertem und biologisch abbaubarem Kunststoff sind die mikrobiellen Aktivitäten. In dieser Dissertation habe ich hochauflösende molekulare Techniken eingesetzt, um das Kernmikrobiom während der Laubstreu- und Totholzzersetzung sowie des Plastikabbaus in landwirtschaftlichen und forstlichen Ökosystemen zu identifizieren. Community-Assembly-Prozesse, Co-Occurrence-Netzwerke und ihre Reaktion auf Umweltfaktoren wurden analysiert. Die Gesamtergebnisse deuten darauf hin, dass die saprotrophen Pilze, insbesondere *Mycena*, die Zusammensetzung der Pilzgemeinschaft stark dominierten, insbesondere während der späten Phase der Zusammensetzung sowohl von Laubstreu als auch von Totholz. Für den Abbau von Polybutylensuccinat-co-adipat (PBSA) habe ich die Anreicherung potenzieller Kunststoffabbauer entdeckt, darunter *Tetracladium*, *Fusarium solani*, *Cladosporium* und *Exophiala*. Einige von ihnen wurden zuvor als Pflanzenpathogene für verschiedene Kulturen (z. B. Zitrusfrüchte und Ackerbohnen) gemeldet, was die Besorgnis über wirtschaftliche Verluste in der Landwirtschaft aufkommen lässt. Bei Bakterien tragen Bakteriengruppen (*Sphingomonas* und *Allorhizobium-Neorhizobium-Pararhizobium-Rhizobium*), die mit dem N-Kreislauf in Verbindung stehen, neben den chemoheterotrophen Bakterien wesentlich zur Zusammensetzung der Bakteriengemeinschaft bei. Die Kopienzahlen des *nifH*-Gens, das ein Schlüsselgen für die Dinitrogenase-Reduktase N₂-fixierender Mikroorganismen ist, wurden beim Abbau von Pflanzenmaterial und Plastik in verschiedenen Ökosystemen quantifiziert. Seine Korrelation mit der Kopienzahl des Pilzgens weist auf direkte und indirekte Beziehungen

zwischen N₂-fixierenden Mikroorganismen und Pilzen hin. Das Co-Occurrence-Netzwerk zeigte unterstützende Ergebnisse für die Wechselwirkungen zwischen Bakterien und Pilzen, und N₂-fixierende Mikroorganismen waren die Schlüsselstein-Taxa in verschiedenen Lebensräumen. Für die Gemeindeversammlung waren die Ergebnisse komplexer und je nach den Substraten und den Ökosystemen, in denen die Substrate abgebaut werden, unterschiedlich. Während des Kunststoffabbaus sind stochastische Prozesse die Hauptprozesse, die die Zusammensetzung der mikrobiellen Gemeinschaft bestimmen. Jedoch, während der Zersetzung von Laubstreu zeigten die deterministischen Prozesse eine zunehmende Bedeutung bei der Steuerung der Zusammensetzung der Bakteriengemeinschaft. Diese Dissertation ist das erste größte Laubstreuersetzungsexperiment in gemäßigten Waldökosystemen und zeigt stoffwechselaktive Tothholzzersetzer auf. Das Plastikabbauexperiment wurde erstmals in gemäßigten Wäldern und in landwirtschaftlichen Ökosystemen unter zukünftigen Klimabedingungen durchgeführt. Insgesamt ermöglichten uns die Ergebnisse dieser umfassenden Dissertation ein tieferes Verständnis darüber, wie die Wechselwirkung zwischen verschiedenen mikrobiellen Reichen bei Pflanzenmaterialien und biobasierten und biologisch abbaubaren Kunststoffzersetzungsprozessen abläuft.

1. INTRODUCTION

1.1.1. Decomposition of plant materials (leaf litter and deadwood) and their impact on ecosystems and environments

Plant biomass covers a large fraction of Earth's surface ¹. A previous study estimated a global biomass amount of approximately 550 gigatons of carbon (Gt C) ². Plant biomass contributes the largest proportion of the global biomass composition (approximately 450 Gt C) ². Terrestrial plant biomass is considered the primary source of global plant biomass ². The leaf area was estimated to be multiple times of the soil surface area ¹. Deadwood and leaf litter significantly contribute to organic C pools and nutrient reservoirs in terrestrial ecosystems ^{3,4}. In forest ecosystems, the organic surface layer, plant litter layer, and detritosphere consist mainly of decomposing leaf litter. Many important biochemical reactions occur in the plant litter layer, such as nutrient (re-)cycling and cation exchange reactions, as well as interactions among microorganisms ⁵⁻⁸. In addition to organic C, leaf litter also conserves large amounts of other important nutrients (including nitrogen (N), phosphorus (P), potassium (K), and other trace elements) captured from soils. These nutrients are stored in leaves much more than in woody stems ^{7,9}. Owing to the high nutrient content in leaf litter and its higher accessibility for organisms and microorganisms, leaf litter often decomposes faster than deadwood litter. Therefore, leaf litter can significantly impact nutrient cycling, nutrient availability, soil fertility, and productivity of terrestrial forest ecosystems ^{3,7,9-11}. Deadwood consists of complex biopolymers including cellulose, hemicellulose, and lignin ¹². Owing to their complex structure and strong bonds, especially in lignin, the decomposition of biopolymers is slow ^{4,13}. Thus, deadwood is rather considered a temporal reservoir of organic C. Deadwood also consists of simple molecules, including organic acids and sugars, which are released and available for microorganisms during the decomposition process ¹².

Leaf litter and deadwood offer habitats not only for the three kingdoms of microorganisms, including archaea, bacteria, and fungi ^{1,3,4,12}, but also for macroorganisms and protists ¹⁴. Bacteria (biomass of 70 Gt C), fungi (biomass of 12 Gt C), and archaea (biomass of 7 Gt C) contributed a large fraction of the global biomass composition following the plant biomass ². While the biomass of prokaryotes (bacteria and archaea) is mostly concentrated in deep subsurface environments (such as aquifers and below the seafloor), more than 90% of fungal biomass is distributed in terrestrial ecosystems ². Nevertheless, microbe-associated senescence or decomposition of leaves and needles has not been sufficiently analyzed as a crucial component of the plant microbiome. The colonization of leaves and needles by microbes is substantially influenced by leaf physicochemical properties, including leaf nutrients (C, P, N, and soluble compounds), leaf pH, and water content ^{3,15}. While many studies have provided valuable insights into leaf-associated bacterial and fungal communities on individual tree species or crops, little is known about the relative importance of tree species identity, tree mycorrhizal associations, and leaf properties on leaf-associated bacterial and fungal microbiomes and their controlling community assembly processes in Central European temperate forests.

1.1.2. Degradation of plastics and their impact on ecosystems and environments

Plastic waste is one of the major causes besides urbanization and industrialization, exploration, and agricultural practices, contributing to environmental pollution across the globe ¹⁶⁻¹⁹. Packaging contributes to the largest plastic market share (45%) due to the global shift from reusable to single-use packaging, followed by building/construction (19%) and consumer/institutional products (12%) ¹⁸. Owing to the variety of their practical uses, plastic consumption and thus also the plastic pollution have multiplied during the last few decades ^{18,20}. By 2050, 12000 Mt of plastic waste will be spread in landfills and natural habitats if the production rate and demand for plastics continue at the current rate ¹⁸. Plastic waste and the

production of non-biodegradable plastics are considered important threats to the environment. Non-biodegradable plastics can be produced either from non-renewable (petroleum-based, such as fossil fuels and coal) or renewable resources (bio-based, such as plant biomass or microbial products). Conventional plastics are mainly petroleum-based non-biodegradable plastics such as polyethylene (PE), polypropylene, and polyvinyl chloride¹⁸. In contrast, some plastics that are produced from plants (e.g., lignin-based plastics, bio-PE, and bio-PE terephthalate) also have certain limitations in biodegradability²¹. Petroleum-based non-biodegradable plastics have disadvantages compared to other groups of plastics in terms of consumption of non-renewable resources, such as fossil fuels and coal, as well as environmental pollution^{22,23}. The production of petroleum-based non-biodegradable plastics also leaves C footprint, an important greenhouse gas^{22,23}. Due to their limited biodegradability, they accumulate in the environment and thus contribute to the major cause of plastic pollution^{17,18}. In terrestrial ecosystems, plastic waste from packaging and agricultural applications are among the main sources of plastic pollution^{18,20}. Recycling and incineration are options for managing plastic waste; in the real world, only 9% of plastic waste has been recycled and 12% has been incinerated¹⁸. The remaining plastic waste is expected to accumulate in landfills or in soil environments through both unintentional and intentional deposit¹⁸. Under natural conditions, these plastic wastes accumulate and release endocrine-disrupting structures from additives. Their molar mass was not reduced, but they were fragmented into smaller particles, microplastics (particle size: 5 millimeter (mm) to 1 micrometer (μm)) and nanoplastics (particle size $<1 \mu\text{m}$)^{24,25}. Micro- and nanoplastics can accumulate in or be transported to various ecosystems, including marine habitats²⁶, agriculture²⁷, landfills, and other natural environments^{18,28}, and potentially enter the human food web through accumulation in animals and plants²⁹. The smaller sizes of such plastics enable their intake by soil macrofauna and aquatic organisms³⁰⁻³². Micro- and nanoplastics ingested by aquatic organisms accumulate in

their organs, such as digestive organs, and thus reduce development and variance in feed habits³¹. In soil environments, they are reported to alter the composition and abundance of microarthropods and nematodes³² and pose a risk to soil fauna such as geophagous bioturbating earthworms (*Aporrectodea rose*)³³. Accumulation of microplastics in soils significantly affects the germination and growth rate of some plants, such as perennial ryegrass (*Lolium perenne*)³³. Studies investigating the ecotoxicology of microplastic waste are mainly based on nonbiodegradable plastics. The ecotoxicology of bio-based and biodegradable plastics on soil microorganisms remains largely unexplored.

1.1.3. Bio-based and biodegradable plastics: Threats or opportunities?

Biodegradable plastics were brought to the market half a century ago with the intention of solving environmental pollution due to excessive plastic waste. Biodegradable plastics have received considerable attention from society as well as the scientific community because of their biodegradability in various environments and environmental conditions²⁰. Early studies focused on plastic degradation in soils and composts environments²⁰, which were later extended to other environments. Biodegradable plastics can be made either from non-renewable resources such as fuels (including polybutylene succinate (PBS), PBS-co-adipate (PBSA), and PB-adipate terephthalate (PBAT)) or from renewable carbon biomass such as starch, cellulose, and plant oil (including poly(lactic acid) (PLA), polyhydroxyalkanoate (PHA), and starch plastics)^{21,22}. The production of these biodegradable plastics, however, has shifted towards being produced from renewable resources (bio-based plastics) owing to the growing awareness of environmental pollution in society³⁴. The production of bio-based polymers offers advantages over petroleum-based polymers, including lower consumption of fossil fuels and oil and thus less greenhouse gas emissions during production as well as after usage^{22,35}. However, bio-based or plant-based polymers are not always biodegradable. In this dissertation, bio-based and biodegradable plastics are plastics produced from renewable plant

materials or by microbial fermentation and can be degraded by microorganisms in various environments^{20,35}. Microorganisms, especially fungi, secrete extracellular carboxylesterase enzymes, such as lipase or cutinase, to degrade the polymer chain of plastics into low-molecular weight compounds, which make them bio-available³⁶. It has been shown that these low-molecular weight compounds are incorporated into microbial biomass and finally released into the environment in the form of carbon dioxide (CO₂) and water³⁶. PBS, PBSA, PLA, and PBAT are commercially available and are promising aliphatic polyesters for biodegradation^{37,38}. Nevertheless, the biodegradation of PLA requires enzyme activity, which in turn requires the presence of more microbes in high abundance. In addition, a temperature above their glass transition temperature (>60 °C) is needed, thus, it is rather compostable polymers^{20,21,37,39}. The breakdown of biodegradable plastics offers further advantages, as the degradation products (monomers) can be utilized by microorganisms²². Some biodegradable plastics can promote plant growth and productivity, such as poly(butylene succinate-co-salicylic acid) copolymers⁴⁰. PBS is widely used in agriculture. Adding non-toxic and biodegradable phenolic compounds, salicylic acid (SA), to PBS can improve the degradability of PBS⁴⁰. During PBS degradation, SA is released into agricultural soils, which can induce crop damage resistance and thus promote plant growth^{40,41}. The plastics of interest in this dissertation are bio-based and biodegradable PBSA. PBSA offers a variety of applications, such as packaging and mulching films²⁰. It has been shown to degrade under agricultural soil conditions²⁰. The degradation products of PBSA can also be utilized by soil microbes in the Szent-Györgyi-Krebs cycle²⁰.

Concerns regarding plastic pollution, ecotoxicology, and its interaction with environmental factors have been growing in recent years. However, the majority of those researches focuses on the pollution of conventional nonbiodegradable plastics and their effects in aquatic ecosystems^{26,30,42}. Studies on plastic degradation in soils have reported that the degradation of

most biodegradable plastics, such as starch blends, PBS, and PBAT, has no adverse environmental impact^{38,43}. However, the enrichment of some groups of microbes, such as plant pathogens, poses a risk to the environment in another aspect. For instance, the enrichment of plant pathogens such as *Cladosporium*⁴⁴ and *F. solani*⁴⁵ during bio-based and biodegradable PBSA degradation processes is potentially harmful to some economically important crops and plants. These plant pathogens are reported to be PBS-based polymers degraders²². However, to date, no study has validated the direct effect of PBSA degradation on plant health. Despite the large amount of plastic waste landing on soils, there are still a limited number of studies investigating its effects on soil health and the environment. Even fewer studies have been conducted on such aspects of bio-based and/or biodegradable plastics^{20,46}, which are intended to replace conventional non-biodegradable plastics in the near future. There is an urgent need to study the biodegradability and impacts of different bio-based and/or biodegradable plastics on soil health and functions under natural soil conditions.

1.1.4. Biodegradability of leaves, deadwood, and bio-based and/or biodegradable plastics:

The importance of microbes and their interactions

Deadwood and leaf litter decomposition are known to be controlled by both abiotic factors such as climate, environmental factors and litter physicochemical properties as well as biotic factors, especially the cross-kingdom interactions between soil bacteria and fungi^{3,47,48}. Leaf litter decomposition is also influenced by leaf physicochemical properties and quality^{49,50}. Different types of symbiosis between host trees and arbuscular mycorrhizal (AM) fungi or ectomycorrhizal (EcM) fungi have been reported to alter nutrient use traits, which subsequently affect leaf physicochemical properties and quality⁴⁹⁻⁵². Soil microbes affect leaf decomposition through symbioses even before leaf senescence. Specifically, AM trees tend to generate higher-quality leaf litter than EcM trees⁵⁰. In temperate forests, leaf litter decomposition rates of leaf litter senesced from AM trees are usually higher than those from

EcM trees⁴⁹. After leaf senescence, microorganisms and cross-kingdom interactions, particularly between bacteria and fungi, are the main drivers of plant litter decomposition³. Bacteria and fungi act as direct decomposers by secreting extracellular enzymes to decompose both simple compounds and complex biopolymers in leaf litter³ (Figure 1). Some specific functional groups of bacteria can facilitate leaf litter decomposition by providing additional macronutrients, such as N and P, for fungal decomposers^{3,53} (Figure 1).

Bacteria, fungi, and their cross-kingdom interactions also play central roles in deadwood decomposition^{4,12}. Specific fungal saprotrophs are the main decomposer as they produce enzymes to catalyze the turnover of complex biopolymer, including cellulose, hemicellulose and lignin in deadwood structure^{3,4,54}. The diverse enzymes produced by fungal saprotrophs include acid phosphatase, β -glucosidase, xylosidase, cellobiohydrolase, N-acetyl-glucosaminidase, laccase, peroxidase, and manganese peroxidase³. N-acetyl-glucosaminidase, acid phosphatase, β -glucosidase, xylosidase, and cellobiohydrolase are hydrolytic enzymes important for the acquisition of P, N, and polymeric C, respectively, during leaf litter and deadwood decomposition³. This group of enzymes is generally produced by brown rot and ascomycetous fungi, such as members of the class Leotiomycetes⁵⁵. Extracellular oxidative enzymes, including laccase, peroxidase, and manganese peroxidases, are secreted by white rotters to catalyze the oxidation of lignin⁴. Basidiomycetes, the second largest fungal phylum, includes most wood- and leaf litter-decomposing species, which have been classified as either white rot or brown rot⁵⁶. Classical white-rot fungi of wood are *Phlebia radiata*, whereas *Stropharia rugosoannulata* represents white-rot fungi of leaf litter⁵⁷. Brown-rot fungi also oxidize lignin directly through hydroxyl radicals generated by the Fenton reaction⁵⁸. The products of deadwood and leaf litter decomposition through enzymatic catalysis (such as glucose, amino acids, and phosphate) are then utilized by microorganisms for metabolism, reproduction, and growth⁵⁹.

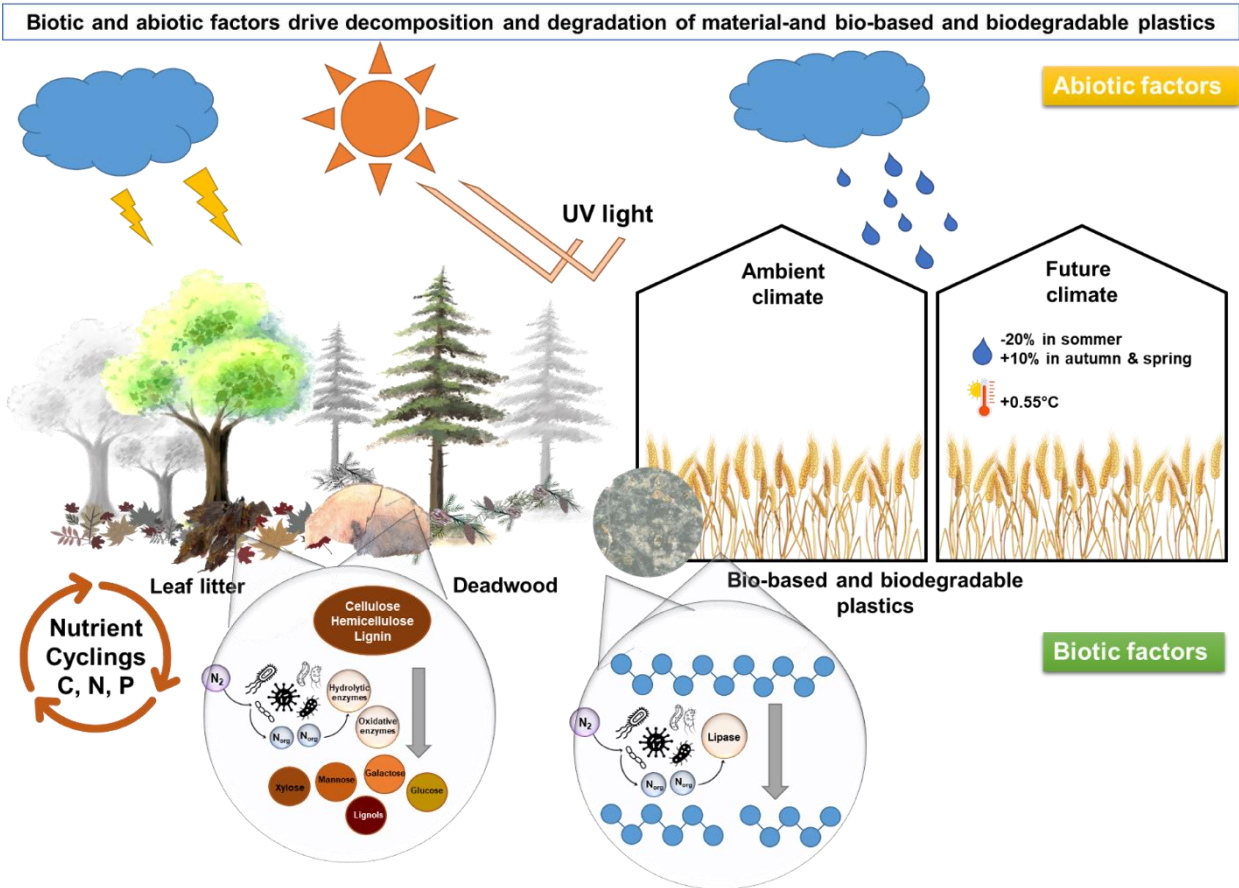


Figure 1. Biotic and abiotic factors drive the decomposition and degradation of plant materials and bio-based and biodegradable PBSA plastics.

Under natural conditions, the degradation of plastics is simultaneously induced by both abiotic (such as light and temperature) and biotic (dominated by microorganisms) factors ³⁸ (Figure 1). Microbial activity, along with the influence of temperature and light, accelerates chemical degradation mechanisms (such as hydrolysis or oxidation). The chemical degradation of plastics results in the cleavage or oxidation of plastic chains, which in turn leads to shorter chains and thus to a lower molar mass ⁶⁰. Soil microbes, including archaea, bacteria, and fungi, play a crucial role in the microbial degradation of biodegradable plastics, such as PBSA and PBAT ^{20,36} (Figure 1). A recent study showed that a PBSA plastic was degraded under natural soil conditions in a conventional farming system (by means of molar mass reduction of up to 33% after approximately one year) ²⁰. The succession of taxonomic and functional compositions of bacteria and fungi was observed during the PBSA degradation processes. The microbial degradation process of PBSA was accelerated after colonization by aquatic fungi

(*Tetracladium*)²⁰. Atmospheric nitrogen (N₂)-fixing bacteria were detected 180 days post-incubation of PBS in soils. They can either facilitate the microbial degradation of PBSA by providing bio-available N, an important nutrient for building PBSA-degrading enzymes (e.g., lipase), or potentially degrade plastics themselves⁶¹ (Figure 1). Despite the important role of soil microbes in plastic degradation, studies investigating this aspect are largely lacking, especially the entire plastisphere microbiome and its cross-kingdom interaction.

1.1.5. Abiotic factors drive decomposition and degradation of plant materials- and bio-based and biodegradable plastics

While biotic factors are considered in certain abiotic conditions as the main driver of plant material decomposition^{4,12}, abiotic factors also play important roles in the decomposition directly by ultraviolet (UV)light, humidity, pH, and temperature⁸ and indirectly by regulating the associated microbial community composition through litter physicochemical properties^{48,62} (Figure 1). Soil structure and texture regulate the water and nutrient dynamics available for soil organisms, whereas soil pH, soil organic matter, temperature, moisture, and soil nutrients determine the activity of microbial decomposer communities⁸. Rainfall has been reported to have a positive effect on litter decomposition rate as soil moisture increases⁸. However, an increase in soil moisture causes anoxic conditions and has a potentially negative impact on aerobic organisms⁶³. The tree species characteristics such as tree anatomy (deciduous or conifer), structure (density), physicochemical properties (water content, pH, and nutrients, including C, N, and lignin content) and external environmental factors (including soil nutrient availability, moisture, and temperature) have a major effect on the colonization of the microbial decomposer communities and thus, the decomposition rate of plant materials^{3,48,64}.

The degradation of plastics under natural conditions is initiated by mechanical, thermal, and hydrolytic processes through weathering conditions³⁸. Abiotic degradation pathways may not

necessarily lead to changes in the polymer structure and reduction of polymer molar mass; rather, they lead to physical degradation mechanisms of plastics (such as cracking, embrittlement, and flaking)⁶⁰. Polymers are fragmented into smaller particles, and the surface area is increased; thus, degradation through chemical or enzymatic attack is more susceptible. Plastic degradation products can be taken up by microbes and subsequently mineralized to water and CO₂ by cellular enzymes^{35,60}. Thus, the degradation rate of microplastics is expected to be higher than that of larger plastic particles owing to their highly active surface⁶⁵.

1.1.6. Climate change impacts on biotic and abiotic factors

Climate change has greatly increased the environmental concerns of society and the scientific community during the past few decades. Plant, animal and microbial communities, the interactions and the ecosystem services vary and change due to the course of available resources, water content, pH, and temperature, which lead to shifts in the organismal composition, activity and to a decline in diversity^{3,4,66}. Climate change directly and indirectly impacts these factors, which are important for microbial growth and survival. Microbes are of high importance for ecosystem services (such as nutrient cycling, contribution to biomass, and decomposition of dead plant materials), on which plants and animals depend¹⁴. Recent studies have suggested that climate change potentially causes a reduction or substantial changes in species diversity and composition, which in turn impacts ecosystem functions and services^{67–71}. Previous studies predicted a reduction in microbial biomass due to the depletion of soluble C and N content caused by climate change^{66,72}. Nevertheless, knowledge on the effect of climate change on microbial community composition, diversity, community assembly, and networks is still scarce.

1.1.7. Community assembly processes control the microbiome during decomposition and degradation of plant materials- and bio-based and biodegradable plastics

Biodiversity is the main driver of ecosystem function. Understanding the assembly processes that govern biodiversity is important for understanding the response of biodiversity and ecosystem functioning to future global changes⁷³. Network analysis and community assembly processes have continued to grow over the past few years. However, such studies on microorganisms are still limited⁷³. Based on niche theory, deterministic processes assumes that species traits, environmental conditions (e.g., temperature, moisture, C-sources, nutrients) and biological interactions (such as synergisms, antagonism, and proto-cooperation) govern community structures⁷³⁻⁷⁷. This follows the “distance–decay” relationship, which is due to the environmental filtering or niche preference of organisms^{73,78}. Thus, it is believed that deterministic processes determine variation in community composition (β -diversity)^{73,78}. However, growing evidence suggests that stochastic processes also significantly drive β -diversity^{73,79}. Stochastic processes based on the neutral theory presuppose that community structures randomly convene, regardless of species characteristics⁷⁵. Stochastic processes include dispersal (immigration) and ecological drift (random births and death)⁷³⁻⁷⁵. Both community assembly processes occurred concurrently. The bacterial and fungal community assembly in leaf litter, as well as in biodegradable plastics, is also simultaneously governed by both stochastic and deterministic processes⁸⁰⁻⁸⁴; however, there is considerable controversy regarding the relative importance of both processes types^{85,86}. Previous studies⁸³⁻⁸⁵ reported a higher contribution of stochasticity (especially ecological drift) in governing bacterial community composition in different ecosystems and habitats (including soils, fresh water, and biodegradable mulch film). Nevertheless, it is still too early to draw general conclusions. Furthermore, studies investigating microbial networks and community assembly processes in biodegradable plastics, especially leaf litter, are limited. The ability to describe the interactions between species is key to gaining a deeper mechanistic understanding of the processes underlying ecosystem functioning. However, interactions between species are sometimes

complex and cannot be described using a simple equation. Ecological networks or co-occurrence networks between species help scientists visualize complex interaction patterns, which are statistically likely between species ⁸⁷. Furthermore, co-occurrence networks have been applied to affiliate the topological role of each taxon as specialists or generalists ^{88,89}. The microbial co-occurrence network visualizes the cross-kingdom interactions of complex microbial taxa and reveals keystone species that predominate communities and functions ⁹⁰. Understanding the ecological networks and ecological stability in relation to environmental conditions will help us predict changes in the system more precisely according to climate or environmental changes.

1.2. High resolution molecular techniques and enzyme analysis

1.2.1. DNA metabarcoding

Cultivation-independent molecular approaches such as next or third next-generation sequencing (NGS) have improved microbiome research. NGS platforms include Illumina MiSeq, Roche GS FLX+, and Ion Torrent PGM ^{91,92}. These sequencing techniques offer several advantages such as high throughput, fast analytical time, read length, accuracy, high quality and comparable data ⁹¹. Illumina sequencing has been widely employed to characterize the microbial community in various environmental samples, including soils ⁹³, leaf litter ⁹⁴, deadwood ⁹⁵, and bio-based and biodegradable PBSA plastic ²¹. Illumina MiSeq is cost efficient and offer several advancements, including coverage sequencing depth up to 600 base pair (bp, 2×300 bp), maximum reads per run up to 25 million reads, running time from 4 to 55 hours (h) and maximum output up to 15 Gigabyte ⁹⁶. Illumina MiSeq is based on the detection of the released fluorescence from the fluorescently labeled reversible-terminator nucleotides during the amplification ⁹² (Figure 2A).

After bioinformatics processing of the raw sequence data, the processed sequences were blasted against bacterial or fungal databases (for example, SILVA or UNITE databases) to gain their taxonomy. The ecological functions of the fungi were then assigned. Currently, there are many annotation tools that help ecologists assign the ecological functions of each fungal genus, for example, LIAS^{97,98}, DEEMY⁹⁹, Fun^{Fun}¹⁰⁰, Notes on genera: Ascomycota¹⁰¹, FUNGuild¹⁰², and FacesOfFungi¹⁰³. Fungal Traits¹⁰⁴ is a newly proposed database that was developed and built from the FUNGuild¹⁰² and Fun^{Fun}¹⁰⁰ databases. However, the choice of annotation tools needs to be considered to select the proper annotation tool and to verify that the manuscripts or previously published articles are comparable.

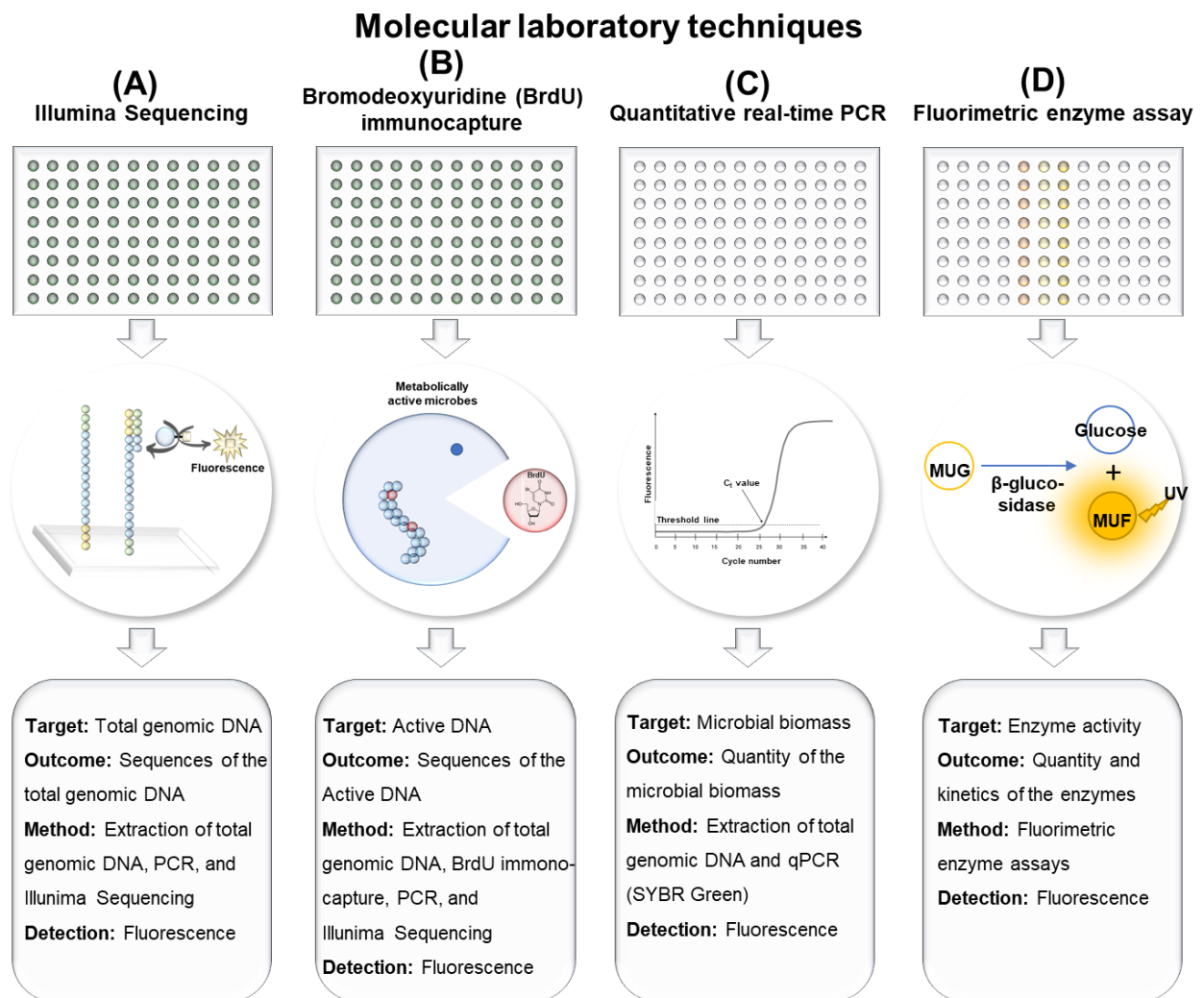


Figure 2 Summary of the laboratory techniques applied in this study. (A) Illumina MiSeq for sequencing of total genomic deoxyribonucleic acid (DNA, Hypotheses I, II, and III), (B) bromodeoxyuridine (BrdU) immunocapture technique incorporating Illumina MiSeq for

sequencing of DNA of metabolically active microorganisms (hypothesis II), (C) quantitative real-time polymerase chain reaction (qPCR) assay for quantifying the microbial biomass or gene copy number (hypotheses I, II, and III), and (D) fluorometric enzyme assays for analyzing the enzyme activity (hypotheses I and II).

1.2.2. Differentiation of active microbial community members by immunocapture technique

NGS molecular techniques target the total genomic DNA of microorganisms, which includes both intracellular DNA in active cells, inactive cells, and extracellular DNA from cell lysis^{95,105}. Thus, the microbial ASV or OTU tables derived from NGS sequencing may lead to under- or overestimation of the relationship between biodiversity and ecosystem functioning⁵⁴. The BrdU immunocapture technique (Figure 2B) is an alternative technique to ribonucleic acid (RNA) sequencing¹⁰⁶ used to determine the microorganisms in targeted environmental samples that are metabolically active in the ecosystems⁵⁴. The BrdU immunocapture technique is based on an excessive supply of BrdU in the outer cytoplasm, which is transported into the cytoplasm and replaces thymidine in the replication of DNA in metabolically active microorganisms, which clearly demonstrates the proliferation of microorganisms in the environment^{107,108} (Figure 2B). The DNA of active microorganisms labeled with BrdU was isolated from the total DNA using specific anti-BrdU antibodies^{107,108}. Not all microbial taxa can uptake BrdU and incorporate it into the cells⁵⁴. Nevertheless, a previous study demonstrated that the majority of studied bacterial strains were able to incorporate BrdU, and all bacterial phyla were detected¹⁰⁹. Incorporating the BrdU immunocapture technique with paired-end Illumina sequencing, both total and active microorganisms can be characterized in targeted ecosystems.

1.2.3. Quantitative real-time PCR assay

Quantitative real-time PCR assay is a revolutionary PCR method that was established in 1991 to monitor DNA amplification in real time based on the detection of fluorescence released

during amplification ¹¹⁰⁻¹¹². SYBR Green- and TaqMan-based qPCR assays are the most popular and widely used qPCR ¹¹². In both methods, the intensity of the released fluorescence was directly proportional to the amplification of the microbial strands, which allowed quantification of the targeted microbial genes. In SYBR Green qPCR assays, the fluorescent dye (SYBR Green) attaches to the newly synthesized double-stranded DNA (dsDNA) and consequently releases the fluorescence that is captured after each qPCR cycle ¹¹² (Figure 2C). In the TaqMan method, dual-labeled probes bind with single-stranded DNA (ssDNA). During amplification, Taq polymerase degrades the dual-labelled probes from ssDNA and generates dsDNA. The degradation releases fluorophore ¹¹². The TaqMan method is more expensive but provides better qPCR efficiency, which is important for the quantification of targeted genes, as compared with the SYBR Green method. However, a recent study reported that with the aid of optimized primers suitable for targeted genes and optimized protocols, the performance and quality of the data obtained from the SYBR Green method were compatible with those obtained using the TaqMan method ¹¹². In this study, the SYBR Green method was used to quantify specific bacterial and fungal biomass. The protocol for SYBR Green qPCR in our laboratory was optimized, and high-performance primers were used to quantify the microbial gene copy. The results from SYBR Green qPCR in our laboratory have been validated in previous studies ^{20,113,114}. The Internal Transcribed Spacer (ITS) primer set (ITS4 and fITS7), bacterial 16S rRNA gene-based primer set (BAC341f and BAC785R) ¹¹⁵, and nitrogenase (*nifH*) gene-based primer sets (*PolF* and *PolR*) ¹¹⁶ were used for the quantification of fungal, bacterial, and *nifH* gene copy numbers, respectively.

1.2.4. Fluorimetric enzyme assays

Enzyme activity analysis is widely employed to investigate ecosystem functioning and its relationship with microbial community composition. Fungi play central role in decomposition of deadwood and plant litter as they secrete various extracellular enzymes to degrade complex

macromolecules, including cellulose, hemicellulose and lignin ^{3,4,54}. In this dissertation, activities of enzymes important for C, N, and P acquisition, including β -glucosidase, cellobiohydrolase, xylosidase, N-acetyl-glucosaminidase, acid phosphatase, laccase, manganese peroxidase, and peroxidase were quantified ^{54,95,117} (Figure 2D). These enzymes catalyze the breakdown of complex macromolecules. β -Glucosidase is an important enzyme that catalyzes the degradation of cellulose, the key structural polysaccharide in plant cell walls ¹¹⁸. N-acetylglucosaminidase catalyses the hydrolysis of N-acetyl glucosamine in chitin ¹¹⁸. Acid phosphatase releases phosphate from organic molecules (including phospholipids and nucleic acids) by catalyzing the hydrolysis of phosphomonoesters ¹¹⁸. Laccase, manganese peroxidase and/or manganese independent peroxidases are important enzymes catalyzing the oxidation of lignin polymer ^{3,4}. Fluorimetric enzyme assays are widely employed to measure the enzyme activity in soils ¹¹⁹. Fluorimetric enzyme assays were used to detect emitted fluorescence using fluorescent dye-conjugated substrates such as 4-methylumbelliferone or 7-amino-4-methylcoumarin ¹¹⁹ (Figure 2D). This assay offers rapid and sensitive detection of enzyme activity ⁵⁹.

2. Synopsis

2.1. Aim and hypotheses

Overall, this dissertation aimed to investigate the leaf litter, deadwood decomposition, and degradation processes of a bio-based and biodegradable PBSA in relation to biotic and abiotic factors. I aimed to characterize the core microbiome responsible for the decomposition of these plant materials and the degradation of PBSA plastic. Furthermore, the relationship between the environmental factors (including tree species, tree mycorrhizal types, land use types, soil and/or leaf physicochemical properties) and the changes in the microbial community composition, community assembly processes, and co-occurrence networks/cross-kingdom

interactions will be analyzed. These core aims will lead to a deeper understanding of the microbial ecology of the decomposition processes and the key players in the microbiome for plant material and plastic decomposition. Furthermore, the link between environmental factors and microbial community compositions, community assembly processes, and co-occurrence networks/cross-kingdom interactions will help us predict the response of the microbiome to expected changes in future climate conditions. In addition, specific groups of microbes (saprotrophic, endophytic, lichenized fungi, plant pathogens, or N₂-fixing bacteria) and their relationship to environmental factors will be further investigated to gain a more complete picture of who lives and proliferates on leaf litter and/or plastic. Additionally, this dissertation will enable us to accurately estimate the potential risk of plastic degradation in the environment.

Overall, I hypothesize that (i) fungi are the main decomposers of all the biopolymers investigated in this dissertation. However, fungi are supported by associated N₂-fixing bacteria, especially in systems or substrates that lack N content, such as dead wood or plastic. Furthermore, I expect that (ii) macronutrients and tree species have an impact on microbial community composition and, thus, the decomposition processes of different biopolymers. Specifically, the following hypothesis was proposed:

Hypotheses part I: Leaf litter decomposition

To identify the ecological functions (such as saprotrophs, plant pathogens, endophytes, etc.) of fungi, many annotation tools have been introduced to assign functional traits to the respective taxa. The choice of annotation tools may lead to different ecological interpretations of the sequencing data. Thus, in the **litter-I** publication, I evaluated the proper annotation tools (FUNGuild *vs.* FungalTraits) and compared whether the ecological interpretations of both annotation tools were comparable. I hypothesized that the functional assignment of fungi based

on the annotation tool FungalTraits is superior in terms of assignment quality and quantity than FUNGuild, as it contains a larger database. However, I hypothesize that the ecological interpretations of both annotation tools are comparable, as FungalTraits were developed from the FUNGuild database. The microbiome of senescing leaves and needles may be important for leaf litter decomposition. Thus, I additionally investigated the specific groups of microbes (saprotrophic, endophytic, lichenized, and plant pathogenic fungi) that inhabit senescing leaves and needles and determined their community assembly processes as well as their corresponding factors to disentangle the importance of each factor on the members of the leaf microbiome. I hypothesized that the community compositions of these initial microbes are mainly governed by deterministic processes, and they are rather specific to leaf/needles of different tree species due to spatial dispersal limitation and specific leaf nutrient traits. Finally, I hypothesized that during leaf litter decomposition, stochastic processes have an increasing contribution in governing the microbial community composition due to the replication, inactivation, and migration processes of the microbes.

Hypotheses part II: deadwood decomposition

In this part of the dissertation, the immunocapture technique was employed to detect which microbial functional groups actively live on decomposing deadwood. I hypothesize that fungi, saprotrophs, and bacteria, especially N₂-fixing bacteria, dominate the microbial community composition. I expect an interaction between these saprotrophs and N₂-fixing bacteria, as a link between N₂-fixing bacteria and deadwood decomposition rate has been introduced in previous studies ^{120,121}. This dissertation is the first assessment of whether N₂-fixing bacteria are metabolically active during fungal deadwood decomposition.

Hypotheses part III: plastic degradation

Here, I expect to detect a high sequence read abundance of previously reported plastic-degrading fungi (such as members of the genera *Tetracladium*, *Cladosporium*, and *F. solani*) in degrading PBSA in forest ecosystems. As the N content in PBSA is almost absent, I hypothesize that an interaction between N₂-fixing bacteria and fungi will occur. I hypothesize that bacterial and fungal communities are governed by both deterministic and stochastic processes, but in different proportions, depending on the ecosystems in which PBSA is being degraded. Additionally, I expect that degrading PBSA favors plant pathogenic microbes (*Cladosporium* and *F. solani*), as this group of microbes also acts as PBSA degraders. I hypothesized that the enrichment of these plant pathogenic microbes poses some risk to specific plants, such as mung bean (*Vigna radiata* L.).

2.2. Study design and study sites

To answer the aims and hypotheses, both field and laboratory experiments were conducted to investigate the decomposition and degradation of plant material and bio-based and biodegradable PBSA plastic under different land cover types, including agricultural land, broad-leaved, and coniferous forest land (Figure 3). The decomposition and degradation of plant material and PBSA plastic experiments were conducted in two forest sites and one agricultural site at the Global Change Experimental Facility (GCEF) (Figure 3). Laboratory experiments were carried out at the Soil Ecology Department, UFZ-Helmholtz Centre for Environmental Research.

2.2.1. Decomposition of leaf/needle of common 12 temperate tree species

To validate the annotation tools for the fungal functional assignment (hypothesis I), FungalTraits and FUNGuild were applied to the fungal sequences of senescing leaves and needles of 12 temperate tree species that grew in a managed mixed forest of Thuringia, Germany (51°12'N 10°18'E) (Figure 3.1). The leaf litter decomposition experiments in this

dissertation were conducted at the same forest site to determine the core microbiome decomposing the leaf litter (Figure 3.1). These 12 tree species include eight deciduous broadleaf (including *Acer pseudoplatanus*, *Carpinus betulus*, *Fagus sylvatica*, *Fraxinus excelsior*, *Populus hybrid*, *Prunus avium*, *Quercus robur*, and *Tilia cordata*), three evergreen (including *Picea abies*, *Pinus sylvestris*, and *Pseudotsuga menziesii*), and one deciduous (*Larix decidua*) coniferous tree species (Figure 3.1).

To investigate the influence of tree mycorrhizal associations on the microbial community, assembly, and network (hypothesis I), tree mycorrhizal types were grouped as follows: broadleaved tree species associated with arbuscular mycorrhizal fungi (AM tree), including *Acer pseudoplatanus*, *Fraxinus excelsior*, and *Prunus avium* (AM_BL). Tree species associated with ectomycorrhizal mycorrhizal fungi (EcM tree) include both broadleaved (EcM_BL including *Carpinus betulus*, *Fagus sylvatica*, *Quercus robur*, and *Tilia cordata*) and coniferous trees (EcM_C including *Picea abies*, *Pinus sylvestris*, *Pseudotsuga menziesii*, and *Larix decidua*).

2.2.2. Decomposition of deadwood

To investigate the active microbiome decomposing deadwood, experiments were conducted independently at a forest site (hypothesis II, Figure 3.2). This included eight plots in a *Fagus sylvatica* and eight plots in a *Picea abies*-dominated forest site.

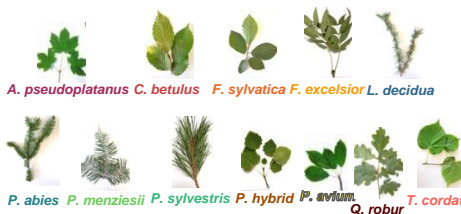
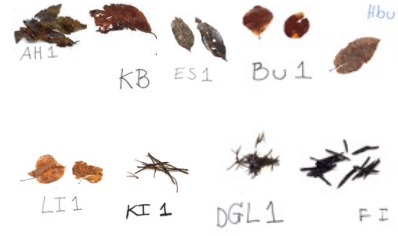

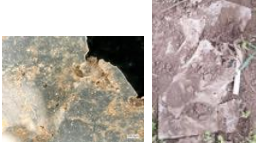



1. Decomposition of leaves and needles of 12 temperate tree species		
Senescing leaves and needles	Decomposing leaves and needles	
<ul style="list-style-type: none"> - Validation of the detection methods. - Characterization of fungi colonizing senescing leaves and needles. 	<ul style="list-style-type: none"> - Characterization of bacteria and fungi colonizing leaves and needles after 200 and 400 days of decomposition. 	
		
2. Decomposition of deadwood		
Experiment in forest site		
<ul style="list-style-type: none"> - Characterization of active bacteria and fungi colonizing deadwood and investigation of their cross-kingdom interaction. 		
3. Decomposition of bio-based and biodegradable plastic, PBSA		
Experiment in agricultural site	Laboratory experiment	Experiment in forest site
 <ul style="list-style-type: none"> - Investigation of their cross-kingdom interaction and co-occurrence network.  <p style="text-align: center;">PBSA</p>	<ul style="list-style-type: none"> - Validating the risk from a plastic-colonizing/decomposing plant pathogen, <i>Fusarium solani</i> to plant health, mung bean (<i>Vigna radiata</i> L.).  <p style="text-align: center;">With PBSA/ N fertilizer</p>  <p style="text-align: center;">No PBSA</p>	<ul style="list-style-type: none"> - Characterization of bacteria and fungi in PBSA under forest site and validating the transferability of the knowledge from agricultural site to forest site. 

Figure 3. Schematic of the study design. To answer the hypotheses, part I of the leaf litter decomposition experiment (Figure 3.1) was conducted in a mixed managed forest. The deadwood decomposition experiment (Figure 3.2) was conducted at forest sites to address hypothesis II. Hypothesis III was assessed by PBSA degradation experiments (Figure 3.3) in agricultural farming, laboratory experiments, and a mixed managed forest.

2.2.3. Degradation of a bio-based and biodegradable plastic, PBSA

To investigate the plastic-degrading microbes in forest ecosystems, a plastic degradation experiment was conducted in a managed mixed forest in Thuringia, Germany (51°12'N 10°18'E) (hypothesis III, Figure 3.3). Plastic films were buried under four tree species from two forest lands, including two broadleaved trees (*F. sylvatica* and *Q. robur*) and two coniferous trees (*P. abies* and *P. sylvestris*). Studies on plastic-degrading microbes in

agricultural sites have been conducted in conventional agricultural farming under ambient and future climate conditions at the world's largest climate change research facility, the GCEF (Hypothesis III, Figure 3.3). The laboratory experiment validating the risk of the plastic-colonizing plant pathogen, *F. solani*, to plant health, mung bean (*V. radiata* L.), was carried out at the Soil Ecology Department, UFZ-Helmholtz Centre for Environmental Research (hypothesis III, Figure 3.3).

2.3. GENERAL DISCUSSION

Part I hypotheses: Leaf litter decomposition

In this study, I used sequencing data from senescing leaves and needles of 12 common temperate forest tree species to verify the choice of annotation tools for assigning the ecological function of fungi associated with different tree species, and finally draw a general conclusion on the choice of annotation tools to be employed for leaf/needle-associated fungi (*Litter 1*, Chapter 3). The FungalTraits annotation tool revealed a higher functional assignment of all functions and saprotrophs across all 12 tree species than FUNGuild. FungalTraits also reveals more accuracy in assigning ecological functions to most fungal groups (*Litter 1*, Chapter 3). These results are not surprising, as FungalTraits included data from FUNGuild¹⁰² and Fun^{Fun}¹⁰⁰. All fungal genera were revised by experts for the highest accuracy. Another advantage of the FungalTraits annotation tool is that it allows users without expert knowledge of the fungal ecological function to properly assign the most common ecological function by providing the primary and secondary lifestyles of each genus¹⁰⁴. The diverse functions of a single fungal genus are not new. Members of the same fungal genus may have different functions within the ecosystem. Some members contribute to more than one ecological function in the environment, depending on the conditions and substrate degradation. For instance, *Fusarium* is generally a plant and animal pathogen in agricultural ecosystems¹²², but it can also act as a¹²³. Thus, the

primary function provided in FungalTraits helps users determine the most common function in each fungal genus. Nevertheless, it is important to specifically assign this function to a particular fungus of interest. They needed to identify the fungal species and individually cross-check with pre-existing literature, regardless of which annotation tools were employed. For an overview of a particular habitat, such as leaves and needles, FungalTraits outperformed ecological assignment (quantity) for all 12 tree species as well as the accuracy of the ecological function being assigned (quality). Nevertheless, the ecological interpretation derived from both annotation tools led to similar conclusions for the saprotrophs (*Litter 1*, Chapter 3). The community composition of fungal saprotrophs assigned by both annotation tools responded significantly to the same environmental factors (water content, location, and nutrient contents, including dissolved organic C (DOC), dissolved mineralized N (N_{Min}), dissolved organic N (N_{Org}), calcium (Ca), iron (Fe), magnesium (Mg), and P content (*Litter 1*, Chapter 3). Tree species was the main factor corresponding to the community composition of fungal saprotrophs derived from both annotation tools (*Litter 1*, Chapter 3). Thus, I conclude that although FungalTraits are superior in terms of assignment quality and quantity compared to FUNGuild, the ecological interpretations derived from these two different annotation tools are comparable. Therefore, the first part of hypothesis I was verified.

For fungi, I found that saprotrophs and plant pathogens dominated the fungal community composition in the initial fungal leaf microbiome (*Litter 1*, Chapter 3). Some of these are endophytes; thus, the presence of these groups in mature/senescing leaves and needles may not be surprising. However, the enrichment of fungal saprotrophs and plant pathogens may have other causes. The high relative sequence read abundance of fungal saprotrophs indicates that mature leaves and needles prepare the leaf microbiome for the upcoming decomposition processes (*Litter 1*, Chapter 3). The enrichment of fungal plant pathogens may be due to intra- and interspecific competition in forest ecosystems (*Litter 2*, Chapter 3). Conspecific negative

density dependence (CNDD) is one of the most important mechanisms regulating tree diversity in mixed forest ecosystems¹²⁴. At our local-scale study site in Central Germany, we determined the CNDD in *C. betulus* and *F. sylvatica* as a higher incidence of foliar disease in *C. betulus* and *F. sylvatica* seedlings growing under their parental tree canopies than in those growing outside of these parental tree canopies (**Figure 4**, additional analysis to *Litter 2*, Chapter 3). Under the tree canopies of *A. pseudoplatanus* and *F. sylvatica*, a high overall foliar disease incidence was observed in seedlings of different tree species (**Figure 4**), which reflects interspecific competition (additional analysis to *Litter 2*, Chapter 3). Under the mature tree canopies of *A. pseudoplatanus* and *F. sylvatica*, where the overall foliar disease incidence of various seedlings was high, we detected high richness and relative sequence read abundance of fungal pathogenic generalists, respectively. In *F. sylvatica*, *Mycosphaerella* (a fungal plant pathogen classified as a generalist) was highly abundant.

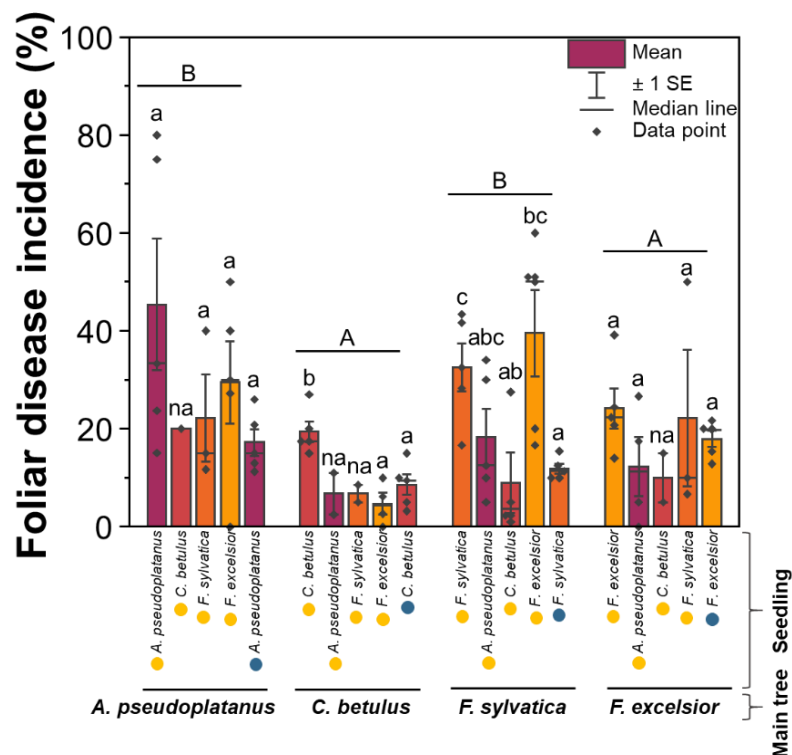


Figure 4 Foliar disease incidence in seedlings of the four broadleaf tree species. Yellow and blue circles indicate the seedlings inside and outside the main tree canopy, respectively. Capital and lowercase letters indicate statistically significant differences among foliar disease incidence in seedlings under main tree canopies and between foliar disease incidence in seedlings under and outside main tree canopies, respectively. Kruskal–Wallis tests and analysis

of variance (ANOVA) were performed for datasets with non-equality of variance and equality of variance, respectively. Na: not assessed. Additional analysis of *Litter 2*, Chapter 3.

In *A. pseudoplantanus*, diverse fungal plant pathogens are classified as generalists, including *Mycosphaerella*, which causes leaf spots in *Acer*¹²⁵, *Fraxinus*¹²⁶, *Fagus*¹²⁷, and *Tilia*¹²⁸. In *C. butulus*, *Erysiphe arcuata* (leaf disease pathogen of *C. butulus*)¹²⁹ were detected and classified as fungal pathogenic specialists. Thus, I propose that fungal plant pathogens living in senescing leaves can cause leaf diseases in seedlings. Community assembly processes based on different approaches revealed divergent results. The phylogenetic normalized stochasticity ratio indicates that the community composition of plant pathogenic fungi in senescing leaves was governed by stochastic processes (ecological drift and homogenizing dispersal), whereas deterministic processes were dominant when the taxonomic normalized stochasticity ratio was applied (*Litter 2*, Chapter 3). This leads to partial verification of the second part of Hypothesis I that the initial leaf microbiome is governed by both deterministic and stochastic processes, depending on the approaches being applied.

Another interesting group of fungi colonizing mature leaves and needles is lichenized fungi. Although it cannot be observed in the necked eyes, this group is diverse when detected by NGS (**Figure 2A**). The lichenized fungal community compositions are shaped by tree species and tree types when all trees and coniferous trees are considered (*Litter 3*, Chapter 3). Notably, leaf/needle nutrients, especially DOC, N_{Org}, nitrite nitrogen, and Fe, significantly shaped both lichenized fungal richness and community composition (**Table 1**, additional analysis to *Litter 3*, Chapter 3). The nutrient acquisition of foliicolous lichens from host leaves remains unclear^{130–133}. This thesis demonstrates the importance of nutrients from the host leaf/needle for lichenized fungal community patterns, which is underexplored and highly novel. Apart from the N produced by the cyanobiont through N₂-fixation¹³³, the results suggest that N_{Min} from host leaves and needles can be an alternative source of N for lichens. N_{Min} and DOC are water-soluble nutrient sources that are immediately available for leave/needle-associated microbes.

C assimilation is driven by photosynthesis in the photobiont, which is highly dependent on water, light, and bio-available N ¹³⁴. During hydration and dry conditions, the differences in water potential between lichen thallus and host substrate, as well as within the lichen symbiont, may act as a suitable environment for nutrient transport ¹³⁵. This thesis provides in-depth evidence that leachable N and C from host leaves and needles may play an important role in structuring both lichenized fungal richness and community composition (**Table 1**, additional analysis to *Litter 3*, Chapter 3). C and N are important elements for anabolic metabolite formation, including the synthesis of carbohydrates, proteins, lipids, and nucleic acids ¹³⁶. Macronutrients affect microbial growth, activity, survival, and reproduction ^{136,137}. Hypothesis I was verified, and different groups of initial fungi associated with senescing leaf/needles were related to leaf nutrients.

Table 1 Goodness-of-fit statistics (R^2) of environmental variables fitted to non-metric multidimensional scaling (NMDS) ordination of lichenized fungal community composition based on relative abundance data. The analysis was performed using the “Vegan” package in R and R Studio. Bold letters indicate statistically significant differences.

	All tree species		Coniferous trees		Broadleaved trees	
	R^2	P	R^2	P	R^2	P
Tree species	0.53	0.001	0.67	0.001	0.32	0.598
Tree type	0.15	0.004	NA	NA	NA	NA
DOC	0.44	0.001	0.42	0.017	0.20	0.192
Ammonium nitrogen	0.07	0.308	0.18	0.194	0.08	0.528
Nitrite nitrogen	0.36	0.001	0.11	0.377	0.37	0.035
Nitrate nitrogen	0.03	0.619	NA	NA	0.09	0.797
N _{Min}	0.09	0.217	0.18	0.193	0.06	0.665
N _{Org}	0.31	0.003	0.27	0.086	0.05	0.711
Ca	0.13	0.079	0.21	0.133	0.14	0.302
Fe	0.18	0.038	0.39	0.018	0.11	0.443
K	0.14	0.057	0.27	0.074	0.29	0.064
Mg	0.10	0.176	0.18	0.210	0.10	0.470
P	0.00	0.981	0.42	0.016	0.30	0.057

This dissertation is the first to conduct a large leaf litter experiment addressing the impact of different tree mycorrhizal association types (nine temperate tree species, covering three tree

mycorrhizal types) on the decomposition rate by governing the microbial community composition, community assembly, and network pattern. Overall, the leaf decomposition rate of broad-leaved arbuscular mycorrhizal trees was significantly higher than that of broad-leaved and coniferous ectomycorrhizal trees (*Litter 4*, Chapter 3). This result is in line with a previous study showing that leaf quality affects leaf litter decomposition rates, in which AM trees are usually higher than EcM trees⁴⁹. The tree mycorrhizal types affected the leaf physicochemical properties and consequently revealed distinct microbial community compositions over time (*Litter 4*, Chapter 3). In the leaves of broadleaved arbuscular and ectomycorrhizal trees, *Alternaria*, *Chaetomium*, and members of the class Leotiomycetes (i.e., from the genera *Hymenoscyphus*, *Mollisia*, and *Tetracladium*) dominated the fungal community composition after 200 days of decomposition (*Litter 4*, Chapter 3). These fungi, especially Leotiomycetes, are known to secrete cellulase⁵⁵ to break down cellulose, hemicellulose, pectin, and chitin. Enrichment of white rot fungi was observed, especially *Mycena*, which produces laccase and manganese peroxidase enzymes^{3,138,139} to decompose lignin. Furthermore, N₂-fixing bacteria, *Sphingomonas*, were identified as module hubs and connectors in the co-occurrence network between bacteria and fungi throughout the decomposition process (*Litter 4*, Chapter 3). This implies that *Sphingomonas* is a keystone species and that a link between N₂-fixing bacteria and fungi exists during the decomposition processes of leaf litter. Furthermore, a link between hydrolytic activity, oxidative enzyme activity, and fungal community composition was observed at both 200 and 400 days (*Litter 4*, Chapter 3). The bacterial community composition was linked to oxidative enzymes on day 400. Generally, the oxidative enzymes (general and manganese peroxidase) measured in this study were strictly produced by fungi¹⁴⁰. The correlation between bacterial community composition and these oxidative enzymes may be due to the fact that some groups of bacteria can act on lignin degradation products, such as *Sphingobium* and *Novosphingobium*¹⁴⁰. During leaf litter decomposition, stochastic processes

were more dominant than deterministic processes in the microbial community composition of senescing leaves and needles (*Litter 4*, Chapter 3). Deterministic processes (mainly variable selection) show increasing importance in governing the bacterial community composition in the later stage of leaf litter decomposition, while in fungal community composition, stochastic processes (mainly ecological drift) are the main assembly processes (*Litter 4*, Chapter 3). This drives the rejection of the second part of hypothesis I for bacteria, but not for fungi.

Part II hypotheses: Deadwood decomposition

The analysis of microorganisms during plant material decomposition using high-resolution molecular techniques such as metabarcoding is not new. In fact, our knowledge of who is responsible for the decomposition of dead plant material is almost complete, with few knowledge gaps. Nevertheless, this knowledge is based on the analysis of total genomic DNA, which contains the DNA of both active and dormant cells. Thus, based on previous knowledge, we only know who is or is living there. The immunocapture technique (**Figure 2**) enables the detection of living microbes and allows a more significant statement of who performs ecosystem functions in the targeted plant materials. This dissertation is among the first to analyze metabolically active microbes that are directly and indirectly involved in deadwood decomposition. The captured metabolically active microbiome is highly dominated by saprotrophic fungi (mainly represented by members of the genus *Mycena*^{3,138,139}) and chemoheterotrophic bacteria (such as *Stenotrophomonas*¹⁴¹, *Massilia*¹⁴², and *Luteibacter*¹⁴³, *Deadwood 1*, Chapter 3). In addition, saprotrophs and bacterial groups related to N cycling (such as *Sphingomonas*¹⁴⁴ and *Rhodanobacter*¹⁴⁵) also co-dominate the active bacterial community composition (*Deadwood 1*, Chapter 3). During deadwood decomposition, nutrients stored in the deadwood are released through the enzymatic cleavage of deadwood compartments. Microbial activity is facilitated by C, N, and other nutrients derived from the decomposition of dead wood. Some bacterial taxa associated with the N cycle are also capable

of fixing N₂, such as *Sphingomonas* and *Allorhizobium-Neorhizobium-Pararhizobium-Rhizobium*¹⁴⁴. In fact, the abundance of *nifH* gene copy numbers is highly correlated with fungal abundance (***Deadwood 1***, Chapter 3). Furthermore, co-occurrence network analyses revealed an interaction between N₂-fixing bacteria and wood-decomposing fungi. Thus, this dissertation is the first to provide evidence for a cross-range interaction between N₂-fixing bacteria and fungi during deadwood decomposition. The first part of hypothesis II was verified as saprotrophic fungi, chemoheterotrophic bacteria, and N₂-fixing bacteria dominated the active microbial community composition, and a correlation between saprotrophs and N₂-fixing bacteria was observed.

Part III hypotheses: Plastic degradation

Potential PBSA-degraders, such as *Cladosporium*, *Exophiala*, and *Tetracladium*, were highly detected in the plastisphere microbiome degraded under different tree species. Furthermore, I found that the potential fungal PBSA decomposers (*Tetracladium*) and N₂-fixing bacteria (including *Methylobacterium*, *Mycobacterium*, and *Allorhizobium-Neorhizobium-Pararhizobium-Rhizobium*) are keystone taxa, indicating their cross-kingdom interactions and their importance during plastic degradation processes (***Plastic 1***, Chapter 3). These findings are in line with a previous study conducted in agricultural farming^{20,146} indicating that these microbes favor PBSA habitats. Additionally, a strong positive correlation between *nifH* and fungal ITS-based gene copy numbers was also detected in forest ecosystems, supporting the assumption of cross-kingdom interactions between N₂-fixing bacteria and fungi in N-limited substrates (PBSA) (***Plastic 1***, Chapter 3). N content is an important nutrient for microbial growth and the production of diverse enzymes¹⁴⁷, including plastic-degrading enzymes (lipase and esterase)¹⁴⁸. In N-poor habitats or substrates, fungi acquire N from nearby environments through the fungal mycelium¹⁴⁹. Another, N source for fungi is the symbiotic interaction with N₂-fixing bacteria which has been observed in different N-poor habitats across different

ecosystems^{3,95,113,121}. During the PBSA degradation processes in forest ecosystems, bacterial community composition is mainly governed by stochastic processes (mainly homogenizing dispersal, *Plastic 1*, Chapter 3). On the other hand, fungal community composition is mainly controlled by stochastic processes (ecological drift and homogenizing dispersal), in which the proportion of deterministic processes (mainly homogeneous selection) increases over time (*Plastic 1*, Chapter 3). Knowledge of community assembly during plastic degradation is still limited, particularly in soil environments. These findings on community assembly in the plastisphere microbiome of forest ecosystems significantly expand the current knowledge on community assembly. The detection of the aforementioned PBSA-degrading microbes and N₂-fixing bacteria on PBSA films in forest ecosystems validates the first part of Hypothesis III.

Cross-kingdom interactions between N₂-fixing bacteria and fungi during PBSA degradation have also been observed in agricultural ecosystems. N₂-fixing bacteria (both symbiotic and non-symbiotic) help PBSA-degrading fungi by providing available N for producing PBSA-degrading enzymes and facilitating fungal growth. N content is the rate-limiting step for N-poor substrate (PBSA) in the laboratory experiment, where I conducted two treatments: i) PBSA incubated in soil and ii) PBSA incubated in soil with the addition of N fertilizer. The results showed that PBSA in the PBSA-N fertilizer treatment was almost completely degraded after 90 days of incubation (*Plastic 2*, Chapter 3). In this treatment, fungal colonization was rapidly enhanced, and N₂-fixing bacteria were almost absent from the system (*Plastic 2*, Chapter 3). This finding suggests that N addition enhances fungal colonization and degradation of PBSA films²¹. In the PBSA treatment without N addition, the enrichment of both symbiotic (undergo symbiosis with plants, especially legumes¹⁵⁰) and non-symbiotic (free-living soil bacteria, not in a direct symbiosis with plants¹⁵¹) N₂-fixing bacteria was observed (*Plastic 2*, Chapter 3). The presence of symbiotic N₂-fixing bacteria on the plastisphere in soils without the presence of any plants indicates that N₂-fixing bacteria can use C from PBSA films as an

alternative C source. This finding is in line with previous studies reporting that N₂-fixing bacteria are capable of both fixing atmospheric N₂ and utilizing a hydrocarbon source from plastic^{61,152}. Hypothesis III on the interaction between N₂-fixing bacteria and fungi was proven in this part of the dissertation (*Plastic 2*, Chapter 3).

In the degradation process of PBSA in agricultural ecosystems, stochastic processes (mainly ecological drift) are the main processes governing both bacterial and fungal community compositions under both ambient and future climates over the course of the degradation process (*Plastic 3*, Chapter 3). This finding is in line with previous studies on aquatic⁸⁴ and terrestrial ecosystems⁸³. On the other hand, future climate will alter the microbial and co-occurrence networks (*Plastic 3*, Chapter 3). The results showed that future climate increased the negative correlation in the bacterial and co-occurrence networks, indicating an increasing antagonistic relationship between bacteria and the interaction patterns between bacteria and fungi. This implies that under future climate conditions, competition between bacteria (especially heterotrophic bacteria) and fungi (saprotrophic fungi) may occur because of limited resources induced by increased temperature, reduced rainfall, and other changes. Nevertheless, this assumption should be verified in future studies. Furthermore, the effect of climate change on the interaction between specific groups of bacteria (particularly N₂-fixing bacteria) and saprotrophic fungi should be investigated to properly estimate the changes in ecosystem functioning. The finding that microbial community compositions on PBSA in agriculture and forest ecosystems are governed by both stochastic and deterministic processes in different proportions led to the validation of Hypothesis III.

As discussed in Hypothesis I, many fungi may have different ecological functions, depending on their habitat and environmental conditions. This is particularly true for potential fungal PBSA degraders. *F. solani* is able to degrade PBSA (*Plastic 4*, Chapter 3) and other various plastics, including PLA, PHA, PBS, plastics^{20,22,146}. On the other hand, *F. solani* was also

reported for their pathogenicity, for example in citrus causing dry root rot ¹⁵³. Thus, an additional laboratory experiment was conducted to evaluate the risk of a high load of PBSA film together with the application of N fertilizer to mung bean health. The results showed that incubating PBSA alone in soils for degradation did not increase the mortality rate of mung beans (*V. radiata* L.), and no disease symptoms were observed (**Plastic 4**, Chapter 3). However, another treatment, incubation of PBSA into soils and adding N fertilizer, revealed contrasting results. *V. radiata* L. showed soybean sudden death syndrome typically causing by *F. solani* ¹⁵⁴ (**Plastic 4**, Chapter 3). To confirm the presence of *F. solani*, specific PCR was performed on the DNA extracted from PBSA films subjected to different treatments. I clearly observed the enrichment of *F. solani* in the treatment of PBSA films with N fertilizer for degradation (**Plastic 4**, Chapter 3). In this treatment, the highest rate of PBSA mass loss was observed (**Plastic 4**, Chapter 3), indicating the ability of *F. solani* to degrade PBSA. In conclusion, the degradation of PBSA films acts as a fungal plant pathogen hub in the soil environment. If the conditions meet (e.g. high N content, water content, pH, etc.), particular fungal plant pathogens can enrich and pose risk to their specific plant hosts, which include also economically important plants and vegetables, in this case mung bean (*V. radiata* L.) (**Plastic 4**, Chapter 3). Thus, this study supports the suggestions of a previous study ²⁰ that bio-based and biodegradable PBSA mulch films should be collected from the field after recycling to prevent possible yield losses in agriculture. The last part of hypothesis III is hereby validated: plant pathogenic fungi are detected on degrading PBSA film and potentially pose a risk to plant health.

2.4. TRANSFERABILITY OF THE KNOWLEDGE

Transferability of the effect of tree mycorrhizal association types on leaf litter decomposition

In this dissertation, I investigated the effects of tree mycorrhizal association types on leaf/needle decomposition in a temperate forest. The results showed that the leaves of broadleaf AM trees decomposed faster than broadleaf or conifer EcM trees did. Another study in temperate forests reported a similar phenomenon ⁴⁹. EcM fungi have been reported to use a slow litter decomposition strategy to reduce competition for nutrients with other accompanying microbes and to prevent the leaching of nutrients ⁴⁹. In contrast, AM fungi that lack saprotrophic ability prefer to take up nutrients from inorganic compounds, which are immediately available for fungi and plants to use ⁴⁹. Thus, tree species associated with AM or EcM fungi will differ in their nutrient traits. These nutrients can be transferred from the root to the leaf/needles. Nutrient traits, in turn, determine the endophytic community composition as well as the colonizing microbial community composition ⁴⁹. In temperate forest ecosystems, the leaves of AM trees are characterized as high-quality leaf litter, as they contain lower lignin:N ratios, which are preferred for faster decomposition ⁴⁹. However, this finding may not be fully applicable to other forest ecosystems such as tropical or subtropical forests. A meta-data study reported that in tropical forests, tree mycorrhizal association does not affect the decomposition rate of leaf litter ^{49,50}. In sub/tropical forests, weather conditions (warm and rainy) significantly lead to a high decomposition rate regardless of the mycorrhizal association; thus, the decomposition rates of AM and EcM leaves are high and not significantly different from one another ⁴⁹. Thus, to predict the decomposition rate, all three predominant factors—climate, litter quality, and forest floor microbial activity and turnover rates—should be considered. Nevertheless, the findings of this dissertation on the relationship between decomposition and mycorrhizal association significantly contribute to the previously published findings for the temperate forest ecosystem in Germany that leaves of broadleaf AM trees decomposed faster than broadleaf or conifer EcM trees.

Transferability of degradation processes of PBSA to other bio-based and/or biodegradable plastics

The PBSA degradation processes in this dissertation were investigated in the natural soil conditions of four ecosystems, including agriculture under ambient and future climates, and broadleaf and conifer forests in temperate climate zones. The results showed that although the soils of these ecosystems may differ in their soil microbial community and activities, the degradation process or molar mass loss of PBSA sheet after one year are basically comparable^{20,113,155}. This may be because PBSA-degrading microbes are able to colonize, inhabit, and dominate PBSA in all ecosystems. Furthermore, the PBSA sheets degraded in the same temperate climate zone. Even though the forest and agricultural sites are more than hundred kilometers away from each other, the main climatic factors, such as temperature, precipitation, and soil moisture, were comparable. A recent study¹⁵⁶ investigated the degradation of bio-based plastics (PLA and PHA) and biodegradable plastic (PBAT) in compost and soils under different climate zones (warm and cool climates) and revealed that degradation in warm climates was faster than in cool climate zones. Furthermore, the degradation of these plastics was significantly slower in soils than in compost in both climate zones¹⁵⁶. The plastic mulch degraded by approximately 20% and 15% within 12 months in Knoxville Mountain and Vernon, respectively¹⁵⁶. Another study¹⁵⁷ investigated the degradation of biodegradable plastics in soil across Japan. The study sites were mostly located in a temperate zone with humid subtropical climate. They also reported that the degradation of different biodegradable plastics is highly dependent on plastic type, climate conditions, and soil properties. The study showed that poly-(3-hydroxy-butylate-valerate) (PHB/V) degraded by 52% within 12 months; poly-(ϵ -caprolactone) (PCL): mean of 52%; PBS:26%; and PBSA: mean of 59%^{20,157}.

Implication of PBSA degradation processes to improve the use in agriculture and the plastic waste management

The findings from the biodegradation of PBSA plastic in agricultural soils greatly contribute to the current knowledge on plastic degradation, as most of the previous publicly available studies were based on laboratory experiments. Here, my experiments revealed that PBSA plastic can be degraded under agricultural soil conditions in temperate zones, where the annual mean temperature is relatively low (mean temperature of 6–9.7°C) ^{20,155} and the precipitation is less than that in the sub/tropical zone. I found similar patterns of the important fungal decomposers that degrade PBSA in different ecosystems (agriculture and forest) as well as in laboratory conditions and their interaction patterns with N₂-fixing bacteria or fertilizer ^{20,21,113,155,158}. This finding can improve plastic degradation, which can help with waste management and pollution problems. Nevertheless, the enrichment of fungal plant pathogens during PBSA degradation is alarming, as potential economic losses of important crops can be expected if the PBSA is buried under the soils after agricultural use as mulching films ^{146,158}. As observed under real field conditions, only approximately 30% of PBSA was degraded after one year of exposure. Thus, the strategy of burying mulch films after each season to save cost and labor may lead to the accumulation of biodegradable plastics in soil over time. Together with the interaction with fertilizer, fungal plant pathogens accumulate in the agricultural soils where the farmer grows their crops. Thus, the findings of this dissertation suggest that first, the development of biodegradable plastics should be further processed to find suitable materials for producing biodegradable plastics with less attraction to plant pathogens and less plastic accumulation once plowed under. Second, until the first suggestion is realized, biodegradable plastic waste should be collected for recycling, incineration, or degradation in landfills.

2.5. CONCLUSION

This comprehensive dissertation investigated the biodegradation of different biopolymers (leaf litter, deadwood, and bio-based and biodegradable plastics) in different ecosystems (temperate mixed forest, agricultural sites, and laboratory). Therefore, I verified the overall hypothesis (i)

that fungi are the main decomposers that decompose different biopolymers due to their abundance and ability to secrete enzyme-degrading biopolymers. I also found evidence that N₂-fixing bacteria commonly co-occurred in decomposing substrates, performed a statistical co-occurrence network, built relationships with fungi, and fixed atmospheric N. Nevertheless, substantial amounts of bacterial saprotrophs have been found in different biopolymers. This indicates that besides fungi, bacterial saprotrophs also participate in the decomposition processes. In all studies, I found that these microbial community compositions significantly corresponded with environmental factors (especially tree species, tree mycorrhizal association types, soil pH, and soil moisture) and substrate nutrients (especially C, N, and Ca content). Tree species have characteristics such as tree physiology, leaf morphology, and different nutrient traits that shape the microbial community composition. Root-mycorrhizal association benefits the tree species in terms of nutrient acquisition through the mycorrhizal mycelium. Depending on the type of mycorrhizal that the trees associate with, the method of acquiring nutrients from the environment and the type of nutrients that the tree achieves will differ. While ectomycorrhizal fungi acquire nutrients in organic form, arbuscular mycorrhizal fungi directly uptake nutrients in inorganic form. Soil pH and moisture are important for the mobility of living cells and nutrient availability. Another factor identified in this dissertation that was important in shaping the microbial community was the nutrient traits of the substrates. Microbes need both macro- and micronutrients for their living, growth, and reproduction. Carbon and N are the backbones of macromolecules, such as proteins, amino acids, and nucleic acids. They are also important for producing enzymes that microbes produce and secrete to decompose the substrates. Thus, I verified the overall hypothesis (ii) that macronutrients and tree species have an impact on microbial community composition and thus the decomposition processes of different biopolymers, in addition to current knowledge.

The research in this comprehensive dissertation contributes greatly to our current knowledge of leaf litter, deadwood decomposition, and PBSA degradation in various ecosystems. The collective results led to the general conclusion that the decomposition rates of plant material and PBSA are highly linked to the presence of white rot (for example, *Mycena*) and plastic-degrading fungi (e.g., *Tetracladium* and *F. solani*), respectively. N₂-fixing bacteria (e.g., *Sphingomonas*) facilitate the fungal decomposition of plant material and PBSA, and the interaction between N₂-fixing bacteria and fungi has been observed in various ecosystems, including agricultural and forest ecosystems, under laboratory conditions. Microbial community assembly analyses showed an important contribution to stochasticity in different habitats than previously expected. Overall, this comprehensive dissertation significantly expands our knowledge and understanding of how the interaction between different microbial kingdoms (especially N₂-fixing bacteria and fungi) occurs, and which community assembly processes govern the microbial community in different habitats and ecosystems. Future studies on leaf litter should employ immunocapture or other high-resolution molecular techniques to capture metabolically active microbes during leaf litter decomposition. Future research on plastic degradation could include other types of bio-based and/or biodegradable plastics (such as PBS, PBAT, Plastarch, and PHA) to draw a more comprehensive conclusion on the degradation of bio-based and/or biodegradable plastics, as the production of these four plastics accounts for more than 70% of the global biodegradable plastic production capacities.

2.6. References

1. Lindow, S. E. & Leveau, J. H. J. Phyllosphere microbiology. *Current Opinion in Biotechnology* **13**, 238–243 (2002).
2. Bar-On, Y. M., Phillips, R. & Milo, R. The biomass distribution on Earth. *Proceedings of the National Academy of Sciences* **115**, 6506–6511 (2018).
3. Purahong, W. *et al.* Life in leaf litter: novel insights into community dynamics of bacteria and fungi during litter decomposition. *Mol. Ecol.* **25**, 4059–4074 (2016).
4. Hoppe, B. *et al.* Linking molecular deadwood-inhabiting fungal diversity and community dynamics to ecosystem functions and processes in Central European forests. *Fungal Diversity* **77**, 367–379 (2016).
5. Ma, X., Razavi, B. S., Holz, M., Blagodatskaya, E. & Kuzyakov, Y. Warming increases hotspot areas of enzyme activity and shortens the duration of hot moments in the root-detritusphere. *Soil Biology and Biochemistry* **107**, 226–233 (2017).
6. Bojko, O. & Kabala, C. Organic carbon pools in mountain soils — Sources of variability and predicted changes in relation to climate and land use changes. *CATENA* **149**, 209–220 (2017).
7. Vergutz, L., Manzoni, S., Porporato, A., Novais, R. F. & Jackson, R. B. Global resorption efficiencies and concentrations of carbon and nutrients in leaves of terrestrial plants. *Ecological Monographs* **82**, 205–220 (2012).
8. Giweta, M. Role of litter production and its decomposition, and factors affecting the processes in a tropical forest ecosystem: a review. *Journal of Ecology and Environment* **44**, 11 (2020).
9. Freschet, G. T., Cornelissen, J. H. C., van Logtestijn, R. S. P. & Aerts, R. Substantial nutrient resorption from leaves, stems and roots in a subarctic flora: what is the link with other resource economics traits? *New Phytologist* **186**, 879–889 (2010).
10. Aerts, R. & de Caluwe, H. Nutritional and plant-mediated controls on leaf litter decomposition of *Carex* Species. *Ecology* **78**, 244 (1997).
11. Hobbie, S. E. Plant species effects on nutrient cycling: revisiting litter feedbacks. *Trends in Ecology & Evolution* **30**, 357–363 (2015).
12. Purahong, W. *et al.* Determinants of deadwood-inhabiting fungal communities in temperate forests: Molecular evidence from a large scale deadwood decomposition experiment. *Front. Microbiol.* **9**, (2018).
13. Floudas, D. *et al.* The Paleozoic origin of enzymatic lignin decomposition reconstructed from 31 fungal genomes. *Science* **336**, 1715–1719 (2012).
14. Krishna, M. P. & Mohan, M. Litter decomposition in forest ecosystems: a review. *Energ. Ecol. Environ.* **2**, 236–249 (2017).
15. Kembel, S. W. *et al.* Relationships between phyllosphere bacterial communities and plant functional traits in a neotropical forest. *Proceedings of the National Academy of Sciences* **111**, 13715–13720 (2014).
16. Jamieson, A. J. *et al.* Microplastics and synthetic particles ingested by deep-sea amphipods in six of the deepest marine ecosystems on Earth. *R Soc Open Sci* **6**, 180667 (2019).
17. Liu, E. K., He, W. Q. & Yan, C. R. 'White revolution' to 'white pollution'—agricultural plastic film mulch in China. *Environ. Res. Lett.* **9**, 091001 (2014).
18. Geyer, R., Jambeck, J. R. & Law, K. L. Production, use, and fate of all plastics ever made. *Science Advances* **3**, e1700782 (2017).
19. Ukaogo, P. O., Ewuzie, U. & Onwuka, C. V. 21 - Environmental pollution: causes, effects, and the remedies. in *Microorganisms for Sustainable Environment and Health* (eds. Chowdhary, P., Raj, A., Verma, D. & Akhter, Y.) 419–429 (Elsevier, 2020). doi:10.1016/B978-0-12-819001-2.00021-8.
20. Purahong, W. *et al.* Back to the future: decomposability of a biobased and biodegradable plastic in field soil environments and its microbiome under ambient and future climates. *Environ. Sci. Technol.* **55**, 12337–12351 (2021).
21. Tanunchai, B. *et al.* Analysis of microbial populations in plastic–soil systems after exposure to high poly(butylene succinate-co-adipate) load using high-resolution molecular technique. *Environmental Sciences Europe* **33**, 105 (2021).

22. Emadian, S. M., Onay, T. T. & Demirel, B. Biodegradation of bioplastics in natural environments. *Waste Management* **59**, 526–536 (2017).
23. Brizga, J., Hubacek, K. & Feng, K. The unintended side effects of bioplastics: carbon, land, and water footprints. *One Earth* **3**, 45–53 (2020).
24. Corradini, F. *et al.* Evidence of microplastic accumulation in agricultural soils from sewage sludge disposal. *Science of The Total Environment* **671**, 411–420 (2019).
25. Allen, S. *et al.* Atmospheric transport and deposition of microplastics in a remote mountain catchment. *Nat. Geosci.* **12**, 339–344 (2019).
26. Browne, M. A. *et al.* Accumulation of microplastic on shorelines worldwide: Sources and sinks. *Environ. Sci. Technol.* **45**, 9175–9179 (2011).
27. Corradini, F. *et al.* Evidence of microplastic accumulation in agricultural soils from sewage sludge disposal. *Science of The Total Environment* **671**, 411–420 (2019).
28. Bosker, T., Bouwman, L. J., Brun, N. R., Behrens, P. & Vijver, M. G. Microplastics accumulate on pores in seed capsule and delay germination and root growth of the terrestrial vascular plant *Lepidium sativum*. *Chemosphere* **226**, 774–781 (2019).
29. Duis, K. & Coors, A. Microplastics in the aquatic and terrestrial environment: sources (with a specific focus on personal care products), fate and effects. *Environmental Sciences Europe* **28**, 2 (2016).
30. de Sá, L. C., Oliveira, M., Ribeiro, F., Rocha, T. L. & Futter, M. N. Studies of the effects of microplastics on aquatic organisms: What do we know and where should we focus our efforts in the future? *Science of The Total Environment* **645**, 1029–1039 (2018).
31. Issac, M. N. & Kandasubramanian, B. Effect of microplastics in water and aquatic systems. *Environ Sci Pollut Res* **28**, 19544–19562 (2021).
32. Lin, D. *et al.* Microplastics negatively affect soil fauna but stimulate microbial activity: insights from a field-based microplastic addition experiment. *Proceedings of the Royal Society B: Biological Sciences* **287**, 20201268 (2020).
33. Boots, B., Russell, C. W. & Green, D. S. Effects of microplastics in soil ecosystems: above and below ground. *Environ. Sci. Technol.* **53**, 11496–11506 (2019).
34. Babu, R. P., O’Connor, K. & Seeram, R. Current progress on bio-based polymers and their future trends. *Prog Biomater* **2**, 8 (2013).
35. Iwata, T. Biodegradable and bio-based polymers: Future prospects of eco-friendly plastics. *Angewandte Chemie International Edition* **54**, 3210–3215 (2015).
36. Zumstein, M. T. *et al.* Biodegradation of synthetic polymers in soils: Tracking carbon into CO₂ and microbial biomass. *Science Advances* **4**, eaas9024 (2018).
37. Gigli, M. *et al.* Influence of chemical and architectural modifications on the enzymatic hydrolysis of poly(butylene succinate). *Green Chem.* **14**, 2885–2893 (2012).
38. Haider, T. P., Völker, C., Kramm, J., Landfester, K. & Wurm, F. R. Plastics of the future? The impact of biodegradable polymers on the environment and on society. *Angewandte Chemie International Edition* **58**, 50–62 (2019).
39. Lambert, S. & Wagner, M. Environmental performance of bio-based and biodegradable plastics: the road ahead. *Chem. Soc. Rev.* **46**, 6855–6871 (2017).
40. Wang, L., Zhang, M., Lawson, T., Kanwal, A. & Miao, Z. Poly(butylene succinate-co-salicylic acid) copolymers and their effect on promoting plant growth. *Royal Society Open Science* **6**, 190504.
41. Sedaghat, M., Tahmasebi-Sarvestani, Z., Emam, Y. & Mokhtassi-Bidgoli, A. Physiological and antioxidant responses of winter wheat cultivars to strigolactone and salicylic acid in drought. *Plant Physiology and Biochemistry* **119**, 59–69 (2017).
42. Horton, A. A., Walton, A., Spurgeon, D. J., Lahive, E. & Svendsen, C. Microplastics in freshwater and terrestrial environments: Evaluating the current understanding to identify the knowledge gaps and future research priorities. *Sci. Total Environ.* **586**, 127–141 (2017).
43. Palsikowski, P. A. *et al.* Ecotoxicity evaluation of the biodegradable polymers PLA, PBAT and its blends using *Allium cepa* as test organism. *J Polym Environ* **26**, 938–945 (2018).
44. El-Dawy, E. G. A. E. M., Gherbawy, Y. A. & Hussein, M. A. Morphological, molecular characterization, plant pathogenicity and biocontrol of *Cladosporium* complex groups associated with faba beans. *Sci Rep* **11**, 14183 (2021).

45. Coleman, J. J. The *Fusarium solani* species complex: ubiquitous pathogens of agricultural importance. *Molecular Plant Pathology* **17**, 146–158 (2016).
46. Kamiya, M., Asakawa, S. & Kimura, M. Molecular analysis of fungal communities of biodegradable plastics in two Japanese soils. *Soil Science and Plant Nutrition* **53**, 568–574 (2007).
47. Berg, B. Litter decomposition and organic matter turnover in northern forest soils. *Forest Ecology and Management* **133**, 13–22 (2000).
48. Purahong, W. *et al.* Characterization of unexplored deadwood mycobiome in highly diverse subtropical forests using culture-independent molecular technique. *Front. Microbiol.* **8**, (2017).
49. Keller, A. B. & Phillips, R. P. Leaf litter decay rates differ between mycorrhizal groups in temperate, but not tropical, forests. *New Phytologist* **222**, 556–564 (2019).
50. Seyfried, G. S., Dalling, J. W. & Yang, W. H. Mycorrhizal type effects on leaf litter decomposition depend on litter quality and environmental context. *Biogeochemistry* **155**, 21–38 (2021).
51. Bonfante, P. & Genre, A. Mechanisms underlying beneficial plant–fungus interactions in mycorrhizal symbiosis. *Nat Commun* **1**, 48 (2010).
52. Jacobs, L. M., Sulman, B. N., Brzostek, E. R., Feighery, J. J. & Phillips, R. P. Interactions among decaying leaf litter, root litter and soil organic matter vary with mycorrhizal type. *Journal of Ecology* **106**, 502–513 (2018).
53. Mieszkin, S. *et al.* Oak decaying wood harbors taxonomically and functionally different bacterial communities in sapwood and heartwood. *Soil Biology and Biochemistry* **155**, 108160 (2021).
54. Wahdan, S. F. M. *et al.* Targeting the active rhizosphere microbiome of *Trifolium pratense* in grassland evidences a stronger-than-expected belowground biodiversity-ecosystem functioning link. *Front. Microbiol.* **12**, (2021).
55. Schneider, T. *et al.* Who is who in litter decomposition? Metaproteomics reveals major microbial players and their biogeochemical functions. *ISME J* **6**, 1749–1762 (2012).
56. Riley, R. *et al.* Extensive sampling of basidiomycete genomes demonstrates inadequacy of the white-rot/brown-rot paradigm for wood decay fungi. *Proceedings of the National Academy of Sciences* **111**, 9923–9928 (2014).
57. Liers, C., Arnstadt, T., Ullrich, R. & Hofrichter, M. Patterns of lignin degradation and oxidative enzyme secretion by different wood- and litter-colonizing basidiomycetes and ascomycetes grown on beech-wood. *FEMS Microbiology Ecology* **78**, 91–102 (2011).
58. Arantes, V. & Goodell, B. Current understanding of brown-rot fungal biodegradation mechanisms: A review. in *Deterioration and Protection of Sustainable Biomaterials* vol. 1158 3–21 (American Chemical Society, 2014).
59. German, D. P. *et al.* Optimization of hydrolytic and oxidative enzyme methods for ecosystem studies. *Soil Biology and Biochemistry* **43**, 1387–1397 (2011).
60. Chamas, A. *et al.* Degradation rates of plastics in the environment. *ACS Sustainable Chem. Eng.* **8**, 3494–3511 (2020).
61. Han, Y. *et al.* Soil type driven change in microbial community affects poly(butylene adipate-co-terephthalate) degradation potential. *Environ. Sci. Technol.* (2021) doi:10.1021/acs.est.0c04850.
62. Rajala, T., Peltoniemi, M., Pennanen, T. & Mäkipää, R. Fungal community dynamics in relation to substrate quality of decaying Norway spruce (*Picea abies* [L.] Karst.) logs in boreal forests. *FEMS Microbiol Ecol* **81**, 494–505 (2012).
63. Arce, M. I. *et al.* Drying and rainfall shape the structure and functioning of nitrifying microbial communities in riverbed sediments. *Frontiers in Microbiology* **9**, (2018).
64. Oberle, B. *et al.* Accurate forest projections require long-term wood decay experiments because plant trait effects change through time. *Global Change Biology* **26**, 864–875 (2020).
65. Gewert, B., Plassmann, M. M. & MacLeod, M. Pathways for degradation of plastic polymers floating in the marine environment. *Environ. Sci.: Processes Impacts* **17**, 1513–1521 (2015).
66. Jansson, J. K. & Hofmockel, K. S. Soil microbiomes and climate change. *Nat Rev Microbiol* **18**, 35–46 (2020).
67. Bellard, C., Bertelsmeier, C., Leadley, P., Thuiller, W. & Courchamp, F. Impacts of climate change on the future of biodiversity. *Ecology Letters* **15**, 365–377 (2012).
68. Wahdan, S. F. M., Buscot, F. & Purahong, W. Future climate alters pathogens-microbiome co-occurrence networks in wheat straw residues during decomposition. *Proceedings* **66**, 22 (2021).

69. Siebert, J., Ciobanu, M., Schädler, M. & Eisenhauer, N. Climate change and land use induce functional shifts in soil nematode communities. *Oecologia* **192**, 281–294 (2020).
70. Grimm, N. B. *et al.* The impacts of climate change on ecosystem structure and function. *Frontiers in Ecology and the Environment* **11**, 474–482 (2013).
71. Cavicchioli, R. *et al.* Scientists’ warning to humanity: microorganisms and climate change. *Nat Rev Microbiol* **17**, 569–586 (2019).
72. Melillo, J. M. *et al.* Long-term pattern and magnitude of soil carbon feedback to the climate system in a warming world. *Science* **358**, 101–105 (2017).
73. Martiny, J. B. H., Eisen, J. A., Penn, K., Allison, S. D. & Horner-Devine, M. C. Drivers of bacterial β -diversity depend on spatial scale. *Proceedings of the National Academy of Sciences* **108**, 7850–7854 (2011).
74. Ramette, A. & Tiedje, J. M. Multiscale responses of microbial life to spatial distance and environmental heterogeneity in a patchy ecosystem. *Proceedings of the National Academy of Sciences* **104**, 2761–2766 (2007).
75. Zhou, J. & Ning, D. Stochastic community assembly: Does it matter in microbial ecology? *Microbiol. Mol. Biol. Rev.* **81**, e00002-17 (2017).
76. Chesson, P. Mechanisms of maintenance of species diversity. *Annual Review of Ecology and Systematics* **31**, 343–366 (2000).
77. Fargione, J., Brown, C. S. & Tilman, D. Community assembly and invasion: An experimental test of neutral versus niche processes. *Proc Natl Acad Sci U S A* **100**, 8916–8920 (2003).
78. Bell, T. Experimental tests of the bacterial distance–decay relationship. *ISME J* **4**, 1357–1365 (2010).
79. Condit, R. *et al.* Beta-diversity in tropical forest trees. *Science* **295**, 666–669 (2002).
80. Junker, R. R., He, X., Otto, J.-C., Ruiz-Hernández, V. & Hanusch, M. Divergent assembly processes? A comparison of the plant and soil microbiome with plant communities in a glacier forefield. *FEMS Microbiology Ecology* **97**, fiab135 (2021).
81. Zhang, H. *et al.* Wheat yellow mosaic enhances bacterial deterministic processes in a plant-soil system. *Science of The Total Environment* **812**, 151430 (2022).
82. Li, C. *et al.* The ecology of the plastisphere: Microbial composition, function, assembly, and network in the freshwater and seawater ecosystems. *Water Research* **202**, 117428 (2021).
83. Ju, Z. *et al.* The succession of bacterial community attached on biodegradable plastic mulches during the degradation in soil. *Frontiers in Microbiology* **12**, (2021).
84. Sun, Y. *et al.* Contribution of stochastic processes to the microbial community assembly on field-collected microplastics. *Environmental Microbiology* **23**, 6707–6720 (2021).
85. Dini-Andreote, F., Stegen, J. C., van Elsas, J. D. & Salles, J. F. Disentangling mechanisms that mediate the balance between stochastic and deterministic processes in microbial succession. *Proceedings of the National Academy of Sciences* **112**, E1326–E1332 (2015).
86. Nemergut, D. R. *et al.* Patterns and processes of microbial community assembly. *Microbiology and Molecular Biology Reviews* **77**, 342–356 (2013).
87. Montoya, J. M., Pimm, S. L. & Solé, R. V. Ecological networks and their fragility. *Nature* **442**, 259–264 (2006).
88. Muszynski, S., Maurer, F., Henjes, S., Horn, M. A. & Noll, M. Fungal and bacterial diversity patterns of two diversity levels retrieved from a late decaying *Fagus sylvatica* under two temperature regimes. *Front. Microbiol.* **11**, (2020).
89. Olesen, J. M., Bascompte, J., Dupont, Y. L. & Jordano, P. The modularity of pollination networks. *PNAS* **104**, 19891–19896 (2007).
90. Ji, L., Tanunchai, B., Wahdan, S. F. M., Schädler, M. & Purahong, W. Future climate change enhances the complexity of plastisphere microbial co-occurrence networks, but does not significantly affect the community assembly. *Science of The Total Environment* 157016 (2022) doi:10.1016/j.scitotenv.2022.157016.
91. Allali, I. *et al.* A comparison of sequencing platforms and bioinformatics pipelines for compositional analysis of the gut microbiome. *BMC Microbiology* **17**, 194 (2017).
92. Quail, M. A. *et al.* A tale of three next generation sequencing platforms: comparison of Ion Torrent, Pacific Biosciences and Illumina MiSeq sequencers. *BMC Genomics* **13**, 341 (2012).

93. Shao, K. *et al.* Illumina sequencing revealed soil microbial communities in a Chinese alpine grassland. *Geomicrobiology Journal* **36**, 204–211 (2019).
94. Tanunchai, B. *et al.* FungalTraits vs. FUNGuild: comparison of ecological functional assignments of leaf- and needle-associated fungi across 12 temperate tree species. *Microb Ecol* (2022) doi:10.1007/s00248-022-01973-2.
95. Purahong, W. *et al.* Cross-kingdom interactions and functional patterns of active microbiota matter in governing deadwood decay. *Proceedings of the Royal Society B: Biological Sciences* **289**, 20220130 (2022).
96. Sequencing Platforms | Compare NGS platform applications & specifications. <https://emea.illumina.com/systems/sequencing-platforms.html>.
97. Triebel, D., Peršoh, D., Nash, T. H., Zedda, L. & Rambold, G. LIAS — An interactive database system for structured descriptive data of Ascomycetes. in *Biodiversity Databases* (CRC Press, 2007).
98. Rambold, G. *et al.* Geographic heat maps of lichen traits derived by combining LIAS light description and GBIF occurrence data, provided on a new platform. *Biodivers Conserv* **25**, 2743–2751 (2016).
99. Agerer R. & Rambold G. DEEMY – An information system for characterization and determination of ectomycorrhizae. [first posted on 2004-06-01; most recent update: 2011-01-10]. *DEEMY* www.deemy.de (2021).
100. Zanne, A. E. *et al.* Fungal functional ecology: bringing a trait-based approach to plant-associated fungi. *Biological Reviews* **95**, 409–433 (2020).
101. Guerreiro, M. A., Wijayawardene, N., Hyde, K. & Peršoh, D. Ecology of Ascomycete genera – A searchable compilation of “Notes on genera: Ascomycota”. *Asian Journal of Mycology* **1**, 146–150 (2018).
102. Nguyen, N. H. *et al.* FUNGuild: An open annotation tool for parsing fungal community datasets by ecological guild. *Fungal Ecology* **20**, 241–248 (2016).
103. Jayasiri, S. C. *et al.* The Faces of Fungi database: fungal names linked with morphology, phylogeny and human impacts. *Fungal Diversity* **74**, 3–18 (2015).
104. Pölme, S. *et al.* FungalTraits: a user-friendly traits database of fungi and fungus-like stramenopiles. *Fungal Divers.* **105**, 1–16 (2020).
105. Probst, M., Ascher-Jenull, J., Insam, H. & Gómez-Brandón, M. The molecular information about deadwood bacteriomes partly depends on the targeted environmental DNA. *Frontiers in Microbiology* **12**, 825 (2021).
106. Bowsher, A. W., Kearns, P. J. & Shade, A. 16S rRNA/rRNA gene ratios and cell activity staining reveal consistent patterns of microbial activity in plant-associated soil. *mSystems* **4**, e00003-19 (2019).
107. Urbach, E., Vergin, K. L. & Giovannoni, S. J. Immunochemical detection and isolation of DNA from metabolically active bacteria. *Appl Environ Microbiol* **65**, 1207–1213 (1999).
108. Borneman, J. Culture-independent identification of microorganisms that respond to specified stimuli. *Applied and Environmental Microbiology* **65**, 3398–3400 (1999).
109. Hellman, M., Berg, J., Brandt, K. K. & Hallin, S. Survey of bromodeoxyuridine uptake among environmental bacteria and variation in uptake rates in a taxonomically diverse set of bacterial isolates. *Journal of Microbiological Methods* **86**, 376–378 (2011).
110. Holland, P. M., Abramson, R. D., Watson, R. & Gelfand, D. H. Detection of specific polymerase chain reaction product by utilizing the 5'----3' exonuclease activity of *Thermus aquaticus* DNA polymerase. *Proceedings of the National Academy of Sciences* **88**, 7276–7280 (1991).
111. Kralik, P. & Ricchi, M. A Basic Guide to real time PCR in microbial diagnostics: Definitions, parameters, and everything. *Frontiers in Microbiology* **8**, (2017).
112. Tajadini, M., Panjehpour, M. & Javanmard, S. H. Comparison of SYBR Green and TaqMan methods in quantitative real-time polymerase chain reaction analysis of four adenosine receptor subtypes. *Adv Biomed Res* **3**, 85 (2014).
113. Tanunchai, B. *et al.* Nitrogen fixing bacteria facilitate microbial biodegradation of a bio-based and biodegradable plastic in soils under ambient and future climatic conditions. *Environ. Sci.: Processes Impacts* **24**, 233–241 (2022).

114. Purahong, W. *et al.* Life on the rocks: First insights into the microbiota of the threatened aquatic rheophyte *Hansenella heterophylla*. *Front. Plant Sci.* **12**, (2021).
115. Klindworth, A. *et al.* Evaluation of general 16S ribosomal RNA gene PCR primers for classical and next-generation sequencing-based diversity studies. *Nucleic Acids Res* **41**, e1 (2013).
116. Poly, F., Monrozier, L. J. & Bally, R. Improvement in the RFLP procedure for studying the diversity of *nifH* genes in communities of nitrogen fixers in soil. *Research in Microbiology* **152**, 95–103 (2001).
117. Kellner, H. *et al.* Widespread occurrence of expressed fungal secretory peroxidases in forest soils. *PLoS ONE* **9**, e95557 (2014).
118. Moorhead, D. L., Sinsabaugh, R. L., Hill, B. H. & Weintraub, M. N. Vector analysis of ecoenzyme activities reveal constraints on coupled C, N and P dynamics. *Soil Biology and Biochemistry* **93**, 1–7 (2016).
119. Marx, M.-C., Wood, M. & Jarvis, S. C. A microplate fluorimetric assay for the study of enzyme diversity in soils. *Soil Biology and Biochemistry* **33**, 1633–1640 (2001).
120. Rinne, K. T. *et al.* Accumulation rates and sources of external nitrogen in decaying wood in a Norway spruce dominated forest. *Funct Ecol* n/a-n/a (2016) doi:10.1111/1365-2435.12734.
121. Hoppe, B. *et al.* Network analysis reveals ecological links between N-fixing bacteria and wood-decaying fungi. *PLoS ONE* **9**, e88141 (2014).
122. Arie, T. *Fusarium* diseases of cultivated plants, control, diagnosis, and molecular and genetic studies. *J Pestic Sci* **44**, 275–281 (2019).
123. Karim, N. F. A., Mohd, M., Nor, N. M. I. M. & Zakaria, L. Saprophytic and potentially pathogenic *Fusarium* species from peat soil in Perak and Pahang. *Trop Life Sci Res* **27**, 1–20 (2016).
124. Bayandala, Fukasawa, Y. & Seiwa, K. Roles of pathogens on replacement of tree seedlings in heterogeneous light environments in a temperate forest: a reciprocal seed sowing experiment. *Journal of Ecology* **104**, 765–772 (2016).
125. Funk, A. & Dorworth, C. E. *Mycosphaerella mycopappi* sp.nov. and its anamorphs on leaves of *Acer macrophyllum*. *Can. J. Bot.* **66**, 295–297 (1988).
126. Wolf, F. A. & Davidson, R. W. Life cycle of *Piggotia fraxini*, causing leaf disease of ash. *Mycologia* **33**, 526–539 (1941).
127. Burke, D. J., Hoke, A. J. & Koch, J. The emergence of beech leaf disease in Ohio: Probing the plant microbiome in search of the cause. *Forest Pathology* **50**, e12579 (2020).
128. Bernadovičová, S. & Ivanová, H. Leaf spot disease on *Tilia cordata* caused by the fungus *Cercospora microsora*. *Biologia* **63**, 44–49 (2008).
129. Chinan, V.-C. & Mânzu, C. C. First report of *Erysiphe arcuata* on *Carpinus betulus* in Romania. *J Plant Pathol* **103**, 405–405 (2021).
130. Anthony, P. A., Holtum, J. A. M. & Jackes, B. R. Shade acclimation of rainforest leaves to colonization by lichens. *Functional Ecology* **16**, 808–816 (2002).
131. Liba, C. m. *et al.* Nitrogen-fixing chemo-organotrophic bacteria isolated from cyanobacteria-deprived lichens and their ability to solubilize phosphate and to release amino acids and phytohormones. *Journal of Applied Microbiology* **101**, 1076–1086 (2006).
132. Grube, M., Cardinale, M., de Castro, J. V., Müller, H. & Berg, G. Species-specific structural and functional diversity of bacterial communities in lichen symbioses. *ISME J* **3**, 1105–1115 (2009).
133. Grimm, M. *et al.* The lichens' microbiota, still a mystery? *Frontiers in Microbiology* **12**, 714 (2021).
134. Palmqvist, K. Tansley review no. 117. carbon economy in lichens. *The New Phytologist* **148**, 11–36 (2000).
135. Potkay, A. *et al.* Water and vapor transport in algal-fungal lichen: Modeling constrained by laboratory experiments, an application for *Flavoparmelia caperata*. *Plant, Cell & Environment* **43**, 945–964 (2020).
136. Prescott, L., Harley, J. & Klein, D. *Microbiology*. (McGraw-Hill Higher Education, 1999).
137. Purahong, W. *et al.* Effects of forest management practices in temperate beech forests on bacterial and fungal communities involved in leaf litter degradation. *Microb Ecol* **69**, 905–913 (2015).
138. Miyamoto, T., Igarashi, T. & Takahashi, K. Lignin-degrading ability of litter-decomposing basidiomycetes from *Picea* forests of Hokkaido. *Mycoscience* **41**, 105–110 (2000).

139. Kellner, H. *et al.* Widespread occurrence of expressed fungal secretory peroxidases in forest soils. *PLoS ONE* **9**, e95557 (2014).
140. de Gonzalo, G., Colpa, D. I., Habib, M. H. M. & Fraaije, M. W. Bacterial enzymes involved in lignin degradation. *Journal of Biotechnology* **236**, 110–119 (2016).
141. Dantur, K. I., Enrique, R., Welin, B. & Castagnaro, A. P. Isolation of cellulolytic bacteria from the intestine of *Diatraea saccharalis* larvae and evaluation of their capacity to degrade sugarcane biomass. *AMB Express* **5**, (2015).
142. Hryniewicz, K., Baum, C. & Leinweber, P. Density, metabolic activity, and identity of cultivable rhizosphere bacteria on *Salix viminalis* in disturbed arable and landfill soils. *Journal of Plant Nutrition and Soil Science* **173**, 747–756 (2010).
143. Tláškal, V. & Baldrian, P. Deadwood-Inhabiting bacteria show adaptations to changing carbon and nitrogen availability during decomposition. *Frontiers in Microbiology* **12**, (2021).
144. Xie, C.-H. & Yokota, A. *Sphingomonas azotifigens* sp. nov., a nitrogen-fixing bacterium isolated from the roots of *Oryza sativa*. *Int J Syst Evol Microbiol* **56**, 889–893 (2006).
145. Kostka, J. E. *et al.* Genome sequences for six *Rhodanobacter* strains, isolated from soils and the terrestrial subsurface, with variable denitrification capabilities. *J Bacteriol* **194**, 4461–4462 (2012).
146. Kantida Juncheed *et al.* Dark side of a bio-based and biodegradable plastic? Assessment of pathogenic microbes associated with poly(butylene succinate-co-adipate) under ambient and future climates using next generation sequencing. *Front. Plant Sci.* doi:doi:10.3389/fpls.2022.966363.
147. Chauhan, R. Nitrogen sources and trace elements influence laccase and peroxidase enzymes activity of *Grammothele fuligo*. *Vegetos* **32**, 316–323 (2019).
148. Fickers, P., Nicaud, J. m., Gaillardin, C., Destain, J. & Thonart, P. Carbon and nitrogen sources modulate lipase production in the yeast *Yarrowia lipolytica*. *Journal of Applied Microbiology* **96**, 742–749 (2004).
149. Brandes, B., Godbold, D. L., Kuhn, A. J. & Jentschke, G. Nitrogen and phosphorus acquisition by the mycelium of the ectomycorrhizal fungus *Paxillus involutus* and its effect on host nutrition. *The New Phytologist* **140**, 735–743 (1998).
150. Mus, F. *et al.* Symbiotic nitrogen fixation and the challenges to its extension to nonlegumes. *Applied and Environmental Microbiology* **82**, 3698–3710 (2016).
151. Roper, M. M. & Gupta, V. V. S. R. Enhancing non-symbiotic N fixation in agriculture. *The Open Agriculture Journal* **10**, (2016).
152. Foght, J. Nitrogen fixation and hydrocarbon-oxidizing bacteria. in *Handbook of Hydrocarbon and Lipid Microbiology* (ed. Timmis, K. N.) 1661–1668 (Springer, 2010). doi:10.1007/978-3-540-77587-4_117.
153. Kurt, Ş., Uysal, A., Soyly, E. M., Kara, M. & Soyly, S. Characterization and pathogenicity of *Fusarium solani* associated with dry root rot of citrus in the eastern Mediterranean region of Turkey. *J Gen Plant Pathol* **86**, 326–332 (2020).
154. Abney, T. S., Richards, T. L. & Roy, K. W. *Fusarium solani* from ascospores of *Nectria haematococca* causes sudden death syndrome of soybean. *Mycologia* **85**, 801–806 (1993).
155. Tanunchai, B. *et al.* Fate of a biodegradable plastic in forest soil: Dominant tree species and forest types drive changes in microbial community assembly, influence the composition of plastisphere, and affect poly(butylene succinate-co-adipate) degradation. *Science of The Total Environment* **873**, 162230 (2023).
156. Sintim, H. Y. *et al.* In situ degradation of biodegradable plastic mulch films in compost and agricultural soils. *Sci Total Environ* **727**, 138668 (2020).
157. Hoshino, A. *et al.* Influence of weather conditions and soil properties on degradation of biodegradable plastics in soil. *Soil Sci. Plant Nutr.* **47**, 35–43 (2001).
158. Scheid, S.-M. *et al.* Interactions Between high load of a bio-based and biodegradable plastic and nitrogen fertilizer affect plant biomass and health: A case study with *Fusarium solani* and mung bean (*Vigna radiata* L.). *J. Polym. Environ.* **30**, 3534–3544 (2022).

3. DECLARATION OF CONTRIBUTION AND PUBLICATIONS

Litter 1: FungalTraits vs. FUNGuild: Comparison of ecological functional assignments of leaf- and needle-associated fungi across 12 temperate tree species (page 52 – 70)

Author: **Benjawan Tanunchai***, Li Ji*, Simon Andreas Schroeter, Sara Fareed Mohamed Wahdan, Shakhawat Hossen, Yoseph Deleegn, François Buscot, Ann-Sophie Lehnert, Eliane Gomes Alves, Ines Hilke, Gerd Gleixner, Ernst-Detlef Schulze, Matthias Noll & Witoon Purahong

*These authors contributed equally to this work.

Status: **Published**

Publication: Microbial Ecology

Publisher: Springer Nature

Date: 5 Feb 2022

IF (2021) = 4.192

Copyright © 2022, The Author(s)

Reprinted with permission from Springer Nature.

Own contribution: samples and metadata collection (60% and 40% were carried out by WP, EDS, SH, SW and YD), DNA analysis: DNA extraction (90% and 10% were carried out by WP and SW), PCR library preparation for sequencing (90% and 10% were carried out by WP and SW), microbial taxonomy and data analyses (80% and 20% were carried out by WP and LJ), visualization (100%), manuscript writing (70% and 30% were carried out by LJ, MN, and WP).

Author Contribution: WP and EDS conceived and designed the study. BT, WP, EDS, SH, YD, and SW collected the samples and metadata. WP and FB contributed reagents and laboratory equipment. BT, WP, and SW led the DNA analysis. SW led bioinformatics. BT, LJ, and WP led the microbial taxonomy and data analyses. SS, IH, GG, ASL, and EGA led the physicochemical analyses. BT, LJ, MN, and WP wrote the manuscript. MN and WP supervised BT. MN, EDS, and FB reviewed and gave comments and suggestions for manuscript. All of the authors gave final approval for manuscript submission.

Litter 2: A poisoned apple: First insights into community assembly and networks of the fungal pathobiome of healthy-looking senescing leaves of temperate trees in mixed forest ecosystem (page 71 – 87)

Author: **Benjawan Tanunchai***, Li Ji*, Simon Andreas Schroeter, Sara Fareed Mohamed Wahdan, Panadda Larpkern, Ann-Sophie Lehnert, Eliane Gomes Alves, Gerd Gleixner, Ernst-Detlef Schulze, Matthias Noll, François Buscot, Witoon Purahong.

*These authors contributed equally to this work.

Status: **Published**

Publication: Frontiers in Plant Science

Publisher: Frontiers Media S.A

Date: 03 November 2022

IF (2021) = 6.627

Copyright © 2022, The Author(s)

Reprinted with permission from Frontiers Media S.A..

Own contribution: samples and metadata collection (60% and 40% were carried out EDS, SW and WP), DNA analysis: DNA extraction (90% and 10% were carried out by SW and WP), PCR library preparation for sequencing (90% and 10% were carried out by SW and WP), microbial taxonomy and data analyses (50% and 50% were carried out by LJ and WP), visualization (70% and 30% were carried out by LJ and WP), manuscript writing (70% and 30% were carried out by LJ and WP).

Author Contribution: WP and E-DS conceived and designed the study. BT, WP, EDS, and SW collected samples and metadata. WP and FB contributed reagents and laboratory equipment. BT, WP, and SW led the DNA analysis. SW led bioinformatics. BT, LJ, and WP led the microbial taxonomy and data analyses. SS, GG, ASL, and EA led the physicochemical analyses. BT, LJ, and WP wrote the manuscript. MN and WP supervised BT. MN, E-DS, PL, and FB reviewed and gave comments and suggestions for manuscript. All authors contributed to the article and approved the submitted version.

Litter 3: More than you can see: Unraveling the ecology and biodiversity of lichenized fungi associated with leaves and needles of 12 temperate tree species using high throughput sequencing. (page 88 – 105)

Author: Benjawan Tanunchai*, Simon Andreas Schroeter*, Li Ji, Sara Fareed Mohamed Wahdan, Shakhawat Hossen, Ann-Sophie Lehnert, Hagen Grünberg, Gerd Gleixner, François Buscot, Ernst-Detlef Schulze, Matthias Noll, Witoon Purahong.

*These authors contributed equally to this work.

Status: Published

Publication: Frontiers in Microbiology

Publisher: Frontiers Media S.A

Date: 16 September 2022

Frontiers in Microbiology, 13.

IF (2021) = 6.064

Copyright © 2022, The Author(s)

Reprinted with permission from Frontiers Media S.A..

Own contribution: samples and metadata collection (60% and 40% were carried out by WP, SS, SH, A-SL, and SW), DNA analysis: DNA extraction (90% and 10% were carried out by WP and SW), PCR library preparation for sequencing (90% and 10% were carried out by WP and SW), microbial taxonomy and data analyses (70% and 30% were carried out by WP

and LJ), visualization (90% and 10% were carried out by WP), manuscript writing (70% and 30% were carried out by SS, MN, and WP).

Author Contribution: WP and E-DS conceived and designed the study. BT, WP, SS, SH, A-SL, and SW collected the samples and metadata. WP and FB contributed reagents and laboratory equipment. BT, WP, and SW led the DNA analysis. SS and GG led the water content and pH measurement. SW led bioinformatics. BT, LJ, and WP led the microbial taxonomy and data analyses. HG performed the fruiting body survey. BT, SS, MN, and WP wrote the manuscript. MN and WP supervised BT. SS, MN, E-DS, and FB reviewed and gave comments and suggestions for the manuscript. All authors gave final approval for manuscript submission.

Litter 4: Tree mycorrhizal type regulates leaf and needle microbial communities, affects microbial assembly and co-occurrence network patterns, and influences litter decomposition rates in temperate forest. (page 106 – 120)

Author: Benjawan Tanunchai*, Li Ji*, Simon Andreas Schroeter, Sara Fareed Mohamed Wahdan, Katikarn Thongsuk, Ann-Sophie Lehnert, Eliane Gomes Alves, Ines Hilke, Gerd Gleixner, François Buscot, Ernst-Detlef Schulze, Matthias Noll, Witoon Purahong.

*These authors contributed equally to this work.

Status: In press, *Frontiers in Plant Science*

IF (2021) = 6.627

Own contribution: experimental set-up (50% and 50% were carried out by WP, SW and EDS), samples and metadata collection (60% and 40% were carried out by LJ, WP, SW, and EDS), DNA analysis: DNA extraction (90% and 10% were carried out by KT and WP), PCR library preparation for sequencing (90% and 10% were carried out by KT and WP), microbial taxonomy and data analyses (70% and 30% were carried out by LJ and WP), visualization (60% and 40% were carried out by LJ and WP), manuscript writing (70% and 30% were carried out by LJ and WP).

Author Contribution: WP and EDS conceived and designed the study. BT, WP, SW and EDS led the experimental set-up. BT, LJ, WP, SW, and EDS collected the samples and metadata. WP, MN, and FB contributed reagents and laboratory equipment. BT, KT and WP led the DNA analysis. SW led bioinformatics. BT, LJ, and WP led the microbial taxonomy, and data analyses. LJ led microbial network and community assembly analyses. SS, IH, GG, ASL, and EGA led the physicochemical analyses. BT, LJ and WP wrote the manuscript. MN and WP supervised BT. MN, AG, EDS, and FB reviewed and gave comments and suggestions for manuscript. All of the authors gave final approval for manuscript submission.

Deadwood 1: Cross-kingdom interactions and functional patterns of active microbiota matter in governing deadwood decay. (page 121 – 131)

Author: Witoon Purahong*, **Benjawan Tanunchai***, Sarah Muszynski*, Florian Maurer, Sara Fareed Mohamed Wahdan, Jonas Malter, François Buscot and Matthias Noll

*These authors contributed equally to this work.

Status: Published

Publication: Proceedings of the Royal Society B: Biological Sciences

Publisher: ROYAL SOCIETY

Date: 8 April 2022

Proceedings of the Royal Society B: Biological Sciences 289, 20220130.

IF (2021) = 5.530

© 2022 The Royal Society

Reprinted with permission from ROYAL SOCIETY.

Own contribution: samples and metadata collection (20% and 70% were carried out by WP, MN, FM, JM, SFMW, and SM), DNA analysis: DNA extraction (90% and 10% were carried out by WP, SM, and SFMW), PCR library preparation for sequencing (90% and 10% were carried out by WP, and SFMW), microbial taxonomy and data analyses (40% and 60% were carried out by WP, SM, FM, and MN), visualization (75% and 25% were carried out by WP, SM, and MN), manuscript writing, review and editing (40% and 60% were carried out by WP, SM, FB, FM, SFMW, JM, and MN).

Author Contribution: W.P.: conceptualization, data curation, formal analysis, funding acquisition, investigation, methodology, resources, supervision, visualization, writing—original draft, writing—review and editing; B.T.: formal analysis, investigation, methodology, writing—original draft, writing—review and editing; S.M.: formal analysis, investigation, methodology, writing—review and editing; F.M.: formal analysis, investigation, writing—review and editing; SFM.W.: data curation, formal analysis, validation, writing—review and editing; J.M.: formal analysis, investigation, writing—review and editing; F.B.: resources, supervision, writing—review and editing; M.N.: conceptualization, formal analysis, funding acquisition, investigation, methodology, resources, supervision, visualization, writing—original draft, writing—review and editing. All authors gave final approval for publication and agreed to be held accountable for the work performed therein.

Plastic 1: Fate of a biodegradable plastic in forest soil: Dominant tree species and forest types drive changes in microbial community assembly, influence the composition of plastisphere, and affect poly(butylene succinate-co-adipate) degradation. (page 132 – 147)

Author: **Benjawan Tanunchai***, Li Ji*, Olaf Schröder, Susanne Julia Gawol, Andreas Geissler, Sara Fareed Mohamed Wahdan, François Buscot, Stefan Kalkhof, Ernst-Detlef Schulze, Matthias Noll, Witoon Purahong.

*These authors contributed equally to this work.

Status: Published

Publication: Science of The Total Environment

Publisher: Elsevier

Date: 15 May 2023

Science of the Total Environment 873 (2023) 162230

IF (2021) = 10.753

© 2023 Elsevier B.V. All rights reserved.

Reprinted with permission from Elsevier.

Own contribution: experimental set-up (50% and 50% were carried out by WP, SW and EDS), samples and metadata collection (60% and 40% were carried out by LJ, WP, SW and EDS), DNA analysis: DNA extraction (90% and 10% were carried out by WP), PCR library preparation for sequencing (90% and 10% were carried out by WP), microbial taxonomy and data analyses (70% and 30% were carried out by WP), manuscript writing (70% and 30% were carried out by WP and LJ).

Author Contribution: WP and EDS conceived and designed the study. BT, WP, SW and EDS led the experimental set-up. BT, LJ, WP, SW, and EDS collected the samples and metadata. WP, MN, and FB contributed reagents and laboratory equipment. BT and WP led the DNA analysis. SW led bioinformatics. BT, and WP led the microbial taxonomy, and data analyses. LJ led microbial network and community assembly analyses. AG performed SEM. MN led quantitative PCR. OS, SJG, and SK led GPC. BT, LJ and WP wrote the manuscript. MN and WP supervised BT. MN, AG, EDS, and FB reviewed and gave comments and suggestions for manuscript. All of the authors gave final approval for manuscript submission.

Plastic 2: Nitrogen fixing bacteria facilitate microbial biodegradation of a bio-based and biodegradable plastic in soils under ambient and future climatic conditions. (page 148 – 157)

Author: Benjawan Tanunchai*, Stefan Kalkhof*, Vusal Guliyev*, Sara Fareed Mohamed Wahdan, Dennis Krstic, Martin Schädler, Andreas Geissler, Bruno Glaser, François Buscot, Evgenia Blagodatskaya, Matthias Noll and Witoon Purahong

*These authors contributed equally to this work.

Status: Published

Publication: Environ. Sci.: Processes Impacts

Publisher: Royal Society of Chemistry (RSC); RSC Publishing

Date: 23 Feb 2022

IF (2021) = 5.334

Environ. Sci.: Processes Impacts 24, 233–241.

Reproduced from Ref. 600097281 with permission from the Royal Society of Chemistry.

Own contribution: Field experiment at GCEF (50% and 50% were carried out by WP and MS), laboratory experimental set-up (70% and 30% were carried out by WP, VG and EB), DNA analysis: DNA extraction (80% and 20% were carried out by WP), PCR library preparation for sequencing (80% and 20% were carried out by WP), mass loss measurement (50% and 50% were carried out by WP), microbial taxonomy and data analyses (50% and 50% were carried out by WP, SK, DK, and VG), visualization (40% and 60% were carried out by WP, SK, DK, and VG), manuscript writing (60% and 40% were carried out by WP, VG, MN, WP, SK, EB, FB, BG, SW, DK, AG, and MS).

Author Contribution: Conceptualization: WP, MN, and SK. Field experiment at GCEF: WP, BT, and MS. Laboratory experimental set-up: VG, BT, WP, and EB. Formal analysis: molecular analysis (BT and WP), *nifH* gene quantification (MN), enzyme analysis (VG and EB), CO₂ measurement (VG and EB), mass loss measurement (WP and BT), SEM (AG), and FTIR (SK and DK). Data analysis: WP, BT, SK, DK, and VG. Bioinformatics: SW. Methodology: WP, MN, SK, and EB. Resources: WP, MN, SK, and EB. Supervision: WP, MN, and EB. Visualization: WP, BT, VG, SK, and DK. Writing – original draft: BT, WP, and VG. Writing – review and editing: MN, WP, SK, EB, FB, BG, SW, DK, AG, and MS.

Plastic 3: Future climate change enhances the complexity of plastisphere microbial co-occurrence networks, but does not significantly affect the community assembly. (page 158 – 164)

Author: Li Ji*, **Benjawan Tanunchai***, Sara Fareed Mohamed Wahdan, Martin Schädler, Witoon Purahong

*These authors contributed equally to this work.

Status: Published

Publication: Science of The Total Environment

Publisher: Elsevier

Date: 20 October 2022

Science of the Total Environment, 157016.

IF (2021) = 10.753

© 2022 Published by Elsevier B.V.

Reprinted with permission from Elsevier.

Own contribution: samples and metadata collection (60% and 40% were carried out by SFMW and WP), DNA analysis: DNA extraction (80% and 20% were carried out by SFMW and WP), PCR library preparation for sequencing (80% and 20% were carried out by SFMW

and WP), microbial taxonomy and data analyses (20% and 80% were carried out by LJ and WP), manuscript writing (40% and 60% were carried out by LJ).

Author Contribution: W.P., M.S. and L.J. conceived and designed the study. B.T., S.F.M.W. and W.P. collected the samples and performed the lab work; L.J. and BT wrote the manuscript. L.J., S.F.M.W. and W.P. led the bioinformatics. All of the authors reviewed and gave comments and suggestions for the manuscript.

Plastic 4: Interactions between high load of a bio-based and biodegradable plastic and nitrogen fertilizer affect plant biomass and health: A case study with *Fusarium solani* and mung bean (*Vigna radiata* L.). (page 165 – 176)

Author: Sarah-Maria Scheid*, Kantida Juncheed*, **Benjawan Tanunchai***, Sara Fareed Mohamed Wahdan, François Buscot, Matthias Noll, Witoon Purahong

*These authors contributed equally to this work.

Status: Published

Publication: Journal of Environmental Polymer Degradation

Publisher: Springer Nature

Date: 30 Mar 2022

J Polym Environ.

IF (2021) = 4.705

Copyright © 2022, The Author(s)

Reprinted with permission from Springer Nature.

Own contribution: study design (50% and 50% were carried out by SS, KJ, MN and WP), laboratory experimental set-up (50% and 50% were carried out by SS, KJ, and WP), samples and metadata collection (40% and 60% were carried out by SS, KJ, and WP), DNA analysis: DNA extraction (50% and 50% were carried out by SS, KJ, and WP), PCR library preparation for sequencing (80% and 20% were carried out by SS, KJ, and WP), visualization (50% and 50% were carried out by SS, KJ, and WP), manuscript writing (40% and 60% were carried out by SS, KJ, and WP).

Author Contribution: SS, KJ, BT, MN and WP conceived and designed the study. SS, KJ, BT and WP led the laboratory experimental set-up. WP, FB and MN contributed reagents and laboratory equipment. BT, SS, KJ and WP led the DNA analysis. SW led bioinformatics. WP and SS led the microbial taxonomy and data analyses. SS, KJ, BT and WP wrote the manuscript. MN and WP supervised SS, KJ, BT. MN, SW and FB reviewed and gave comments and suggestions for manuscript. All of the authors gave final approval for manuscript submission.



FungalTraits vs. FUNGuild: Comparison of Ecological Functional Assignments of Leaf- and Needle-Associated Fungi Across 12 Temperate Tree Species

Benjawan Tanunchai^{1,2} · Li Ji^{1,3} · Simon Andreas Schroeter⁴ · Sara Fareed Mohamed Wahdan^{1,5} · Shakhawat Hossen^{1,6} · Yoseph Delelegn¹ · François Buscot^{1,7} · Ann-Sophie Lehnert⁴ · Eliane Gomes Alves⁴ · Ines Hilke⁴ · Gerd Gleixner⁴ · Ernst-Detlef Schulze⁴ · Matthias Noll^{2,6} · Witoon Purahong¹

Received: 11 October 2021 / Accepted: 21 January 2022
© The Author(s) 2022

Abstract

Recently, a new annotation tool “FungalTraits” was created based on the previous FUNGuild and Fun^{Fun} databases, which has attracted high attention in the scientific community. These databases were widely used to gain more information from fungal sequencing datasets by assigning fungal functional traits. More than 1500 publications so far employed FUNGuild and the aim of this study is to compare this successful database with the recent FungalTraits database. Quality and quantity of the assignment by FUNGuild and FungalTraits to a fungal internal transcribed spacer (ITS)–based amplicon sequencing dataset on amplicon sequence variants (ASVs) were addressed. Sequencing dataset was derived from leaves and needles of 12 temperate broadleaved and coniferous tree species. We found that FungalTraits assigned more functional traits than FUNGuild, and especially the coverage of saprotrophs, plant pathogens, and endophytes was higher while lichenized fungi revealed similar findings. Moreover, ASVs derived from leaves and needles of each tree species were better assigned to all available fungal traits as well as to saprotrophs by FungalTraits compared to FUNGuild in particular for broadleaved tree species. Assigned ASV richness as well as fungal functional community composition was higher and more diverse after analyses with FungalTraits compared to FUNGuild. Moreover, datasets of both databases showed similar effect of environmental factors for saprotrophs but for endophytes, unidentical patterns of significant corresponding factors were obtained. As a conclusion, FungalTraits is superior to FUNGuild in assigning a higher quantity and quality of ASVs as well as a higher frequency of significant correlations with environmental factors.

Keywords Amplicon sequence variants · Endophytes · Functional assignment · Fungal amplicon sequencing · ITS · Lichenized fungi · Plant pathogens · Saprotrophs

Benjawan Tanunchai and Li Ji contributed equally.

✉ Matthias Noll
Matthias.noll@hs-coburg.de

✉ Witoon Purahong
witoon.purahong@ufz.de

François Buscot
francois.buscot@ufz.de

¹ Department of Soil Ecology, UFZ-Helmholtz Centre for Environmental Research, Theodor-Lieser-Str. 4, 06120 Halle (Saale), Germany

² Bayreuth Center of Ecology and Environmental Research (BayCEER), University of Bayreuth, Bayreuth, Germany

³ Key Laboratory of Sustainable Forest Ecosystem Management-Ministry of Education, School of Forestry, Northeast Forestry University, 150040 Harbin, People’s Republic of China

⁴ Max Planck Institute for Biogeochemistry, Biogeochemical Processes Department, Hans-Knöll-Str. 10, 07745 Jena, Germany

⁵ Botany Department, Faculty of Science, Suez Canal University, Ismailia 41522, Egypt

⁶ Institute of Bioanalysis, Coburg University of Applied Sciences and Arts, Coburg, Germany

⁷ German Centre for Integrative Biodiversity Research (iDiv) Halle-Jena-Leipzig, Deutscher Platz 5e, 04103 Leipzig, Germany

Introduction

Fungi play a pivotal role in terrestrial ecosystems and exert important ecological functions including decomposition, transformation, and effective utilization of organic substrates, facilitating the cycling processes [1]. The understanding of fungal community diversity associated with leaf decomposition provides new insights into changes in biodiversity and forest ecosystem functions under climate change scenarios [2, 3]. Leaf properties (especially pH, availability of N and C nutrients) vary greatly among different host tree species and tree types and are known to shape the microbial community composition and microbial functional groups [4–6]. However, little attention has been paid to the fungal community functions related to leaves and needles of temperate tree species [7] and their relation to the host tree species. A functional guild summarizes a functional group composed of different phylogenetic taxa, which employs similar utilization of the same substrate type. Nevertheless, not all fungal groups perform consistent ecological functions, potentially resulting in guild bias in the relationships between the relative abundance of fungal communities and ecological functions. Some fungal groups even have overlapping niches under certain conditions [8–10]. Less is known until recently on how different fungal guilds interplay in facilitating and competitive modes in different host tree species. The interaction between fungal guilds can impact the decomposition rate of organic matter through the priming effect (additional carbon input) or the Gadgil effect (competition between saprotrophs and ectomycorrhizas for limited organic resources) [11–13]. Saprotrophs and plant pathogens are the two main guilds inhabiting the leaf litter. Saprotrophs exert a variety of functions in forest debris (e.g., dead wood and leaf litter), soil carbon, and nutrient cycling [14], while plant pathogens usually exhibit saprophytic activities after leaf senescence (in the early stage of decomposition) [15]. These characteristics can lead to differences of the functional richness between the saprotrophs and plant pathogens in different habitats. Therefore, identifying and evaluating how fungal guilds and their richness in the respective functional diversity response to the variation in host tree species and diversity is a crucial issue for microbial ecology and biodiversity. The functional assignment to phylogenetic datasets is an important step to assess fungal community functions and guild differentiation.

In recent years, several relatively efficient and accurate databases or molecular tools that depict and identify fungal functions have been established, for example LIAS [16, 17], DEEMY [18], Fun^{Fun} [19], Notes on genera: Ascomycota [20], FUNGuild [21], and FacesOfFungi [22]. LIAS

focuses on lichens, lichenicolous fungi, and non-lichenized Ascomycetes, whereas DEEMY focuses on ectomycorrhizal fungi [16, 18]. FacesOfFungi is a broad database and includes three main fungal groups, Ascomycota, Basidiomycota, basal fungi as well as fungus-like organisms [22]. Notes on genera: Ascomycota has been built up from FacesOfFungi by focusing on habitats, substrates, gross biotic interactions, and trophic modes of Ascomycetes [20]. FUNGuild is a database for the comparison of fungal functions and can link fungal gene sequencing information with the ecological functions of fungi, as well as identify the nutrient types used by fungi at the genus level and conduct the specific functional classifications [21]. Fun^{Fun} database has been developed from FUNGuild by addition of data on various number of traits at the genus and species levels (including cellular, ecological, and biochemical traits) [19]. The FUNGuild annotation tool proposed by Nguyen et al. (2016) for analyzing the functional guilds of fungal communities [21] has received more attention and has been applied to perform the fungal ecological functions in terrestrial and aquatic ecosystems [23–28]. The script is written in Python and licensed under GNU General Public License. FUNGuild's script works by matching terms in the taxonomy column of the OTU table to those in the database in the GitHub repository [21]. Even though FUNGuild has been used to analyze the functions of fungi to a certain extent, the functions of 59% of soil fungi and 20% of saprophytic organisms have not yet been resolved [21]. This tool has certain limitations as it is based on existing literature and data. Therefore, the fungal taxon and functional group datasets still need to be updated with higher resolution.

Based on the previous fungal functional annotation tools, FUNGuild [21] and Fun^{Fun} [19], the recent work by Pölme et al. developed the FungalTraits tool and reannotated 10,210 genera of fungi and 151 genera of Stramenopila associated with 17 characteristic lifestyles [29]. They manually classified and assigned the 697,413 fungal ITS sequences and obtained the 92,623 fungal characteristics and host information (at 1% dissimilarity threshold). Compared with FUNGuild, FungalTraits clearly provides the most commonly occurring lifestyle as primary lifestyle and additional relevant lifestyle as secondary lifestyles. Furthermore, FungalTraits introduced the “aquatic_habitat” feature, which allows fungi to be classified as marine, freshwater, more extensive aquatic, or partial aquatic organisms, because many previous aquatic species were usually annotated to root or soil environments. They unravelled that it may be necessary to parse accidental spores of terrestrial fungi from functional groups that naturally grow in water or similar substrates [29]. In addition, FungalTraits has also expanded the “growth_form” field, with 15 characteristic states covering amoeba, filamentous, mycelium, and various single-cell

forms related to fungi and Strametes. For ectomycorrhizal fungi, the evolutionary characters “ectomycorrhiza_lineage” and “ectomycorrhiza_exploration_type” are introduced. In addition, they collected specific information about primary and secondary symbiotic photosynthetic organisms in the literature to annotated information about lichen traits [29].

Until now, more than 1500 publications (last accessed 16.12.2021) have employed FUNGuild to annotate sequencing datasets to ecological functions. Due to the large number of previous studies using FUNGuild, it is necessary to compare the performance and the ecological interpretation provided by the two annotation tools (FUNGuild vs. FungalTraits). Our study aimed to compare state-of-the-art methods (FungalTraits vs. FUNGuild) for leaf- and needle-associated fungal functional diversity analyses. We investigated the leaf- and needle-associated fungi of 12 temperate tree species in Central Europe forests and validated the consistency of using the two functional annotation tools. We hypothesize that (1) for overall and for all main fungal guilds, FungalTraits outperforms FUNGuild as it contains a higher number of fungal genera in its database; (2) both functional annotation tools provide consistent results for interpreting the richness and community composition of the leaf- and needle-associated fungi across 12 temperate tree species.

Materials and Methods

Study Site and Sampling

This study was conducted in the Hainich-Dün region of Thuringia, Germany (51°12' N 10°18'E). Elevations range from 100 to 494 m above sea level, the mean annual precipitations from 600 to 800 mm, and the mean annual temperatures from 6 to 7.5 °C (average temperatures in January = 0.65 °C and July = 17.17 °C). The parent material is Triassic limestone, which is covered by a Pleistocene loess layer of variable thickness (ca. 10–50 cm) at most sites. The litter layer consists mainly of past years foliage (1 to 3 cm). The main soil type is a Cambisol on limestone as bed-rock. The soil pH is weakly acidic (5.1 ± 1.1 ; mean \pm SD).

In October 2019, we collected senescing leaves and needles from 60 tree individual (12 tree species, five true replicates (trees), minimum 200-g leaves or needles per tree individual). These tree species include 8 broadleaved (including *Acer pseudoplatanus*, *Carpinus betulus*, *Fagus sylvatica*, *Fraxinus excelsior*, *Populus* sp., *Prunus avium*, *Quercus robur*, and *Tilia cordata*) and 4 coniferous tree species (including *Picea abies*, *Larix decidua*, *Pinus sylvestris*, and *Pseudotsuga menziesii*). Sampling was carried out with gloves and sterilized plastic bags, and leaves and needles from each tree were separately packed and transported under cooled conditions to the lab. In the laboratory, each leaf

and needle were frozen at -80 °C for subsequent molecular approaches.

DNA Extraction and Illumina Sequencing

Healthy-looking leaves (up to 10 leaves per tree individual depending on the size of the leaves) and needles (from five branches per tree individual) were subsampled and prepared for DNA extraction. Briefly, we removed loosely adherent dust particles and microbes from leaf and needle samples by vortexing them with a maximum speed for 5 min in sterile Tween solution (0.1% vol/vol), and this step was repeated three times. The samples were then washed three to five times using deionized water. Finally, leaf and needle samples were incubated for 1 h in sterile water at room temperature. Each composite sample was then ground using liquid nitrogen and pestle, homogenized, then stored at -20 °C for further analysis. Fungal community attached firmly to the leaf and needle samples (~120 mg homogenized leaves and needles) was then subjected to DNA extraction using DNeasy PowerSoil Kit (Qiagen, Hilden, Germany) and a Precellys 24 tissue homogenizer (Bertin Instruments, Montigny-le-Bretonneux, France) according to the manufacturer's instructions. The presence and quantity of genomic DNA were checked using NanoDrop ND-1000 spectrophotometer (Thermo Fisher Scientific, Dreieich, Germany), and the extracts were stored at -20 °C. Leaf- and needle-associated fungi were characterized by fungal internal transcribed spacer (ITS)-based amplicon sequencing on the Illumina MiSeq sequencing platform, as outlined earlier [30]. For establishing fungal amplicon libraries, the fungal ITS2 gene was amplified using the fungal primer pair FITS7 [5-GTG ARTCATCGAATCTTTG-3] [31] and ITS4 primer [5-TCC TCCGCTTATTGATATGC-3] [32] with Illumina adapter sequences. Amplifications were performed using 20- μ L reaction volumes with 5 \times HOT FIRE Pol Blend Master Mix (Solis BioDyne, Tartu, Estonia). The amplified products were visualized by gel electrophoresis and purified using an Agencourt AMPure XP kit (Beckman Coulter, Krefeld, Germany). Illumina Nextera XT Indices were added to both ends of fungal amplicons. The products from three technical replicates were then pooled in equimolar concentrations. Paired-end sequencing (2×300 bp) was performed on the pooled PCR products using a MiSeq Reagent kit v3 on an Illumina MiSeq system (Illumina Inc., San Diego, CA, USA) at the Department of Soil Ecology, Helmholtz Centre for Environmental Research, Germany.

Bioinformatics

The ITS rDNA sequences corresponding to the forward and reverse primers were trimmed from the demultiplexed raw reads using cutadapt [33]. Paired-end sequences were

quality-trimmed, filtered for chimeras, and merged using the DADA2 package [34] through the pipeline dada2 [30]. Assembled reads fulfilling the following criteria were retained for further analyses: a minimum length of 70 nt, quality scores at least equal to 9 with maximum expected error score of 5 for forward and reverse sequences, and no ambiguous nucleotides. Merging was conducted with 2 mismatches allowed and a minimum overlap of 20 nucleotides required for fungal sequences. High-quality reads were clustered into 2480 amplicon sequence variants (ASVs) for fungi after chimera removal. Fungal ASVs were classified against the UNITE v7.2 database [35]. Set of ASVs were classified using the Bayesian classifier as implemented in the mothur classify.seqs command, with a cut-off of 60. The ASV method is used to infer the biological sequences in the sample, as described previously [36]. Rare ASVs (singletons), which potentially represent artificial sequences, were removed. The dataset was then rarefied. Finally, we obtained 2451 rarefied fungal ASVs with the minimum sequencing depths of 21,967 sequences per sample. Presence/Absence datasets for fungi were used in the statistical analyses. The rarefaction curves of all the samples are provided in the Supplementary Figure S1. The fungal ecological function of each ASV was determined using FUNGuild [21] and FungalTraits [29] according to the authors' instructions.

Physiochemical analyses

Wet leaf and needle samples were shaken for 1 h in falcon tubes with 30 mL milliQ water to leach water-soluble components from their surfaces. The leachates were centrifuged for 5 min at 3500 rpm, decanted, and filtered through pre-flushed 0.45- μ m regenerated cellulose syringe filters. The remaining leaf/needle material was dried for two weeks at 40 °C for dry weight determination. All quantification results are given in reference to the dry weight. The pH of the leachates was determined using pH paper with a scale precision of 0.2 pH units. N_{org} was calculated as the difference: $N_{org} = TN_b - N_{min}$. TN_b was analyzed using a sum parameter analyzer with high temperature combustion and chemiluminescence detection (Mitsubishi TN-100; a1 envirosciences, Düsseldorf, Germany). For N_{Min} quantification, a flow injection analyzer (Quikchem QC85S5; Lachat Instruments, Hach Company, Loveland CO, USA) with corresponding manifolds for the nitrogen measurement of ammonium $N_{NH_4^+}$, nitrite $N_{NO_2^-}$, and nitrate- plus nitrite $N_{NO_3^-+NO_2^-}$ was used. DOC was quantified as non-purgeable organic carbon (NPOC) with a sum parameter analyzer using high-temperature combustion and infrared detection (vario TOC cube, Elementar Analysensysteme GmbH, Langenselbold, Germany). Nutrient ions, Ca, Fe, K, Mg, and P content were determined using Inductively Coupled Plasma–Optical

Emission Spectrometry (ICP–OES, PerkinElmer Inc., Waltham, MA, USA) according to manufacturers' specifications. All method details on physiochemical analyses are provided in supplementary material.

Statistical analysis

The datasets were tested for normality using the Jarque–Bera JB test and for the equality of group variances using *F*-test (for two datasets) and Levene's test (for more than two datasets). The statistical differences between proportions of functional assignment by FUNGuild and FungalTraits were performed using *T*-test (for normal distributed data) and Mann–Whitney *U* test (for non-normal distributed data). Effects of tree species and tree types on fungal community composition were visualized and tested with cluster analysis (based on presence-absence data, paired group algorithms, and the Jaccard distance measure) and one-way PERMANOVA (based on presence-absence data and the Jaccard distance measure), over 999 permutations were run. The correlation analyses were performed using Pearson's *r* (for normal distributed data) and Spearman's ρ (for non-normal distributed data). The statistical differences of ASV richness among different tree species were performed using one-way ANOVA with Tukey's post hoc test or KW test with Mann–Whitney *U* test. All statistical analyses were performed using PAST version 2.17 [37].

Results

Overall Performances of Ecological Function Assignments of FUNGuild and FungalTraits

In total, we assigned functions to 1,395 ASVs (accounted for 57% of total ASVs) using both FUNGuild and FungalTraits annotation tools (Table 1 and Fig. 1). In these total assigned ASVs, 70% and 89% were assigned functions by FUNGuild and FungalTraits, respectively (Table 1 and Fig. 1a). The remaining 30% that were not assigned functions by FUNGuild were assigned solely by FungalTraits and vice versa. 977 ASVs (~40% of total ASVs) could not functionally be assigned by both FUNGuild and FungalTraits. As suggested by Nguyen et al. [21], genera with confidence level of “possible” (in total 349 ASVs) were classified as “uncertained” and excluded from the functional analyses in this study (Table 1 and Supplementary Table S1). Overall, we found that the proportion of the total fungal functional assignment by FungalTraits (average of all tree species = 60%) was significantly higher than those by FUNGuild (average of all tree species = 43%) (Fig. 1a). We found a consistent pattern when considering each fungal guild (including saprotroph, plant pathogen, and endophyte) (Fig. 1b–d). The proportions

Table 1 Number of ASVs assigned functions by FUNGuild and FungalTraits

Functions	Total number of ASVs assigned to functions by both annotation tools	Total number of ASVs assigned to functions by FUNGuild	Total number of ASVs assigned to functions by FungalTraits	Shared ASVs
All functions	1395	982	1240	827
Animal pathogen/animal parasite	48	21	48	21
Ectomycorrhiza	13	8	13	8
Endophyte	19	8	13	2
Epiphyte	50	5	45	0
Ericoid mycorrhiza	1	1	NA	NA
Fungal parasite/mycoparasite	57	7	57	7
Lichen parasite	18	6	18	6
Lichenized fungi	60	59	54	53
Multifunction	317	317	NA	NA
Plant pathogen	405	216	400	211
Saprotroph	654	334	585	265
Sooty mold	7	NA	7	NA
Unassigned	1354	1120	1211	977
Uncertained (FUNGuild with confidence level of “possible”)	349*	349*	0	0

*79 ASVs are shared ASVs between “uncertained” in FUNGuild and “unassigned” in FungalTraits

of the functional assignment of these fungal guilds by FungalTraits were also significantly higher than those by FUNGuild, especially for saprotrophs (FungalTraits = 30% and FUNGuild = 14%), plant pathogens (FungalTraits = 20% and FUNGuild = 10%), and endophytes (FungalTraits = 0.24% and FUNGuild = 0.08%). Considering main fungal guilds, FUNGuild assigned only 53 and 51% of plant pathogens and saprotrophs, respectively. Contrarily, FungalTraits assigned up to 99% of these main fungal guilds. Furthermore, 98 and 79% of plant pathogens and saprotrophs, respectively, assigned by FUNGuild were also assigned by FungalTraits. However, for lichenized fungi, we found no significant difference between the proportions of functional assignment by both annotation tools ($P > 0.05$) (Fig. 1e). FUNGuild and FungalTraits shared 88% of total lichenized fungal ASVs. Remarkably, all ASVs assigned functions such as animal pathogen/animal parasite, ectomycorrhiza, fungal parasite/mycoparasite, and lichen parasite by FUNGuild were subset of those assigned by FungalTraits (Table 1). Epiphyte was, however, an exception. There was no shared epiphytic ASV between both annotation tools.

Specific Performances of Ecological Function Assignments of FUNGuild and FungalTraits Across 12 Temperate Tree Species

Based on individual tree species, we also found that FungalTraits provided a significantly higher proportion of the

total fungal functional assignment compared to FUNGuild (Fig. 2). This pattern was consistent across all 12 tree species. Among broadleaved tree species, *Populus* sp. revealed the highest proportion of the total fungal functional assignments by FungalTraits, whereas *F. sylvatica* has the lowest proportion (Figs. 1 and 2). Remarkably, the differences between these proportions assigned by both annotation tools were much higher in broadleaved tree species compared to coniferous tree species. The highest difference was found in broadleaved *Populus* sp. (31%), while the lowest difference was observed for *P. abies* (7%). While the proportions of overall fungal functional assignments by FungalTraits were much higher in broadleaved tree species compared to coniferous tree species, FUNGuild provided similar proportions across all tree species. The consistent patterns were found in saprotrophs. The proportions of saprotrophic fungal functional assignments by FungalTraits were significantly higher than those by FUNGuild across 12 tree species. The differences between them were also higher in broadleaved tree species (13–24%) compared to coniferous tree species (7–18%).

FUNGuild vs. FungalTraits: Interpretation of Richness and Community Composition of Main Fungal Guilds

We found a significant correlation between the percentage points of total functional assignments by FUNGuild and

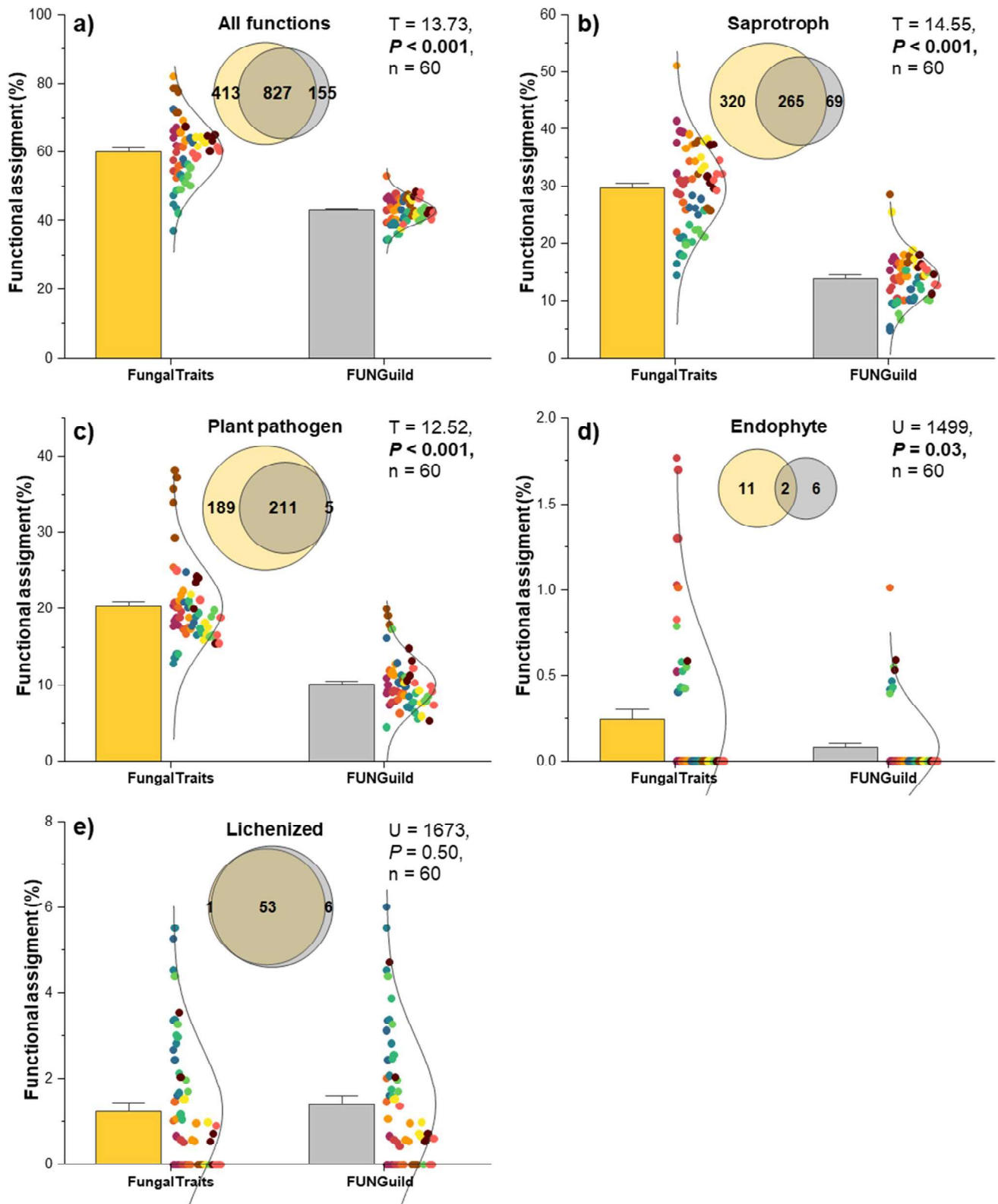
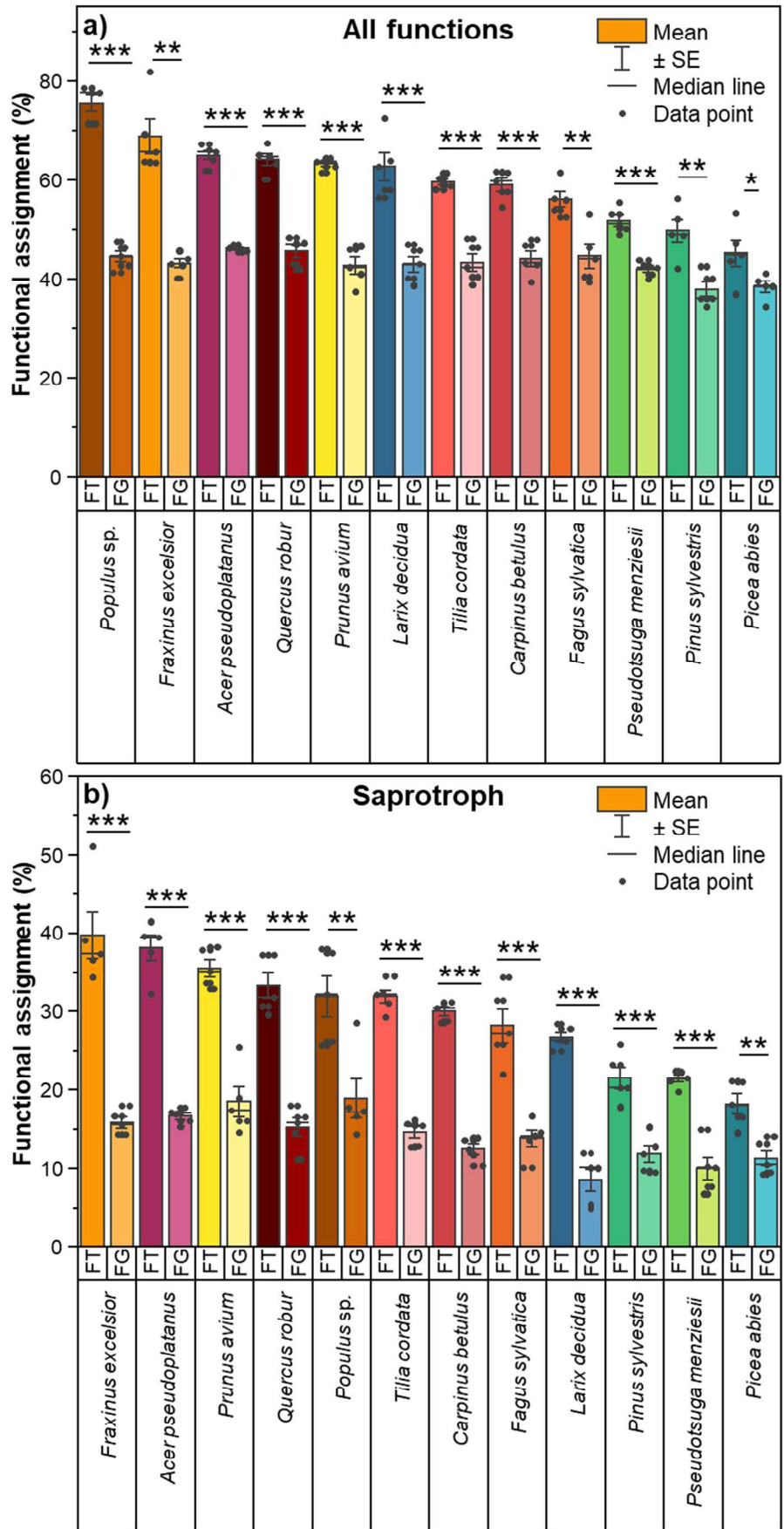


Fig. 1 Proportions of functional assignments and Venn diagrams of (a) all functions, (b) saprotrophs, (c) plant pathogens, (d) endophytes, and (e) lichenized fungi by FungalTraits and FUNGuild. The statistical differences were performed using T -test (for normal distributed data) and Mann–Whitney U test (for non-normal distributed

data). Color code of each data point refers to leaves and needles of respective tree species identity and is similar to the color code of Fig. 2. Data used for Venn diagrams are provided in Supplementary Table S3–S6

Fig. 2 Bar plots of functional assignments of (a) all functions and (b) saprotrophs across 12 tree species. Median of average proportion with standard error are denoted. FT and FG stand for FungalTraits and FUNGuild, respectively. Yellow–red–brown color tone refers to the broadleaved tree species and blue–green color tone refers to the coniferous tree species. The statistical differences between proportions of functional assignments by FungalTraits and FUNGuild in each tree species were performed using *T*-test ($P < 0.05 = *$, $P < 0.01 = **$, $P < 0.001 = ***$)



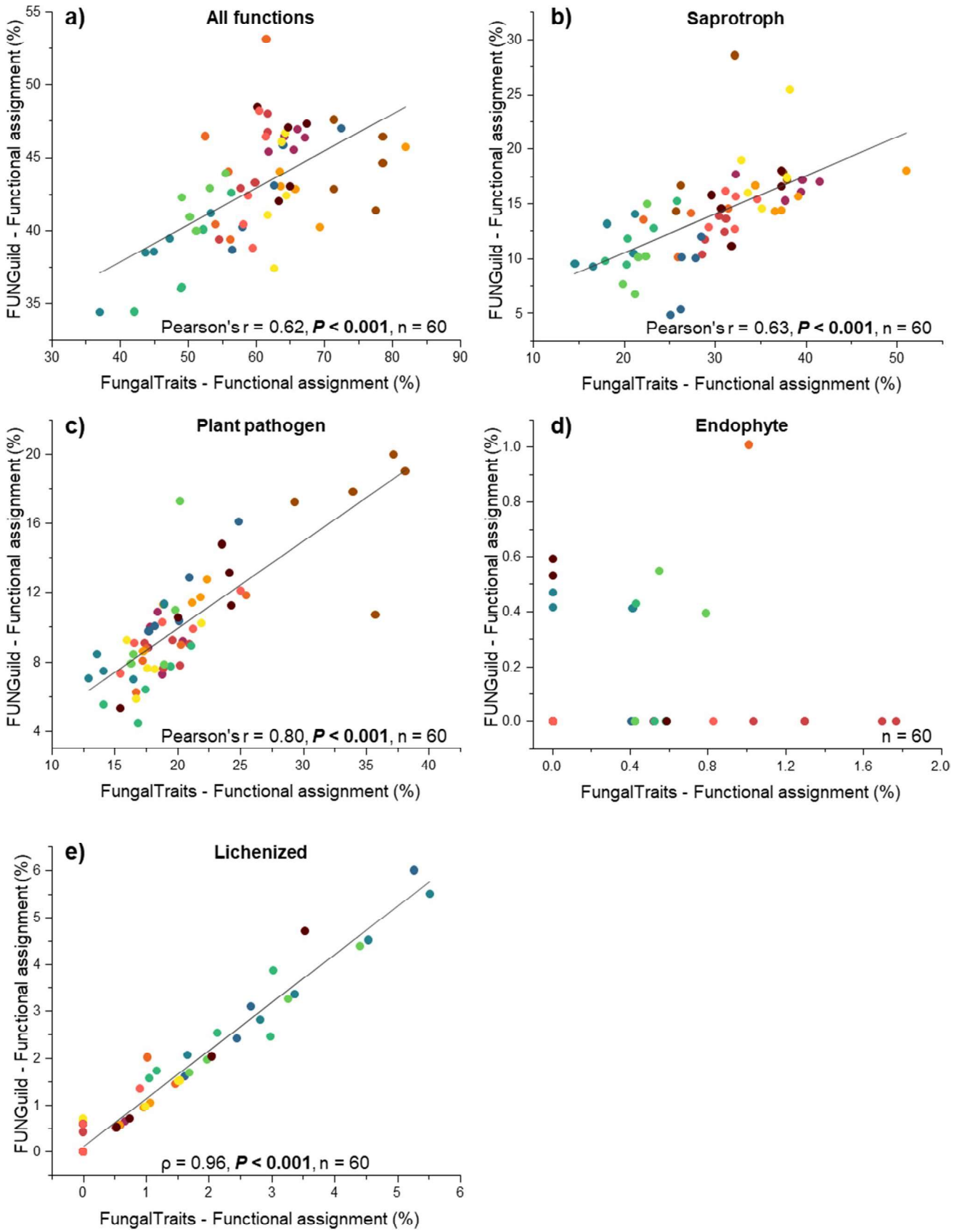


Fig. 3 Linear regressions between proportions of functional assignments by FungalTraits and FUNGuild for (a) all functions, (b) saprotrophs, (c) plant pathogens, (d) endophytes, and (e) lichenized fungi. The statistical differences were performed using Pearson's r (for normal distributed data) and Spearman's ρ (for non-normal distributed data)

FungalTraits (Pearson's $r=0.62$, $P<0.001$) (Fig. 3a). However, the correlations were different among fungal guilds. We found that lichenized fungi revealed the highest significant correlation between proportions of functional assignment by FUNGuild and FungalTraits ($\rho=0.96$, $P<0.001$), followed by plant pathogens (Pearson's $r=0.80$, $P<0.001$). A significant, but lower correlation, was found for saprotrophs (Pearson's $r=0.63$, $P<0.001$). Contrarily, no correlation was observed for endophytes ($P>0.05$).

Likewise, the consistent results of the effect of tree species and tree types (broadleaved vs. coniferous trees) on richness and community composition were highly correlated to fungal guilds (Figs. 4, 5, and 6). For lichenized fungi, such results from FUNGuild and FungalTraits are almost identical. We found that needles of all coniferous trees harboured significantly higher richness of lichenized fungi as compared to the broadleaved trees (Fig. 4). An exception was found for *Q. robur*, which exhibited similar richness as compared with *L. decidua*, *P. sylvestris*, and *P. menziesii*. *Picea abies* and *Populus* sp. harboured highest and lowest richness. For fungal community composition, we found that almost all needle samples of coniferous trees clustered together into one clade with few broadleaved trees (Fig. 5). The majority of leaf samples from broadleaved trees (*Populus* sp., *A. pseudoplatanus*, *F. sylvatica*, *T. cordata*) contained no lichenized fungi and clustered together on the left side of the plot. The effects of tree species ($F_{\text{tree species, FG}}=1.52$, $P=0.0001$ and $F_{\text{tree species, FT}}=1.52$, $P=0.0001$, respectively) and tree types ($F_{\text{tree type, FG}}=3.29$, $P=0.0001$ and $F_{\text{tree type, FT}}=3.32$, $P=0.0001$, respectively) on lichenized fungal community composition based on FUNGuild and FungalTraits were almost identical.

On the other hand, for saprotrophs, the results from FUNGuild and FungalTraits were partly inconsistent (Figs. 4 and 6). Both functional annotation tools showed that tree species and tree types significantly affect the richness of saprotrophic fungi and *Populus* sp. harboured the lowest richness. However, FUNGuild and FungalTraits showed that *A. pseudoplatanus* and *F. excelsior*, respectively, harboured the highest saprotrophic richness (Fig. 4). Nevertheless, we found strong correlations for all tree species of both saprotrophic (Pearson's $r=0.82$, $P<0.001$) and lichenized ($\rho=0.96$, $P<0.001$) fungal richness obtained by FUNGuild and FungalTraits (Fig. 4e and f). For saprotrophic fungal community composition derived from FUNGuild and FungalTraits, we found that all leaf samples of coniferous trees

separated from broadleaved trees (Fig. 6). However, based on FUNGuild, we detected two clades belong to broadleaved trees (*Populus* sp. separated from other broadleaved trees) and two clades belong to coniferous trees (*L. decidua* separated from other coniferous trees) (Fig. 6a) whereas based on FungalTraits, we detected two clades, each belonged to coniferous and broadleaved trees (one *Populus* sp. sample separated from other trees) (Fig. 6b).

FUNGuild vs. FungalTraits: Factors Shaping Community Composition of Main Fungal Guilds

We found similar patterns of factors shaping the saprotrophic community composition derived from FUNGuild and FungalTraits. Here, tree species and tree type were the main factors shaping the saprotrophic community composition (Table 2). Besides tree species and tree type, we also found that water content, the majority of water-leachable leaf/needle nutrient compounds (DOC, organic (N_{Org}) and inorganic (mineralized) N (N_{Min} , $N_{\text{NH}_4^+}$, and $N_{\text{NO}_2^-}$) as well as Ca, Fe, Mg, and P content), and location significantly corresponded with saprotrophic community composition of both annotation tools (Table 2). In the endophytic community, where no correlation between proportions of functional assignment by FUNGuild and FungalTraits was detected, unidentical patterns of factors were found (Table 2). Tree species was the main factor shaping endophytic community composition of both annotation tools along with P content. However, when FUNGuild was employed, we obtained longitude as another main factor significantly corresponded with endophytic community composition. On the other hand, when FungalTraits was applied, Ca and K content were found to be additional factors that significantly corresponded with endophytic community composition (Table 2).

Variation partitioning analysis revealed similar results for saprotrophs derived from both FUNGuild and FungalTraits (Supplementary Table S2). Tree species alone explained the largest variation (45% of total explainable variance) in the saprotrophic community composition of both annotation tools, followed by leaf/needle nutrients (FUNGuild: 6% and FungalTraits: 3% of total explainable variance). Water content/pH and location alone did not explain the saprotrophic community compositions. The combinations of these factors revealed similar percentage of total explainable variance in saprotrophic community composition of both annotation tools. In the endophytic community composition obtained from FUNGuild, tree species, leaf/needle nutrients, location, and the combination of these three factors explained 46%, 26%, 18%, and 10%, respectively, of total explainable variance (Supplementary Table S2). In the endophytic community composition obtained from FungalTraits, only two factors (tree species and leaf/needle nutrients) were used to

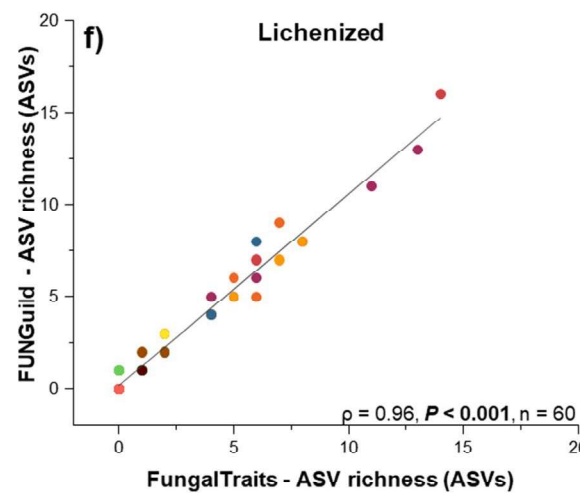
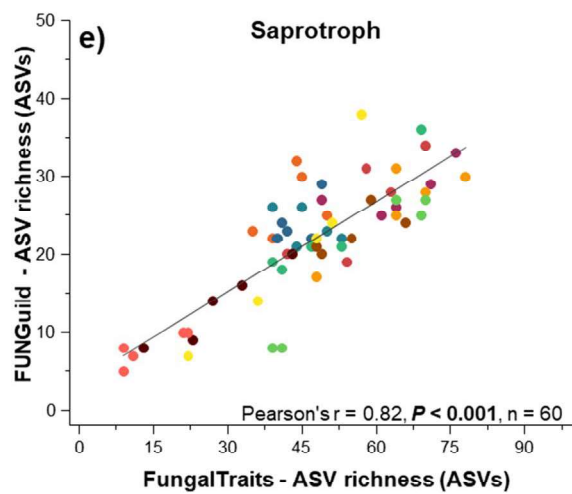
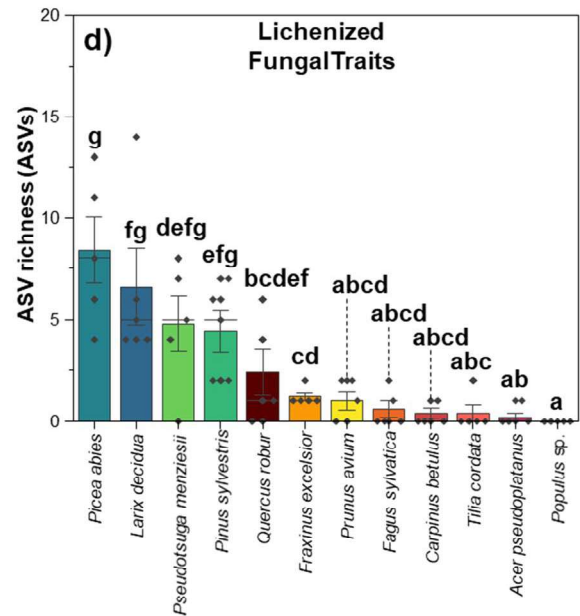
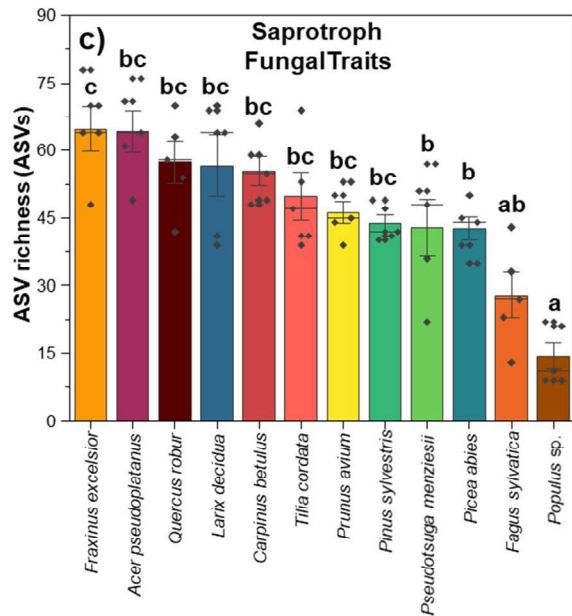
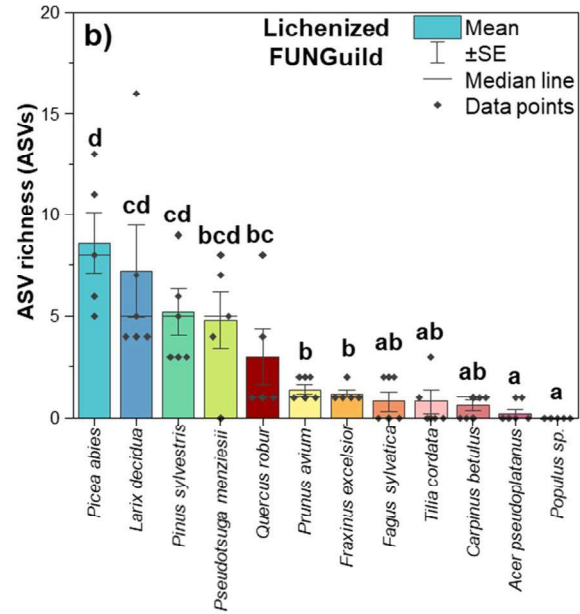
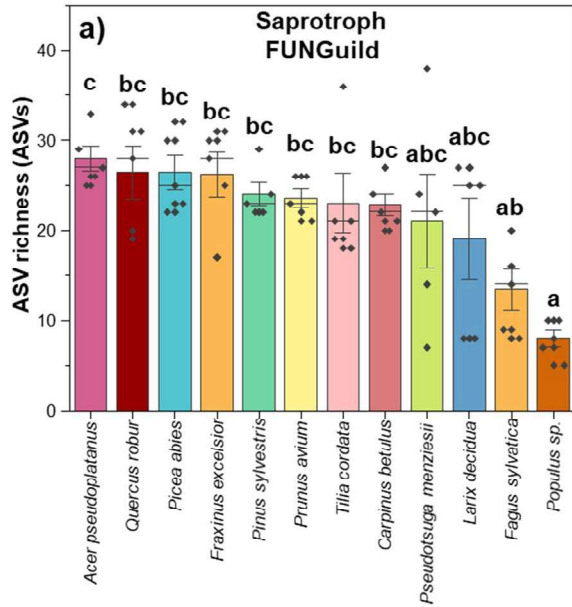


Fig. 4 Average ASV richness of fungal saprotrophs (a, c) and lichenized fungi (b, d) across 12 tree species obtained by FUNGuild (a, b) and FungalTraits (c, d) and correlations between ASV richness values obtained by FUNGuild and FungalTraits for fungal saprotrophs (e) and lichenized fungi (f). Median of average proportion with standard error are denoted. Yellow–red-brown color tone refers to the broadleaved tree species and blue-green color tone refers to the coniferous tree species. The statistical differences of ASV richness among different tree species were performed using ANOVA or KW test. Correlations were determined using Pearson's r and Spearman's rank correlation coefficients

explain the variation (Supplementary Table S2). Sixty-six percent, 18%, and 16% of total explainable variance were explained by tree species, leaf/needle nutrient, and the combination of these two factors, respectively.

Discussion

Performance of Ecological Function Assignments of FUNGuild and FungalTraits

FUNGuild has been routinely used for functional annotations of mycobiome members across different ecosystems and biomes encompassing both terrestrial and aquatic environments [23, 38–42]. Many studies detected specific responses of a defined set of fungal guilds to different environmental factors which cannot be detected based on the total community analyses [40, 43]. A recent study based on total and active microbiome also illustrates that some ecosystem functions are related to the changes in richness, abundances, and community composition of specific fungal guilds [39]. While FUNGuild is based on a publicly available Python script to annotate fungal functions, FungalTraits works in similar way with the same Python script but offers a more user-friendly Excel-based database and a web-based interface for users without Python expertise [29]. As FungalTraits proof-checked all entries from FUNGuild and included a large set of additional entries, the database FungalTraits encompasses a more comprehensive and faster annotation. FungalTraits receives high attention in the scientific community and has been already applied for investigating fungal guilds in some terrestrial ecosystems [44, 45]. Due to the large number of previous studies using FUNGuild, it is necessary to compare the performance and the ecological interpretation provided by these two annotation tools with high scientific reputation. FungalTraits has been applied together with FUNGuild to annotate functional groups of fungi associated with Orchidaceae [45]. The authors of that study successfully demonstrated symbiont switching and shifts of trophic mode of fungi associated with Orchidaceae. FungalTraits was also successfully applied to annotate the fungal guilds for wood-inhabiting

fungi [44]. In this current study, we used the data on mycobiome associated with senescing leaves and needles of 12 temperate tree species to compare the performance and the results obtained by FUNGuild and FungalTraits. Our results clearly show that FungalTraits outperforms FUNGuild in terms of percent functional assignment quantity and quality. The average value of percent functional assignment of FungalTraits reaches 60% and in *Populus* sp., such value reaches 76%. The average value of percent functional assignment of FUNGuild is 43% (ranging from 38–46%). These values are consistent with the percentage points of functional assignment of FUNGuild reported before in many publications [39, 46, 47]. Nevertheless, it is known that the percentage points of functional assignments of taxonomically dependent functional annotation tool highly depends on the quality and quantity of the database backbone of each sequence data, taxonomic identification and functional description [48]. The better performance of FungalTraits is not surprising as it contains a higher number of fungal genera in its database than FUNGuild [21, 29]. Interestingly, we found that the values of percentage points of functional assignments are relatively constant across different tree species when FUNGuild is applied, such value varied greatly when FungalTraits is applied. Furthermore, for FungalTraits-derived datasets, the percentage points of functional assignments are higher for deciduous trees (including broadleaved trees and *L. decidua*) and lower for the remaining coniferous trees (Fig. 2).

FUNGuild vs. FungalTraits: There Are Some Similarities but also Some Differences

Our current study demonstrates that the quality of functional annotations and the resulting interpretations derived from FUNGuild and FungalTraits are relatively similar; however, they are not identical. Furthermore, the degrees of similarity greatly depend on which fungal guilds were considered. While the results on the effect of tree species and tree types on richness and community composition of lichenized fungi are almost identical when FUNGuild and FungalTraits are applied, for saprotrophic fungi, we could detect some discrepancies between these two annotation tools (Fig. 3). Low discrepancies are expected for plant pathogens as correlations between proportions of percentage points of functional assignments of FUNGuild and FungalTraits are high. In contrast, we expected high discrepancies for endophytes as we detected no correlation (Fig. 3). Such discrepancies derive from the fact that there are mismatches of functional assignments between FUNGuild and FungalTraits. We now identified these mismatches for fungal genera associated with our datasets (Supplementary Table S3–S6). For example, the genus *Fusarium* was assigned to “plant pathogen” as a primary function in FungalTraits. In turn, FUNGuild assigned *Fusarium* to “Animal Pathogen-Endophyte-Lichen

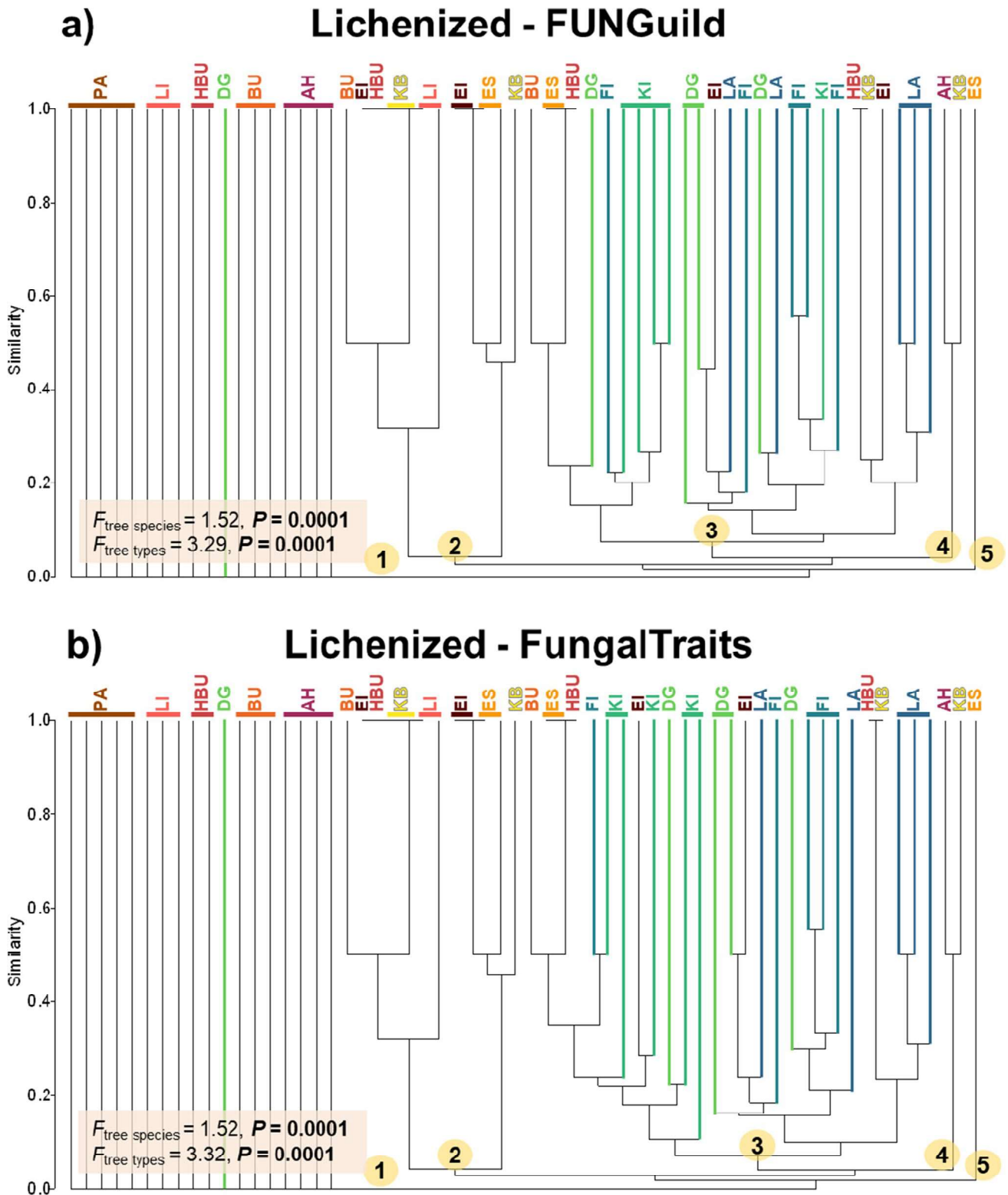


Fig. 5 Community composition of lichenized fungi derived from FUNGuild (a) and FungalTraits (b) of five independent leaf/needle replicates. Yellow–red–brown color tone refers to the broadleaved tree species and blue–green color tone the coniferous tree species. Numbers in yellow circle indicate different clades in the dendrogram for lichen cluster analysis. Species abbreviations for broadleaved tree

species are as follows: AH: *Acer pseudoplatanus*, BU: *Fagus sylvatica*, EI: *Quercus robur*, ES: *Fraxinus excelsior*, HBU: *Carpinus betulus*, KB: *Prunus avium*, LI: *Tilia cordata*, and PA: *Populus* sp., and coniferous tree species are: DG: *Pseudotsuga menziesii*, FI: *Picea abies*, KI: *Pinus sylvestris*, and LA: *Larix decidua*. Effects of tree species and tree types were tested with one-way PERMANOVA

parasite-Plant Pathogen-Soil Saprotroph-Wood Saprotroph” with confidence level “possible”. According to the original FUNGuild article, function with confidence level “possible” should be excluded or interpreted with caution. Confidence level “possible” in FUNGuild may contain genera with split ecologies (they perform different or even conflicting functions depending on life stage and environmental conditions). Another example for the mismatch is the identification of genus *Cenangium*. *Cenangium* is classified as “foliar endophyte” in FungalTraits, while it is identified as “saprotroph” with confidence level “probable” in FUNGuild. According to recent research, *Cenangium* was identified as endophyte, saprotroph, and plant pathogen [49, 50], which is consistent with the “Comment on lifestyle” in FungalTraits [29].

Apart from mismatches, FUNGuild identified two or more functions (with confidence level “probable”) for a single fungal taxon; thus, it is difficult to make decision which function or both functions are most likely fitting to this fungus. Nevertheless, it is quite common to report all functions obtained by FUNGuild for a single taxon when the confidence level is at least “probable”. Another possibility for the discrepancy is that FUNGuild can annotate functions to fungi at a higher taxonomic rank (such as family). For example, we found that four fungal ASVs belonged to *Pannariaceae*, *Candelariaceae*, and *Ramalinaceae*, which were annotated as lichenized fungi using FUNGuild (with probable and highly probable confidence levels), but the same ASVs cannot be annotated to any function by FungalTraits. As demonstrated before, FUNGuild and FungalTraits can be applied together to maximize the number of fungal functional annotations and to remove ambiguous annotations. However, based on the results of our datasets, FungalTraits alone already yielded successful functional assignments for high proportions of the fungal community. Adding the functions specifically annotate with FUNGuild to the FungalTraits datasets can increase the percentage points of the total functional assignment by approximately 6%. Apart from the primary lifestyle (function), FungalTraits also provides other interesting information on secondary lifestyle, endophytic interaction capability, plant pathogenic capacity, preferred substrate type, decay type, habitat characteristics, animal biotrophic capacity, hosts, growth form, fruitbody type, Hymenium type, ectomycorrhiza exploration type, ectomycorrhizal lineage, and photobiont.

FUNGuild vs. FungalTraits: Factors Shaping Community Composition of Main Fungal Guilds

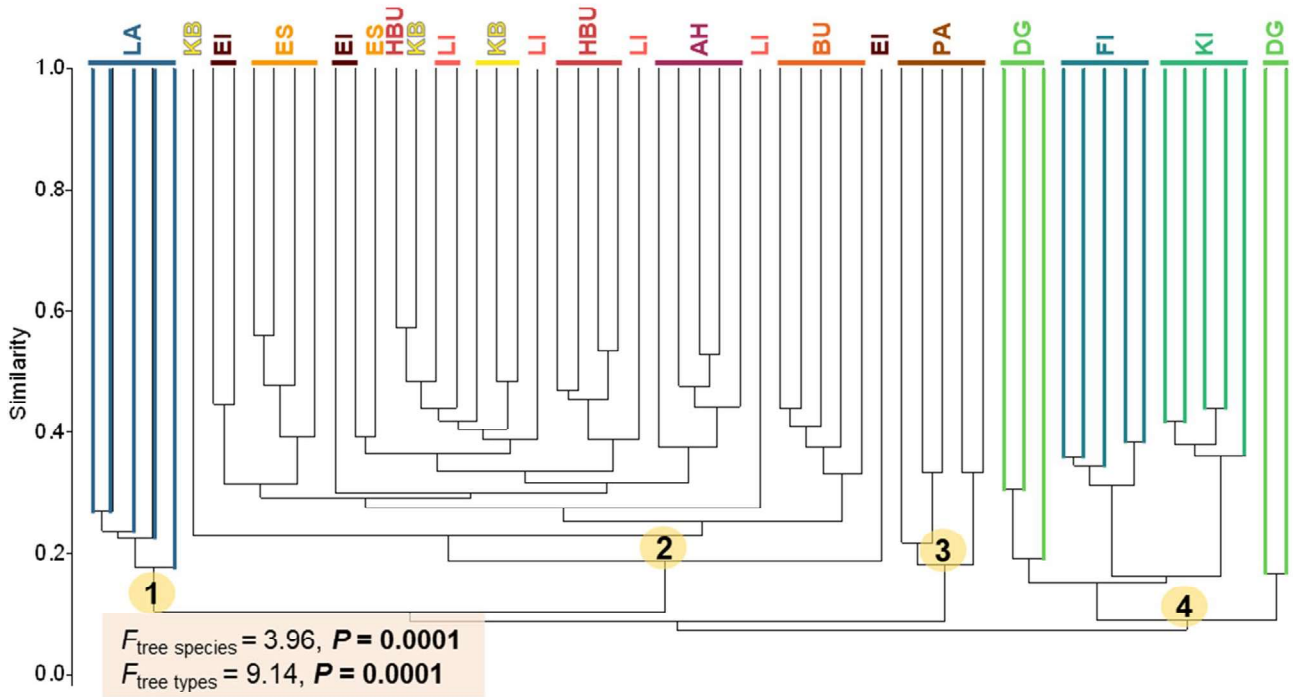
Saprotrophic fungi are among the most important fungal groups driving important ecosystem functions such as accelerating the decomposition rate, enabling the nutrients accessibility and availability for themselves and other microbes [51, 52]. FungalTraits assigns substantially higher number

of saprotrophic ASVs (89% of the total assigned saprotrophic ASVs) compared to FUNGuild (51% of the total assigned saprotrophic ASVs). The shared ASVs assigned by both annotation tools account to only ~41% of the total assigned saprotrophic ASVs and only moderate correlation is obtained (Pearson’s $r=0.63$, $P<0.001$). This is due to the reannotation process of the fungal genera in FungalTraits. Some changes are made to some specific fungal genera by the experts of the field during this process. Nevertheless, we detect similar patterns of factors that shape the saprotrophic community composition derived from both annotation tools. In both datasets, we found that tree species and tree type are the main factors that significantly shape saprotrophic community composition, along with water content and nutrients (water-leachable DOC amount, water-leachable organic and inorganic nitrogen species ($N_{NH_4^+}$, $N_{NO_3^-}$, N_{Min} , N_{Org}), Ca, Fe, Mg, and P content), and location. These findings are in line with previously published studies [53, 54]. The microbial macronutrients (such as C, N, and Ca) and transition metal (Fe) have been previously reported to shape the fungal community in different forest management practices [53]. These nutrients are essential elements in macromolecules and also required for many important enzymatic and metabolic processes which are important for microbial growth and activity [53]. In contrast to the results of saprotrophs, the shared ASVs of endophytes account only to 11% of the total assigned endophytic ASVs and no correlation is observed. Longitude is an additional main factor shaping the endophytic community composition of FUNGuild, while Ca and K content solely significantly correspond with those of FungalTraits. The different patterns of significant factors might lead to a different ecological interpretation of endophytes.

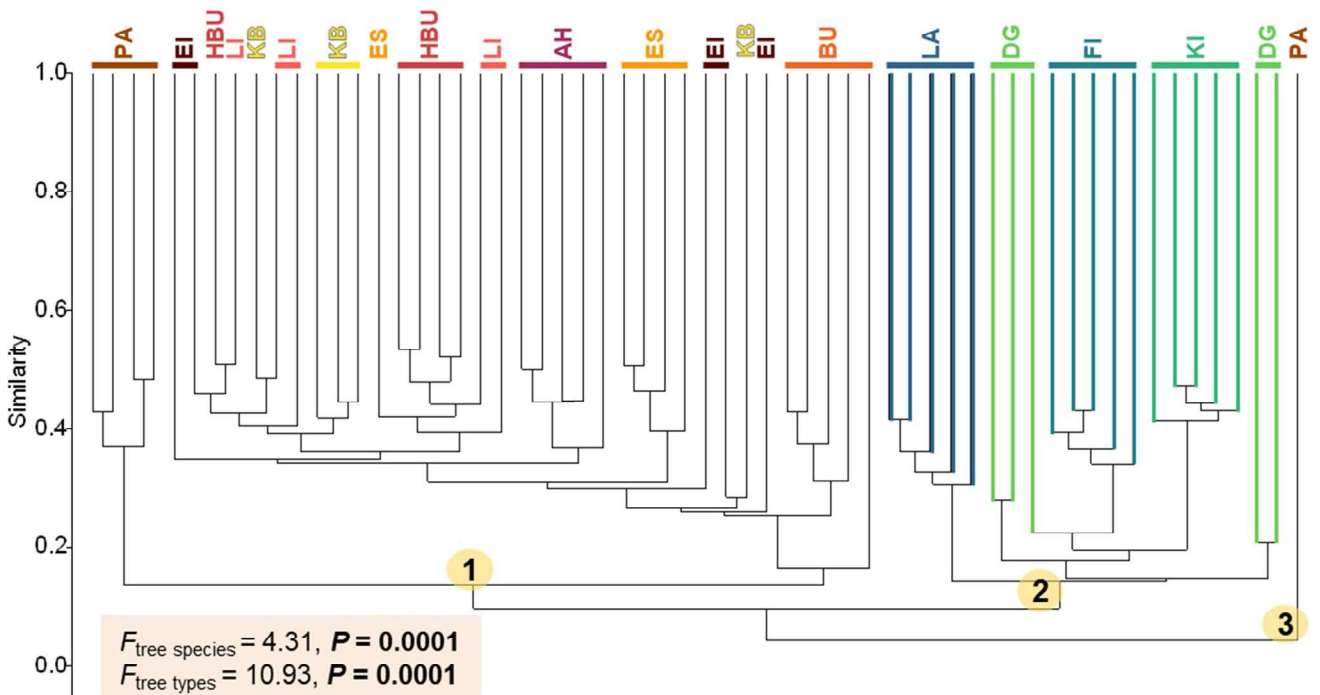
Unexpected High Diversity of Lichens Associated with Senescing Leaves and Needles: Implication and Future Study

In this study, we revealed a high diversity of lichens associated with senescing leaves and needles assigned by both FUNGuild and FungalTraits. In total, we are able to assign 60 lichenized fungal ASVs that were assigned to 21 genera. The proportion of lichenized fungal assignments obtained from both annotation tools is highly correlated and shared ASVs account to ~88% of the total assigned lichenized fungal ASVs. FUNGuild provides six more lichenized fungal ASV assignments compared to those of FungalTraits. Among these, four ASVs are not identified at genus level and functions are only assigned on family level. We found a potential controversial issue for the functional assignment of the genus *Sphaerulina* as FUNGuild classifies *Sphaerulina* as lichenized fungi with the confidence level “highly probable”, while FungalTraits assigns in the primary and

a) Saprotroph - FUNGuild



b) Saprotroph - FungalTraits



secondary lifestyles of this genus as “saprotroph” and “plant pathogen”, respectively. A recent study, however, reports *Sphaerulina* as lichenicolous fungi [55], while other studies

attributed them as plant pathogen [56, 57]. Therefore, careful double and crosschecking with published datasets is mandatory to verify database outputs especially at low confidence

Fig. 6 Community composition of saprotrophic fungi derived from FUNGuild (a) and FungalTraits (b) of five independent leaf/needle replicates. Yellow–red–brown color tone refers to the broadleaved tree species and blue–green color tone the coniferous tree species. Numbers in yellow circle indicate different clades in the dendrogram for saprotroph cluster analysis. Species abbreviations for broadleaved tree species are: AH: *Acer pseudoplatanus*, BU: *Fagus sylvatica*, EI: *Quercus robur*, ES: *Fraxinus excelsior*, HBU: *Carpinus betulus*, KB: *Prunus avium*, LI: *Tilia cordata*, and PA: *Populus sp.*, and coniferous tree species are: DG: *Pseudotsuga menziesii*, FI: *Picea abies*, KI: *Pinus sylvestris*, and LA: *Larix decidua*. Effects of tree species and tree types were tested with one-way PERMANOVA

level. FUNGuild provided information on growth morphology and habitat, while FungalTraits additionally provided information on fruitbody type, hymenium type, and primary photobiont of the assigned lichens. Most of the lichens (55 out of 60 ASVs) detected in this study are associated with senescing needles of coniferous tree species (Supplementary Table S1). We observed lichens on the branches of all coniferous tree species used in this study. Our work showed that lichens associated with senescing leaves and needles were both foliicolous lichens (their development starts directly on leaves or needles) and lichens that accidentally grow onto the leaves or needles from the bark of adjacent branches (their development does not start on leaves or needles) [58]. This current work sheds light solely on richness of lichens as influenced by tree species and tree types. Future studies should focus on the effects of tree species, tree types, leaf/needle physicochemical properties, and geographical distances on richness and community composition of lichens.

FUNGuild vs. FungalTraits: Similarities and Differences of the Assignments of Arbuscular and Ectomycorrhizal Fungi

Our present study emphasizes on the functional assignments and the performances of the annotation tools, FUNGuild and FungalTraits, in the leaf/needle-associated fungal communities. However, in nature, mycorrhizal fungi are also considered as important functional groups associated with plants and play crucial role in promoting their performances [59, 60]. Thus, for the sake of completeness, we further evaluate the functional assignment of arbuscular (AMF) and ectomycorrhizal (EcM) fungi using FUNGuild [21] and FungalTraits [29]. As AMF are mostly derived from the phylum Glomeromycota, we simply compare all 51 AMF genera from both annotation tools. All assigned AMF genera are covered by FungalTraits alone and 20 AMF genera from FungalTraits are absent from the FUNGuild database (Supplementary Table S7). These new 20 AMF genera are erected in previous studies published between the year 2018 and 2019 [61–64]. However, FUNGuild assigns AMF already at family, order, and phylum level (Glomeromycota). For the analysis of EcM, we employ a dataset from a recently published study investigating EcM in soils at different elevation levels (830 and 1300 m a.s.l) [65]. We assign 26 EcM genera by both annotation tools. FungalTraits covers all 26 EcM genera and FUNGuild assigns 25 EcM genera (Supplementary Figure S2). The fungal genus, *Pustularia*, cannot be assigned to the ecological function by FUNGuild. Members

Table 2 Goodness-of-fit statistics (R^2) of environmental variables fitted to the nonmetric multidimensional scaling (NMDS) ordination of saprotrophic and endophytic fungal community based on presence/absence data and Jaccard distance measure. Bold letter indicates statistical significances

	Saprotroph				Endophyte			
	FUNGuild		FungalTraits		FUNGuild		FungalTraits	
	R^2	P	R^2	P	R^2	P	R^2	P
Tree species	0.86	0.001	0.89	0.001	0.74	0.044	0.77	0.007
Tree type	0.51	0.001	0.61	0.001	0.01	0.886	0.08	0.304
Water content	0.11	0.042	0.14	0.020	0.02	0.949	0.15	0.339
pH	0.06	0.184	0.08	0.090	0.41	0.213	0.19	0.199
DOC	0.50	0.001	0.54	0.001	0.15	0.613	0.26	0.107
$N_{NH_4^+}$	0.15	0.008	0.23	0.004	0.19	0.538	0.20	0.202
$N_{NO_2^-}$	0.42	0.001	0.41	0.001	0.05	0.843	0.10	0.469
$N_{NO_3^-}$	0.04	0.311	0.03	0.317	ND	ND	0.25	0.218
N_{Min}	0.16	0.008	0.20	0.006	0.15	0.607	0.26	0.151
N_{Org}	0.36	0.001	0.40	0.001	0.03	0.935	0.30	0.085
Ca	0.50	0.001	0.53	0.001	0.01	0.956	0.39	0.016
Fe	0.15	0.009	0.20	0.001	0.03	0.929	0.03	0.808
K	0.01	0.695	0.04	0.329	0.59	0.074	0.44	0.017
Mg	0.26	0.003	0.31	0.001	0.12	0.708	0.31	0.059
P	0.30	0.001	0.31	0.001	0.68	0.034	0.40	0.018
Latitude	0.65	0.001	0.66	0.001	0.02	0.938	0.14	0.296
Longitude	0.17	0.007	0.15	0.010	0.87	0.004	0.24	0.124

of this genus were previously reported as EcM [66, 67]. Nevertheless, both annotation tools refer to the same ecological interpretation (Supplementary Figure S2). The richness and community composition of EcM significantly differ at different elevation levels. On the basis of this information, we conclude that the performances of FUNGuild and FungalTraits in assigning AMF and EcM are not different.

Conclusions

Functional assignment of fungal amplicon sequencing datasets is of pivotal interest to infer a more mechanistic understanding of phylogenetic information and to ease the assessment of ecosystem processes of the respective habitat. The quantity and quality of fungal functional annotations were significantly better in FungalTraits than in FunGuild for evaluating the functional guilds on senescing leaves and needles of 12 temperate tree species. The transferability to other environments and research tasks should be addressed in upcoming studies.

Supplementary Information The online version contains supplementary material available at <https://doi.org/10.1007/s00248-022-01973-2>.

Acknowledgements The community composition data have been computed at the High-Performance Computing (HPC) Cluster EVE, a joint effort of both the Helmholtz Centre for Environmental Research—UFZ and the German Centre for Integrative Biodiversity Research (iDiv) Halle-Jena-Leipzig. We thank Beatrix Schnabel and Melanie Günther for their help with Illumina sequencing. Li Ji appreciates the financial support by the China Scholarship Council (No. 20190660038).

Author Contribution WP and EDS conceived and designed the study. BT, WP, EDS, SH, YD, and SW collected the samples and metadata. WP and FB contributed reagents and laboratory equipment. BT, WP, and SW led the DNA analysis. SW led bioinformatics. BT, LJ, and WP led the microbial taxonomy and data analyses. SS, IH, GG, ASL, and EGA led the physicochemical analyses. BT, LJ, MN, and WP wrote the manuscript. MN and WP supervised BT. MN, EDS, and FB reviewed and gave comments and suggestions for manuscript. All of the authors gave final approval for manuscript submission.

Funding Open Access funding enabled and organized by Projekt DEAL. This work has been partially funded by the internal research budget to Department of Soil Ecology, UFZ-Helmholtz Centre for Environmental Research.

Data availability The ITS rRNA gene sequences were deposited in the National Center for Biotechnology Information (NCBI) Sequence Read Archive under the accession number PRJNA753096.

Declarations

Institutional Review Board Statement Ethical review and approval were waived for this study as ethical considerations of humans or animals were not addressed.

Informed Consent Statement Not applicable.

Conflict of Interest The authors declare no competing interests.

Open Access This article is licensed under a Creative Commons Attribution 4.0 International License, which permits use, sharing, adaptation, distribution and reproduction in any medium or format, as long as you give appropriate credit to the original author(s) and the source, provide a link to the Creative Commons licence, and indicate if changes were made. The images or other third party material in this article are included in the article's Creative Commons licence, unless indicated otherwise in a credit line to the material. If material is not included in the article's Creative Commons licence and your intended use is not permitted by statutory regulation or exceeds the permitted use, you will need to obtain permission directly from the copyright holder. To view a copy of this licence, visit <http://creativecommons.org/licenses/by/4.0/>.

References

- van der Heijden MGA, Klironomos JN, Ursic M et al (1998) Mycorrhizal fungal diversity determines plant biodiversity, ecosystem variability and productivity. *Nature* 396:69–72. <https://doi.org/10.1038/23932>
- Osono T (2011) Diversity and functioning of fungi associated with leaf litter decomposition in Asian forests of different climatic regions. *Fungal Ecol* 4:375–385. <https://doi.org/10.1016/j.funeco.2011.02.004>
- Bani A, Pioli S, Ventura M et al (2018) The role of microbial community in the decomposition of leaf litter and deadwood. *Appl Soil Ecol* 126:75–84. <https://doi.org/10.1016/j.apsoil.2018.02.017>
- Purahong W, Wubet T, Lentendu G, et al (2018) Determinants of deadwood-inhabiting fungal communities in temperate forests: molecular evidence from a large scale deadwood decomposition experiment. *Front Microbiol* 9. <https://doi.org/10.3389/fmicb.2018.02120>
- Joly F-X, Fromin N, Kiikkilä O, Hättenschwiler S (2016) Diversity of leaf litter leachates from temperate forest trees and its consequences for soil microbial activity. *Biogeochemistry* 129:373–388. <https://doi.org/10.1007/s10533-016-0239-z>
- Chapman SK, Newman GS, Hart SC et al (2013) Leaf litter mixtures alter microbial community development: mechanisms for non-additive effects in litter decomposition. *PLoS ONE* 8:e62671. <https://doi.org/10.1371/journal.pone.0062671>
- Baldrian P, Kolařík M, Štursová M et al (2012) Active and total microbial communities in forest soil are largely different and highly stratified during decomposition. *ISME J* 6:248–258. <https://doi.org/10.1038/ismej.2011.95>
- Clemmensen KE, Finlay RD, Dahlberg A et al (2015) Carbon sequestration is related to mycorrhizal fungal community shifts during long-term succession in boreal forests. *New Phytol* 205:1525–1536. <https://doi.org/10.1111/nph.13208>
- Bödeker ITM, Lindahl BD, Olson Å, Clemmensen KE (2016) Mycorrhizal and saprotrophic fungal guilds compete for the same organic substrates but affect decomposition differently. *Funct Ecol* 30:1967–1978. <https://doi.org/10.1111/1365-2435.12677>
- Shigyo N, Hirao T (2021) Saprotrophic and ectomycorrhizal fungi exhibit contrasting richness patterns along elevational gradients in cool-temperate montane forests. *Fung Ecol* 50:101036. <https://doi.org/10.1016/j.funeco.2020.101036>
- Fernandez CW, Kennedy PG (2016) Revisiting the ‘Gadgil effect’: do interguild fungal interactions control carbon cycling in forest soils? *New Phytol* 209:1382–1394. <https://doi.org/10.1111/nph.13648>

12. Bhatnagar JM, Peay KG, Treseder KK (2018) Litter chemistry influences decomposition through activity of specific microbial functional guilds. *Ecol Monogr* 88:429–444. <https://doi.org/10.1002/ecm.1303>
13. Kohout P, Charvátová M, Štursová M et al (2018) Clearcutting alters decomposition processes and initiates complex restructuring of fungal communities in soil and tree roots. *ISME J* 12:692–703. <https://doi.org/10.1038/s41396-017-0027-3>
14. Baldrian P (2017) Forest microbiome: diversity, complexity and dynamics. *FEMS Microbiol Rev* 41:109–130. <https://doi.org/10.1093/femsre/fuw040>
15. Otsing E, Barantal S, Anslan S et al (2018) Litter species richness and composition effects on fungal richness and community structure in decomposing foliar and root litter. *Soil Biol Biochem* 125:328–339. <https://doi.org/10.1016/j.soilbio.2018.08.006>
16. Triebel D, Peršoh D, Nash TH, et al (2007) LIAS — an interactive database system for structured descriptive data of Ascomycetes. In: *Biodiversity Databases*. CRC Press
17. Rambold G, Zedda L, Coyle JR et al (2016) Geographic heat maps of lichen traits derived by combining LIAS light description and GBIF occurrence data, provided on a new platform. *Biodivers Conserv* 25:2743–2751. <https://doi.org/10.1007/s10531-016-1199-2>
18. Agerer R., Rambold G. (2021) DEEMY – An information system for characterization and determination of ectomycorrhizae. [first posted on 2004–06–01; most recent update: 2011–01–10]. In: DEEMY. www.deemy.de
19. Zanne AE, Abarenkov K, Afkhami ME et al (2020) Fungal functional ecology: bringing a trait-based approach to plant-associated fungi. *Biol Rev* 95:409–433. <https://doi.org/10.1111/brv.12570>
20. Guerreiro MA, Wijayawardene N, Hyde K, Peršoh D (2018) Ecology of Ascomycete genera – a searchable compilation of “Notes on genera: Ascomycota.” *Asian Journal of Mycology* 1:146–150
21. Nguyen NH, Song Z, Bates ST et al (2016) FUNGuild: an open annotation tool for parsing fungal community datasets by ecological guild. *Fungal Ecol* 20:241–248. <https://doi.org/10.1016/j.funeco.2015.06.006>
22. Jayasiri SC, Hyde KD, Ariyawansa HA et al (2015) The Faces of Fungi database: fungal names linked with morphology, phylogeny and human impacts. *Fung Div* 74:3–18. <https://doi.org/10.1007/s13225-015-0351-8>
23. Talbot JM, Martin F, Kohler A et al (2015) Functional guild classification predicts the enzymatic role of fungi in litter and soil biogeochemistry. *Soil Biol Biochem* 88:441–456
24. Zhao D, Shen F, Zeng J et al (2016) Network analysis reveals seasonal variation of co-occurrence correlations between Cyanobacteria and other bacterioplankton. *Sci Total Environ* 573:817–825. <https://doi.org/10.1016/j.scitotenv.2016.08.150>
25. Luis P, Saint-Genis G, Vallon L et al (2019) Contrasted ecological niches shape fungal and prokaryotic community structure in mangroves sediments. *Environ Microbiol* 21:1407–1424. <https://doi.org/10.1111/1462-2920.14571>
26. Schmidt R, Mitchell J, Scow K (2019) Cover cropping and no-till increase diversity and symbiotroph:saprotroph ratios of soil fungal communities. *Soil Biol Biochem* 129:99–109. <https://doi.org/10.1016/j.soilbio.2018.11.010>
27. Gallardo CA, Baldrian P, López-Mondéjar R (2020) Litter-inhabiting fungi show high level of specialization towards biopolymers composing plant and fungal biomass. *Biol Fertil Soils* 57:77–88
28. Ji L, Yang Y, Yang L (2021) Seasonal variations in soil fungal communities and co-occurrence networks along an altitudinal gradient in the cold temperate zone of China: a case study on Oakley Mountain. *CATENA* 204:105448. <https://doi.org/10.1016/j.catena.2021.105448>
29. Pöhlme S, Abarenkov K, Henrik Nilsson R et al (2020) Fungal-Traits: a user-friendly traits database of fungi and fungus-like stramenopiles. *Fungal Diversity* 105:1–16. <https://doi.org/10.1007/s13225-020-00466-2>
30. Weißbecker C, Schnabel B, Heintz-Buschart A (2020) Dadasnake, a Snakemake implementation of DADA2 to process amplicon sequencing data for microbial ecology. *GigaScience* 9 <https://doi.org/10.1093/gigascience/giaa135>
31. Ihrmark K, Bödeker ITM, Cruz-Martinez K et al (2012) New primers to amplify the fungal ITS2 region – evaluation by 454-sequencing of artificial and natural communities. *FEMS Microbiol Ecol* 82:666–677. <https://doi.org/10.1111/j.1574-6941.2012.01437.x>
32. White TJ, Bruns TD, Lee S, Taylor J (1990) Amplification and direct sequencing of fungal ribosomal RNA genes for phylogenetics. In: Innis MA, Gelfand DH, Sninsky JJ, White TJ (eds) *PCR protocols: A guide to methods and applications*. Academic Press, San Diego, pp 315–322
33. Martin M (2011) Cutadapt removes adapter sequences from high-throughput sequencing reads. *EMBnet.journal* 17:10–12. <https://doi.org/10.14806/ej.17.1.200>
34. Callahan BJ, McMurdie PJ, Rosen MJ et al (2016) DADA2: High-resolution sample inference from Illumina amplicon data. *Nat Methods* 13:581–583. <https://doi.org/10.1038/nmeth.3869>
35. Kõljalg U, Nilsson RH, Abarenkov K et al (2013) Towards a unified paradigm for sequence-based identification of fungi. *Mol Ecol* 22:5271–5277. <https://doi.org/10.1111/mec.12481>
36. Callahan BJ, McMurdie PJ, Holmes SP (2017) Exact sequence variants should replace operational taxonomic units in marker-gene data analysis. *ISME J* 11:2639–2643. <https://doi.org/10.1038/ismej.2017.119>
37. Hammer Ø, Harper DAT, Ryan PD (2001) PAST: paleontological statistics software package for education and data analysis. *Palaeontol Electron* 4:9
38. Prada-Salcedo LD, Goldmann K, Heintz-Buschart A et al (2021) Fungal guilds and soil functionality respond to tree community traits rather than to tree diversity in European forests. *Mol Ecol* 30:572–591. <https://doi.org/10.1111/mec.15749>
39. Wahdan SFM, Heintz-Buschart A, Sansupa C, et al (2021) Targeting the active rhizosphere microbiome of *Trifolium pratense* in grassland evidences a stronger-than-expected belowground biodiversity-ecosystem functioning link. *Front Microbiol* 12 <https://doi.org/10.3389/fmicb.2021.629169>
40. Weißbecker C, Wubet T, Lentendu G, et al (2018) Experimental evidence of functional group-dependent effects of tree diversity on soil fungi in subtropical forests. *Front Microbiol* 9 <https://doi.org/10.3389/fmicb.2018.02312>
41. Nawaz A, Purahong W, Lehmann R et al (2018) First insights into the living groundwater mycobiome of the terrestrial biogeosphere. *Water Res* 145:50–61. <https://doi.org/10.1016/j.watres.2018.07.067>
42. Nawaz A, Purahong W, Lehmann R, et al (2016) Superimposed pristine limestone aquifers with marked hydrochemical differences exhibit distinct fungal communities. *Front Microbiol* 6 <https://doi.org/10.3389/fmicb.2016.00666>
43. Wang P, Chen Y, Sun Y, et al (2019) Distinct biogeography of different fungal guilds and their associations with plant species richness in forest ecosystems. *Front Ecol Evol* 7 <https://doi.org/10.3389/fevo.2019.00216>
44. Lepinay C, Jirásková L, Tláškal V et al (2021) Successional development of fungal communities associated with decomposing deadwood in a natural mixed temperate forest. *J Fungi* 7:412. <https://doi.org/10.3390/jof7060412>
45. Wang D, Jacquemyn H, Gomes SIF et al (2021) Symbiont switching and trophic mode shifts in Orchidaceae. *New Phytol* 231:791–800. <https://doi.org/10.1111/nph.17414>
46. Purahong W, Hossen S, Nawaz A, et al (2021) Life on the rocks: first insights into the microbiota of the threatened aquatic

- rheophyte *Hanseniella heterophylla*. *Front Plant Sci* 12:https://doi.org/10.3389/fpls.2021.634960
47. Ottosson E, Kubartová A, Edman M et al (2015) Diverse ecological roles within fungal communities in decomposing logs of *Picea abies*. *FEMS Microbiol Ecol* 91:fiv012. <https://doi.org/10.1093/femsec/fiv012>
 48. Sansupa C, Wahdan SFM, Hossen S et al (2021) Can we use Functional Annotation of Prokaryotic Taxa (FAPROTAX) to assign the ecological functions of soil bacteria? *Appl Sci* 11:688. <https://doi.org/10.3390/app11020688>
 49. Ryu M, Mishra RC, Jeon J et al (2018) Drought-induced susceptibility for *Cenangium ferruginosum* leads to progression of *Cenangium* -dieback disease in *Pinus koraiensis*. *Sci Rep* 8:16368. <https://doi.org/10.1038/s41598-018-34318-6>
 50. Wrzosek M, Ruskiewicz-Michalska M, Sikora K et al (2017) The plasticity of fungal interactions. *Mycol Progress* 16:101–108. <https://doi.org/10.1007/s11557-016-1257-x>
 51. Fang M, Liang M, Liu X et al (2020) Abundance of saprotrophic fungi determines decomposition rates of leaf litter from arbuscular mycorrhizal and ectomycorrhizal trees in a subtropical forest. *Soil Biol Biochem* 149:107966. <https://doi.org/10.1016/j.soilbio.2020.107966>
 52. Marañón-Jiménez S, Radujković D, Verbruggen E et al (2021) Shifts in the abundances of saprotrophic and ectomycorrhizal fungi with altered leaf litter inputs. *Front Plant Sci* 12:1452. <https://doi.org/10.3389/fpls.2021.682142>
 53. Purahong W, Kapturska D, Pecyna MJ et al (2015) Effects of forest management practices in temperate beech forests on bacterial and fungal communities involved in leaf litter degradation. *Microb Ecol* 69:905–913. <https://doi.org/10.1007/s00248-015-0585-8>
 54. Prescott CE, Grayston SJ (2013) Tree species influence on microbial communities in litter and soil: Current knowledge and research needs. *For Ecol Manage* 309:19–27. <https://doi.org/10.1016/j.foreco.2013.02.034>
 55. Diederich P, Lawrey JD, Ertz D (2018) The 2018 classification and checklist of lichenicolous fungi, with 2000 non-lichenized, obligately lichenicolous taxa. *bryo* 121:340–425. <https://doi.org/10.1639/0007-2745-121.3.340>
 56. Qin R, LeBoldus JM (2014) The infection biology of *Sphaerulina musiva*: clues to understanding a forest pathogen. *PLoS ONE* 9:e103477. <https://doi.org/10.1371/journal.pone.0103477>
 57. Søndreli KL, Keriö S, Frost K et al (2020) Outbreak of *Septoria* Canker caused by *Sphaerulina musiva* on *Populus trichocarpa* in Eastern Oregon. *Plant Dis* 104:3266–3266. <https://doi.org/10.1094/PDIS-03-20-0494-PDN>
 58. Lücking R, Wirth V, Ahrens M (2009) Foliicolous lichens in the black forest, Southwest-Germany. *Carolinaea* 67:23–31
 59. Jiang Y, Luan L, Hu K et al (2020) Trophic interactions as determinants of the arbuscular mycorrhizal fungal community with cascading plant-promoting consequences. *Microbiome* 8:142. <https://doi.org/10.1186/s40168-020-00918-6>
 60. Kurth F, Zeitler K, Feldhahn L et al (2013) Detection and quantification of a mycorrhization helper bacterium and a mycorrhizal fungus in plant-soil microcosms at different levels of complexity. *BMC Microbiol* 13:205. <https://doi.org/10.1186/1471-2180-13-205>
 61. Baltruschat H, Santos VM, da Silva DKA et al (2019) Unexpectedly high diversity of arbuscular mycorrhizal fungi in fertile Chernozem croplands in Central Europe. *CATENA* 182:104135. <https://doi.org/10.1016/j.catena.2019.104135>
 62. Błaszczowski J, Niezgoda P, Goto BT, Kozłowska A (2018) *Halonatospora* gen. nov. with *H. pansihalos* comb. nov. and *Glomus bareae* sp. nov. (Glomeromycota; Glomeraceae). *Botany* 96:737–748. <https://doi.org/10.1139/cjb-2018-0107>
 63. Walker C, Gollotte A, Redecker D (2018) A new genus, *Planticonsortium* (Mucoromycotina), and new combination (*P. tenue*), for the fine root endophyte, *Glomus tenue* (basonym *Rhizophagus tenuis*). *Mycorrhiza* 28:213–219. <https://doi.org/10.1007/s00572-017-0815-7>
 64. Błaszczowski J, Niezgoda P, de Paiva JN et al (2019) *Sieverdingia* gen. nov., *S. tortuosa* comb. nov., and *Diversispora peloponnesiaca* sp. nov. in the Diversisporaceae (Glomeromycota). *Mycol Progress* 18:1363–1382. <https://doi.org/10.1007/s11557-019-01534-x>
 65. Ji L, Shen F, Liu Y et al (2022) Contrasting altitudinal patterns and co-occurrence networks of soil bacterial and fungal communities along soil depths in the cold-temperate montane forests of China. *CATENA* 209:105844. <https://doi.org/10.1016/j.catena.2021.105844>
 66. Tedersoo L, Arnold AE, Hansen K (2013) Novel aspects in the life cycle and biotrophic interactions in Pezizomycetes (Ascomycota, Fungi). *Mol Ecol* 22:1488–1493. <https://doi.org/10.1111/mec.12224>
 67. Rudawska M, Leski T (2021) Ectomycorrhizal fungal assemblages of nursery-grown Scots pine are influenced by age of the seedlings. *Forests* 12:134. <https://doi.org/10.3390/f12020134>

Litter 1 – Supplementary Information

FungalTraits vs. FUNGuild: Comparison of ecological functional assignments of leaf- and needle-associated fungi across 12 temperate tree species

Author: Benjawan Tanunchai*, Li Ji*, Simon Andreas Schroeter, Sara Fareed Mohamed Wahdan, Shakhawat Hossen, Yoseph Delelegn, François Buscot, Ann-Sophie Lehnert, Eliane Gomes Alves, Ines Hilke, Gerd Gleixner, Ernst-Detlef Schulze, Matthias Noll & Witoon Purahong

*These authors contributed equally to this work.

Status: Published

Publication: Microbial Ecology

Publisher: Springer Nature

Date: 5 Feb 2022

Copyright © 2022, The Author(s)

Reprinted with permission from Springer Nature.

Available online at: <https://doi.org/10.1007/s00248-022-01973-2>

Or please see separate attachments



OPEN ACCESS

EDITED BY

Xiangming Xu,
National Institute of Agricultural
Botany (NIAB), United Kingdom

REVIEWED BY

Yongqi Shao,
Zhejiang University, China
Yu Fukasawa,
Tohoku University, Japan



*CORRESPONDENCE

Witoon Purahong
witoon.purahong@ufz.de
François Buscot
francois.buscot@ufz.de

†These authors have contributed
equally to this work

SPECIALTY SECTION

This article was submitted to
Plant Pathogen Interactions,
a section of the journal
Frontiers in Plant Science

RECEIVED 13 June 2022

ACCEPTED 05 October 2022

PUBLISHED xx xx 2022

CITATION

Tanunchai B, Ji L, Schroeter SA,
Wahdan SFM, Larpkern P, Lehnert A-S,
Alves EG, Gleixner G, Schulze E-D,
Noll M, Buscot F and Purahong W
(2022) A poisoned apple: First
insights into community assembly
and networks of the fungal
pathobiome of healthy-looking
senescing leaves of temperate
trees in mixed forest ecosystem.
Front. Plant Sci. 13:968218.
doi: 10.3389/fpls.2022.968218

COPYRIGHT

© 2022 Tanunchai, Ji, Schroeter,
Wahdan, Larpkern, Lehnert, Alves,
Gleixner, Schulze, Noll, Buscot and
Purahong. This is an open-access article
distributed under the terms of the
Creative Commons Attribution License
(CC BY). The use, distribution or
reproduction in other forums is
permitted, provided the original
author(s) and the copyright owner(s)
are credited and that the original
publication in this journal is cited, in
accordance with accepted academic
practice. No use, distribution or
reproduction is permitted which does
not comply with these terms.

A poisoned apple: First insights into community assembly and networks of the fungal pathobiome of healthy-looking senescing leaves of temperate trees in mixed forest ecosystem

Benjawan Tanunchai^{1,2†}, Li Ji^{1,3†}, Simon Andreas Schroeter⁴, Sara Fareed Mohamed Wahdan^{1,5}, Panadda Larpkern⁶, Ann-Sophie Lehnert⁴, Eliane Gomes Alves⁴, Gerd Gleixner⁴, Ernst-Detlef Schulze⁴, Matthias Noll^{2,7}, François Buscot^{1,8*} and Witoon Purahong^{1*}

¹UFZ-Helmholtz Centre for Environmental Research, Department of Soil Ecology, Halle (Saale), Germany, ²Bayreuth Center of Ecology and Environmental Research (BayCEER), University of Bayreuth, Bayreuth, Germany, ³School of Forestry, Central South of Forestry and Technology, Changsha, China, ⁴Max Planck Institute for Biogeochemistry, Biogeochemical Processes Department, Jena, Germany, ⁵Department of Botany and Microbiology, Faculty of Science, Suez Canal University, Ismailia, Egypt, ⁶Bodhivijjalaya College, Srinakharinwirot University, Nakhon Nayok, Thailand, ⁷Institute for Bioanalysis, Coburg University of Applied Sciences and Arts, Coburg, Germany, ⁸German Centre for Integrative Biodiversity Research (iDiv), Halle-Jena-Leipzig, Leipzig, Germany

Despite the abundance of observations of foliar pathogens, our knowledge is severely lacking regarding how the fungal pathobiome is structured and which processes determine community assembly. In this study, we addressed these questions by analysing the fungal pathobiome associated with the senescing leaves and needles of 12 temperate tree species. We compared fungal pathogen load in the senescing leaves and demonstrated that healthy-looking leaves are inhabited by diverse and distinct fungal pathogens. We detected 400 fungal pathogenic ASVs belonging to 130 genera. The pathogenic generalist, *Mycosphaerella*, was found to be the potential most significant contributor to foliar disease in seedlings. The analyses of assembly process and co-occurrence network showed that the fungal pathogenic communities in different tree types are mainly determined by stochastic processes. However, the homogenising dispersal highly contributes in broadleaf trees, whereas ecological drift plays an important role in conifer trees. The deterministic assembly processes (dominated by variable selection) contributed more in broadleaf trees as compared to coniferous trees. We found that pH and P levels significantly correspond with fungal pathogenic community compositions in both tree types. Our study provides the first insight and mechanistic understanding into the community assembly, networks, and

complete taxonomy of the foliar fungal pathobiome in senescing leaves and needles.

KEYWORDS

foliar fungal pathogens, next generation sequencing, deterministic processes, stochastic processes, homogenising dispersal, ecological drift

Q5

Q6 Introduction

Mixed forest ecosystems have recently received considerable attention due to their advantages over monospecific forests in the context of global climate change but also in relation with both economic and ecological aspects (Clasen et al., 2011; Gamfeldt et al., 2013; Almeida et al., 2018). Mixed forests have been reported to have a better risk–return relation compared to monocultures, which are associated with higher risks and lower returns (Clasen et al., 2011). The net present value (defined as appropriately discounted and summed net revenues gained or caused by the management) of mixed beech forests can reach the annual gains up to 113 € ha⁻¹ yr⁻¹ as compared with 72 € ha⁻¹ yr⁻¹ for beech monocultures (Clasen et al., 2011). In addition to this economic perspective, mixed forests, especially those based on natural regeneration (forests that are allowed to maintain natural growth cycles with minimal human intervention), exhibit ecological advantages over monospecific forests, including promoting biodiversity and ecosystem functions, maintaining tree genetic diversity, increasing resilience to climate change, and enhancing high resistance to biotic and abiotic hazards (Griess et al., 2012; Almeida et al., 2018; Ehbrecht et al., 2021). To date, mixed forest ecosystem covers more than 200 million ha worldwide or about 5% of the global forest area (FAO and UNEP, 2020). In Germany, the mixed forest area increased to ~58% of the total forest area in 2012 (Wilke, 2017).

In mixed forest ecosystems, niche partitioning and competitions (intra- and interspecific competitions) play important roles in shaping tree species community composition and diversity. The sources for fungal leaf pathogens are shedding leaves and/or fungal bodies of pathogenic fungi (Sánchez Márquez et al., 2011; Bayandala et al., 2016). Senescing leaves may attract diverse fungal functional groups, including fungal pathogens (Tanunchai et al., 2022). However, such knowledge in temperate tree species, including their taxonomy, assembly processes, specificity and factors corresponding to their community composition, is still largely unexplored. For evergreen coniferous trees, senescing leaves shed over the year and thus represent continuous input of fungal pathogens to the soil system. Conversely, senescing leaves of coniferous and broadleaves

deciduous trees mainly shed during autumn, creating a large seasonal wave of fungal pathogens into the soil system. Interactions among microbial taxa can be complex as different taxa can express antagonistic, competitive, or mutualistic interactions (Montoya et al., 2006; Deng et al., 2012; Tyc et al., 2014). Investigating interactions among different microbial taxa within a community and their responses to environmental changes enables a better understanding of ecological mechanisms and outcomes (Sheng et al., 2019). To achieve this comprehensive analytic perspective, ecological network approaches have been intensively applied to investigate the complexity of interactions among different microbial taxa (Montoya et al., 2006; Deng et al., 2012; Toju et al., 2014). In general, environmental filtering by mean of substrate physicochemical properties is considered as a main process shaping the community in plant debris (Purahong et al., 2016); however, the community assembly may be largely explained by stochastic processes (Abrego, 2021). This issue has never been addressed for the senescing leaves of diverse temperate tree species.

Despite the importance of foliar fungal pathogens in regulating tree diversity and community composition in temperate forests, our knowledge of their ecology and community assembly remains limited. Specifically, it remains unclear which factors shape foliar fungal pathobiome community composition, which processes (stochastic vs. deterministic) determine their community assembly, and how their community structure is organized. In this study, we used a high–resolution molecular approach (Next Generation Sequencing) to obtain a better understanding of the fungal pathobiome of healthy-looking senescing leaves among 12 temperate tree species growing in a managed mixed forest at the Central Germany. We aimed to determine (i) which ecological processes determine the pathobiome community assembly, (ii) how foliar fungal pathobiome communities are structured, (iii) which factors determine richness and community composition of the foliar fungal pathogens, and (iv) which tree species that act as fungal pathogen hub in this forest ecosystem.

Materials and methods

Study site and sampling

The study site is located in a managed mixed forest of Thuringia, Germany (51°12'N 10°18'E) and is characterized by mean annual precipitation from 600 to 800 mm, mean annual temperature from 6 to 7.5°C, and elevations from 100 to 494 m above sea level. The main soil type is Cambisol on limestone as bed-rock. The soil pH is weakly acidic (5.1 ± 1.1 ; mean \pm SD). In October 2019, a minimum 200-g healthy-looking senescing leaves and needles of 12 mature tree species (5 true replicates/tree individual per tree species, in total 60 samples) were collected in a separate sterile plastic bag with new clean gloves. In this current study, we characterized the healthy-looking senescing leaf as green leaves without visible leaf disease symptoms from branches at the lower part of the crown of the mature tree (3 years old). These 12 tree species include 8 deciduous broadleaf (including *Acer pseudoplatanus*, *Carpinus betulus*, *Fagus sylvatica*, *Fraxinus excelsior*, *Populus hybrid.*, *Prunus avium*, *Quercus robur*, and *Tilia cordata*), 3 evergreen (including *Picea abies*, *Pinus sylvestris*, and *Pseudotsuga menziesii*), and 1 deciduous (*Larix decidua*) coniferous tree species. Leaf samples were transported on ice to the laboratory within 3 h and stored at -80°C for further analysis.

Q11

DNA extraction and illumina sequencing

To prepare for deoxyribonucleic acid (DNA) extraction, up to 10 healthy-looking leaves and needles from 5 branches per individual tree were subsampled. Leaf and needle samples were washed three times with 0.1% sterile Tween to remove loosely attached dust particles. The samples were then washed three to five times using deionized water and incubated for 1 h in sterile water to remove the Tween bubbles. By washing leaves with Tween solution, the endophytic and strongly attached epiphytic microorganisms were subjected to the DNA extraction. Leaf and needle samples were ground using liquid nitrogen and sterile nails, homogenized, and stored at -20°C for further analysis. The DNA extraction of senescing leaves and needles and associated microbes was performed using DNeasy PowerSoil Kit (Qiagen, Hilden, Germany) and a Precellys 24 tissue homogenizer (Bertin Instruments, Montigny-le-Bretonneux, France) according to the manufacturer's instructions. The presence and quantity of genomic DNA was checked using NanoDrop ND-1000 spectrophotometer (Thermo Fisher Scientific, Dreieich, Germany), and the extracts were stored at -20°C .

Leaf-associated fungi were characterized by fungal internal transcribed spacer (ITS)-based amplicon sequencing on the Illumina MiSeq sequencing platform, as outlined previously [34]. To establish fungal amplicon libraries, the fungal ITS2

gene was amplified using the fungal primer pair fITS7 [5'-GTGARTCATCGAATCTTTG-3'] (Ihrmark et al., 2012) and ITS4 [5'-TCCTCCGCTTATTGATATGC-3'] (White et al., 1990) with Illumina adapter sequences. Amplifications were performed using 20- μL reaction volumes with 5 \times HOT FIRE Pol Blend Master Mix (Solis BioDyne, Tartu, Estonia). The amplified products were visualized by gel electrophoresis and purified using an Agencourt AMPure XP kit (Beckman Coulter, Krefeld, Germany). Illumina Nextera XT Indices were added to both ends of the fungal amplicons. The products from three technical replicates were then pooled in equimolar concentrations. Paired-end sequencing (2×300 base pair (bp)) was performed on the pooled polymerase chain reaction (PCR) products using a MiSeq Reagent kit v3 on an Illumina MiSeq system (Illumina Inc., San Diego, CA, United States) at the Department of Soil Ecology, Helmholtz Centre for Environmental Research, Germany. The ITS ribosomal ribonucleic acid (rRNA) gene sequences are deposited in the National Center for Biotechnology Information (NCBI) Sequence Read Archive under the accession number PRJNA753096.

Bioinformatics

The ITS ribosomal DNA (rDNA) sequences corresponding to the forward and reverse primers were trimmed from the demultiplexed raw reads using cutadapt (Martin, 2011). Paired-end sequences were quality-trimmed, filtered for chimeras, and merged using the DADA2 package (Callahan et al., 2016) through the dada-snake pipeline (Weißbecker et al., 2020). Assembled reads fulfilling the following criteria were retained for further analysis: a minimum length of 70 nucleotides (nt), quality scores at least equal to 9 with maximum expected error score of 5 for forward and reverse sequences and no ambiguous nucleotides. Merging was conducted with an allowance for 2 mismatches and a minimum overlap of 20 nt required for fungal sequences. High-quality reads of fungi were clustered into 2480 amplicon sequence variants (ASVs) after chimera removal. Fungal ASVs were classified against the UNITE v7.2 database (Kõljalg et al., 2013). ASV sets were classified using the Bayesian classifier (Wang et al., 2007) in the mothur classify.seqs command with a cut-off of 60. The ASV method was used to infer biological sequences in the sample, as described previously (Callahan et al., 2017). Rare ASVs (singletons), which may represent artificial sequences, were removed. After, 2,451 fungal ASVs with minimum sequencing depths of 21,967 sequences per sample were obtained. We used a Mantel test based on Bray–Curtis distance measure with 999 permutations to assess the correlation between the whole matrix and a rarified matrix for fungal data sets. The results indicated that the rarefaction dataset highly represents the whole fungal matrix ($R_{\text{Mantel}} = 0.997$, $P = 0.001$). Among these, 400 ASVs were classified as plant pathogens according to FungalTraits database

(Pölme et al., 2020). The information on plant pathogenic ASVs with average relative abundances (ranged from 8–67%) and taxonomic information is provided in Supplementary Table S1. The 400 plant pathogenic ASVs were again rarified to the minimum read of 1,245, except one and two replicates of *P. avium* and *P. abies*, were not rarified, to confirm the consistency of the plant pathogenic ASV richness.

Investigation of the fate of plant pathogens

We preliminary investigated the fate of these plant pathogens in senescing leaves and needles after 200 and 400 days of the decomposition. The collected senescing leaves and needles were oven dried at 25°C for 14 days. Three grams of oven-dried senescing leaves and needles were filled into a nylon bag (2 mm mesh, 5 mm holes), placed back under the same tree individuals and allowed to decomposed. After 200 and 400 days of decomposition, leaf/needle samples were collected in a separate sterile plastic bag with new clean gloves and transported on ice to the laboratory within 3 h and stored at –80°C for further analysis. The decomposing leaf/needle samples were processed with the same procedures for sample preparation, DNA extraction as well as bioinformatics as described above.

Leaf physiochemical analyses

To obtain water-leachable components, senescing leaf and needle samples were shaken in 30 mL milliQ water for 1 h in falcon tubes, centrifuged for 5 min at 3500 rpm, decanted, and filtered. The remaining leaf/needle material was dried for two weeks at 40°C to determine dry weight, which was used as reference for all subsequent qualifications. Leachate pH was determined using pH paper with a scale precision of 0.2 units. Organic nitrogen (N_{org}) was calculated as the difference: $N_{org} = \text{Total nitrogen (TN)} - \text{mineralized nitrogen (N}_{Min})$. TN was analyzed using a sum parameter analyzer with high temperature combustion and chemiluminescence detection (Mitsubishi TN-100; a1 envirosciences, Düsseldorf, Germany). For N_{Min} quantification, a flow injection analyzer (Quikchem QC85S5; Lachat Instruments, Hach Company, Loveland CO, USA) was used with corresponding manifolds to measure ammonium nitrogen. N_{NH_4} nitrite nitrogen N_{NO_2} , and nitrate- plus nitrite nitrogen $N_{NO_3+NO_2}$ content. Dissolved organic carbon (DOC) was quantified as non-purgeable organic carbon with a sum parameter analyzer using high-temperature combustion and infrared detection (vario TOC cube, Elementar Analysensysteme GmbH, Langenselbold, Germany). The nutrient content, Ca, Fe, K, Mg, and P analyses were carried out using inductively coupled plasma–optical emission spectrometry “Arcos” (Spectro, Kleve, Germany) equipped with a 27.12 MHz free-running

LDMOS generator and ORCA optical system. The complete methods for leaf physiochemical analyses are provided in the Supplementary Material.

Network analyses and generalist and specialist determination

The plant pathogenic network analysis was constructed based on Random Matrix Theory using the molecular ecological network analysis pipeline (<http://ieg4.rccc.ou.edu/mena/>). Spearman rank correlation coefficients was analyzed between any two pairs of ASVs based on sequencing reads. The intra-module connectivity value (Z_i) and inter-module connectivity value (P_i) for each node were used to identify keystone species in the network. For detailed information regarding theories, algorithms, and procedures, refer to Deng et al., 2012 and Zhou et al., 2011. The plant pathogenic networks were visualized using Gephi v0.9.2. The co-occurrence network between tree species and fungal plant pathogens was visualized in Cytoscape v. 3.8.0. Specialist/generalist classification of the taxonomic dataset in this study was performed using EcolUtils package in R version 4.0.4 based on niche width and permutation algorithms. R code for specialist/generalist classification in this study is provided in Supplementary Material.

Community assembly analyses

To quantify the relative proportion of deterministic and stochastic processes in community assembly, the phylogenetic normalized stochasticity ratio (pNST) and beta nearest taxon indices (β NTI) based on the null model theory were calculated using ‘iCAMP’ package in R (Stegen et al., 2013; Ning et al., 2020; Sun et al., 2021). The fungal ITS gene sequences obtained by Illumina sequencing have been recently used to construct the phylogenetic and null model analyses for determining the assembly processes of fungal communities (Gyeong et al., 2021; Wang et al., 2022; Zhao et al., 2022). Although 18S nuclear ribosomal small subunit rRNA gene (SSU) is more appropriate and commonly applied to construct the phylogenetic tree of fungi than the ITS gene, it has lower hypervariable domains in fungi (Schoch et al., 2012). Thus, it had inferior taxonomic resolution as compared with the ITS. In this current study, we focus more on the taxonomic identification of fungi, so the ITS region was chosen as the region for detecting plant pathogenic fungi. Nevertheless, the ITS regions (full ITS, ITS1, and ITS2) have been successfully used to construct relatively reliable phylogenetic tree of many fungal genera (Porter and Brian Golding, 2011; Dissanayake et al., 2018; Purahong et al., 2019). Thus, the results from pNST derived from the ITS sequences should be interpreted with caution. In addition to β NTI, the Raup–Crick (RC_{bray}) null model based on Bray–Curtis

dissimilarity was further calculated to quantify dispersal-based stochastic ecological processes generating the turnover of community composition (Stegen et al., 2015). Briefly, for pNST index, deterministic and stochastic assembly were determined when $pNST < 50\%$ and $pNST > 50\%$, respectively. For the βNTI , homogeneous and variable selection are indicated by $\beta NTI < -2$ and $\beta NTI > +2$, respectively. The relative importance of dispersal limitation and homogenizing dispersal processes were assessed by $|\beta NTI| < 2$ but $RCbray > +0.95$ and $RCbray < -0.95$, respectively, and the undominated process was estimated by $|\beta NTI| < 2$ and $|RCbray| < 0.95$ (Stegen et al., 2015). Apart from pNST analysis, we have analyzed microbial assembly based on the taxonomic normalized stochasticity ratio (tNST) according to Ning et al., 2019.

Statistical analyses

The datasets were tested for normality using the Jarque–Bera test and for equality of group variances using *F*-test (for two datasets) and Levene's test (for more than two datasets). The differences among the generalists, and specialists were tested using Kruskal-Wallis test and one-way analysis of variance (ANOVA) for the data sets with non- and equality of variance, respectively. The statistical differences between the generalists and specialist in each tree species were performed using *t*-test. The statistical differences of ASV richness among different tree species were performed using one-way ANOVA with Tukey's *post-hoc* test. Effects of tree species on fungal plant pathogenic community composition were tested using non-metric multidimensional scaling (NMDS), permutational multivariate ANOVA, and analysis of similarities based on observed relative abundance and the Bray–Curtis distance measure as well as presence/absence data and the Jaccard distance measure, over 999 permutations. The relationship between plant pathogenic community compositions and different factors was analyzed using a goodness-of-fit statistic based on observed relative abundance and the Bray–Curtis distance measure as well as presence/absence data and the Jaccard distance measure. To differentiate the effect of an individual factor as well as their combining effect, we performed the variance partitioning analysis. The amounts of variation in plant pathogenic community compositions, explained by various factors, were estimated through variation partitioning using the Vegan package in R. R code for goodness-of-fit statistic and variance partitioning analysis in this study is provided in Supplementary Material. All statistical analyses were performed using PAST version 2.17 (Hammer et al., 2001), R, and RStudio version 4.0.4 (RStudio Team, 2019).

Results

Fungal pathobiome characteristics

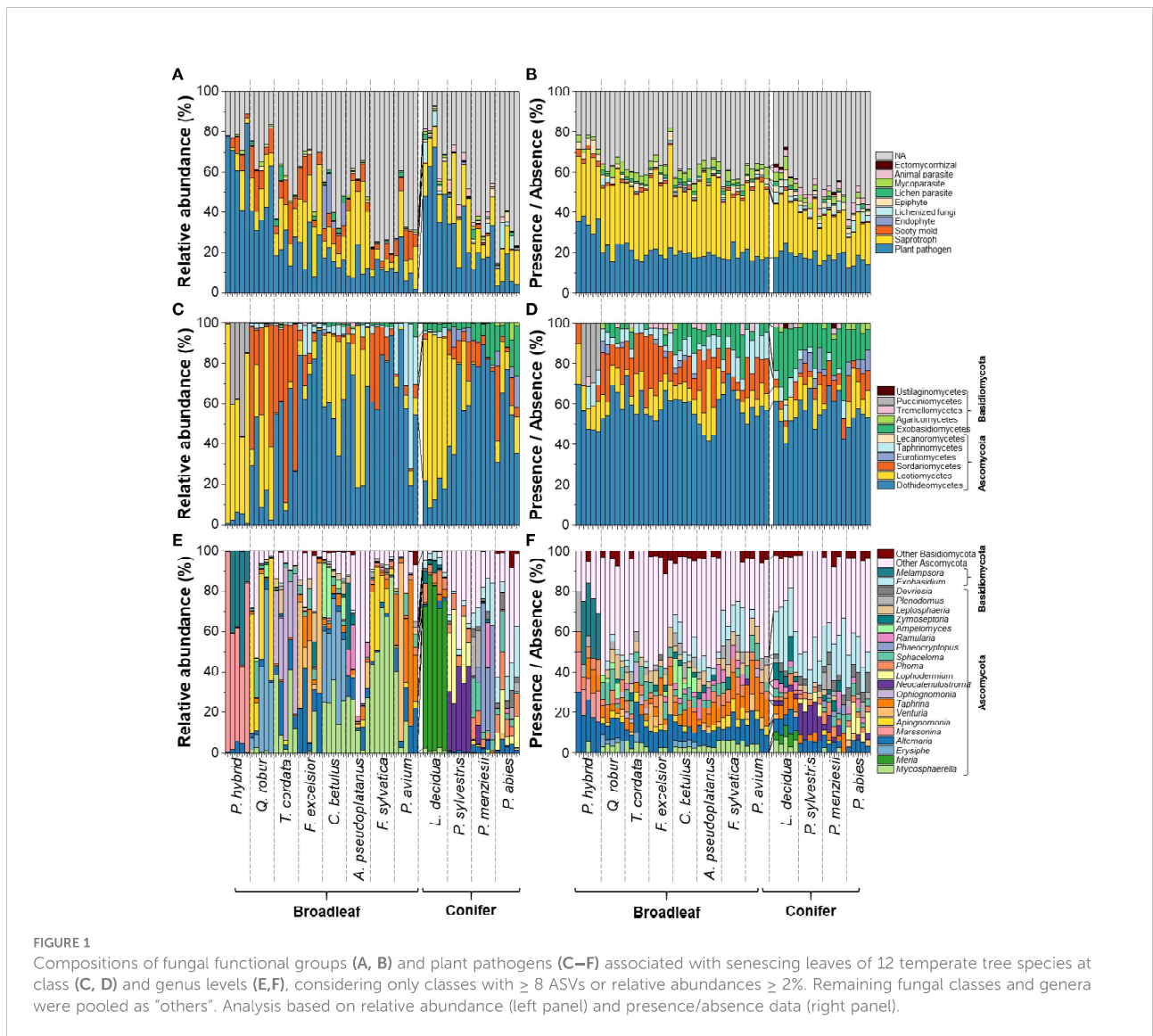
In this study, the fungal community compositions associated with healthy-looking leaves and needles of 12 temperate tree species were analysed (Figure 1). We detected 400 fungal pathogenic ASVs belonging to 130 genera (Supplementary Table S1). Fungal plant pathogens contributed the highest proportion among all fungal functional groups, especially in leaves and needles of *P. hybrid*, *L. decidua*, and *Q. robur* with Leotiomycetes (represented by *Marssonina*, *Meria*, and *Erysiphe*) contributing up to 99, 87, and 80% of fungal plant pathogens, respectively (Figure 1). Leaves and needles of other tree species were dominated by fungal pathogenic genera in Dothideomycetes, including *Mycosphaerella*, *Alternaria*, and *Venturia*. Among these 400 fungal pathogenic ASVs, 214 ASVs and 16 ASVs revealed saprotrophic and endophytic lifestyle as secondary lifestyles, respectively. 75 ASVs have the foliar endophytic interaction capability (Supplementary Table S1).

Diverse fungal pathogens detected in 12 temperate tree species

In line with the relative abundance data, *P. hybrid* also showed the highest percentage of plant pathogenic ASV richness relative to the total fungal groups, and *P. abies* revealed the lowest percentage of ASV richness (Figure 2). *Larix decidua* harbored a high relative abundance and the highest fungal pathogenic ASV richness (Figure 2). In contrast to *L. decidua*, *P. hybrid* revealed the highest relative abundance but the lowest ASV richness of fungal pathogens.

Community compositions and specificity of fungal pathogens

Leaves and needles of 12 temperate tree species harboured distinct fungal pathogenic community compositions based on both relative abundance and presence/absence data (Figure 3, Supplementary Figure S1 and Supplementary Table S2A, B). In this study, 240 ASVs (accounting for 60% of the total plant pathogenic ASVs) were specific to one tree species. Only four plant pathogenic ASVs (*Alternaria* ASV55, ASV56, ASV86, and *Neoscochyta* ASV227) were detected across all 12 temperate tree species (Figure 3B and Supplementary Table S1). In this current study, fungal pathogenic generalists and specialists showed significantly different relative abundances and richness across most studied temperate tree species (Figures 3D, E). The highest relative abundance of fungal pathogenic generalists and



specialists was found in *F. sylvatica* and *P. hybrid*, respectively (Figure 3D). *Acer pseudoplatanus* exhibited the highest ASV richness of fungal pathogenic generalists, followed by *C. betulus* and *L. decidua* (Figure 3E). Remarkably, *L. decidua* and *Q. robur* harboured significantly higher ASV richness of generalists as compared with specialists, and *P. hybrid* also harboured similar ASV richness of generalists and specialists, but 90–99% relative abundance of their plant pathogens belonged to specialists.

Are there any tree species that act as fungal pathogen hub in this forest ecosystem?

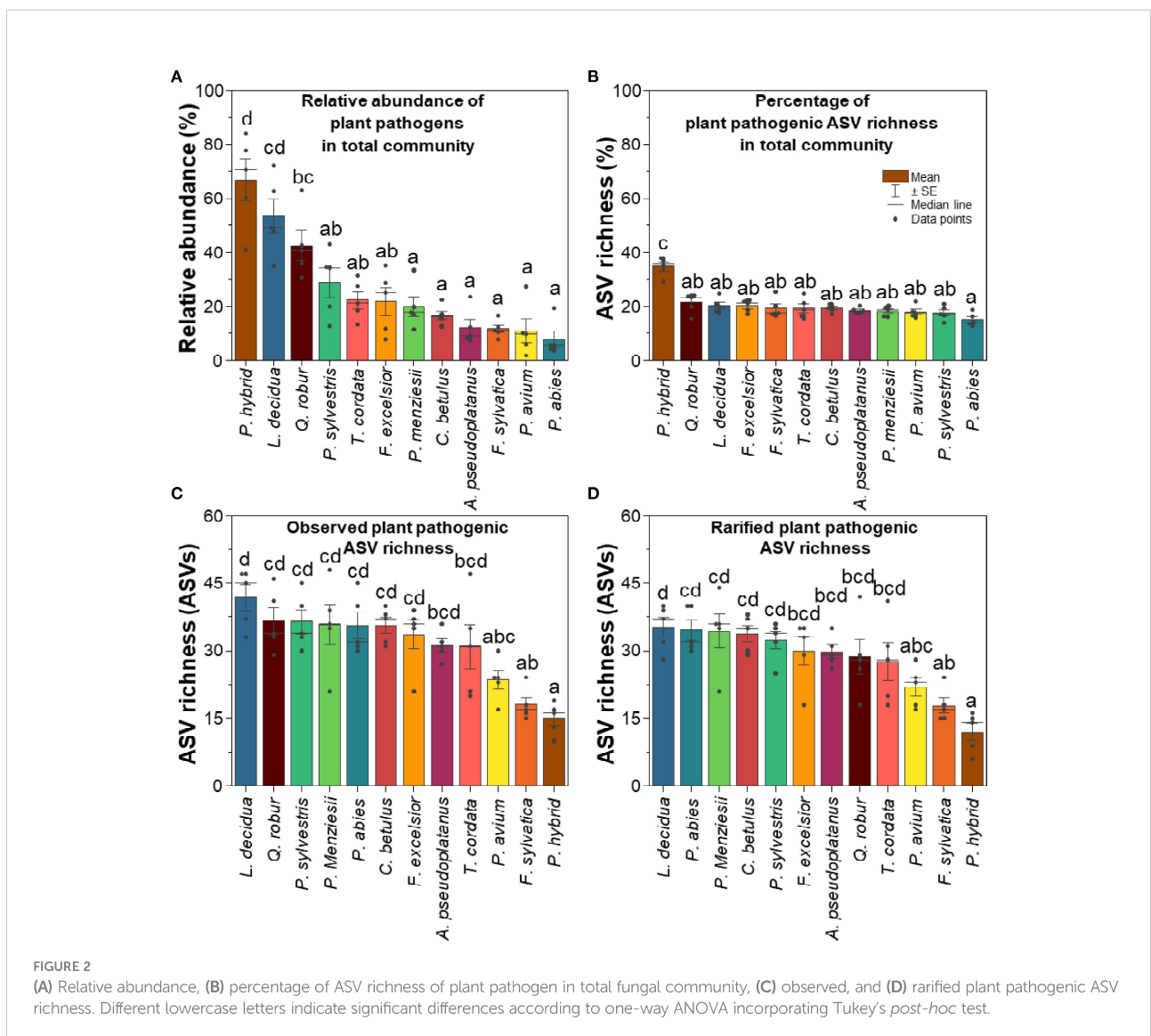
In general, no specific mature tree species were found to behave as a fungal pathogen hub. However, some tree species

harboured significantly more fungal plant pathogens. *P. menziesii* harboured the highest number of plant pathogenic fungal ASVs (97 ASVs), followed by *Q. robur* (96 ASVs), *L. decidua* (95 ASVs), *A. pseudoplatanus* (81 ASVs), and *F. excelsior* (80 ASVs). *P. hybrid* harboured the lowest number of plant pathogenic fungal ASVs (29 ASVs). Among 400 plant pathogenic fungal ASVs, 240 ASVs connected with only one tree species (Supplementary Figure S2). 156 plant pathogenic fungal ASVs build network with two to 11 tree species and four ASVs were detected in all 12 tree species. Furthermore, some tree species harboured significantly more fungal pathogenic generalists, including *A. pseudoplatanus* (25 ASVs), *F. excelsior* (23 ASVs), and *Q. robur* (22 ASVs).

Assembly processes: Deterministic vs. stochastic

Analysis using the phylogenetic normalized stochasticity ratio (pNST) and beta nearest taxon index (β NTI) showed that the assembly processes of fungal pathogens were highly dominated by stochastic processes (Figure 4). However, the contribution of stochasticity of plant pathogens in broadleaf tree species was significantly lower than that in coniferous tree species. Based on β NTI, the stochastic assembly processes comprised mainly of undominated processes (UP) or ecological drift, homogenizing dispersal (HP). However, the patterns are different in broadleaf and coniferous trees. The homogenizing dispersal process dominated the stochastic assembly processes in broadleaf tree species and ecological drift in coniferous tree species. The deterministic assembly

processes contributed more in broadleaf trees (~20% estimated by pNST and ~10% by β NTI) as compared to coniferous trees (5–10%) (Figure 4). Deterministic assembly processes were dominated by variable selection (VS) with a small contribution of homogeneous selection (HS). We further calculated the normalized stochasticity ratio based on the taxonomic turnover (tNST). High tNST value was observed in broadleaved group ($P < 0.05$, Supplementary Figure S3A). Based on the tNST value, broadleaf and conifer trees revealed 36.5% and 28.4% proportions of stochasticity, respectively (Supplementary Figure S3B).



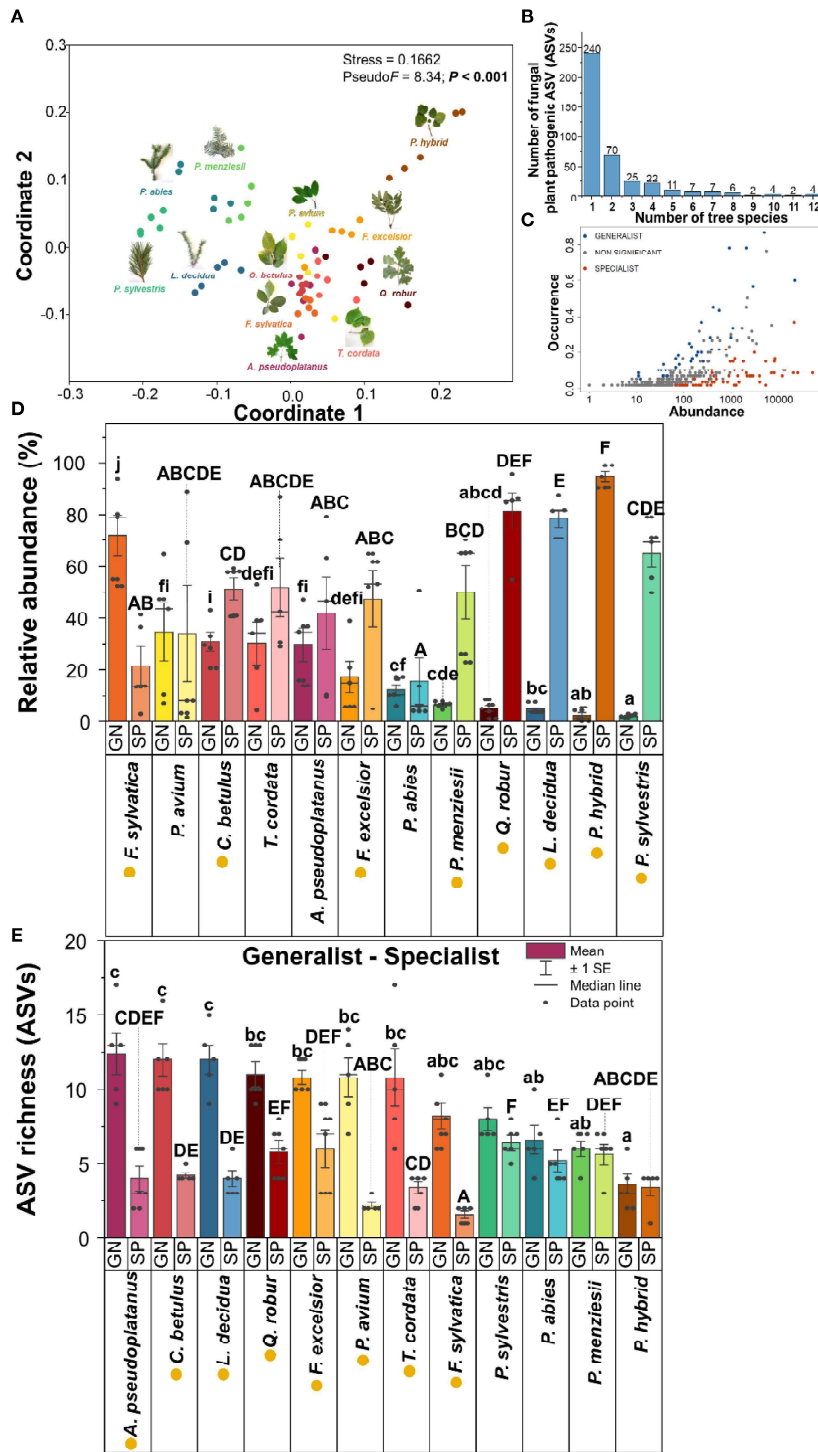


FIGURE 3

Fungal plant pathogenic community compositions and their specificity: NMDS ordinations of plant pathogenic community compositions based on relative abundance and Bray–Curtis distance similarity (A), number of fungal plant pathogenic ASVs detected in various number of tree species (B), the abundance and the occurrence of generalists and specialists of fungal plant pathogens (C), relative abundance (D), and ASV richness (E) of fungal plant pathogenic generalists and specialists in each tree species. Generalist and specialist classification refers only to our taxonomic data from the local scale experiment. Capital and lowercase letters in Figures 3D, E indicate statistically significant differences (Kruskal–Wallis test and ANOVA were performed for the data sets with non- and equality of variance, respectively) among fungal plant pathogenic specialists (SP) and generalists (GN), respectively. The yellow circle in the front of tree species name indicates statistically significant differences (*t*-test) between fungal plant pathogenic generalist and specialist in each tree species.

Factors determining fungal pathogenic community composition

Based on relative abundance data, the fungal pathogenic community compositions in broadleaf and coniferous tree species were shaped mainly by tree species identity ($R^2 = 0.87-0.88$, $P = 0.001$) (Figure 5). In coniferous tree species, the pH, latitude, and longitude of each tree individual were additional primary factors that shaped fungal pathogenic community composition ($R^2 = 0.71-0.86$, $P = 0.001$). Leaf nutrients such as C, N, K, Mg, and P also significantly correlated with fungal pathogenic community composition in coniferous tree species. In broadleaf tree species, we also detected correspondence of the plant pathogenic community composition with pH, Ca, and P. Similar pattern of the factors determining the fungal pathogenic community compositions was found on the presence/absence data. The tree species identity ($R^2 = 0.83-0.91$, $P = 0.001$) mainly shaped the fungal pathogenic community compositions in broadleaf and coniferous tree species (Supplementary Figure

S4). Leaf/needle water content, pH, latitude, and longitude as well as leaf nutrients (C, N, K, Mg, and P) were also important factors that shaped fungal pathogenic community composition ($R^2 = 0.37-0.91$, $P = 0.024-0.001$).

All studied factors that significantly corresponded with the plant pathogenic community composition were used in the variation partitioning analysis. These factors explained 68% and 92% of variation in relative abundance data of plant pathogen community compositions of broadleaf and coniferous tree species, respectively (Figures 5B, C). In broadleaf trees, tree species alone explained the highest variation in fungal pathogenic community composition (78% of the total explainable variance). Nutrients alone explained 7% of the variation in fungal pathogenic community composition in broadleaf trees and their combining effect with tree species explained 7%. In coniferous trees, nutrient abundance alone explained the highest variation (17% of the total explainable variance), followed by tree species and pH/water content. Combining effect of nutrients and tree species explained 13%

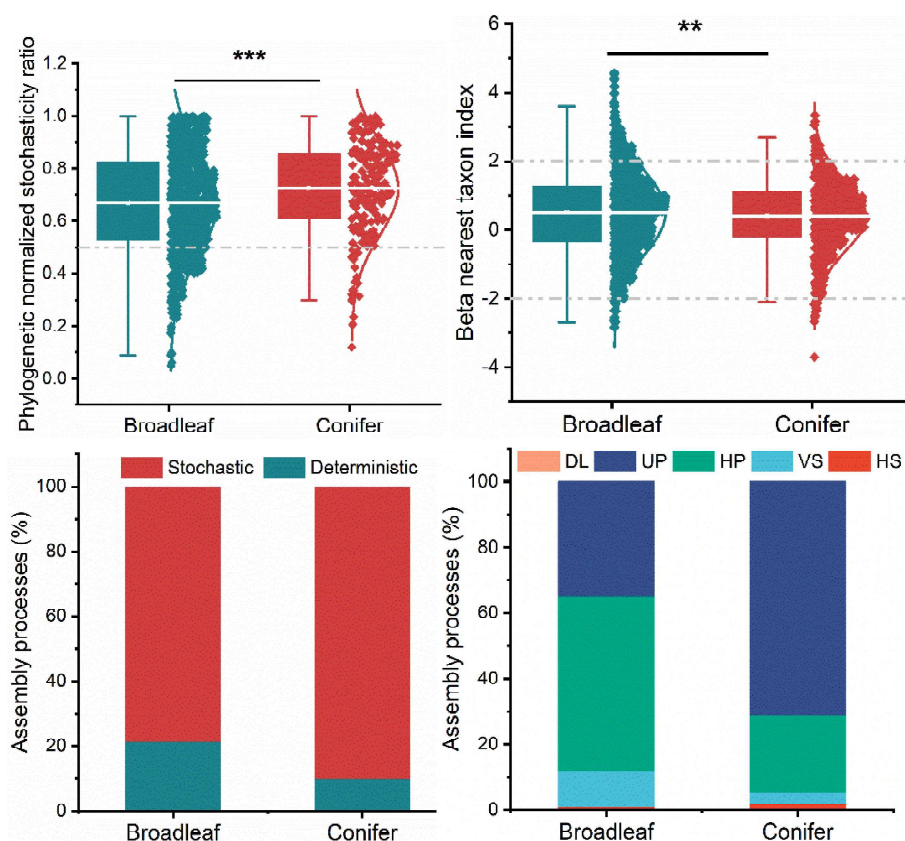


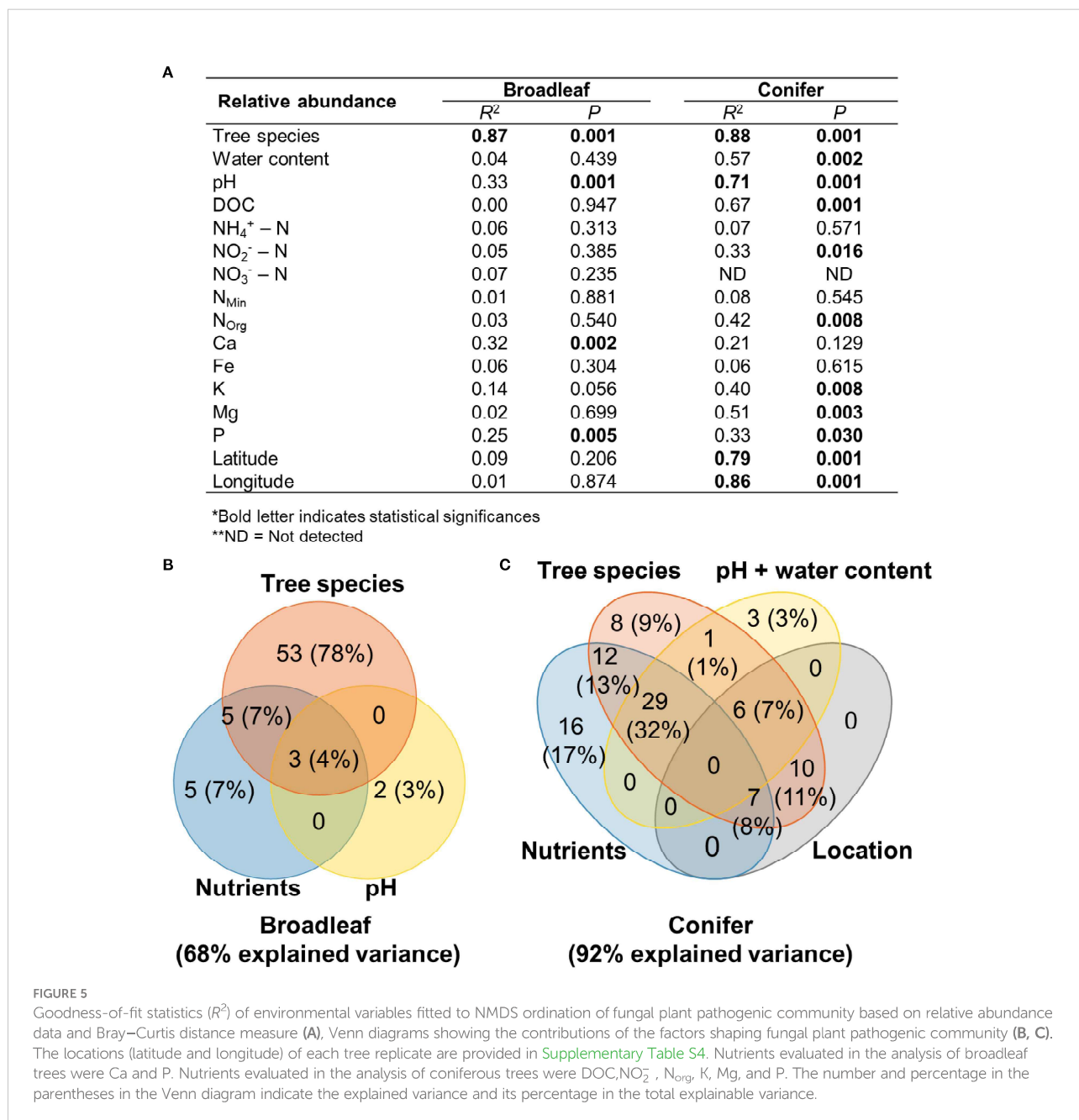
FIGURE 4 Deterministic vs. stochastic assembly processes in broadleaf and conifer trees based on phylogenetic normalized stochasticity ratio (pNST) and beta nearest taxon index (βNTI). Stochastic processes: DL = dispersal limitation, UP = undominated processes, HP = homogenizing dispersal; deterministic processes: VS = variable selection, HS = homogeneous selection. Note: The non-dominant processes ($|RC_{bray}| < 0.95$) were drift and diversification.

Q24

of the variation in fungal pathogenic community composition in coniferous trees. Location (latitude and longitude) alone did not explain the variation in the fungal pathogenic community in coniferous trees. Tree species identity, nutrients, pH/water content, and their combined effects explained more than 70% of the explainable variance in both tree types.

While tree species, nutrients, pH, water content, and location explained large proportion of variation in plant pathogen community compositions based on relative abundance data, they explain 25% and 41% of those based on presence/absence data in broadleaf and coniferous tree species,

respectively (Supplementary Figures S4B, C). Nevertheless, similar pattern of variation partitioning was found. In broadleaf trees, tree species alone explained the highest variation in fungal pathogenic community composition (68% of the total explainable variance), followed by nutrients (4%). Combining effect of nutrients and tree species explained 5% of variation in fungal pathogenic community composition. In coniferous trees, nutrient abundance alone also explained the highest variation (12% of the total explainable variance), followed by tree species and pH/water content. Combining effect of nutrients and tree species explained 5% of the



Q25

variation in fungal pathogenic community composition in coniferous trees. Location (latitude and longitude) alone did not explain the variation in the fungal pathogenic community in both broadleaf and coniferous trees.

Different co-occurrence network patterns in broadleaf and coniferous trees

To evaluate the interactions among fungal pathogenic taxa and the co-occurrence network patterns of both tree types, two ecological networks for broadleaf and coniferous tree species were constructed (Figure 6). The main topological parameters in

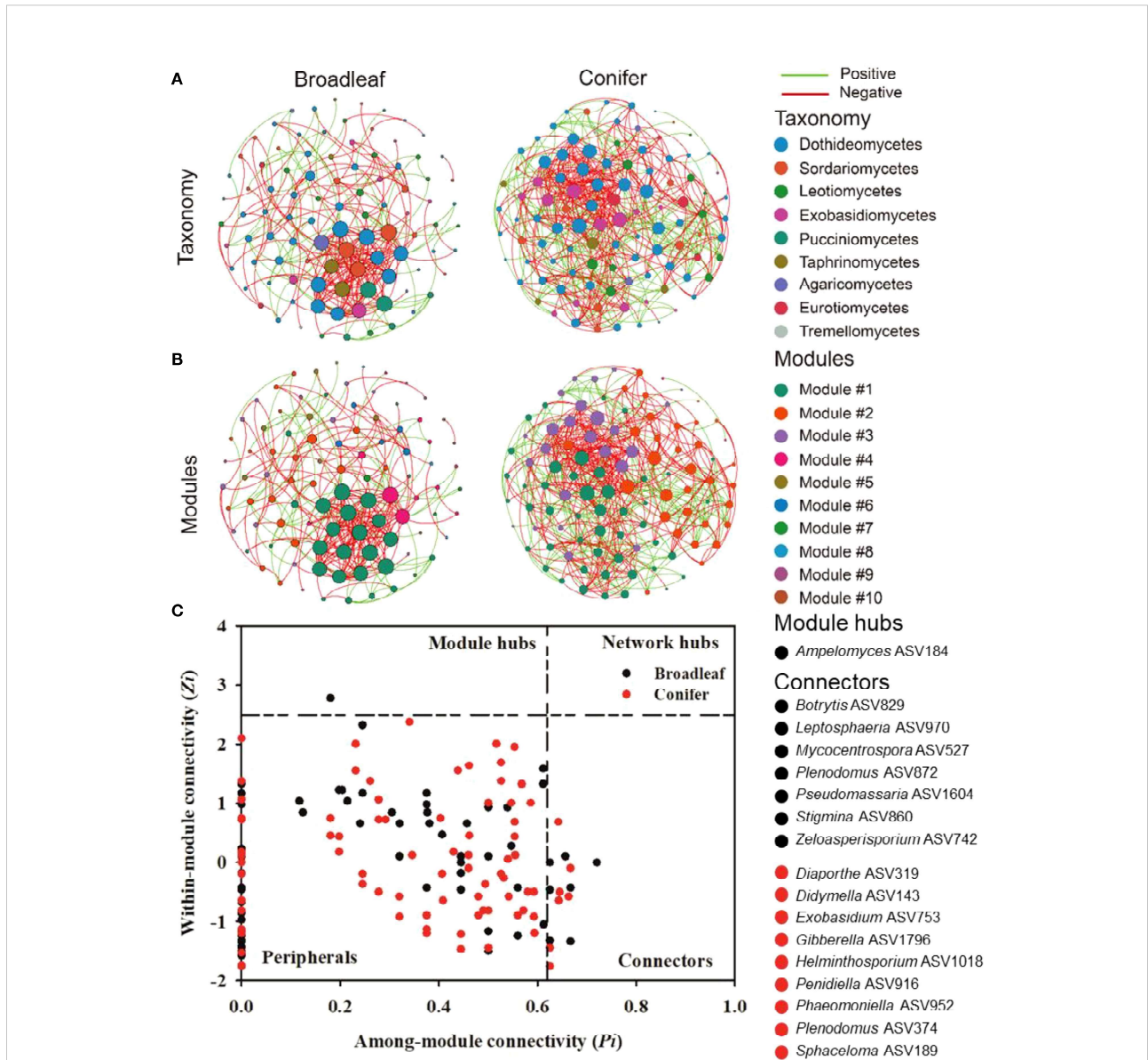


FIGURE 6 Taxonomic (A), modular networks (B), and topological roles of each ASVs in the plant pathogenic co-occurrence networks (C) in broadleaf and coniferous tree species. The green (co-presence, positive) and red links (mutual exclusion, negative) in the co-occurrence networks represent significant Spearman's correlations ($P < 0.05$). Each node in Fig. 6a and b represents one ASV. The size of each node is proportional to the degree. The node color indicates the corresponding taxonomic assignment at the class (A) and modular level (B). The nodes in Fig. 6c with $Z_i > 2.5$ but $P_i < 0.62$ are identified as module hubs, and those with $P_i > 0.62$ but $Z_i < 2.5$ represent connectors. The network hubs are characterized with $Z_i > 2.5$ and $P_i > 0.62$, and the peripherals are characterized with $Z_i < 2.5$ and $P_i < 0.62$ according to Olesen et al., 2007. Nodes in broadleaf 10 (4 big modules), conifer 4 (3 big modules > 10% of the notes) modules.

the empirical network were higher than in the random network, which implied a nonrandom pattern. The plant pathogenic network in coniferous trees was more complex than those in broadleaf trees, revealing a lower average path distance, average clustering coefficient, and modularity but higher average degree (Supplementary Table S3). Notably, the percentage of negative links (63.5%) in the coniferous network was lower than in broadleaf trees (75.5%). Furthermore, we detected 10 and four modules (functional units or subcommunities) in the networks of broadleaf and coniferous trees, respectively. However, the numbers of large modules (modules with more than 10% nodes) were similar in both tree types (4 large modules in broadleaf and 3 large modules in coniferous trees).

Based on Z_i and P_i tests, the potential topological roles of the plant pathogen taxa were explored (Figure 6C). One node belonging to *Ampelomyces* ASV184 was identified as a module hub in broadleaf trees. We detected seven and eight connectors belonging to diverse plant pathogenic genera in the broadleaf and coniferous networks, respectively. The keystone species (module hub/connectors) were distinct between the tree types. The fungal pathogenic module hub, *Ampelomyces* ASV184, was classified as a specialist and detected solely in *C. betulus*. Conversely, connectors were distributed across different tree species. Among them, four connectors were classified as pathogenic generalists, including *Botrytis* ASV829, *Gibberella* ASV1796, *Pseudomassaria* ASV1604, and *Sphaeloma* ASV189.

Fate of plant pathogens

After 200 days of decomposition, 81 out of 130 plant pathogenic fungal genera were detected in the decomposing leaves and needles. The proportion of *Alternaria* increased from 4% to 49% of the sequence reads of the considered plant pathogens. *Phoma* (18%) and *Rhizosphaera* (10%) co-dominated along the plant pathogenic fungal genera along with *Alternaria*. After 400 days of decomposition, 79 out of 130 plant pathogenic genera continued to colonize the decomposing leaves and needles. *Alternaria* (48%) and *Phoma* (21%) hyperdominated the sequence read of the 79 plant pathogens.

Discussion

Pathobiome of 12 common temperate tree species

We successfully accessed the pathobiomes in senescing leaves and needles of the 12 common temperate tree species, which allowed us to compare fungal pathogen load among different tree species. Our current study reveals diverse and tree species distinct fungal pathogens associated with senescing

leaves and needles of the 12 common temperate tree species, which is appropriate to be considered as the database for foliar fungal pathogens in Thuringia forest (Supplementary Table S1). With the aid of the high-resolution molecular approach (Illumina MiSeq) used in this study, our understanding of foliar fungal pathobiome communities was significantly extended. Despite the fact that our experiment focused at the local scale, we detected highly diverse and abundant fungal pathogens associated with senescing leaves and needles of 12 temperate tree species. The majority of these fungal pathogens were species-specific. In *F. sylvatica*, the plant pathogenic generalist *Mycosphaerella* ASV14 (UNITE name: *Mycosphaerella punctiformis*) was highly abundant. In *A. pseudoplatanus*, diverse fungal pathogenic generalists were detected, including *Mycosphaerella* ASV14. *Mycosphaerella* spp. have been reported to cause leaf spot in different tree species, including *Acer* (Funk and Dorworth, 1988), *Fraxinus* (Wolf and Davidson, 1941), *Fagus* (Burke et al., 2020), and *Tilia* (Bernadovičová and Ivanová, 2008). In *C. butulus*, we also detected a high richness of fungal pathogenic generalists and high relative abundances of *Mycosphaerella* ASV14 and the fungal pathogenic specialist *Erysiphe* ASV42 (UNITE name: *Erysiphe arcuata*), which has previously been reported as leaf disease pathogen in *C. butulus* (Chinan and Mânzu, 2021). Apart from the previously described hosts of foliar plant pathogens (airborne pathogen propagules and spore) (Bayandala et al., 2016), we suggest that fungal pathogens inhabiting senescing leaves can act as an agent to cause foliar disease in seedlings which is in line with a previous study on contribution of leaf litter on *Mycosphaerella* leaf disease (Sánchez Márquez et al., 2011). In Figure 7, we summarize the aforementioned hosts of foliar pathogens, which the mature tree uses to regulate seedling density. Furthermore, we preliminarily investigated the fate of these plant pathogens in senescing leaves and needles during the decomposition process (Figure 7). In senescing leaves, fungal pathogenic community composition was dominated by diverse fungal genera, including *Marssonina*, *Meria*, *Erysiphe*, *Apiognomonia*, and *Melampsora*. After 200 days of leaf decomposition, the high diversity and relative abundance of the previously detected foliar fungal pathogenic community are maintained. Nevertheless, the relative abundance of the foliar pathogens strongly declines after 400 days of decomposition. *Alternaria* is hyper-dominant with some contributions of *Phoma* at 200 and 400 days. Thus, decomposing leaf litter can be an important agent causing foliar disease in seedlings and even saplings over seasons.

The hosts of fungal pathogens and the fate of the 400 fungal pathogenic ASVs (130 genera) associated with senescing leaves.

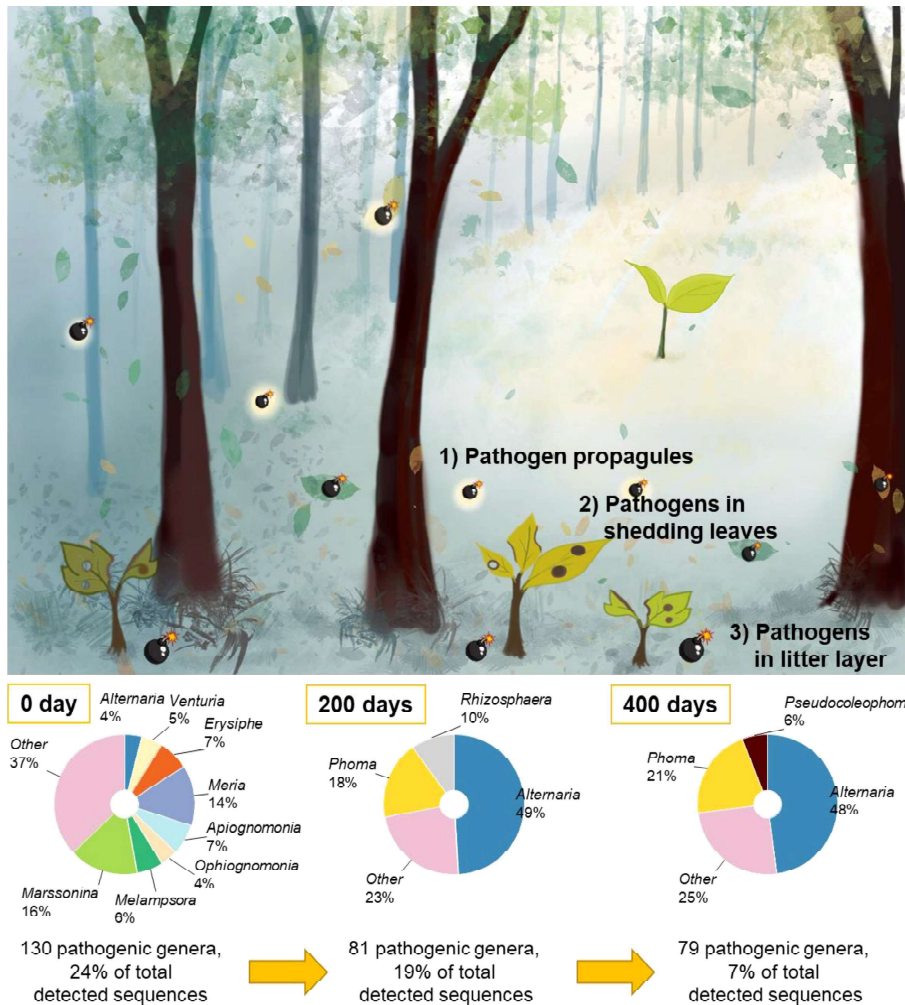


FIGURE 7 Fungal pathogen hosts (left panel) and the fate of the 400 fungal pathogenic ASVs (131 genera) associated with senescing leaves (right panel). Leaf-associated fungal pathogens at 200 and 400 days were characterized by fungal internal transcribed spacer (ITS)-based amplicon sequencing on the Illumina MiSeq sequencing with the same bioinformatics.

Pathobiome community assembly is highly determined by stochastic processes

Understanding the process governing fungal plant pathogenic community assembly is important for identifying driving factors. Some studies have focused on environmental filtering and seek factors to describe the community, but the community assembly may be largely explained by stochastic processes (Abrego, 2021). This study demonstrates that the fungal pathobiome associated with leaves and needles of 12 common temperate tree species are determined mainly by stochastic processes based on pNST, specifically homogenizing

dispersal and undominated processes (ecological drift). Based on tNST, deterministic processes play more important role as compared with stochastic processes. The controversial results of pNST and tNST were also demonstrated in a previous study based on bacterial 16S rRNA amplicon (Tai et al., 2020). This may due to the calculation of the microbial attributes from different dimensions of diversity (including taxonomic, phylogenetic, functional, etc.). Thus, the results should be interpreted with caution. Nevertheless, stochasticity based on the tNST also reveals substantial proportion in governing fungal plant pathogenic community assembly in both broadleaf (36.5%) and coniferous trees (28.4%). Tree species is the main factor that shapes fungal pathogenic communities in both broadleaf and

coniferous tree species. The results of negative networks and stochasticity suggest that the systems in both tree types follow the colonization–extinction stochasticity assumption (unpredictability in arrival and establishment of different species) (Abrego, 2021). This implies that the fungal pathobiome colonizing the leaf habitat exhibits unpredictable systematic variation in species, which can be driven by the colonization–competition trade-off (Tilman, 1994; Abrego, 2021). We determined the contribution of deterministic processes, mainly by variable selection (VS). We found that pH and P levels significantly correspond with fungal pathogenic community compositions in both tree types. Other important factors in broadleaf or coniferous trees are water content, C, N, and other leaf nutrients. Tree species can also determine leaf nutrients such as Ca, P, and N. In this study, we found the importance of both nutrients alone as well as their combined effect with tree species in explaining the variation in plant pathogenic fungal community. These factors were previously reported to shape microbial community composition associated with decomposing leaf of European beech in Germany (Purahong et al., 2016). These microbial macronutrients are important for microbial growth, reproductivity, and activity (Prescott et al., 1999; Purahong et al., 2015; Purahong et al., 2016).

Conclusion

Our study is the first to investigate community assembly, networks, and the complete taxonomy of foliar fungal pathobiome, which different tree species may use for inter- and intraspecific competition in mixed temperate forests. Shedding the foliar fungal pathogens with senescing leaf seems to be an effective strategy as it can be repeated over years and the healthy mature tree would not be affected much by their own foliar fungal pathogens. Future studies should focus on the fate of fungal pathogens (colonization–extinction dynamics) and how their interaction change during the leaf decomposition process.

Q13 Data availability statement

The datasets presented in this study can be found in online repositories. The names of the repository/repositories and accession number(s) can be found in the article/Supplementary Material.

Q16 Author contributions

WP and E-DS conceived and designed the study. BT, WP, E-DS, and SW collected samples and metadata. WP and FB

contributed reagents and laboratory equipment. BT, WP, and SW led the DNA analysis. SW led bioinformatics. BT, LJ, and WP led the microbial taxonomy and data analyses. SS, GG, A-SL, and EA led the physicochemical analyses. BT, LJ, and WP wrote the manuscript. MN and WP supervised BT. MN, E-DS, PL, and FB reviewed and gave comments and suggestions for manuscript. All authors contributed to the article and approved the submitted version.

Funding

This work was partially funded by the internal research budget of WP to Department of Soil Ecology, UFZ-Helmholtz Centre for Environmental Research.

Acknowledgments

Community composition data were computed at the High-Performance Computing (HPC) Cluster EVE, a joint effort of both the Helmholtz Centre for Environmental Research - UFZ and the German Centre for Integrative Biodiversity Research (iDiv) Halle-Jena-Leipzig. We thank Beatrix Schnabel and Melanie Günther for their help with Illumina sequencing.

Conflict of interest

The authors declare that the research was conducted in the absence of any commercial or financial relationships that could be construed as a potential conflict of interest.

Publisher's note

All claims expressed in this article are solely those of the authors and do not necessarily represent those of their affiliated organizations, or those of the publisher, the editors and the reviewers. Any product that may be evaluated in this article, or claim that may be made by its manufacturer, is not guaranteed or endorsed by the publisher.

Supplementary material

The Supplementary Material for this article can be found online at: <https://www.frontiersin.org/articles/10.3389/fpls.2022.968218/full#supplementary-material>

References

- Abrego, N. (2021). Wood-inhabiting fungal communities: Opportunities for integration of empirical and theoretical community ecology. *Fungal Ecol.*, 101112. doi: 10.1016/j.funeco.2021.101112
- Almeida, I., Rösch, C., and Saha, S. (2018). Comparison of ecosystem services from mixed and monospecific forests in southwest Germany: A survey on public perception. *Forests* 9, 627. doi: 10.3390/f9100627
- Bayandala, F., Fukasawa, Y., and Seiwa, K. (2016). Roles of pathogens on replacement of tree seedlings in heterogeneous light environments in a temperate forest: a reciprocal seed sowing experiment. *J. Ecol.* 104, 765–772. doi: 10.1111/1365-2745.12552
- Bernadovičová, S., and Ivanová, H. (2008). Leaf spot disease on *Tilia cordata* caused by the fungus *Cercospora microsora*. *Biologia* 63, 44–49. doi: 10.2478/s11756-008-0003-5
- Burke, D. J., Hoke, A. J., and Koch, J. (2020). The emergence of beech leaf disease in Ohio: Probing the plant microbiome in search of the cause. *For. Pathol.* 50, e12579. doi: 10.1111/efp.12579
- Callahan, B. J., McMurdie, P. J., and Holmes, S. P. (2017). Exact sequence variants should replace operational taxonomic units in marker-gene data analysis. *ISME J.* 11, 2639–2643. doi: 10.1038/ismej.2017.119
- Callahan, B. J., McMurdie, P. J., Rosen, M. J., Han, A. W., Johnson, A. J. A., and Holmes, S. P. (2016). DADA2: High-resolution sample inference from illumina amplicon data. *Nat. Methods* 13, 581–583. doi: 10.1038/nmeth.3869
- Chinan, V.-C., and Mânzu, C. C. (2021). First report of *Erysiphe arcuata* on *Carpinus betulus* in Romania. *J. Plant Pathol.* 103, 405–405. doi: 10.1007/s42161-020-00739-4
- Clasen, C., Griess, V. C., and Knoke, T. (2011). Financial consequences of losing admixed tree species: A new approach to value increased financial risks by ungulate browsing. *For. Policy Economics* 13, 503–511. doi: 10.1016/j.forpol.2011.05.005
- Deng, Y., Jiang, Y.-H., Yang, Y., He, Z., Luo, F., and Zhou, J. (2012). Molecular ecological network analyses. *BMC Bioinf.* 13, 113. doi: 10.1186/1471-2105-13-113
- Dissanayake, A. J., Purahong, W., Wubet, T., Hyde, K. D., Zhang, W., Xu, H., et al. (2018). Direct comparison of culture-dependent and culture-independent molecular approaches reveal the diversity of fungal endophytic communities in stems of grapevine *Vitis vinifera*. *Fungal Diversity* 90, 85–107. doi: 10.1007/s13225-018-0399-3
- Ehbrecht, M., Seidel, D., Annighöfer, P., Kreft, H., Köhler, M., Zemp, D. C., et al. (2021). Global patterns and climatic controls of forest structural complexity. *Nat. Commun.* 12, 519. doi: 10.1038/s41467-020-20767-z
- FAO and UNEP (2020). “The state of the world’s forests 2020,” in *Forests, biodiversity and people*(Rome). doi: 10.4060/ca8642en
- Funk, A., and Dorworth, C. E. (1988). *Mycosphaerella mycopappi* sp.nov. and its anamorphs on leaves of *Acer macrophyllum*. *Can. J. Bot.* 66, 295–297. doi: 10.1139/b88-048
- Gamfeldt, L., Snäll, T., Bagchi, R., Jonsson, M., Gustafsson, L., Kjellander, P., et al. (2013). Higher levels of multiple ecosystem services are found in forests with more tree species. *Nat. Commun.* 4, 1340. doi: 10.1038/ncomms2328
- Griess, V. C., Acevedo, R., Härtl, F., Staupendahl, K., and Knoke, T. (2012). Does mixing tree species enhance stand resistance against natural hazards? a case study for spruce. *For. Ecol. Manage.* 267, 284–296. doi: 10.1016/j.foreco.2011.11.035
- Gyeong, H., Hyun, C.-U., Kim, S. C., Tripathi, B. M., Yun, J., Kim, J., et al. (2021). Contrasting early successional dynamics of bacterial and fungal communities in recently deglaciated soils of the maritime Antarctic. *Mol. Ecol.* 30, 4231–4244. doi: 10.1111/mec.16054
- Hammer, Ø., Harper, D. A. T., and Ryan, P. D. (2001). PAST: Paleontological statistics software package for education and data analysis. *Palaeontol. Electron.* 4, 9.
- Ihrmark, K., Bödeker, I. T. M., Cruz-Martinez, K., Friberg, H., Kubartova, A., Schenck, J., et al. (2012). New primers to amplify the fungal ITS2 region – evaluation by 454-sequencing of artificial and natural communities. *FEMS Microbiol. Ecol.* 82, 666–677. doi: 10.1111/j.1574-6941.2012.01437.x
- Köljal, U., Nilsson, R. H., Abarenkov, K., Tedersoo, L., Taylor, A. F. S., Bahram, M., et al. (2013). Towards a unified paradigm for sequence-based identification of fungi. *Mol. Ecol.* 22, 5271–5277. doi: 10.1111/mec.12481
- Martin, M. (2011). Cutadapt removes adapter sequences from high-throughput sequencing reads. *EMBnet.journal* 17, 10–12. doi: 10.14806/ebj.17.1.200
- Montoya, J. M., Pimm, S. L., and Solé, R. V. (2006). Ecological networks and their fragility. *Nature* 442, 259–264. doi: 10.1038/nature04927
- Ning, D., Deng, Y., Tiedje, J. M., and Zhou, J. (2019). “A general framework for quantitatively assessing ecological stochasticity,” in *Proceedings of the National Academy of Sciences*, Vol. 116. 16892–16898. doi: 10.1073/pnas.1904623116
- Ning, D., Yuan, M., Wu, L., Zhang, Y., Guo, X., Zhou, X., et al. (2020). A quantitative framework reveals ecological drivers of grassland microbial community assembly in response to warming. *Nat. Commun.* 11, 4717. doi: 10.1038/s41467-020-18560-z
- Olesen, J. M., Bascompte, J., Dupont, Y. L., and Jordano, P. (2007). The modularity of pollination networks. *PNAS* 104, 19891–19896. doi: 10.1073/pnas.0706375104
- Pölme, S., Abarenkov, K., Henrik Nilsson, R., Lindahl, B. D., Clemmensen, K. E., Kauserud, H., et al. (2020). FungalTraits: a user-friendly traits database of fungi and fungus-like stramenopiles. *Fungal Diversity* 105, 1–16. doi: 10.1007/s13225-020-00466-2
- Porter, T. M., and Brian Golding, G. (2011). Are similarity- or phylogeny-based methods more appropriate for classifying internal transcribed spacer (ITS) metagenomic amplicons? *New Phytol.* 192, 775–782. doi: 10.1111/j.1469-8137.2011.03838.x
- Prescott, L. M., Harley, J. P., and Klein, D. A. (1999). *Microbiology* (WCB/McGraw-Hill). Available at: <https://books.google.de/books?id=kddfQgAACAAJ>.
- Purahong, W., Kapturska, D., Pecyna, M. J., Jariyavidyanont, K., Kaunzner, J., Juncheed, K., et al. (2015). Effects of forest management practices in temperate beech forests on bacterial and fungal communities involved in leaf litter degradation. *Microb. Ecol.* 69, 905–913. doi: 10.1007/s00248-015-0585-8
- Purahong, W., Mapook, A., Wu, Y.-T., and Chen, C.-T. (2019). Characterization of the *Castanopsis carlesii* deadwood mycobiome by pacbio sequencing of the full-length fungal nuclear ribosomal internal transcribed spacer (ITS). *Front. Microbiol.* 10. doi: 10.3389/fmicb.2019.00983
- Purahong, W., Wubet, T., Lentendu, G., Schloter, M., Pecyna, M. J., Kapturska, D., et al. (2016). Life in leaf litter: novel insights into community dynamics of bacteria and fungi during litter decomposition. *Mol. Ecol.* 25, 4059–4074. doi: 10.1111/mec.13739
- RStudio Team (2019). *RStudio: Integrated development for r* (Boston, MA: RStudio, Inc.). Available at: <https://rstudio.com/>.
- Sánchez Márquez, S., Bills, G. f., and Zabalgoitia, I. (2011). Fungal species diversity in juvenile and adult leaves of eucalyptus globulus from plantations affected by *Mycosphaerella* leaf disease. *Ann. Appl. Biol.* 158, 177–187. doi: 10.1111/j.1744-7348.2010.00449.x
- Schoch, C. L., Seifert, K. A., Huhndorf, S., Robert, V., Spouge, J. L., Levesque, C. A., et al. (2012). Nuclear ribosomal internal transcribed spacer (ITS) region as a universal DNA barcode marker for fungi. *PNAS* 109, 6241–6246. doi: 10.1073/pnas.1117018109
- Sheng, Y., Cong, W., Yang, L., Liu, Q., and Zhang, Y. (2019). Forest soil fungal community elevational distribution pattern and their ecological assembly processes. *Front. Microbiol.* 10. doi: 10.3389/fmicb.2019.02226
- Stegen, J. C., Lin, X., Fredrickson, J. K., Chen, X., Kennedy, D. W., Murray, C. J., et al. (2013). Quantifying community assembly processes and identifying features that impose them. *ISME J.* 7, 2069–2079. doi: 10.1038/ismej.2013.93
- Stegen, J. C., Lin, X., Fredrickson, J. K., and Konopka, A. E. (2015) Estimating and mapping ecological processes influencing microbial community assembly (Accessed March 24, 2022).
- Sun, Y., Zhang, M., Duan, C., Cao, N., Jia, W., Zhao, Z., et al. (2021). Contribution of stochastic processes to the microbial community assembly on field-collected microplastics. *Environ. Microbiol.* 23, 6707–6720. doi: 10.1111/1462-2920.15713
- Tai, X., Li, R., Zhang, B., Yu, H., Kong, X., Bai, Z., et al. (2020). Pollution gradients altered the bacterial community composition and stochastic process of rural polluted ponds. *Microorganisms* 8, 311. doi: 10.3390/microorganisms8020311
- Tanunchai, B., Ji, L., Schroeter, S. A., Wahdan, S. F. M., Hossen, S., Delelegn, Y., et al. (2022). FungalTraits vs. FUNGuild: comparison of ecological functional assignments of leaf- and needle-associated fungi across 12 temperate tree species. *Microb. Ecol.* doi: 10.1007/s00248-022-01973-2
- Tilman, D. (1994). Competition and biodiversity in spatially structured habitats. *Ecology* 75, 2–16. doi: 10.2307/1939377
- Toju, H., Guimarães, P. R., Olesen, J. M., and Thompson, J. N. (2014). Assembly of complex plant–fungus networks. *Nat. Commun.* 5, 273. doi: 10.1038/ncomms6273
- Tyc, O., van den Berg, M., Gerards, S., van Veen, J. A., Raaijmakers, J. M., de Boer, W., et al. (2014) Impact of interspecific interactions on antimicrobial activity among soil bacteria (Accessed June 13, 2022).

1591	Wang, Q., Garrity, G. M., Tiedje, J. M., and Cole, J. R. (2007). Naive Bayesian classifier for rapid assignment of rRNA sequences into the new bacterial taxonomy. <i>Appl. Environ. Microbiol.</i> 73, 5261–5267. doi: 10.1128/AEM.00062-07	1644
1592		1645
1593	Wang, W., Wang, H., Cheng, X., Wu, M., Song, Y., Liu, X., et al. (2022). Different responses of bacteria and fungi to environmental variables and corresponding community assembly in Sb-contaminated soil. <i>Environ. pollut.</i> 298, 118812. doi: 10.1016/j.envpol.2022.118812	1646
1594		1647
1595		1648
1596	Weißbecker, C., Schnabel, B., and Heintz-Buschart, A. (2020). Dadasnake, a snakemake implementation of DADA2 to process amplicon sequencing data for microbial ecology. <i>GigaScience</i> 9. doi: 10.1093/gigascience/giaa135	1649
1597		1650
1598	White, T. J., Bruns, T. D., Lee, S., and Taylor, J. (1990). “Amplification and direct sequencing of fungal ribosomal RNA genes for phylogenetics,” in <i>PCR protocols: A guide to methods and applications</i> . Eds. M. A. Innis, D. H. Gelfand, J. J. Sninsky and T. J. White (San Diego: Academic Press), 315–322.	1651
1599		1652
1600		1653
1601		1654
1602		1655
1603		1656
1604		1657
1605		1658
1606		1659
1607		1660
1608		1661
1609		1662
1610		1663
1611		1664
1612		1665
1613		1666
1614		1667
1615		1668
1616		1669
1617		1670
1618		1671
1619		1672
1620		1673
1621		1674
1622		1675
1623		1676
1624		1677
1625		1678
1626		1679
1627		1680
1628		1681
1629		1682
1630		1683
1631		1684
1632		1685
1633		1686
1634		1687
1635		1688
1636		1689
1637		1690
1638		1691
1639		1692
1640		1693
1641		1694
1642		1695
1643		1696

Litter 2 – Supplementary Information

A poisoned apple: First insights into community assembly and networks of the fungal pathobiome of healthy-looking senescing leaves of temperate trees in mixed forest ecosystem

Author: Benjawan Tanunchai*, Li Ji*, Simon Andreas Schroeter, Sara Fareed Mohamed Wahdan, Panadda Larpkern, Ann-Sophie Lehnert, Eliane Gomes Alves, Gerd Gleixner, Ernst-Detlef Schulze, Matthias Noll, François Buscot, Witoon Purahong.

*These authors contributed equally to this work.

Status: Published

Publication: Frontiers in Plant Science

Publisher: Frontiers Media S.A

Date: 03 November 2022

IF (2021) = 6.627

Copyright © 2022, The Author(s)

Reprinted with permission from Frontiers Media S.A..

Available online at: <https://doi.org/10.3389/fpls.2022.968218>

Or please see separate attachments



OPEN ACCESS

EDITED BY

Saskia Bindschedler,
Université de Neuchâtel, Switzerland

REVIEWED BY

Pulak Maitra,
Polish Academy of Sciences
(PAN), Poland
Carles Castaño,
Swedish University of Agricultural
Sciences, Sweden
Davide Francioli,
University of Hohenheim, Germany

*CORRESPONDENCE

Witoon Purahong
witoon.purahong@ufz.de
Matthias Noll
Matthias.noll@hs-coburg.de

†These authors have contributed
equally to this work

SPECIALTY SECTION

This article was submitted to
Terrestrial Microbiology,
a section of the journal
Frontiers in Microbiology

RECEIVED 29 March 2022

ACCEPTED 12 August 2022

PUBLISHED 16 September 2022

CITATION

Tanunchai B, Schroeter SA, Ji L,
Wahdan SFM, Hossen S, Lehnert A-S,
Grünberg H, Gleixner G, Buscot F,
Schulze E-D, Noll M and Purahong W
(2022) More than you can see:
Unraveling the ecology and
biodiversity of lichenized fungi
associated with leaves and needles of
12 temperate tree species using
high-throughput sequencing.
Front. Microbiol. 13:907531.
doi: 10.3389/fmicb.2022.907531

COPYRIGHT

© 2022 Tanunchai, Schroeter, Ji,
Wahdan, Hossen, Lehnert, Grünberg,
Gleixner, Buscot, Schulze, Noll and
Purahong. This is an open-access
article distributed under the terms of
the Creative Commons Attribution
License (CC BY). The use, distribution
or reproduction in other forums is
permitted, provided the original
author(s) and the copyright owner(s)
are credited and that the original
publication in this journal is cited, in
accordance with accepted academic
practice. No use, distribution or
reproduction is permitted which does
not comply with these terms.

More than you can see: Unraveling the ecology and biodiversity of lichenized fungi associated with leaves and needles of 12 temperate tree species using high-throughput sequencing

Benjawan Tanunchai^{1,2†}, Simon Andreas Schroeter^{3†}, Li Ji^{1,4},
Sara Fareed Mohamed Wahdan^{1,5}, Shakhawat Hossen^{1,6},
Ann-Sophie Lehnert³, Hagen Grünberg⁷, Gerd Gleixner³,
François Buscot^{1,8}, Ernst-Detlef Schulze³, Matthias Noll^{2,6*}
and Witoon Purahong^{1*}

¹Department of Soil Ecology, UFZ-Helmholtz Centre for Environmental Research, Halle (Saale), Germany, ²Bayreuth Center of Ecology and Environmental Research, University of Bayreuth, Bayreuth, Germany, ³Biogeochemical Processes Department, Max Planck Institute for Biogeochemistry, Jena, Germany, ⁴School of Forestry, Central South of Forestry and Technology, Changsha, China, ⁵Department of Botany and Microbiology, Faculty of Science, Suez Canal University, Ismailia, Egypt, ⁶Institute of Bioanalysis, Coburg University of Applied Sciences and Arts, Coburg, Germany, ⁷Preßwitzer Straße, Unterwellenborn, Germany, ⁸German Centre for Integrative Biodiversity Research (iDiv) Halle-Jena-Leipzig, Leipzig, Germany

Currently, lichen surveys are generally based on the examination of fruiting bodies. Lichens in the mycelial stage, in spores, or awaiting conditions for fruiting body formation are usually overlooked, even though they are important for maintaining biodiversity and ecosystem functions. This study aimed to explore the lichenized fungal community composition and richness associated with leaves and needles of 12 temperate tree species using Illumina MiSeq-based amplicon sequencing of the internal transcribed spacer (ITS) 2 region. *Picea abies* harbored the highest richness and number of lichenized fungal species. We found that the lichenized fungus *Physcia adscendens* dominated the leaves and needles of the most temperate tree species. Eleven lichenized fungal species detected in this study were recorded for the first time on leaves and needles. In addition, we identified *Athallia cerinella*, *Fellhanera bouteillei*, and *Melanohalea exasperata* that are on the German national red lists. Lichenized fungal richness was higher in conifer compared to broadleaf trees. Overall, tree species (within coniferous trees) and tree types (broadleaved vs. coniferous trees) harbored significantly different lichenized fungal community compositions pointing out the importance of host species. Diversity and community composition patterns of lichenized fungi were correlated mainly with tree species. Our study demonstrates that the diversity

of foliicolous lichens associated with leaves and needles of 12 temperate tree species can be appropriately analyzed and functionally assigned using the ITS-based high-throughput sequencing. We highlighted the importance of conifers for maintaining the biodiversity of foliicolous lichens. Based on the discovery of many red list lichens, our methodological approach and results are important contributions to subsequent actions in the bio-conversation approaches.

KEYWORDS

ITS2, *Physcia adscendens*, red-list lichenized fungi, foliicolous lichens, Illumina MiSeq

Introduction

Lichens are widely distributed in terrestrial ecosystems contributing to ecosystem functions such as biomass production and nutrient cycling, including carbon (C), nitrogen (N), and phosphorous (P) cycling (Plitt, 1919; Knops et al., 1996; Belnap et al., 2003; Asplund and Wardle, 2017). They are rich in nutrients (such as N and P) and, thus, significantly contribute to mineral cycling (Knops et al., 1996; Grimm et al., 2021). The occurrence and status of many lichens have been used for a long time as a bio-indicator for environmental air pollution (SO₂), such pollution decreases photosynthesis and respiration rate in lichens (Beekley and Hoffman, 1981). Some other lichens have been proposed as passive monitors for climate change as their occurrence corresponds to the amount of humidity in the air (Lücking et al., 2009). Lichen diversity has been used to track the drivers of global change (e.g., temperature) as its diversity responds to the temperature (Matos et al., 2017). Lichens occupy a long-lived ecological niche in which symbiotic interactions occur with various lichen-associated microorganisms (mainly fungus, green algae, and/or cyanobacterium) (Grimm et al., 2021). Nowadays, lichens have been known to further host prokaryotes, lichenicolous fungi, and viruses (Cardinale et al., 2006; Petrzik et al., 2019; Grimm et al., 2021). A recent study revealed a complete carbon (C) cycling in a lichen symbiotic interaction between algal, fungal, and lichen partners (ten Veldhuis et al., 2020). The mycobiont shapes the thallus structure of lichens that allows better nutrient accessibility, whereas the photobiont (green algae) trades off C in form of sugar and O₂ produced by photosynthesis to other microorganisms in the lichen symbiosis (Pinokiyo et al., 2006; ten Veldhuis et al., 2020; Grimm et al., 2021). Furthermore, the respiratory CO₂ generated by the mycobiont can also be used by the photobiont (ten Veldhuis et al., 2020). The cyanobiont (a cyanobacterium) may be involved in both N₂-fixation and photosynthesis as part of the symbiotic interactome (Grimm et al., 2021).

Lichen thalli play important roles both to secure the adherence of lichens onto different substrata and to embed

and expose the photobiont to solar radiation (Grube and Hawksworth, 2007). Common lichen thallus forms are crustose (crust-like) and foliose (leaf-like) forms (Grube and Hawksworth, 2007; Grimm et al., 2021). Lichens that epiphytically colonize on live leaves/needles are so-called foliicolous lichens (Anthony et al., 2002; Pinokiyo et al., 2006). According to a previous study (Lücking et al., 2009), foliicolous lichens were re-classified into four groups: (i) truly foliicolous, (ii) ubiquitous, (iii) facultatively foliicolous, and (iv) accidentally foliicolous lichens. The differences among these foliicolous lichens are the variety of their substrates as outlined earlier (Lücking et al., 2009). Briefly, truly foliicolous lichens develop mainly on leaves and needles, while ubiquitous lichens can grow on various substrata, including leaves and needles, bark, rocks, and soils (Triebel et al., 2007; Lücking et al., 2009). Facultatively foliicolous lichens can change their lifestyle to grow on leaves or needles under certain limitations or environmental conditions (Lücking et al., 2009). These first three foliicolous lichen groups are considered truly foliicolous lichens as they start their development and complete their life cycles on leaves/needles, while the accidentally foliicolous lichens (iv) start growing from adjacent branches and overgrow evergreen needles (Lücking et al., 2009).

Leaves and needles of different tree species differed in various traits including nutrition, the persistence of leaves and needles onto the trees [deciduous (shedding) vs. evergreen (non-shedding)], specific leaf area, shapes, pH, and water content. The persistence of leaves and needles plays an important role in the presence of foliicolous lichens as they need at least 2–3 years to develop thalli with reproductive organs to achieve their life cycle (Lücking and Bernecker-Lücking, 2002). There is still controversial discussion on the nutrient uptake of foliicolous lichens from host leaves and needles (Anthony et al., 2002). Some believed that lichens can access the nutrients of their host leaves and needles, whereas some believed that lichens only epiphytically live there without using the nutrient from the hosts, but absorb light and shade their host leaves (Anthony et al., 2002). While the nutrient uptake of lichens from the host leaf is in debate, other environmental factors, such as

leaf water content and pH, were reported to be important factors controlling lichenized fungi (Spier et al., 2010; Potkay et al., 2020). Lichens are poikilohydric organisms, they passively receive water from their substrates and environment (e.g., air humidity) (Lange et al., 1968; Grimm et al., 2021). The substrate preference, occurrence, and activity of lichens directly correspond with air humidity and moisture dynamics (Lücking et al., 2009; Potkay et al., 2020).

High-throughput or Next-Generation Sequencing approaches have revolutionized lichen biodiversity research (Grimm et al., 2021). The sequencing results, however, largely depend on the choice of barcode locus. Banchi et al. (2018) proposed the use of the internal transcribed spacer 2 (ITS2) gene to access the taxonomy and diversity of lichen mycobiome. They successfully detected and identified diverse lichenized fungal operational taxonomic units (OTUs). The fungal ITS gene is one of the most commonly targeted regions for detecting fungi, especially for the environmental sequencing substrates, such as leaf, soil, and wood. More than 2.6 million ITS sequences have been deposited in the UNITE database and the International Nucleotide Sequence Databases (Karsch-Mizrachi et al., 2018; Nilsson et al., 2019) (last accessed 28.03.2022). A large number of available sequences offers better accessibility for the molecular identification of fungi (Nilsson et al., 2009, 2019). UNITE database is a recently published web-based database containing more than one million public fungal ITS sequences for reference (Nilsson et al., 2019). These ITS sequences are clustered into UNITE species hypotheses that enable us to consistently identify and compare microbes from different datasets obtained from independent molecular techniques at the species level (Nilsson et al., 2019). This is the first time that the lichenized fungal diversity and community composition associated with leaves and needles of the 12 common temperate tree species are characterized using Illumina MiSeq and the most recent bioinformatic pipeline, Divisive Amplicon Denoising Algorithm 2 (DADA2) (Callahan et al., 2016). Lichens and their diversity have been used as important biological indicators for monitoring environmental quality (Abas, 2021). Studying lichenized fungal diversity and community composition is a crucial step in biodiversity conservation (Purahong et al., 2019).

This current study aims to (i) investigate the diversity and community composition of lichenized fungi associated with leaves and needles of 12 temperate tree species using high-throughput sequencing technique (Illumina MiSeq) based amplicon sequencing of the ITS2 region and the most recent bioinformatic pipeline (based on DADA2) in combination with the UNITE species hypothesis, and (ii) identify the corresponding factors shaping the diversity and community composition patterns of lichenized fungi. These factors include tree species, tree type, water content, pH, and location. We hypothesize that (i) our state-of-the-art sequencing approach is able to obtain overlooked lichenized fungi associated with leaves/needles of 12 temperate tree species at fine taxonomic

levels, such as genus or species levels; and (ii) tree species and tree types are the significant factors shaping the diversity and community composition pattern of lichenized fungi associated with leaves/needles of 12 temperate tree species.

Materials and methods

Study site and sampling

The sampling site was located in the Hainich-Dün region of Thuringia, Germany (51°12'N 10°18'E, elevations ranging from 100 to 494 m above sea level) (Supplementary Figure S1). The characteristics of the study site are 600–800 mm mean annual precipitations and 6–7.5°C mean annual temperatures. The main soil type is a Cambisol on limestone as bedrock with the soil pH of 5.1. In total, a minimum of 200 g of healthy-looking leaves and needles were collected from branches at the lower part of the crown of the 60 mature trees (3-years-old leaves and needles, 12 temperate tree species, and 5 replicate tree individuals per species) in October 2019. The 12 temperate tree species consisted of eight broadleaved (including *Acer pseudoplatanus*, *Carpinus betulus*, *Fagus sylvatica*, *Fraxinus excelsior*, *Populus hybrid*, *Prunus avium*, *Quercus robur*, and *Tilia cordata*) and four coniferous tree species (including *Picea abies*, *Larix decidua*, *Pinus sylvestris*, and *Pseudotsuga menziesii*). *Fagus sylvatica* and *Picea abies* are the dominant tree species in this site. Leaves and needles of an individual tree were sampled in a separate sterilized plastic bag using new clean gloves. One set of samples was sent on ice to the physicochemical laboratory for water content and pH determination and another set of samples was transported on ice to the molecular laboratory within 3 h and stored at –80°C until further processing.

Water content and pH measurement

To measure water content and leaf pH, wet leaf and needle samples were shaken for 1 h in falcon tubes with 30 mL Milli-Q water. The leachates were centrifuged for 5 min at 5,000×g, decanted, and filtered through pre-flushed 0.45 µm regenerated cellulose syringe filters. The remaining leaf/needle material was dried for 2 weeks at 40°C for dry weight determination. The pH of the leachates was determined using pH paper with a scale precision of 0.2 pH units.

DNA extraction and Illumina sequencing

DNA extraction and Illumina sequencing were done according to Tanunchai et al. (2022). In our previous study (Tanunchai et al., 2022), we compared FUNGuild and FungalTraits to assign fungal ASVs to lichenized fungi;

however; we did not tackle the ecological aspect of those datasets. Briefly, for the preparation for the DNA extraction, up to 10 healthy-looking leaves and needles were carefully selected from five branches per tree individual to avoid contamination from the fungi living on branches. Loosely attached fungal mycelium and dust particles were removed from the leaf and needle sample by three-times washing with sterile Tween solution (0.1% vol/vol), then three to five times with MiliQ sterile water or until no bobble, and finally, incubated for 1 h in sterile water at room temperature. The samples were then ground using liquid N₂ and sterilized nails, homogenized, then stored at -20°C for further analysis. The total fungal community attached firmly to the leaf and needle samples (~120 mg homogenized leaves and needles) was then subjected to DNA extraction using the DNeasy PowerSoil kit (Qiagen, Hilden, Germany) and a Precellys 24 tissue homogenizer (Bertin Instruments, Montigny-le-Bretonneux, France) according to the manufacturer's instructions. The total fungi were characterized by the fungal internal transcribed spacer (ITS)-based amplicon sequencing on the Illumina MiSeq sequencing platform, as outlined earlier (Weißbecker et al., 2020). The fungal ITS2 gene was amplified using the fungal primer pair fITS7 [5'-GTCTCG TGGGCTCGGAGATGTGTATAAGAGACAGNNNGTGART CATCGAATCTTTG-3' and 5'-GTCTCGTGGGCTCGGAGA TGTGTATAAGAGACAGNNNGTGARTCATCGAATCTT TG-3'] (Ihrmark et al., 2012) and ITS4 primer [5'-TCGTCGG CAGCGTCAGATGTGTATAAGAGACAGNNNNNTCCTCC GCTTATTGATATGC-3' and 5'-TCGTCGGCAGCGTCAGAT GTGTATAAGAGACAGNNNNNTCCTCCGCTTATTGAT ATGC-3'] (White et al., 1990) with Illumina adapter sequences. Amplifications were performed using 20 µL reaction volumes with 5× HOT FIRE Pol Blend Master Mix (Solis BioDyne, Tartu, Estonia). The amplified products were visualized by gel electrophoresis (fragment size length ~400 bp). Negative control was sequenced along with the samples. Paired-end sequencing (2 × 300 bp) was performed on the pooled PCR products (three technical replicates, ~45 µL reaction volumes) using a MiSeq Reagent kit v3 on an Illumina MiSeq system (Illumina Inc., San Diego, CA, United States) at the Department of Soil Ecology, Helmholtz Centre for Environmental Research, Germany as outlined earlier (Tanunchai et al., 2022).

Bioinformatics

Bioinformatics analysis was conducted according to Tanunchai et al. (2022). Briefly, the ITS rRNA gene paired-end sequences were quality-trimmed from the demultiplexed raw reads using cutadapt (Martin, 2011), filtered for chimeras, and merged using the DADA2 package (Callahan et al., 2016) through the pipeline dada2 (Weißbecker et al., 2020). Assembled reads fulfilling the following criteria were retained for further analyses: a minimum length of 70 nt, quality scores

at least equal to 9 nt with a maximum expected error score of 5 nt for forward and reverse sequences, and no ambiguous nt. Merging was conducted with two mismatches allowed and a minimum overlap of 20 nucleotides required for fungal sequences. Fungal ASVs were classified against the UNITE v7.2 database (Kõljalg et al., 2013). A set of ASVs was classified using the Bayesian classifier as implemented in the mothur classify.seqs command, with a cut-off of 60 (Wang et al., 2007). DADA2 offers an advantage against the conventional OTU method as it results in less spurious sequences, which consequently reduces the inflation of the microbial richness. The inflation of the microbial richness is considered an important problem for OTU-based analyses (Callahan et al., 2016). The fungal raw reads were rarefied. A total of 2,451 rarefied fungal ASVs with the minimum sequencing depths of 21,967 sequences per sample were obtained. The fungal ecological function of each ASV was determined using FUNGuild (Nguyen et al., 2016) and FungalTraits (Pöhlme et al., 2020) according to the authors' instructions. We assigned 59 lichenized fungal ASVs (accounting for 2.4% of total fungal ASVs and 0.87% of total fungal sequencing reads) by FUNGuild and FungalTraits (removing one fungal ASV with ambiguous ecological functions, *Sphaerulina*) (Tanunchai et al., 2022). Species of 59 lichenized fungal ASVs were identified by UNITE database based on UNITE species hypothesis. Lichenized fungal ASVs with identical UNITE species hypothesis and SH code were merged into a single species. In total, 28 lichenized fungal species were obtained. Relative abundance and richness of lichenized fungal species were used for further analyses. LIAS (Triebel et al., 2007) and peer-reviewed publications (Lücking, 1999; Lücking and Cáceres, 2002; Pinokiyo et al., 2006; Lücking et al., 2009; Grube, 2010) were used to affiliate traits to the lichenized fungal ASVs, such as identify distribution, substrata, record on leaf, and thallus forms. To confirm the ITS-based sequencing identification of lichenized fungi, we performed the fruiting body survey on the same temperate trees and collected visible fruiting bodies for microscopic examination.

Statistical analysis

The datasets were tested for normality using the Jarque-Bera JB test and for the equality of group variances using the *F*-test (for two datasets) and Levene's test (for more than two datasets). To test the effect of tree species on lichenized fungal community composition, data of tree species with more than three replicates were considered. Effects of tree species and tree types on lichenized fungal community composition were visualized with principle coordinate analysis (based on relative abundance data and the Bray-Curtis distance measure) and tested with one-way PERMANOVA (based on relative abundance data and the Bray-Curtis distance measure), over 999 permutations of each run. The correlation analyses between pH, leaf/needle water content,

and lichenized fungal species richness were performed using Spearman's rank correlation (ρ). The statistical differences in ASV richness among different tree species were performed using one-way ANOVA. All statistical analyses were performed using PAST version 2.17 (Hammer et al., 2001), R and RStudio version 4.0.4 (RStudio Team, 2019).

Specialist/generalist classification of the taxonomic dataset in this study was performed using the "EcolUtils" package in R and RStudio version 4.0.4 based on niche width and permutation algorithms. The indicator species were identified using the "indicspecies" package in R and RStudio version 4.0.4 based on the association between species patterns and combinations of groups of sites. The goodness-of-fit statistics (R^2) of environmental variables fitted to the nonmetric multidimensional scaling (NMDS) ordination of lichenized fungal community composition were performed using the "Vegan" package in R and RStudio. The function "envfit" in the Vegan package fits environmental vectors or factors onto an ordination.

Results

Lichenized fungi associated with leaves and needles of 12 temperate tree species

Twenty-eight lichenized fungal species from 23 different genera were obtained (Figure 1; Table 1). In total, we assigned 11,508 fungal reads to lichenized fungal species (accounting for 0.87% of total fungal sequencing reads). Lichenized fungal reads of 11,324 (98%) were obtained from coniferous trees, while only 184 reads (2%) were obtained from broadleaved trees. The lichenized fungal genus, *Physcia* (accounting for 72.1% relative sequence read abundance of the total lichenized fungal community composition) dominated the lichenized fungal community composition across temperate tree species (including all coniferous tree and broadleaved trees; except the tree species maple, linden, and poplar), followed by lichenized fungal genera *Bacidia* (16.3%) and *Scoliciosporum* (2.9%) (Figure 1A). Similar patterns were found for lichenized fungal community composition associated with needles of coniferous trees, *Physcia* (72.5%), *Bacidia* (16.5%), and *Scoliciosporum* (2.7%) covered more than 90% relative abundance of the lichenized fungal community composition (Figure 1C). In broadleaved trees, *Physcia* (accounting for 46.2% relative sequence read abundance of the broadleaved associated lichenized fungal community composition) dominated the lichenized fungal community, followed by fungal genera, *Xanthoria* (16.8%), *Scoliciosporum* (14.7%), and *Lecania* (7.1%) (Figure 1B). The lichenized fungal genus *Physcia* is mainly represented by *Physcia adscendens* (Fr.) H. Olivier (Figure 1D). *Scoliciosporum chlorococcum* (Stenh.) Vezda co-dominated lichenized fungal community composition along with *Physcia*

adscendens in three broadleaved tree species. In leaves of *Acer pseudoplatanus*, only *Phaeophyscia orbicularis* (Neck.) Moberg was detected and no lichenized fungi were detected in the leaves of the *Populus hybrid* (Figure 1D).

The lichenized fungal species detected in this study were classified into two main types of lichens according to their thallus form, (i) crustose (e.g., *Amandinea punctata*, *Fellhanera bouteillei*, and *Lecanora dispersa*) and (ii) foliose (e.g., *Hypogymnia physodes*, *Physcia adscendens*, and *Polycauliona candalaria*) (Table 1). Some lichens also had more than one thallus form, e.g., *Fellhanera bouteillei* (crustose and leprose) and *Polycauliona candalaria* (foliose and subfruticose). The foliicolous lichen, *F. bouteillei*, which was found on needles of young planted *Picea abies*, was recorded as red-list species with the status "threatened with extinction" according to the German national red lists (Wirth et al., 2011). In addition, two other lichenized fungal species with the red-list status of highly threatened (*Athallia cerinella* (Nyl.) Arup, Frödén and Söchting on leaves of *Quercus robur* and *Melanohalea exasperata* (De Not.) O. Blanco, A. Crespo, Divakar, Essl., D. Hawksw. and Lumbsch on needles of planted *Larix decidua*) were observed (Table 1). On the other hand, *Bacidia arnoldiana* (Körb.) V. Wirth and Vezda and *Melanohalea exasperata* were listed with the status "threatened" according to the red-list species of Thuringia (Eckstein and Grünberg, 2021). Moreover, we identified seven indicator species for coniferous tree species [including *Lecania cyrtella*, *Pezizomycotina (Sarea resiniae)*, *Polycauliona candalaria*, *Scoliciosporum chlorococcum*, *Squamarina* sp., *P. adscendens*, and *Xanthoria coomae*] (Table 1). Based on niche width and permutation algorithms, we assigned three lichenized fungal specialists (including *Bacidia neosquamulosa*, *Cliostomum* sp., and *Micarea* sp.) and two generalists (including *P. adscendens* and *X. coomae*) (Table 1).

Link between next-generation sequencing and fruiting body data sets for species identification of lichenized fungi

To confirm the ITS-based sequencing identification of lichenized fungi, we collected the fruiting bodies for microscopic examination from the same temperate trees. There were 10 out of 28 lichenized fungal species detected by NGS that were also found by the fruiting body survey (Table 1). These lichens include *Athallia cerinella*, *Buellia griseovirens*, *Candelariella* sp., *Hypogymnia physodes*, *Lecania cyrtella*, *Melanelixia subaurifera*, *Phaeophyscia orbicularis*, *Physcia adscendens*, *P. alnophila*, and *X. coomae*. However, five lichenized species (*A. cerinella*, *B. griseovirens*, *Candelariella* sp., *L. cyrtella*, and *P. orbicularis*)

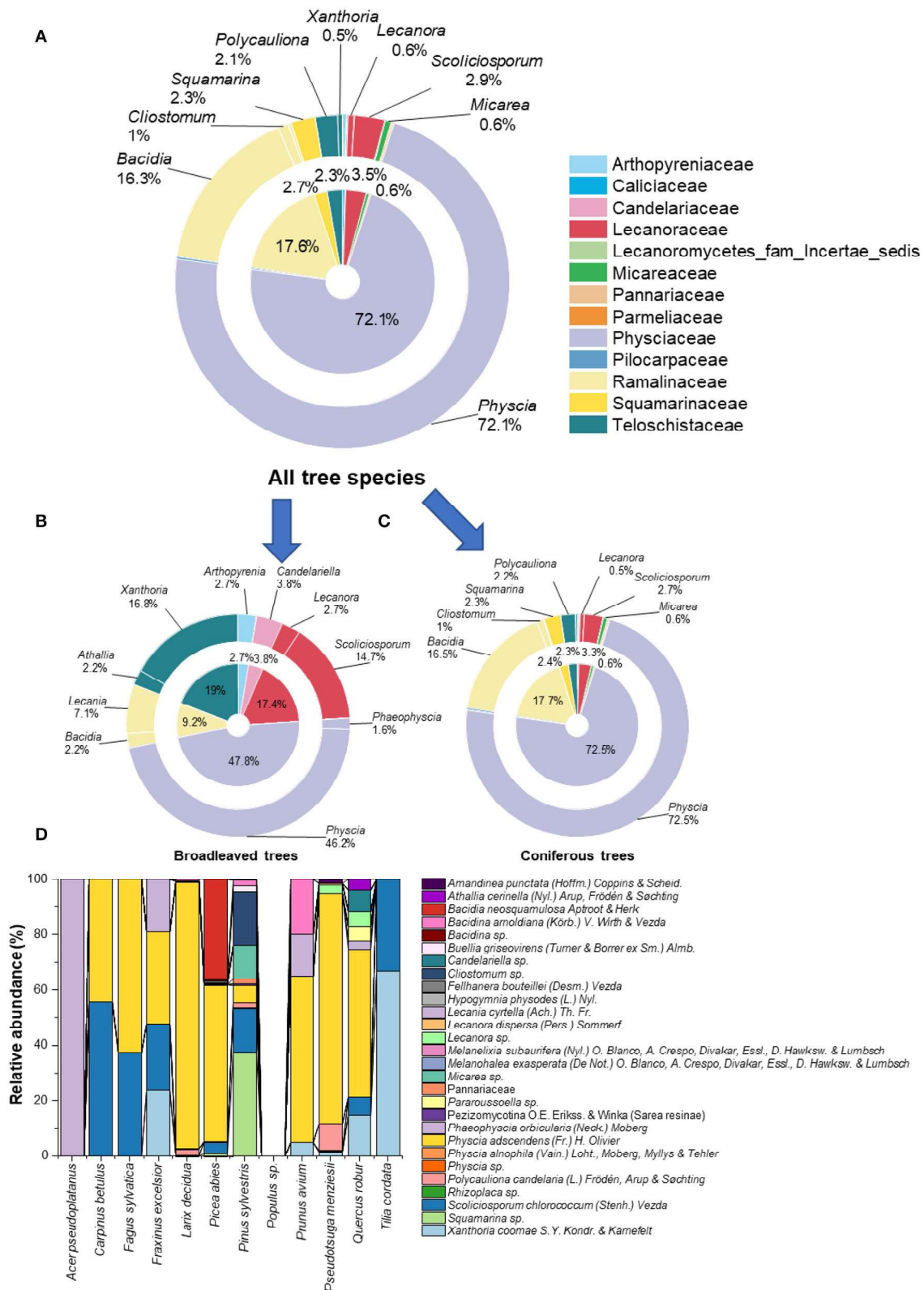


FIGURE 1 Proportion of lichenized fungi (at family- and genus level) associated with leaves and needles of all tree species (A), leaves of broadleaved tree species (B), needles of coniferous tree species (C), and proportion of lichenized fungi (at species-level) (D) associated with leaves and needles of 12 temperate tree species ($n = 5$ tree replicates). No lichenized fungi were detected in *Populus* sp. (*Populus hybrid*). Color codes in (A–C) refer to lichenized fungal family given in the top-right of the figure.

TABLE 1 UNITE species hypothesis of lichenized fungi associated with leaves and needles of 12 temperate tree species with the information on its global distribution, red-list status (recorded in Germany), indicator species, substrate, record on leaf/needle, and thallus form.

Final UNITE species hypothesis (percent match > 97%)	Host tree species	Indicator species for	Fruiting body survey record in Germany	Sequence record in Germany	Red-list status (Germany)	Red-list status (Thuringia)	Global occurrence (LIAS)	Substrata (LIAS)	Record on leaf/needle	Thallus form (LIAS)
<i>Amandinea punctata</i> (Hoffm.) Coppins and Scheid.	DG, KI	NA	NA	NA	Not threatened	Not threatened	Worldwide	Wood, bark, cork, plant surface, trunks, branches, twigs, rock	Yes	Crustose
<i>Athallia cerinella</i> (Nyl.) Arup, Frödén and Sochting	EI	NA	BU	NA	Highly threatened	NA	Australia, Europe, Americas	Wood, bark, cork, plant surface, trunks, branches, twigs	NA	Crustose
<i>Bacidia neosquamulosa</i> Aptroot and Herk	FI	NA	NA	NA	Not threatened	NA	Europe, Americas	Bark, cork, plant surface, trunks, branches, twigs	NA	Crustose, squamulose, subsquamulose
(Specialist)										
<i>Bacidia arnoldiana</i> (Körb.) KB, KI, LA V. Wirth and Vezda	KB, KI, LA	NA	NA	NA	Not threatened	Threatened	Asia, Europe, Americas	Rock	Yes (accidentally foliicolous lichen)	Crustose
<i>Bacidia</i> sp.	FI	NA	NA	NA	NA	NA	NA	NA	NA	NA
<i>Buellia griseovirens</i> (Turner and Borrer ex Sm.) Almb.	KI	NA	BU	NA	Not threatened	Not threatened	Australia, Europe, Americas	Wood, bark, cork, plant surface, trunks, branches, twigs	NA	Crustose
<i>Candelariella</i> sp.	EI, FI, LA	NA	BU	NA	NA	NA	NA	NA	NA	NA
<i>Clotostomum</i> sp.	KI	NA	NA	NA	NA	NA	NA	NA	NA	NA
(Specialist)										
<i>Fellhanera bouteillei</i> (Desm.) Vezda	FI	NA	NA	NA	Threatened with extinction	Not threatened	Worldwide except Africa and Antarctica	Bark, cork, plant surface, trunks, branches, twigs, leaves, fronds, needles, rock	Yes (ubiquitous foliicolous lichen)	Leprose, crustose
<i>Hypogymnia physodes</i> (L.) Nyl.	FI, LA	NA	FI, LA	NA	Not threatened	Not threatened	Worldwide except Antarctica and Australia	Soil, humus, turf, detritus, dead leaves, mosses, wood, bark, cork, plant surface, trunks, branches, twigs, rock	Yes	Foliose

(Continued)

TABLE 1 (Continued)

Final UNITE species hypothesis (percent match > 97%)	Host tree species	Indicator species for	Fruiting body survey record in Germany	Sequence record in Germany	Red-list status (Germany)	Red-list status (Thuringia)	Global occurrence (LIAS)	Substrata (LIAS)	Record on leaf/needle	Thallus form (LIAS)
<i>Lecanora cyrtella</i> (Ach.) Th. Fr.	AH, ES, FI, KB	FI	BU	NA	Not threatened	Not threatened	Worldwide except Antarctica and Australia	Bark, cork, plant surface, trunks, branches, twigs	NA	Crustose
<i>Lecanora dispersa</i> (Pets.) Sommerf.	DG	NA	NA	NA	Not threatened	NA	Worldwide except Antarctica	Soil, humus, turf, detritus, dead leaves, bark, cork, plant surface, trunks, branches, twigs, rock	Yes	Crustose
<i>Lecanora</i> sp.	Coniferous trees (except KI) and EI	NA	NA	NA	NA	NA	NA	NA	NA	NA
<i>Melanelixia subaurifera</i> (Nyl.) O. Blanco, A. Crespo, Divakar, Essl., D. Hawksw. and Lumbsch	FI	NA	FI, LA	NA	Not threatened	Not threatened	Asia, Europe, Americas	Mosses, wood, bark, cork, plant surface, trunks, branches, twigs, rock	NA	Foliose
<i>Melanohalea exasperata</i> (De La Not.) O. Blanco, A. Crespo, Divakar, Essl., D. Hawksw. and Lumbsch	De LA	NA	NA	NA	Highly threatened	Threatened	Worldwide except Antarctica and Australia	Wood, bark, cork, plant surface, trunks, branches, twigs, rock	NA	Foliose
<i>Micarex</i> sp. (Specialist)	KI	NA	NA	NA	NA	NA	NA	NA	NA	NA
Pannariaceae sp.	KI	NA	NA	Yes	NA	NA	NA	NA	NA	NA
<i>Pararoussoella</i> sp.	EI	NA	NA	Yes	NA	NA	NA	NA	NA	NA
<i>Pezizomycotina</i> O.E. Erikss. and Winka (<i>Sarea resiniae</i>)*	KI	NA	NA	Yes	Near threatened	NA	Europe, Americas	Bark, cork, plant surface, trunks, branches, twigs	NA	Crustose
<i>Phaeophyscia orbicularis</i> (Neck.) Moberg	EI	NA	BU	Yes	Not threatened	Not threatened	Worldwide except Antarctica	Bark, cork, plant surface, trunks, branches, twigs, rock	NA	Foliose

(Continued)

TABLE 1 (Continued)

Final UNITE species hypothesis (percent match > 97%)	Host tree species	Indicator species for	Fruiting body survey record in Germany	Sequence record in Germany	Red-list status (Germany)	Red-list status (Thuringia)	Global occurrence (LIAS)	Substrata (LIAS)	Record on leaf/needle	Thallus form (LIAS)
<i>Physcia adscendens</i> (Fr.) H. Olivier (Generalist)	All coniferous tree and broadleaved trees (except AH, LI, PA)	DG, FI, and LA	BU, FI, LA	Yes	Not threatened	Not threatened	Worldwide	Wood, bark, cork, plant surface, trunks, branches, twigs, rock	Yes (accidentally foliicolous lichen)	Foliose
<i>Physcia alnophila</i> (Vain.) Lohlt, Moberg, Myllys and Tehler	LA	NA	LA	NA	NA	NA	Europe, Americas	NA	NA	Foliose
<i>Physcia</i> sp.	FI, LA	NA	NA	Yes	NA	NA	NA	NA	NA	NA
<i>Polycauliona candelaria</i> (L.) Frödén, Arup and Sochting	Coniferous trees (except FI)	DG and LA	NA	Yes	Not threatened	NA	Worldwide except Australia	Wood, bark, cork, plant surface, trunks, branches, twigs, rock	NA	Foliose, subfruticose
<i>Rhizoplaca</i> sp.	DG, KI	NA	NA	NA	NA	NA	NA	NA	NA	NA
<i>Scoliciosporum chlorococcum</i> (Stenh.) Vezda	Coniferous trees (except LA) and broadleaved trees (except AH, KB, PA)	FI and KI	NA	NA	Not threatened	Vulnerable fungi	Europe, Americas	Bark, cork, plant surface, trunks, branches, twigs	NA	Crustose
<i>Squamarina</i> sp.	Coniferous trees (except DG)	FI and KI	NA	NA	NA	NA	NA	NA	NA	NA
<i>Xanthoria</i> <i>come</i> S.Y. Kondr. and Kärmefelt	Coniferous trees (except KI) and EI, ES, KB, LI	DG, EI, and ES	BU, FI, LA	Yes	NA	NA	NA	Bark	NA	Foliose
(Generalist)										

*According to UNITE database, it was identified as *Sarea resiniae* (Near threatened), however, the UNITE species hypothesis identified it as *Pezizomycotina* O.E. Erikss. and Winka. Thus, we exclude it from the red-list species. Information about specialism and generalism is given with the species name. Host tree species abbreviations are: AH, *Acer pseudoplatanus*; BU, *Ficus sylvatica*; DG, *Pseudotsuga menziesii*; EI, *Quercus robur*; ES, *Fraxinus excelsior*; FI, *Picea abies*; HBU, *Carpinus betulus*; KB, *Prunus avium*; KI, *Pinus sylvestris*; LA, *Larix decidua*; LI, *Tilia cordata*; PA, *Populus hybrid*; NA, Not assigned. Information from the lichens and non-lichenized ascomycetes (LIAS) was taken from Triebel et al. (2007). Bold letters indicate red-list status and generalist/specialist.

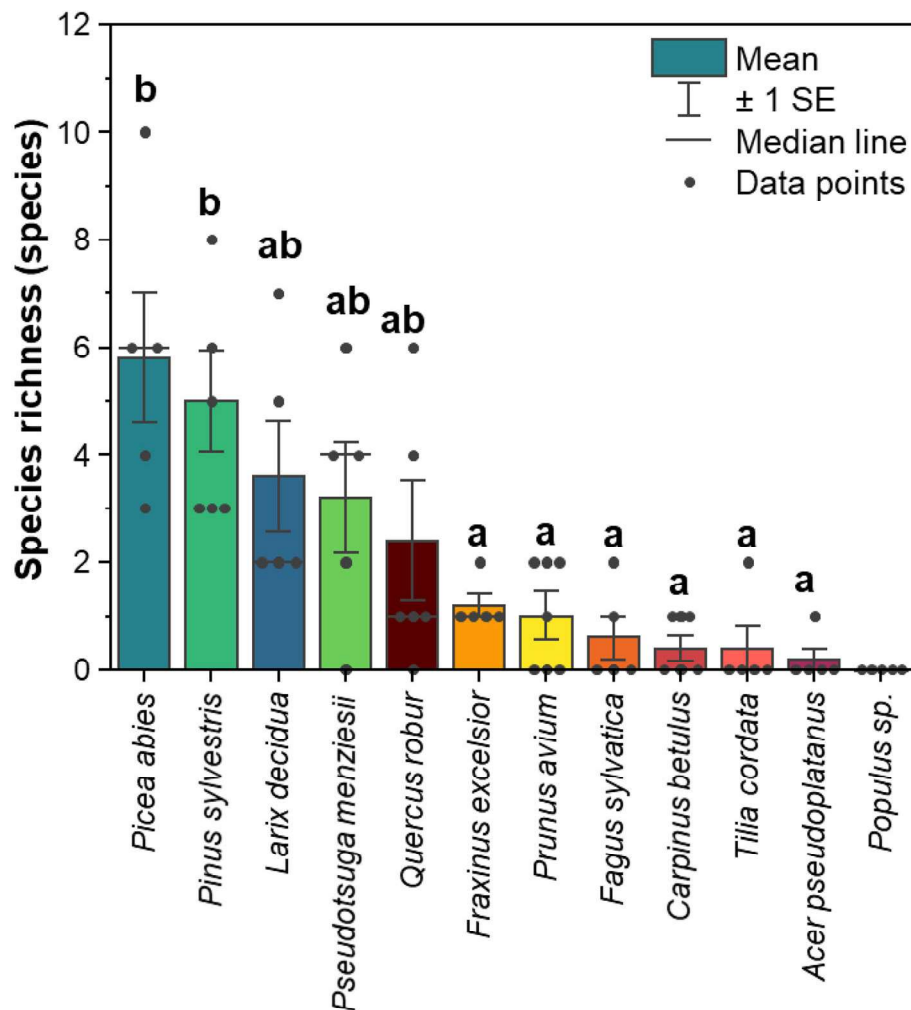


FIGURE 2

Mean of species richness of lichenized fungi associated with leaves and needles of 12 temperate tree species ($n = 5$ tree replicates). Yellow-red-brown color tone refers to the broadleaved tree species and blue-green color tone refers to the coniferous tree species. The statistical differences ($P < 0.05$) as indicated by letters between species richness among different tree species [excluding *Populus sp.* (*Populus hybrid*)] were performed using one-way ANOVA.

detected by NGS were found on different host trees than those examined in the fruiting body survey.

Richness of lichenized fungi associated with leaves and needles of 12 temperate tree species

The richness of lichenized fungal species (merge of ASVs with identical UNITE species hypothesis) was higher in coniferous trees than in broadleaved trees (Figure 2). Among coniferous trees, *Picea abies* harbored the highest species richness (average of five replicate trees = 5.8 species, ranging from 3 to 10 species), while *Pseudotsuga menziesii* revealed the

lowest species richness (average of five replicate trees = 3.2 species, ranged from 0 to 6 species). *Quercus robur* harbored the highest species richness (average of five replicate trees = 2.4 species, ranging from 0 to 6 species) among broadleaved trees, whereas, in *Populus hybrid*, no lichenized fungi were detected.

A similar pattern was found when we considered the total number of lichenized fungal species detected in each tree species. In total, conifers harbored 25 out of 28 lichenized fungal species. Among conifers, *Picea abies* harbored the highest number of lichenized fungal species (13 species), followed by *Pinus sylvestris* (12 species), *Larix decidua* (11 species), and *Pseudotsuga menziesii* (8 species). In total, broadleaved tree species harbored 10 out of 28 lichenized fungal species. Among broadleaved tree species, *Quercus robur* harbored the highest number of lichenized fungal species (eight species), followed

by *Fraxinus excelsior* (four species), and *Prunus avium* (four species). *Carpinus betulus*, *Fagus sylvatica*, and *Tilia cordata* harbored two lichenized fungal species, and *Acer pseudoplatanus* harbored solely one lichenized fungal species [*Lecania cyrtella* (Ach.) Th. Fr.].

Leaves and needles and environmental factors shaped lichenized fungal community composition

Overall, the lichenized fungal community compositions significantly differed among 11 temperate tree species (PseudoF = 2.94, $P < 0.001$; Figure 3A). The lichenized fungal community compositions associated with needles of *Pinus sylvestris* and *Larix decidua* were significantly different from those of almost all other tree species (Supplementary Table S1). Considering coniferous tree species, the lichenized fungal community compositions also significantly differed (PseudoF = 5.39, $P < 0.001$; Figure 3B), except for *Picea abies* and *Pseudotsuga menziesii* (Supplementary Table S1). Considering broadleaved tree species (*Fraxinus excelsior*, *Prunus avium*, and *Quercus robur*), no significant difference was detected (PseudoF = 0.93, $P > 0.05$; Supplementary Figure S2).

The goodness of fit tests showed that tree species, tree type, and water content significantly corresponded with the lichenized fungal community composition (Table 2). When needles of coniferous trees were considered, tree species, pH, and longitude significantly corresponded with lichenized fungal community composition. The lichenized fungal richness of all tree species had no significant correlation with pH and water content (Figure 4). However, when considering broadleaved and conifer trees separately, pH ($\rho = 0.50$, $P = 0.030$) was found to be the important factor that significantly positively correlated with lichenized fungal species richness of conifer and water content positively correlated with those of broadleaf ($\rho = 0.58$, $P = 0.011$) (Figure 4).

Discussion

The detection of lichenized fungi living on leaves and needles using high-throughput sequencing technique based on the amplicon sequencing of the ITS2 region

The observation of lichens by the experts was traditionally based on the presence and microscopic observations of fruiting bodies. In our study site, we observed lichens by eye on branches and needles of coniferous tree species, such as *Fellhanera*, *Physcia*, and *Xanthoria* (Figure 5). The contamination from lichens that grow on branches was unlikely as the leaf and

needle samples were carefully selected, separated from branches, and washed three times with 0.1% sterile tween and five times with MiliQ sterile water. A high-resolution molecular technique based on the ITS2 region allowed the identification of the lichenized fungal taxonomy at fine taxonomic levels (genus or species level). This is consistent with a recent study (Banchi et al., 2018), which demonstrated that the fungal ITS2 gene can be efficiently used to access the taxonomy and diversity of lichen mycobiome. In fact, the fungal ITS gene is one of the most commonly targeted regions for detecting diverse groups of fungi, including saprotrophs, pathogens, endophytes, and lichenized fungi. Previous studies clearly reported the distinctiveness between lichenized fungi and fungal endophytes living in both lichen thalli and plants in terms of taxonomy, diversity, transmission mode, and evolutionary history (Arnold et al., 2009; U'Ren et al., 2010). In this study, we specifically select the lichenized fungal group for the analysis which is assigned function by the most successful and recently published annotation tools, FUNGuild (Nguyen et al., 2016) and FungalTraits (Pöhlme et al., 2020). We confirmed the lichenized fungal species using UNITE species hypothesis (Nilsson et al., 2019) and previously published literature, including LIAS (Triebel et al., 2007) and peer-reviewed publications (Lücking, 1999; Lücking and Cáceres, 2002; Pinokiyo et al., 2006; Lücking et al., 2009; Grube, 2010).

Frequently overlooked high diversity of lichenized fungi were found on leaves and needles of 12 temperate tree species

More than 60% (17 out of 28 species) of lichenized fungal species were identified at the species level using the UNITE species hypothesis (Nilsson et al., 2019). Overall, we detected two times more diverse lichenized fungal species using NGS as compared to the traditional fruiting body survey (Table 1). Specifically, only 10 lichens were observed by a fruiting body survey and under the microscope. *P. adscendens* is one of the most widespread lichenized fungi detected in high relative abundance across both broadleaved (*Carpinus betulus*, *Fraxinus excelsior*, *Fagus sylvatica*, *Prunus avium*, and *Quercus robur*) and coniferous tree species (*Larix decidua*, *Picea abies*, *Pseudotsuga menziesii*, and *Pinus sylvestris*) in a temperate forest of Central Germany. *Physcia adscendens* is foliose lichen previously recorded worldwide (Triebel et al., 2007). It was classified as accidentally foliicolous lichen (Lücking et al., 2009) as it starts developing on branches and overgrown leaves. Accidentally foliicolous lichens are not considered truly foliicolous lichens, which would need at least 2 years to develop thalli with reproductive organs and complete their life cycle on leaves (Lücking and Bernecker-Lücking, 2002). Thus, the presence of *P. adscendens* on leaves and needles of deciduous

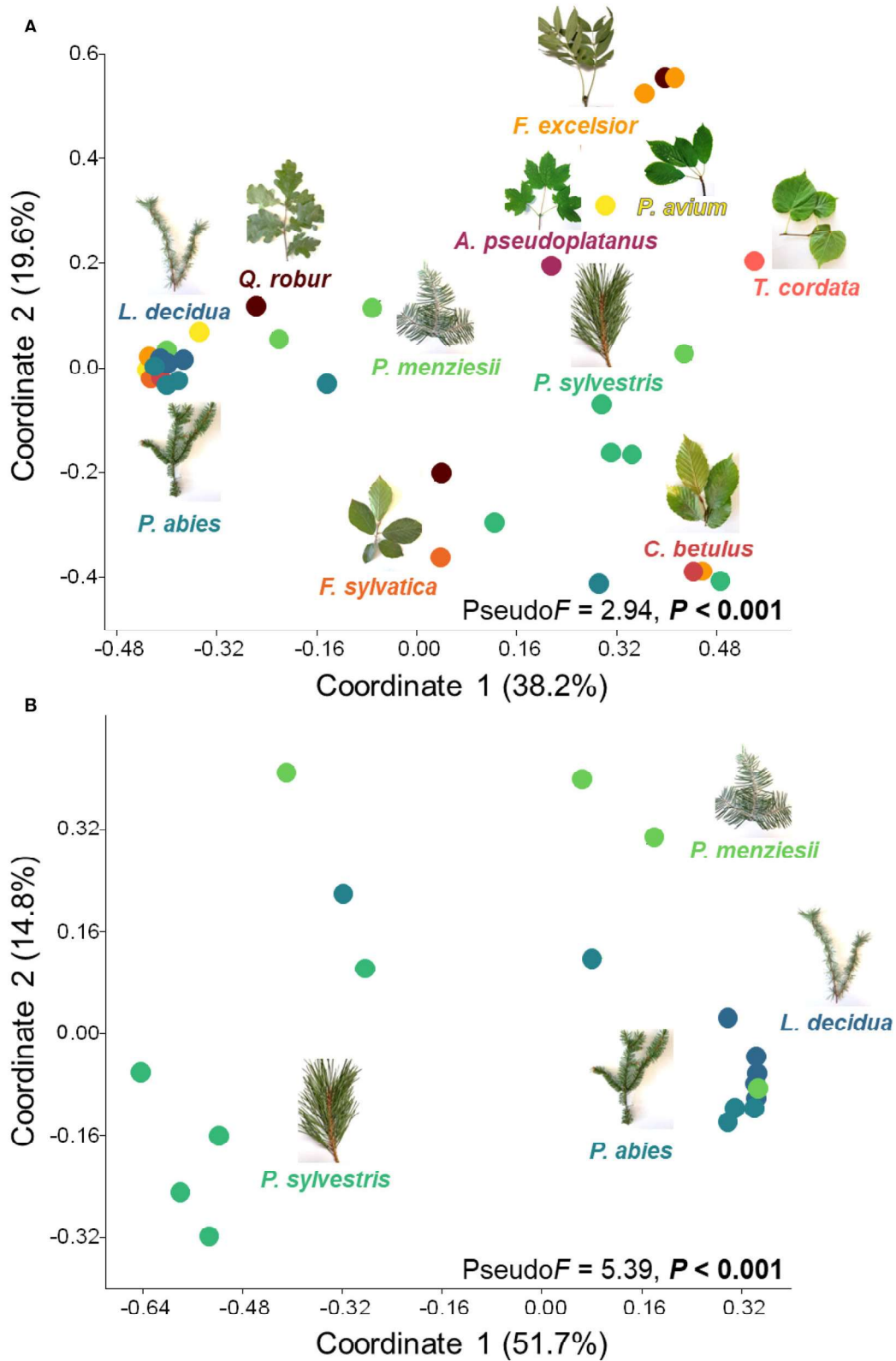
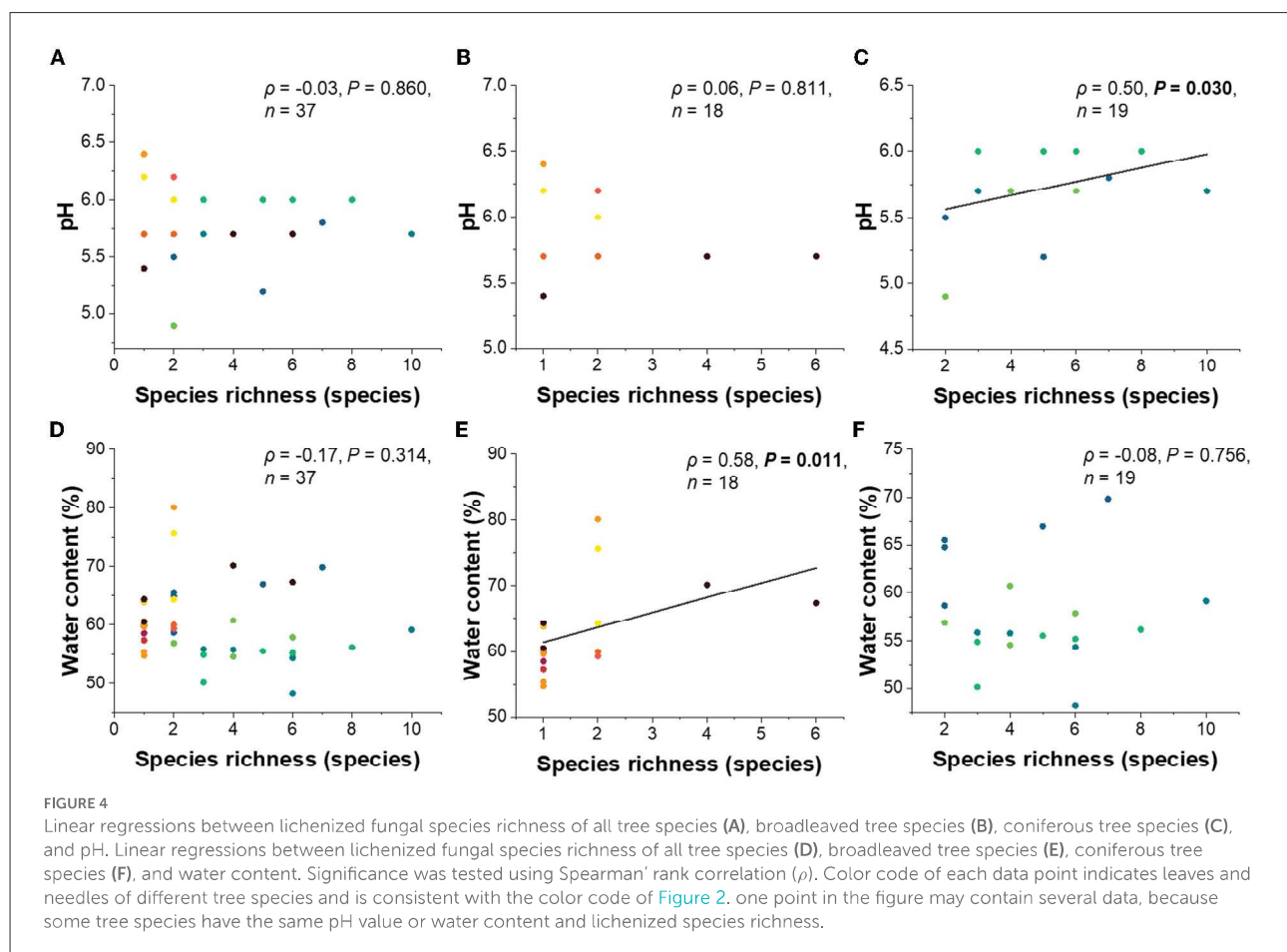


FIGURE 3
Principal coordinates showing lichenized fungal community compositions in all tree species (A) and coniferous tree species (B). Effects of tree species (only tree species that contain lichenized fungi in more than three replicates are considered) were tested with one-way PERMANOVA (based on relative abundance data and the Bray-Curtis distance measure). *Populus hybrid.* was excluded from the analysis. Color code of each data point indicates leaves and needles of different tree species and is consistent with the color code of Figure 2.

TABLE 2 Goodness-of-fit statistics (R^2) of environmental variables fitted to the nonmetric multidimensional scaling (NMDS) ordination of lichenized fungal community composition based on relative abundance data for three comparisons: (i) leaves and trees of all tree species, and separately for (ii) coniferous or (iii) broadleaved trees.

	(i) All tree species		(ii) Coniferous trees		(iii) Broadleaved trees	
	R^2	P	R^2	P	R^2	P
Tree species	0.53	0.001	0.67	0.001	0.32	0.598
Tree type	0.15	0.004	NA	NA	NA	NA
pH	0.11	0.146	0.37	0.031	0.00	0.981
Water content	0.25	0.008	0.14	0.284	0.27	0.096
Latitude	0.13	0.105	0.19	0.190	0.10	0.491
Longitude	0.11	0.135	0.36	0.023	0.21	0.190

Bold letter indicates statistical significances. The data on leaf/needle water content and pH are provided in Supplementary Figure S3.



trees, which shed their leaves or needles annually, may not be surprising.

In this study, needles of coniferous tree species harbor more rich and diverse lichenized fungal species as compared with leaves of broadleaved deciduous tree species. Specifically, needles of *Picea abies* harbored the highest richness and number of lichenized fungal species. Lichenized fungal community

composition on needles of deciduous *Larix decidua* differs from other evergreen coniferous tree species. The high lichenized fungal species richness on needles of coniferous tree species may be explained by first, the persistence of evergreen needles which allows the development of lichens to achieve their life cycle (Lücking and Bernecker-Lücking, 2002). Second, fungal hyphae may attach better to the cuticular crust of needles.

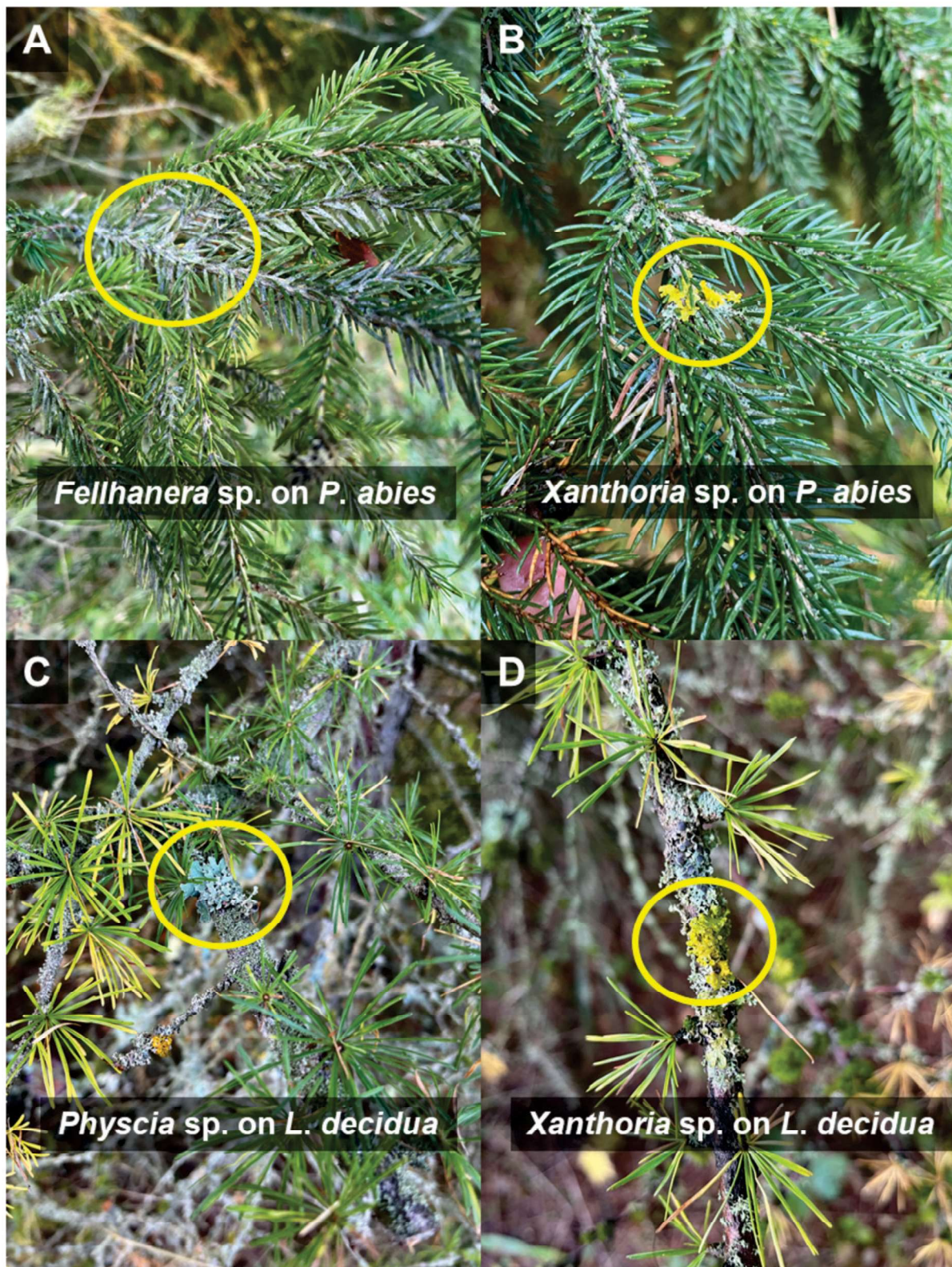


FIGURE 5

Lichens with visible fruiting bodies growing on branches and needles of *Picea abies* (A,B) and *Larix decidua* (C,D). The identification of lichens was performed by Hagen Grünberg, Lichen-Expert Thüringen.

The main type of substrate or habitat, on which lichens were previously recorded, were bark, wood, and branches (Table 1) (Triebel et al., 2007). Interestingly, among the 17 lichenized fungal species, only six lichenized fungi were previously reported on leaves and only three lichenized fungi were classified as foliicolous lichens [*F. bouteillei* (Desm.) Vezda, *H. physodes*, and *Lecanora dispersa*] (Table 1). Other 11 lichenized fungi are recorded for the first time on leaf and needle substrata. These lichenized fungi included *A. cerinella*, *B. neosquamulosa*, *B. griseovirens*, *L. cyrtella*, *M. subaurifera*, *M. exasperata*, *P. orbicularis*, *P. alnophila*, *P. candelaria*, *S. chlorococcum*, and *X. coomae* (Table 1). These lichenized fungi are likely to be new potential accidentally foliicolous lichens. Furthermore, the Illumina MiSeq molecular technique is also able to capture red-list lichenized fungi, which are listed in the German national red lists with the status of “highly threatened” and “threatened with extinction” (Wirth et al., 2011). These include *A. cerinella*, *F. bouteillei*, and *M. exasperata*. To date, there is still no evidence of the free-living lichenized fungi (Tuovinen et al., 2015). The foliicolous or red-list lichenized fungi detected using the NGS could be in the life states of mycelium, in spores, or in the initial state to produce a fruiting body (Glassman et al., 2016; Purahong et al., 2022).

Monitoring and conservation aspects of lichenized fungi using the high-throughput sequencing technique

The monitoring of lichens can be limited to those that have a fruiting body and can be observed under a microscope. However, overlooked or even invisible lichens living on leaves and needles may also play roles in the ecosystems such as indicator species for tree species and some are red-list lichenized fungal species. We found the importance of conifer needles as a habitat for foliicolous lichens as they harbored 98% of the lichenized fungal sequence reads and 89% of the lichenized fungal species (25/28 species) detected in this study. Thus, the maintenance of conifer trees is important for biodiversity conservation as they host a broad diversity of foliicolous lichens. This knowledge of lichen substrates is crucial to develop and apply targeted bio-conservation strategies (Purahong et al., 2019). Next-generation sequencing combined with the use of annotation tools (such as FungalTraits and FUNGuild) allows scientists without expert knowledge of lichens to identify this group of fungi and assign their functions. The sequencing database needs to be expanded to include verified DNA samples from described lichens so that we can get a more complete picture of invisible lichens. Our study is preliminary showing that lichens associated with

leaves and needles are more diverse than so far expected by microscopic fruiting body surveys or examinations by the naked eye.

Factors determining community composition patterns and richness of lichenized fungi

Tree species and tree type are known to determine the fungal community composition in deadwood of different tree species due to the different physicochemical properties (Bantle et al., 2014a,b; Purahong et al., 2018). Consistent with those observations, the majority of lichenized fungal community compositions are shaped by the leaves and needle substrate of the respective tree species and tree types when separately considering all trees and coniferous trees. However, few generalists such as *P. adscendens* were independent of their substrate, indicating that overgrowing and displacing other lichens is its main life strategy. The colonization of lichenized fungi on leaves of broadleaved trees seems to be rather independent of the tree species as we found no relationship between the two. Leaves and needles of different tree species differed in various traits including nutrition, persistence, specific leaf area, shapes, pH, and water content. However, there is no solid evidence that lichens can uptake nutrients from host leaves and needles. Follicolous lichens usually grow onto evergreen needles as they develop thalli with reproductive organs and complete their life cycle (Lücking and Bernecker-Lücking, 2002). However, in our study, we were also able to detect lichenized fungi on deciduous tree species, including *Larix decidua* as well as broadleaved trees. We also detect algae and cyanobacteria in leaves and needles across the 12 temperate tree species. Our study is considered among the first to demonstrate the specificity of lichenized fungi on different host leaves/needles.

Conclusion

The monitoring of lichens is generally based on fruiting body surveys. Overlooked or even invisible lichens are thus usually neglected. Here, we demonstrated that Next-Generation Sequencing can be used to augment the lichen monitoring, which adds significantly to previous knowledge. Conifers showed a higher lichenized fungal richness compared to broadleaved trees. Moreover, the lichenized fungal generalist, *P. adscendens* was the most successful lichenized fungi dominating the majority of leaves and needles of the temperate tree species. We conclude that conifers are important for maintaining the biodiversity of foliicolous lichens. Future studies should investigate the interactions among lichenized

fungi and environmental conditions that favor the conservation of lichens.

Data availability statement

The datasets presented in this study can be found in online repositories. The names of the repository/repositories and accession number(s) can be found at: <https://www.ncbi.nlm.nih.gov/>, PRJNA753096.

Author contributions

WP and E-DS conceived and designed the study. BT, WP, SS, SH, A-SL, and SW collected the samples and metadata. WP and FB contributed reagents and laboratory equipment. BT, WP, and SW led the DNA analysis. SS and GG led the water content and pH measurement. SW led bioinformatics. BT, LJ, and WP led the microbial taxonomy and data analyses. HG performed the fruiting body survey. BT, SS, MN, and WP wrote the manuscript. MN and WP supervised BT. SS, MN, E-DS, and FB reviewed and gave comments and suggestions for the manuscript. All authors gave final approval for manuscript submission.

Funding

This work has been partially funded by the internal research budget of WP to the Department of Soil Ecology, UFZ-Helmholtz Centre for Environmental Research. LJ appreciates the financial support from the China Scholarship Council (No. 201906600038).

References

- Abas, A. (2021). A systematic review on biomonitoring using lichen as the biological indicator: a decade of practices, progress and challenges. *Ecol. Indic.* 121, 107197. doi: 10.1016/j.ecolind.2020.107197
- Anthony, P. A., Holtum, J. A. M., and Jackes, B. R. (2002). Shade acclimation of rainforest leaves to colonization by lichens. *Funct. Ecol.* 16, 808–816. doi: 10.1046/j.1365-2435.2002.00688.x
- Arnold, A. E., Miadlikowska, J., Higgins, K. L., Sarvate, S. D., Gugger, P., Way, A., et al. (2009). A phylogenetic estimation of trophic transition networks for ascomycetous fungi: Are lichens cradles of symbiotrophic fungal diversification? *Syst. Biol.* 58, 283–297. doi: 10.1093/sysbio/syp001
- Asplund, J., and Wardle, D. A. (2017). How lichens impact on terrestrial community and ecosystem properties. *Biol. Rev.* 92, 1720–1738. doi: 10.1111/brv.12305
- Banchi, E., Stankovic, D., Fernández-Mendoza, F., Gionchetti, F., Pallavicini, A., and Muggia, L. (2018). ITS2 metabarcoding analysis complements lichen mycobiome diversity data. *Mycol. Progress* 17, 1049–1066. doi: 10.1007/s11557-018-1415-4
- Bantle, A., Borken, W., Ellerbrock, R. H., Schulze, E. D., Weisser, W. W., and Matzner, E. (2014a). Quantity and quality of dissolved organic carbon

Acknowledgments

The community composition data have been computed at the High-Performance Computing (HPC) Cluster EVE, a joint effort of both the Helmholtz Centre for Environmental Research—UFZ and the German Centre for Integrative Biodiversity Research (iDiv) Halle-Jena-Leipzig. We thank Beatrix Schnabel and Melanie Günther for their help with Illumina sequencing. SS gratefully acknowledges funding from the Collaborative Research Centre AquaDiva (CRC1076).

Conflict of interest

The authors declare that the research was conducted in the absence of any commercial or financial relationships that could be construed as a potential conflict of interest.

Publisher's note

All claims expressed in this article are solely those of the authors and do not necessarily represent those of their affiliated organizations, or those of the publisher, the editors and the reviewers. Any product that may be evaluated in this article, or claim that may be made by its manufacturer, is not guaranteed or endorsed by the publisher.

Supplementary material

The Supplementary Material for this article can be found online at: <https://www.frontiersin.org/articles/10.3389/fmicb.2022.907531/full#supplementary-material>

released from coarse woody debris of different tree species in the early phase of decomposition. *For. Ecol. Manage.* 329, 287–294. doi: 10.1016/j.foreco.2014.06.035

Bantle, A., Borken, W., and Matzner, E. (2014b). Dissolved nitrogen release from coarse woody debris of different tree species in the early phase of decomposition. *For. Ecol. Manage.* 334, 277–283. doi: 10.1016/j.foreco.2014.09.015

Beekley, P. K., and Hoffman, G. R. (1981). Effects of sulfur dioxide fumigation on photosynthesis, respiration, and chlorophyll content of selected lichens. *Bryologist* 84, 379–389. doi: 10.2307/3242857

Belnap, J., Büdel, B., and Lange, O. L. (2003). "Biological soil crusts: structure, function, and management," in *Biological Soil Crusts: Structure, Function, and Management Ecological Studies*, eds J. Belnap and O. L. Lange (Berlin, Heidelberg: Springer).

Callahan, B. J., McMurdie, P. J., Rosen, M. J., Han, A. W., Johnson, A. J. A., and Holmes, S. P. (2016). DADA2: high-resolution sample inference from Illumina amplicon data. *Nat. Methods* 13, 581–583. doi: 10.1038/nmeth.3869

Cardinale, M., Puglia, A. M., and Grube, M. (2006). Molecular analysis of lichen-associated bacterial communities. *FEMS Microbiol. Ecol.* 57, 484–495. doi: 10.1111/j.1574-6941.2006.00133.x

- Eckstein, J., and Grünberg, H. (2021). Rote Liste der Flechten (Lichenes) Thüringens. 4. Fassung, Stand: 11/2020. *Naturschutzreport, Nr. 30/2021 - Rote Listen Thüringens*, 402–424.
- Glassman, S. I., Levine, C. R., DiRocco, A. M., Battles, J. J., and Bruns, T. D. (2016). Ectomycorrhizal fungal spore bank recovery after a severe forest fire: some like it hot. *ISME J.* 10, 1228–1239. doi: 10.1038/ismej.2015.182
- Grimm, M., Grube, M., Schiefelbein, U., Zühlke, D., Bernhardt, J., and Riedel, K. (2021). The lichens' microbiota, still a mystery? *Front. Microbiol.* 12, 714. doi: 10.3389/fmicb.2021.623839
- Grube, M. (2010). Follicolous lichens. *Bryologist* 113, 224–226. doi: 10.1639/0007-2745-113.1.224
- Grube, M., and Hawksworth, D. L. (2007). Trouble with lichen: the re-evaluation and re-interpretation of thallus form and fruit body types in the molecular era. *Mycol. Res.* 111, 1116–1132. doi: 10.1016/j.mycres.2007.04.008
- Hammer, Ø., Harper, D. A. T., and Ryan, P. D. (2001). PAST: paleontological statistics software package for education and data analysis. *Palaeontol. Electron.* 4, 9.
- Ihrmark, K., Bödeker, I. T. M., Cruz-Martinez, K., Friberg, H., Kubartova, A., Schenck, J., et al. (2012). New primers to amplify the fungal ITS2 region—evaluation by 454-sequencing of artificial and natural communities. *FEMS Microbiol. Ecol.* 82, 666–677. doi: 10.1111/j.1574-6941.2012.01437.x
- Karsch-Mizrachi, I., Takagi, T., Cochrane, G., and on behalf of the International Nucleotide Sequence Database Collaboration (2018). The international nucleotide sequence database collaboration. *Nucleic Acids Res.* 46, D48–D51. doi: 10.1093/nar/gkx1097
- Knops, J. M. H., Nash, T. H., and Schlesinger, W. H. (1996). The influence of epiphytic lichens on the nutrient cycling of an oak woodland. *Ecol. Monogr.* 66, 159–179. doi: 10.2307/2963473
- Köljal, U., Nilsson, R. H., Abarenkov, K., Tedersoo, L., Taylor, A. F. S., Bahram, M., et al. (2013). Towards a unified paradigm for sequence-based identification of fungi. *Mol. Ecol.* 22, 5271–5277. doi: 10.1111/mec.12481
- Lange, O. L., Schulze, E. D., and Koch, W. (1968). Photosynthese von Wüstenflechten am natürlichen Standort nach Wasserdampfaufnahme aus dem Luftraum. *Naturwissenschaften* 55, 658–659. doi: 10.1007/BF01081508
- Lücking, R. (1999). Follicolous lichens and their lichenicolous fungi from Ecuador, with a comparison of lowland and montane rain forest. *Willdenowia* 29, 299–335. doi: 10.3372/wi.29.2924
- Lücking, R., and Bernecker-Lücking, A. (2002). Distance, dynamics, and diversity in tropical rainforests: an experimental approach using follicolous lichens on artificial leaves. I. Growth performance and succession. *Ecotropica* 8, 1–13.
- Lücking, R., and Cáceres, M. (2002). Follicolous lichens of the world - Part I: Genera and selected species. *Field Guides*. Available online at: <https://fieldguides.fieldmuseum.org/guides/guide/130> (accessed September 1, 2021).
- Lücking, R., Wirth, V., and Ahrens, M. (2009). Follicolous lichens in the black forest, Southwest-Germany. *Carolinea* 67, 23–31.
- Martin, M. (2011). Cutadapt removes adapter sequences from high-throughput sequencing reads. *EMBnet J.* 17, 10–12. doi: 10.14806/ej.17.1.200
- Matos, P., Geiser, L., Hardman, A., Glavich, D., Pinho, P., Nunes, A., et al. (2017). Tracking global change using lichen diversity: towards a global-scale ecological indicator. *Methods Ecol. Evol.* 8, 788–798. doi: 10.1111/2041-210X.12712
- Nguyen, N. H., Song, Z., Bates, S. T., Branco, S., Tedersoo, L., Menke, J., et al. (2016). FUNGuild: an open annotation tool for parsing fungal community datasets by ecological guild. *Fungal Ecol.* 20, 241–248. doi: 10.1016/j.funeco.2015.06.006
- Nilsson, R. H., Larsson, K.-H., Taylor, A. F. S., Bengtsson-Palme, J., Jeppesen, T. S., Schigel, D., et al. (2019). The UNITE database for molecular identification of fungi: handling dark taxa and parallel taxonomic classifications. *Nucleic Acids Res.* 47, D259–D264. doi: 10.1093/nar/gky1022
- Nilsson, R. H., Ryberg, M., Abarenkov, K., Sjökvist, E., and Kristiansson, E. (2009). The ITS region as a target for characterization of fungal communities using emerging sequencing technologies. *FEMS Microbiol. Lett.* 296, 97–101. doi: 10.1111/j.1574-6968.2009.01618.x
- Petrzik, K., Koloniuk, I., Sehádová, H., and Sarkisova, T. (2019). Chrysovirus inhabiting symbiotic fungi of lichens. *Viruses* 11, 1120. doi: 10.3390/v11121120
- Pinokiyo, A., Singh, K. P., and Singh, J. S. (2006). Leaf-colonizing lichens: their diversity, ecology and future prospects. *Curr. Sci.* 90, 509–518.
- Plitt, C. C. (1919). A short history of lichenology. *Bryologist* 22, 77–xii. doi: 10.1639/0007-2745(1919)22[77:ASHOL]2.0.CO;2
- Pölme, S., Abarenkov, K., Henrik Nilsson, R., Lindahl, B. D., Clemmensen, K. E., Kausserud, H., et al. (2020). FungalTraits: a user-friendly traits database of fungi and fungus-like stramenopiles. *Fungal Divers* 105, 1–16. doi: 10.1007/s13225-020-00466-2
- Potkay, A., Veldhuis, M.-C., ten, Fan, Y., Mattos, C. R. C., Ananyev, G., and Dismukes, G. C. (2020). Water and vapor transport in algal-fungal lichen: modeling constrained by laboratory experiments, an application for Flavoparmelia caperata. *Plant Cell Environ.* 43, 945–964. doi: 10.1111/pce.13690
- Purahong, W., Günther, A., Gminder, A., Tanunchai, B., Gossner, M. M., Buscot, F., et al. (2022). City life of mycorrhizal and wood-inhabiting macrofungi: Importance of urban areas for maintaining fungal biodiversity. *Landsc. Urban Plan.* 221, 104360. doi: 10.1016/j.landurbplan.2022.104360
- Purahong, W., Wubet, T., Krüger, D., and Buscot, F. (2019). Application of next-generation sequencing technologies to conservation of wood-inhabiting fungi. *Conserv. Biol.* 33, 716–724. doi: 10.1111/cobi.13240
- Purahong, W., Wubet, T., Lentendu, G., Hoppe, B., Jariyavidyanont, K., Arnstadt, T., et al. (2018). Determinants of deadwood-inhabiting fungal communities in temperate forests: molecular evidence from a large scale deadwood decomposition experiment. *Front. Microbiol.* 9, 2120. doi: 10.3389/fmicb.2018.02120
- RStudio Team (2019). *RStudio: Integrated Development for R*. RStudio, Inc., Boston, MA. Available online at: <https://rstudio.com/> (accessed February, 2021).
- Spier, L., van Dobben, H., and van Dort, K. (2010). Is bark pH more important than tree species in determining the composition of nitrophytic or acidophytic lichen floras? *Environ. Pollut.* 158, 3607–3611. doi: 10.1016/j.envpol.2010.08.008
- Tanunchai, B., Ji, L., Schroeter, S. A., Wahdan, S. F. M., Hossen, S., Deleegn, Y., et al. (2022). FungalTraits vs. FUNGuild: comparison of ecological functional assignments of leaf- and needle-associated fungi across 12 temperate tree species. *Microb. Ecol.* doi: 10.1007/s00248-022-01973-2
- ten Veldhuis, M.-C., Ananyev, G., and Dismukes, G. C. (2020). Symbiosis extended: exchange of photosynthetic O₂ and fungal-respired CO₂ mutually power metabolism of lichen symbionts. *Photosyn. Res.* 143, 287–299. doi: 10.1007/s11120-019-00702-0
- Triebel, D., Peršoh, D., Nash, T. H., Zedda, L., and Rambold, G. (2007). “LIAS — An interactive database system for structured descriptive data of Ascomycetes,” in *Biodiversity Databases: Techniques, Politics, and Applications*, ed G. B. Curry (Boca Raton, FL: CRC Press), 73, 99–110.
- Tuovinen, V., Svensson, M., Kubartová, A., Ottosson, E., Stenlid, J., Thor, G., et al. (2015). No support for occurrence of free-living *Cladonia* mycobionts in dead wood. *Fungal Ecol.* 14, 130–132. doi: 10.1016/j.funeco.2014.12.003
- U'Ren, J. M., Lutzoni, F., Miadlikowska, J., and Arnold, A. E. (2010). Community analysis reveals close affinities between endophytic and endolichenic fungi in mosses and lichens. *Microb. Ecol.* 60, 340–353. doi: 10.1007/s00248-010-9698-2
- Wang, Q., Garrity, G. M., Tiedje, J. M., and Cole, J. R. (2007). Naive Bayesian classifier for rapid assignment of rRNA sequences into the new bacterial taxonomy. *Appl. Environ. Microbiol.* 73, 5261–5267. doi: 10.1128/AEM.00062-07
- Weißbecker, C., Schnabel, B., and Heintz-Buschart, A. (2020). Dadasnake, a Snakemake implementation of DADA2 to process amplicon sequencing data for microbial ecology. *GigaScience* 9, g135. doi: 10.1093/gigascience/g135
- White, T. J., Bruns, T. D., Lee, S., and Taylor, J. (1990). “Amplification and direct sequencing of fungal ribosomal RNA genes for phylogenetics,” in *PCR Protocols: A Guide to Methods and Applications*, eds M. A. Innis, D. H. Gelfand, J. J. Sninsky, and T. J. White (San Diego: Academic Press), 315–322.
- Wirth, V., Hauck, M., von Brackel, W., Cezanne, R., de Bruyn, U., Dürhammer, O., et al. (2011). Rote Liste und Artenverzeichnis der Flechten und flechtenbewohnenden Pilze Deutschlands. *Naturschutz und Biologische Vielfalt* 70, 7–122.

Litter 3 – Supplementary Information

More than you can see: Unraveling the ecology and biodiversity of lichenized fungi associated with leaves and needles of 12 temperate tree species using high throughput sequencing.

Author: **Benjawan Tanunchai***, Simon Andreas Schroeter*, Li Ji, Sara Fareed Mohamed Wahdan, Shakhawat Hossen, Ann-Sophie Lehnert, Hagen Grünberg, Gerd Gleixner, François Buscot, Ernst-Detlef Schulze, Matthias Noll, Witoon Purahong.

*These authors contributed equally to this work.

Status: **Published**

Publication: Frontiers in Microbiology

Publisher: Frontiers Media S.A

Date: 16 September 2022

Frontiers in Microbiology, 13.

Copyright © 2022, The Author(s)

Reprinted with permission from Frontiers Media S.A..

Available online at: <https://doi.org/10.3389/fmicb.2022.907531>

Or please see separate attachments



OPEN ACCESS

EDITED BY

Luciano Kayser Vargas,
State Secretariat of Agriculture, Livestock
and Irrigation, Brazil

REVIEWED BY

Raffaella Balestrini,
National Research Council (CNR), Italy
Franck Stefani,
Agriculture and Agri-Food Canada
(AAFC), Canada

Q4

*CORRESPONDENCE

Benjawan Tanunchai
✉ benjawan.tanunchai@hs-coburg.de

Witoon Purahong

✉ witoon.purahong@ufz.de

Matthias Noll

✉ Matthias.noll@hs-coburg.de

†These authors have contributed equally to
this work

RECEIVED 13 June 2023

ACCEPTED 24 October 2023

PUBLISHED xx xx 2023

CITATION

Tanunchai B, Ji L, Schroeter SA,
Wahdan SFM, Thongsuk K, Hilke J,
Gleixner G, Buscot F, Schulze E-D, Noll M
and Purahong W (2023) Tree mycorrhizal
type regulates leaf and needle microbial
communities, affects microbial assembly
and co-occurrence network patterns, and
influences litter decomposition rates in
temperate forest.
Front. Plant Sci. 14:1239600.
doi: 10.3389/fpls.2023.1239600

COPYRIGHT

© 2023 Tanunchai, Ji, Schroeter, Wahdan,
Thongsuk, Hilke, Gleixner, Buscot, Schulze,
Noll and Purahong. This is an open-access
article distributed under the terms of the
Creative Commons Attribution License
(CC BY). The use, distribution or
reproduction in other forums is permitted,
provided the original author(s) and the
copyright owner(s) are credited and that
the original publication in this journal is
cited, in accordance with accepted
academic practice. No use, distribution or
reproduction is permitted which does not
comply with these terms.

Tree mycorrhizal type regulates leaf and needle microbial communities, affects microbial assembly and co-occurrence network patterns, and influences litter decomposition rates in temperate forest

Q1 Q2

Benjawan Tanunchai^{1,2,3*†}, Li Ji^{1,4†}, Simon Andreas Schroeter⁵, Sara Fareed Mohamed Wahdan^{1,6}, Katikarn Thongsuk¹, Ines Hilke⁵, Gerd Gleixner⁵, François Buscot^{1,7}, Ernst-Detlef Schulze⁵, Matthias Noll^{2,3*} and Witoon Purahong^{1*}

Q3 Q14

Q5

¹Department of Soil Ecology, UFZ-Helmholtz Centre for Environmental Research, Halle (Saale), Germany, ²Institute of Bioanalysis, Coburg University of Applied Sciences and Arts, Coburg, Germany, ³Bayreuth Center of Ecology and Environmental Research (BayCEER), University of Bayreuth, Bayreuth, Germany, ⁴School of Forestry, Central South of Forestry and Technology, Changsha, China, ⁵Max Planck Institute for Biogeochemistry, Biogeochemical Processes Department, Jena, Germany, ⁶Department of Botany and Microbiology, Faculty of Science, Suez Canal University, Ismailia, Egypt, ⁷German Centre for Integrative Biodiversity Research (iDiv) Halle-Jena-Leipzig, Leipzig, Germany

Q7 Q6

Q8

Tree mycorrhizal types (arbuscular mycorrhizal fungi and ectomycorrhizal fungi) alter nutrient use traits and leaf physicochemical properties and, thus, affect leaf litter decomposition. However, little is known about how different tree mycorrhizal species affect the microbial diversity, community composition, function, and community assembly processes that govern leaf litter-dwelling microbes during leaf litter decomposition. In this study, we investigated the microbial diversity, community dynamics, and community assembly processes of nine temperate tree species, including broadleaved arbuscular mycorrhizal, broadleaved ectomycorrhizal, and coniferous ectomycorrhizal tree types, during leaf litter decomposition. The leaves and needles of different tree mycorrhizal types significantly affected the microbial richness and community composition during leaf litter decomposition. Leaf litter mass loss was related to higher sequence reads of a few bacterial functional groups, particularly N-fixing bacteria. Furthermore, a link between bacterial and fungal community composition and hydrolytic and/or oxidative enzyme activity was found. The microbial communities in the leaf litter of different tree mycorrhizal types were governed by different proportions of determinism and stochasticity, which changed throughout litter decomposition. Specifically, determinism (mainly variable selection) controlling bacterial community composition increased over time. In contrast, stochasticity (mainly ecological drift) increasingly governs fungal community composition. Finally, the co-occurrence network analysis

Q9

showed greater competition between bacteria and fungi in the early stages of litter decomposition and revealed a contrasting pattern between mycorrhizal types. Overall, we conclude that tree mycorrhizal types influence leaf litter quality, which affects microbial richness and community composition, and thus, leaf litter decomposition.

KEYWORDS

ecological drift, variable selection, N fixing bacteria, enzyme activity, arbuscular mycorrhiza, ectomycorrhiza

Introduction

The decomposition of plant litter plays a crucial role in regulating carbon (C) and nutrient cycles in terrestrial forest ecosystems (Aerts and de Caluwe, 1997; Hobbie, 2015). Leaf litter highly contributes to the detritosphere, an interphase between the above- and belowground in forest ecosystems where intensive interactions among microbes occur (Ma et al., 2017). Leaf litter decomposition rates determine the velocity of nutrient turnover and transfer from primary producers to other organisms (Keller and Phillips, 2019). Thus, litter decomposition contributes significantly to nutrient availability, soil fertility, and productivity of terrestrial forest ecosystems (Aerts and de Caluwe, 1997; Hobbie, 2015). Litter decomposition is controlled by both abiotic factors, such as climate, environmental factors, and physicochemical properties of the litter, and biotic factors, especially cross-kingdom interactions between soil bacteria and fungi (Berg, 2000; Purahong et al., 2016). Leaf litter decomposition in forest ecosystems can even be influenced by soil microbes before leaf senescence has begun, through the symbiosis between host trees and mycorrhizal fungi (Jacobs et al., 2018; Keller and Phillips, 2019; Seyfried et al., 2021). Forest trees are associated with two dominant types of fungi, namely, arbuscular mycorrhizal (AM) and ectomycorrhizal (EcM) fungi, to improve their nutrient uptake, growth, and fitness (Bonfante and Genre, 2010). These different types of symbioses between AM and EcM trees have been demonstrated to alter nutrient use traits that significantly affect leaf physicochemical properties and quality (Keller and Phillips, 2019; Seyfried et al., 2021). Specifically, EcM trees tend to produce lower quality leaf litter than AM trees (Seyfried et al., 2021). In temperate forests, such differences in leaf quality have been reported to affect leaf litter decomposition rates, which are usually higher in AM trees than in EcM trees (Keller and Phillips, 2019). Leaf litter nitrogen (N) content and tree phylogeny have been identified as significant factors that explain the difference in litter decomposition rates between AM and EcM trees (Keller and Phillips, 2019). Furthermore, competition between EcM fungi and saprotrophs in EcM-dominated forests can negatively affect litter decomposition in EcM trees (Seyfried et al., 2021). However, little is known about how different tree mycorrhizal types affect microbial diversity, community composition, and function during leaf litter decomposition. The mechanisms underlying the assembly of

microbial communities and their cross-kingdom interactions in plant litter of AM and EcM trees remain largely unexplored (Purahong et al., 2016; Abrego, 2021). Several studies have shown that fungal community assembly in temperate forests is governed by stochastic processes (dispersal limitation and drift), whereas both stochastic and deterministic processes dominate the bacterial community assembly (Osburn et al., 2021; Zhang et al., 2022). However, this information may not be fully applicable to microbes living in leaf litter, and the relative importance of each specific assembly process may vary greatly between the leaf litter of different tree mycorrhizal types and decomposition stages.

Cross-kingdom interactions, particularly between bacteria and fungi, are the main drivers of plant litter decomposition (Purahong et al., 2016). However, the dynamics of cross-kingdom interactions during litter decomposition and among different mycorrhizal types have not yet been investigated. While both bacteria and fungi play an important role as direct decomposers through the production and secretion of extracellular plant compound-degrading enzymes, different functional groups of bacteria act as facilitators by providing additional macronutrients such as N and phosphorus (P) for fungal decomposers (Purahong et al., 2016; Mieszkin et al., 2021; Purahong et al., 2022). Tree mycorrhizal type can alter the abundance and microbial community composition of leaf litter-dwelling microbes due to its significant impact on soil microbial communities (Singavarapu et al., 2021) and leaf litter properties (Seyfried et al., 2021). Thus, the key microbial players in leaf litter decomposition, as well as their interactions with biotic and abiotic factors, may differ greatly among the tree mycorrhizal types. However, this has not been tested yet.

The objectives of this study were to i) investigate microbial diversity, community composition, and environmental factors in nine tree species representing different tree mycorrhizal types; ii) investigate microbial community assembly over time; iii) investigate the dynamics of co-occurrence network patterns of different tree mycorrhizal types over time and identify their associated keystone microbial taxa; and vi) investigate the relationship between microbial functions (enzyme activities) and microbial communities. We hypothesized that i) tree mycorrhizal types determine microbial richness and community composition through their specific initial physicochemical properties of the leaves and needles and ii) microbial community assembly differs among different tree mycorrhizal types and over time. We expected

different co-occurrence network patterns and their associated keystone microbial taxa over time and among different tree mycorrhizal types.

Materials and methods

Study site, experimental setup, and design

Q13 The leaf litter decomposition experiment was conducted at the study site located in the Hainich-Dün region of Thuringia, Germany (51°12'N, 10°18'E). Mature leaves and needles were collected, oven-dried at 25°C for 14 days, and returned under their mother tree. Further details of the experimental design and study site have been published elsewhere (Tanunchai et al., 2022a) and in the Supplementary Material.

In October 2019, at least 200 g of mature leaves and needles were collected from three tree mycorrhizal types, each of which was represented by three tree species. Five true tree replicates were collected for each tree species, at a minimum of 5 m apart (45 trees in total). The tree mycorrhizal types investigated in this study were i) broadleaved arbuscular mycorrhizal trees (AM_BL; *Acer pseudoplatanus*, *Fraxinus excelsior*, and *Prunus avium*), ii) broadleaved ectomycorrhizal trees (EcM_BL; *Fagus sylvatica*, *Carpinus betulus*, and *Tilia cordata*), and iii) coniferous ectomycorrhizal trees (EcM_C; *Picea abies*, *Pinus sylvestris*, and *Pseudotsuga menziesii*). The collected mature leaves and needles were oven-dried at 25°C for 14 days. A nylon bag (2 mm mesh, 5 mm holes) was filled with 3 g of oven-dried leaves and needles. The nylon bags were then placed under the same mother tree to mimic the actual situation of leaf litter decomposition in the environment. After 200 and 400 days of decomposition, leaf/needle samples were collected in separate sterile plastic bags with new clean gloves, transported on ice to the laboratory within 3 h, and stored at -80°C for further analysis. Another set of samples was sent on ice to the physicochemical laboratory to determine leaf/needle water content, pH, and nutrients. All further analyses are summarized in the experimental scheme (Supplementary Material).

Physicochemical and enzyme analyses

Q15 The procedures for the physicochemical analyses were published by Tanunchai et al. (2022). Total leaf C (TC), total leaf N (TN), nutrient (Ca, Fe, K, Mg, and P contents), dissolved organic C (DOC), dissolved organic N (N_{org}), and dissolved inorganic N (N_{min}) contents were analyzed. Leachable components were extracted by incubating wet leaf and needle samples in 30 mL of MilliQ water for 1 h at room temperature. Five potential enzymatic activities, including three hydrolytic enzymes (β -glucosidase, N-acetylglucosaminidase, and acid phosphatase) and two oxidative enzymes (general peroxidase and manganese peroxidase) (Purahong et al., 2016), were measured in homogenized leaves and needles. More details on the physicochemical and enzymatic analyses are provided in the Supplementary Material.

DNA extraction, Illumina sequencing, and bioinformatics

The procedures for DNA extraction, Illumina sequencing, and bioinformatics have been published by Tanunchai et al. (2022). Further details are provided in the Supplementary Material. Briefly, leaf and needle samples were washed three times in sterile Tween solution (0.1% vol/vol), washed three to five times using deionized water, and then incubated for 1 h in sterile water. The ground leaf samples (~120 mg homogenized leaves and needles) were subjected to DNA extraction using the DNeasy PowerSoil Kit (Qiagen, Hilden, Germany) and a Precellys 24 tissue homogenizer (Bertin Instruments, Montigny-le-Bretonneux, France) according to the manufacturer's instructions.

The microbial communities associated with leaves and needles **Q16** were profiled by amplification and sequencing of two genetic markers: the fungal internal transcribed spacer 2 (ITS2) within the nuclear ribosomal DNA (rDNA) and the bacterial 16S rDNA V4 region (Weißbecker et al., 2020). The fungal ITS2 region was amplified using the fungal universal primer pair fITS7 [5'-GTGARTCATCGAATCTTTG-3'] (Ihrmark et al., 2012) and ITS4 primer [5'-TCCTCCGCTTATTGATATGC-3'] (White et al., 1990) with Illumina adapter sequences. The 16S rDNA V4 region was amplified using the universal bacterial primer pair 515F (5'-GTGCCAGCMGCCGCGGTAA-3') and 806R (5'-GGACTACHVGGGTWTCTAAT-3') (Caporaso et al., 2011) with Illumina adapter **Q17** sequences. Paired-end sequencing (2 × 300 bp) was performed on the pooled PCR products using a MiSeq Reagent kit v3 on an Illumina MiSeq system (Illumina Inc., San Diego, CA, USA) at the Department of Soil Ecology, Helmholtz Centre for Environmental Research, Germany.

Bioinformatics

The 16S and ITS2 sequences corresponding to the forward and reverse primers were trimmed from the demultiplexed raw reads using Cutadapt (Martin, 2011). The paired-end sequences were quality-trimmed, filtered for chimeras, and assembled using the DADA2 package (Callahan et al., 2016) through the pipeline dada2 (Weißbecker et al., 2020). Assembled reads that met these criteria were retained for further analysis. High-quality reads were clustered into 15,213 bacterial and 5,030 fungal amplicon sequence variants (ASVs) after chimera removal. Rare ASVs (singletons) were removed as they may represent artificial sequences. The datasets were then rarefied to the minimum sequencing depth of bacterial and fungal sequence reads (21,000 sequences per sample). The bacterial sequencing data of mature leaves and needles (at 0 days) were not considered for rarefaction because their minimum sequence reads were 2,733 reads, which is approximately eight times lower than the minimum reads of the total samples. The richness at the different rarefaction depths of these samples was determined (Table S1). Finally, 14,773 rarefied bacteria and 4,896 fungal ASVs were obtained. Using absolute sequence reads instead of relative sequence read abundances

reflects to a higher degree the PCR pitfalls, as reviewed earlier (Wintzingerode et al., 1997); therefore, the use of relative sequence read abundances is recommended (Schloss et al., 2009). To avoid sequencing bias, normalizing the data by rarefaction is recommended. After rarefaction to a minimum of 21,000 sequence reads, both bacterial and fungal rarefaction curves showed saturation, which implies that a large majority of the microbes in the community were included after rarefaction. The rarefaction curves of all samples reached saturation (Supplementary Material), which is a prerequisite for less biased sequence comparisons between samples (Schloss et al., 2009). Nevertheless, it should be noted that the rarefied data usually differ from the raw sequence read data, which may lead to a different pattern in the analyzed results, which in turn may affect ecological interpretation. Thus, the Mantel test based on the Bray–Curtis distance with 999 permutations was applied to evaluate the correlation between the whole matrix and a rarefied matrix for bacterial and fungal datasets (Tanunchai et al., 2022b). The results indicated that the rarefaction dataset was highly representative of the entire bacterial and fungal matrices ($R_{\text{Mantel, bacteria}} = 0.998, P = 0.001$; $R_{\text{Mantel, fungi}} = 0.996, P = 0.001$). Datasets of relative sequence read abundance were used for statistical analyses. It is also important to note that sequencing data provide only information regarding the occurrence and relative abundance of taxa, but it is not a direct measure of the absolute abundance of the taxa in the samples. To approximate the absolute abundances, further methods, such as the incorporation of internal standards of known quantity (Harrison et al., 2021) or quantitative PCR (Tanunchai et al., 2023), should be considered. The metabolic functional profiles of leaf-associated bacterial communities in nine temperate tree species were predicted using Tax4Fun2 in R (v4.0.5) (Wemheuer et al., 2020, 2). The fungal ecological function of each ASV was determined using FungalTraits (Pölme et al., 2020; Tanunchai et al., 2022a), according to the authors' instructions. Further details are provided in the Supplementary Material.

Network and community assembly analyses

Based on the random matrix theory (RMT), we constructed co-occurrence networks of cross-kingdoms inhabiting mature and decomposing leaves using the molecular ecological network analysis pipeline (MENA, <http://ieg4.rccc.ou.edu/mena/>). The network analysis was performed following the four steps described in previous studies (Zhou et al., 2011; Deng et al., 2012): 1) metagenomic/amplification sequence read collection, 2) data standardization, 3) pairwise similarity estimation, and 4) adjacent matrix construction according to an RMT-based approach. Further details are provided in the Supplementary Material. All networks were visualized with Gephi v0.9.2. All of the above parameters were calculated using the “iCAMP” package in R with the code provided by Ning et al. (2020) (<https://github.com/DaliangNing/iCAMP1>).

Statistical analysis

The datasets were tested for normality using the Jarque–Bera test and for equality of group variances using the *F*-test (for two datasets) and Levene's test (for more than two datasets). The effects of time, tree species, and tree mycorrhizal type on microbial community composition were visualized using non-metric multidimensional scaling (NMDS) and tested using analysis of similarities (ANOSIM) and non-parametric multivariate analysis of variance (NPMANOVA) based on relative abundance data and the Bray–Curtis distance measure. Over 999 permutations were performed. The relationship between different environmental factors, enzyme activities, and microbial community composition was analyzed using a goodness-of-fit statistic based on normalized relative abundance and the Bray–Curtis distance measure. The effects of time, tree species, and tree mycorrhizal type on leaf litter mass loss, microbial ASV richness, leaf physicochemical properties, and enzyme activities were tested using repeated measures analysis of variance (ANOVA) with Fisher's least significant difference (LSD) *post-hoc* test. Log transformation was used when necessary. All statistical analyses were performed using the PAST version 2.17, SPSS version 29.0.0.0, R, and RStudio version 4.2.1.

Results

Microbial succession during leaf litter decomposition

Details of the general overview of the leaf and needle microbiomes in forest ecosystems are provided in the Supplementary Material. We found three patterns of microbial succession over decomposition time. First, some microbes were enriched at 200 and 400 days of decomposition and were not initially detected in mature leaves and needles. These microbes included bacteria (*Caulobacter* ASV10, *Flavobacterium* ASV38, *Brevundimonas* ASV44, *Rhizobiaceae* ASV48, *Polaromonas* ASV51, and ASV54; Figures S1, S2; Table S2) and fungi (*Botryosphaerales* ASV12, *Herpotrichia* ASV30, *Chaetomium* ASV8, and ASV19; Figures S3, S4; Table S3). While the enrichment of such bacteria at 200 and 400 days was consistent across all tree mycorrhizal types, the enrichment of fungi was more specific to some tree mycorrhizal types. *Botryosphaerales* ASV12 was enriched only on needles of the EcM_C tree, specifically of *P. menziesii* (Figures S1, S2). *Chaetomium* spp. were enriched in the leaves of AM_BL (*P. avium*) and EcM_BL trees (*T. cordata*, Figures S3, S4). Second, the relative sequence read abundances of *Sphingomonas* ASV6, *Massilia* ASV11, *Helotiales* ASV10, *Aureobasidium* ASV9, *Mycosphaerellaceae* ASV31, and *Didymellaceae* ASV24 were reduced at 200 and 400 days (Figures S1–S4). The majority of these taxa were initially highly enriched in the leaves of both AM_BL and EcM_BL trees. Third, some microbes were enriched after 200 days of decomposition. These microbes include bacteria (*Pseudomonas* ASV4, *Pedobacter* ASV9,

Microbacteriaceae ASV8, and *Luteibacter* ASV17) and fungi (*Alternaria* ASV2, *Tetracladium* ASV14, and *Mollisia* ASV17). While the enrichment of such bacteria at 200 days was consistent across all tree mycorrhizal types (especially for EcM_C trees), the enrichment of fungi was specific to AM_BL and/or EcM_BL trees (Figures S1–S4). Interestingly, *Phoma* (ASV7) was highly enriched in *P. sylvestris* needles at 400 days of decomposition (Figure S4).

The absolute number of reads was checked to validate the interpretation of the relative abundance data. Similar patterns were observed in this study. First, *Caulobacter* ASV10, *Flavobacterium* ASV38, *Brevundimonas* ASV44, *Rhizobiaceae* ASV48, *Polaromonas* ASV51, *Polaromonas* ASV54, *Botryosphaerales* ASV12, *Herpotrichia* ASV30, *Chaetomium* ASV8, and ASV19 were initially not detected but were enriched at 200 and 400 days of decomposition (Table S4). Second, the absolute number of reads of *Sphingomonas* ASV6, *Massilia* ASV11, *Helotiales* ASV10, *Aureobasidium* ASV9, *Mycosphaerellaceae* ASV31, and *Didymellaceae* ASV24 declined mainly after 400 days (Table S4). Third, *Pseudomonas* ASV4, *Pedobacter* ASV9, *Microbacteriaceae* ASV8, *Luteibacter* ASV17, *Alternaria* ASV2, *Tetracladium* ASV14, and *Mollisia* ASV17 were also enriched after 200 days of decomposition (Table S4).

Tree species and mycorrhizal types drive changes in the microbial communities, ASV richness, and thus, leaf litter decomposition over time

The microbial community composition in mature and decomposing leaves and needles differed among tree species, mycorrhizal types, and decomposition times (bacteria: $R_{ANOSIM} = 0.94$, $F_{NPMANOVA} = 11.46$, $P < 0.001$; fungi: $R_{ANOSIM} = 0.95$, $F_{NPMANOVA} = 7.54$, $P < 0.001$; Figure 1; Table S5). Tree species, tree mycorrhizal types, and sampling time significantly influenced the bacterial and fungal community composition across all sampling times (bacteria: $R^2 = 0.15–0.94$, $P < 0.001$; fungi: $R^2 = 0.52–0.97$, $P < 0.001$, Table 1). While tree mycorrhizal type was detected as the main factor determining the bacterial and fungal community composition only at 0 days ($R^2 = 0.77–0.88$, $P < 0.001$), tree species was the main factor controlling the microbial community composition at all sampling times ($R^2 = 0.87–0.97$, $P < 0.001$, Table 1). Sampling time was also the main factor that significantly altered bacterial community composition ($R^2 = 0.85$, $P < 0.001$, Table 1).

Tree mycorrhizal types also significantly affected microbial richness throughout the decomposition period (Table S6; Figure 1). Microbial richness was the highest in the needles of EcM_C trees at 0 days. In addition, we found that decomposition time significantly affected bacterial richness. The bacterial richness in the leaves and needles of all mycorrhizal types increased significantly with time (Figure 1; Table S6). However, no significant effect of decomposition time on fungal richness was observed (Table S6). Fungal richness observed in the leaves of AM_BL and EcM_BL trees tended to increase over time, while the

fungal richness in the needles of EcM_C trees decreased after 200 days of incubation.

The tree mycorrhizal type and decomposition time significantly influenced the mass loss of the leaves and needles (Figure 2). Mass losses were the lowest in ectomycorrhizal conifers [at 200 days, values ranged from $14.8\% \pm 2.2\%$ (mean \pm SE), and at 400 days, values ranged from $54.1\% \pm 3.6\%$ (mean \pm SE)] and the highest in AM_BL trees [at 200 days, values ranged from $47.7\% \pm 4.0\%$ (mean \pm SE), and at 400 days, values ranged from $80.1\% \pm 4.1\%$ (mean \pm SE)] (Figure 2). Tree species also had a marginally significant effect on mass loss.

Different assembly patterns in litter-associated bacterial and fungal communities across tree mycorrhizal types

Based on the null model, the relative contribution of ecological stochasticity to bacterial and fungal community assembly was calculated. The pNST values of the litter-associated bacterial communities of all trees at 400 days were lower than those at 0 days, and the relative proportion of variable selection increased over time (Figure 3A, $P < 0.05$). Compared with AM_BL trees, the bacterial communities inhabiting EcM_BL and EcM_C trees had a higher pNST value ($P < 0.05$), suggesting that fewer stochastic processes were observed in AM_BL trees. For fungi, the pNST values of the AM_BL and EcM_BL trees increased with decomposition time (Figure 3C, $P < 0.05$). In contrast, the pNST value of EcM_C trees at 200 days was the lowest.

At 200 and 400 days of decomposition, the community assembly of litter-associated bacteria was mainly controlled by variable selection processes, whereas the fungal community was governed by drift (Figures 3B, 5D). In addition, a higher proportion of drift in the litter-associated bacterial community was found in the EcM_C trees (Figure 3B). More importantly, a higher drift process of the litter-associated fungal community was observed at 200 and 400 days (Figure 3D).

The microbial co-occurrence network and keystone taxa are important for leaf and needle decomposition

The co-occurrence networks between bacteria and fungi (interkingdom) varied between the mycorrhizal types and sampling times (Figure 4). The divergent network topology showed an obvious shift between broadleaved (AM_BL and EcM_BL) and coniferous (EcM_C) trees (Figures 4A–C). Notably, the network complexity of the interkingdom network was higher in EcM_BL trees than in the AM_BL and EcM_C groups (Table S7). Compared with conifers, the litter-associated interkingdom at 0 days and 200 days in AM_BL and EcM_BL trees had more nodes and a higher average degree (Table S7). The lower percentage of negative links in EcM_C trees indicated that the interkingdom network in conifers was more connected among ASVs and that there was less competition among ASVs than in broadleaved trees

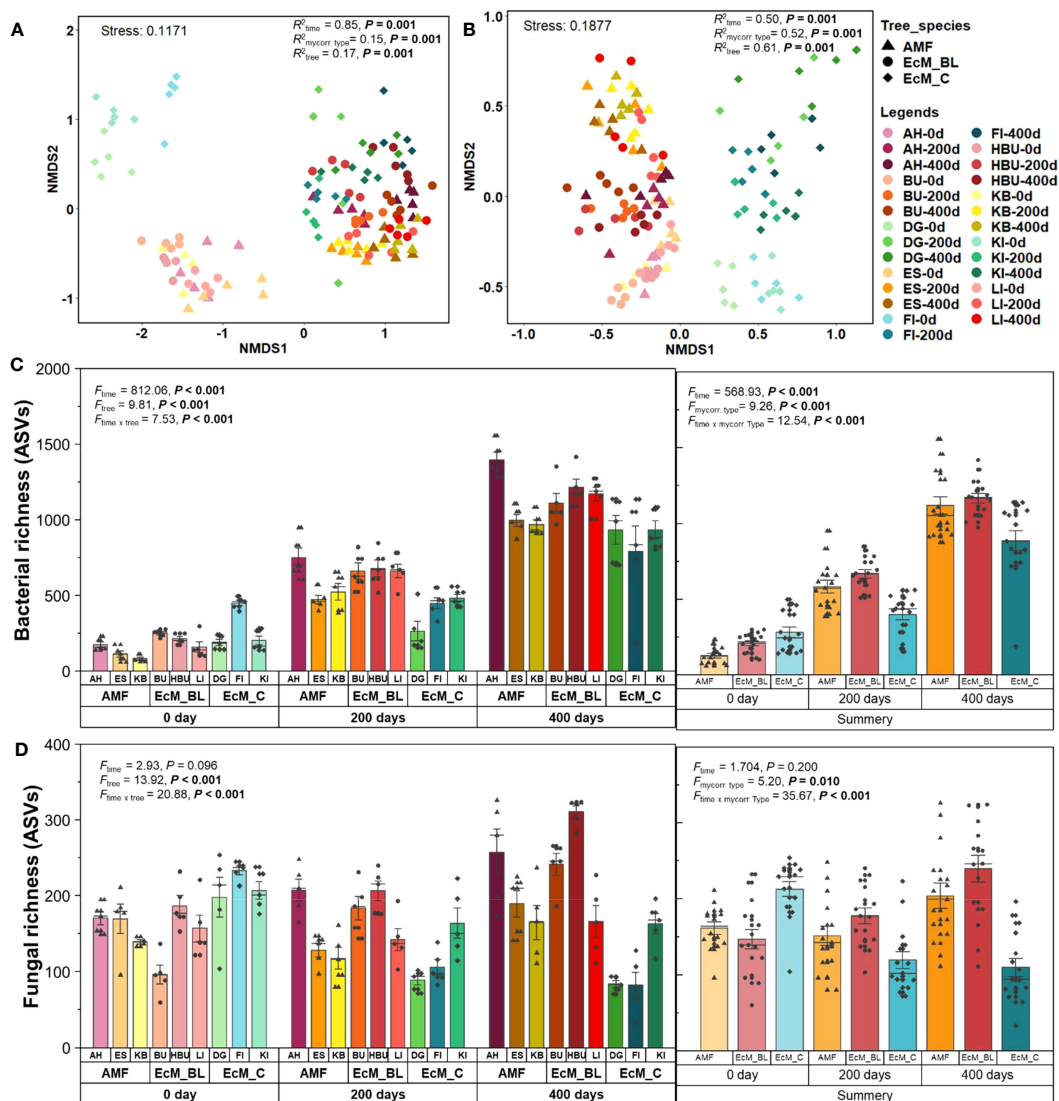


FIGURE 1

Non-metric multidimensional scaling (NMDS) ordinations of bacterial (A) and fungal (B) community compositions in leaf and needle decomposition based on relative abundance. ASV richness (number of ASVs) for bacteria (C) and fungi (D) in leaf and needle decomposition. The legends for each NMDS data point are provided in the upper right of the figure. AM_BL, broadleaved arbuscular mycorrhizal trees (including AH, *Acer pseudoplatanus*; ES, *Fraxinus excelsior*; and KB, *Prunus avium*); EcM_BL, broadleaved ectomycorrhizal trees (including BU: *Fagus sylvatica*, HBU: *Carpinus betulus*, and LI: *Tilia cordata*); EcM_C, coniferous ectomycorrhizal trees (including FI, *Picea abies*; KI, *Pinus sylvestris*; and DG, *Pseudotsuga menziesii*). The results of PERMANOVA and ANOSIM are presented in Table S5. Statistical differences between microbial ASV richness among different tree species and tree mycorrhizal types were tested using repeated measures analysis of variance (ANOVA) with Fisher's least significant difference (LSD) *post-hoc* test.

(Table S7). Interestingly, the total number of links and the proportion of negative links from all mycorrhizal types increased at 200 days and then decreased at 400 days, indicating more competition at a later stage of litter decomposition in forests (Table S7). N-fixing bacteria (*Brevundimonas*, *Methylobacterium*, *Methylorubrum*, *Pseudomonas*, and *Sphingomonas*), saprotrophic fungi (*Chalara*, *Coprinellus*, *Hypholoma*, *Praetumpfia*, and *Tothia*), and plant pathogenic fungi (*Neocateulostroma*, *Pleurophoma*, *Truncatella*, and *Venturia*) were identified as network module hubs and connectors (Figure 5). *Sphingomonas* was identified as network connectors and/or module hubs in co-occurrence networks across sampling times.

Factors influencing the leaf and needle microbial communities

Overall, we found that the tree mycorrhizal types influenced most of the leaf physicochemical properties ($P < 0.001$, Table S6). We found that plot factors and leaf physicochemical properties were also significantly correlated with the microbial community composition (both bacteria and fungi, Table 1). The plot factors and leaf physicochemical properties that showed significant responses to microbial community composition across all sampling times included soil water content ($R^2 = 0.23\text{--}0.65$, $P < 0.001$), latitude ($R^2 = 0.42\text{--}0.70$, $P < 0.001$), leaf water content, pH, total C, N:P ratio, Ca, Fe, and Mg ($R^2 = 0.15\text{--}0.72$, $P < 0.05\text{--}0.001$). Latitude was also the

Q32 TABLE 1 Goodness-of-fit statistics (R^2) of environmental variables fitted to the non-metric multidimensional scaling (NMDS) ordination of bacterial and fungal communities in all tree species based on relative abundance data and Bray–Curtis distance measure.

Factors	All sampling times		0 days		200 days		400 days	
	Bac	Fun	Bac	Fun	Bac	Fun	Bac	Fun
Tree factors								
Tree mycorrhizal type	0.15***	0.52***	0.77***	0.88***	0.59***	0.61***	0.62***	0.64***
Tree species	0.17***	0.61***	0.94***	0.97***	0.87***	0.91***	0.90***	0.94***
Time factor								
Sampling times	0.85***	0.50***	NA	NA	NA	NA	NA	NA
Plot factors								
Soil water content	0.23***	0.43***	0.41***	0.45***	0.65***	0.64***	0.37***	0.43***
Soil pH	0.14**	0.04	0.44***	0.40***	0.33***	0.17*	0.27**	0.15*
Latitude	0.42***	0.58***	0.63***	0.70***	0.47***	0.61***	0.65***	0.64***
Longitude	0.10**	0.17***	0.15*	0.12	0.05	0.35***	0.18*	0.40***
Leaf physicochemical properties								
Leaf water content	0.16***	0.22***	0.22**	0.18*	0.49***	0.42***	0.40***	0.39***
Leaf pH	0.36***	0.30***	0.19*	0.27**	0.45***	0.30***	0.28***	0.36***
C	0.41***	0.52***	0.72***	0.55***	0.49***	0.58***	0.37***	0.34**
DOC	0.60***	0.25***	0.62***	0.56***	0.15*	0.06	0.11	0.07
N	0.37***	0.19***	0.17*	0.16*	0.09	0.07	0.03	0.17*
N _{min}	0.10**	0.06*	0.34**	0.23**	0.08	0.07	0.02	0.04
N _{org}	0.37***	0.07**	0.60***	0.46***	0.23**	0.03	0.04	0.03
C:N ratio	0.57***	0.35***	0.17*	0.12	0.23**	0.21**	0.13	0.27**
C:P ratio	0.12***	0.13***	0.20*	0.35***	0.08	0.07	0.25**	0.20**
N:P ratio	0.19***	0.21***	0.66***	0.67***	0.16*	0.15*	0.26**	0.22**
Ca	0.36***	0.39***	0.66***	0.60***	0.40***	0.38***	0.33***	0.26**
Fe	0.29***	0.24***	0.25**	0.26**	0.23**	0.34***	0.34***	0.21*
K	0.06*	0.06*	0.03	0.02	0.04	0.19*	0.18*	0.08
Mg	0.23***	0.26***	0.48***	0.43***	0.37***	0.43***	0.17*	0.15*
P	0.25***	0.17***	0.35***	0.38***	0.11	0.09	0.39***	0.35***

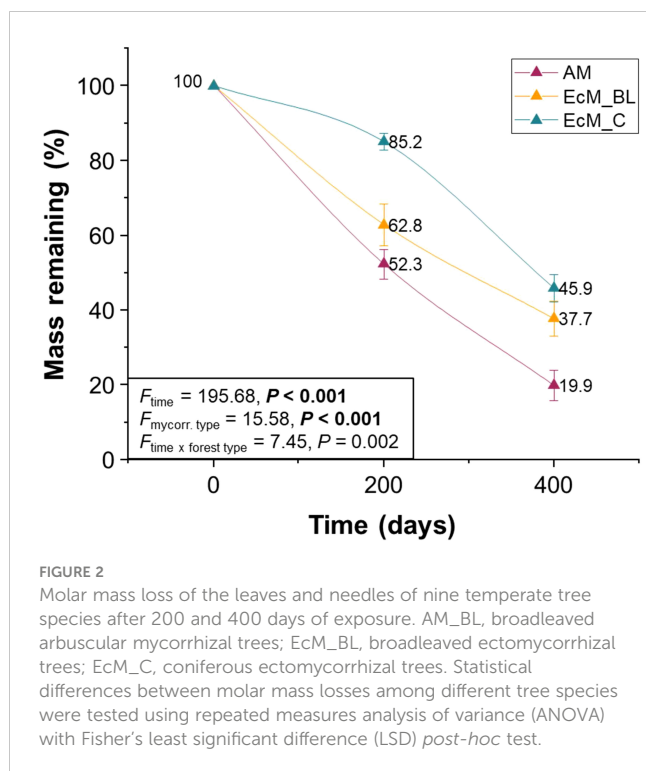
Bold values indicate statistical significance with $R^2 \geq 0.70$.

* $P < 0.05$, ** $P < 0.01$, *** $P < 0.001$.

main factor corresponding to the fungal community composition ($R^2 = 0.70$, $P < 0.001$, Table 1), while total C was another main factor for bacterial community composition ($R^2 = 0.72$, $P < 0.001$, Table 1). Notably, DOC and N content (total N, dissolved inorganic N, and organic N) were significantly correlated with bacterial and fungal communities only at 0 days ($R^2 = 0.17$ – 0.62 , $P < 0.05$ – 0.001).

When considering AM_BL, EcM_BL, and EcM_C separately, we found similar and dissimilar patterns of factors corresponding to bacterial and fungal community compositions (Table S8). Similar patterns that were observed across all considerations (AM_BL, EcM_BL, and EcM_C) were as follows: i) tree species was the main factor affecting the fungal community composition across all sampling times ($R^2 = 0.83$ – 1.00 , $P < 0.001$), and ii) sampling times

were the main factors corresponding to both bacterial and fungal community compositions ($R^2 = 0.79$ – 0.90 , $P < 0.001$). The leaf and soil pH patterns were the first to differ. Leaf pH correlated significantly with bacterial and fungal community composition at most sampling times (except bacterial composition at time point 0 days, Table S8). While leaf pH continued to significantly correlate with microbial community composition in AM_BL trees at 200 and 400 days, soil pH became more important for the microbial community composition in EcM_BL and EcM_C at 200 and 400 days (Table S8). Second, total C and DOC showed no significant correlation with the microbial community composition of AM_BL trees at 0 days, but they were significantly correlated with the microbial community composition of EcM_BL trees and were the



main factors determining the microbial community composition of EcM_C trees (Table S8). Third, C:P and N:P ratios were the main factors that significantly corresponded to the fungal community composition in EcM_C trees at 0 days and C:N, C:P, and N:P ratios at 400 days; however, in other tree mycorrhizal types, they showed only moderate correlation or no correlation with the microbial community composition (Table S8). Details of enzyme activities and their association with microbial communities are provided in the Supplementary Material.

Discussion

Microbial richness, community composition, and their corresponding factors in nine tree species representing different tree mycorrhizal types

The results of this study confirmed our hypothesis that the mycorrhizal type of the tree affects nutrient acquisition and, thus, the nutrient traits of mature leaves and needles, which in turn determine the microbial community composition in the mature leaves and needles (Figure 1; Table 1). The effect of mycorrhizal type on microbial community composition was high at time 0 (mature leaves and needles) and decreased at later stages of decomposition. Previous studies (Bonfante and Genre, 2010; Jacobs et al., 2018; Keller and Phillips, 2019; Seyfried et al., 2021) have reported that tree mycorrhizal types play an important role in determining the nutrient traits of leaf litter and, thus, in selecting the phyllosphere microbiome prior to leaf senescence. Indeed, we found that the patterns of microbial community composition were correlated with

nutrient content in different tree mycorrhizal types (Table 1). In mature leaves and needles before leaf senescence, DOC and N content (total N, dissolved inorganic N, and organic N) were more important than the decomposition time. Leachable C and N are the key components in the production of leaf litter-decomposing enzymes (Hoppe et al., 2014; Purahong et al., 2016). These two factors, namely, the initial phyllosphere microbiome and nutrient traits in the leaf litter, represent leaf litter quality and will later determine the leaf litter decomposition rate (Strickland et al., 2009). Indeed, we found that the leaf litter of AM trees decomposed faster than the leaves and needles of EcM broadleaves and conifers. This finding is consistent with a previous study of investigation on leaf litter decomposition in temperate forests (Keller and Phillips, 2019).

The succession of microbial community composition during leaf litter decomposition and its relationship to leaf litter quality is of great interest to scientists in various fields, especially ecology, microbiology, and forestry (Purahong et al., 2016; Tláškal et al., 2016). Nevertheless, previous studies (Purahong et al., 2016; Tláškal et al., 2016) have investigated microbial succession or only bacterial succession in one or two tree species. In this study, we revealed the microbial community dynamics and succession during leaf litter decomposition of nine temperate tree species, including broadleaf AM, broadleaf EcM, and conifer EcM. *Caulobacter*, *Flavobacterium*, *Brevundimonas*, *Rhizobiaceae*, *Polaromonas*, *Botryosphaeriales*, *Herpotrichia*, and *Chaetomium* were able to enrich the decomposing leaves and needles at 200 and 400 days, whereas *Sphingomonas*, *Massilia*, *Helotiales*, *Aureobasidium*, *Mycosphaerellaceae*, and *Didymellaceae* were drastically reduced at 200 and 400 days (Figures S1–S4). Interestingly, fungal enrichment was more specific to certain mycorrhizal tree types. Nevertheless, an increase in the relative abundance of a taxon can be explained by several different scenarios (Harrison et al., 2021). Thus, the absolute number of reads was checked to validate the above interpretation. The enrichment patterns of these microbes were mostly conserved when the absolute count of the sequence reads was considered. Nevertheless, further methods, such as the incorporation of internal standards of known quantity (Harrison et al., 2021) or quantitative PCR (Tanunchai et al., 2023), should be considered to better and directly approximate the absolute abundances in samples.

More cross-kingdom competition in the early stages of different mycorrhizal litter decomposition

The relationship between bacteria and fungi (co-occurrence network patterns) differed among the tree mycorrhizal types during the decomposition period, which was consistent with our hypothesis. Network analysis can be used to determine how the environment affects an underlying network of ecological dependencies (Montoya et al., 2006). Given the characteristics of leaf habitats, cross-kingdom interactions in leaf microbial networks respond rapidly to environmental fluctuations (Barranca et al., 2015). Identifying bacterial and fungal associations within and between litter decomposition communities is critical for

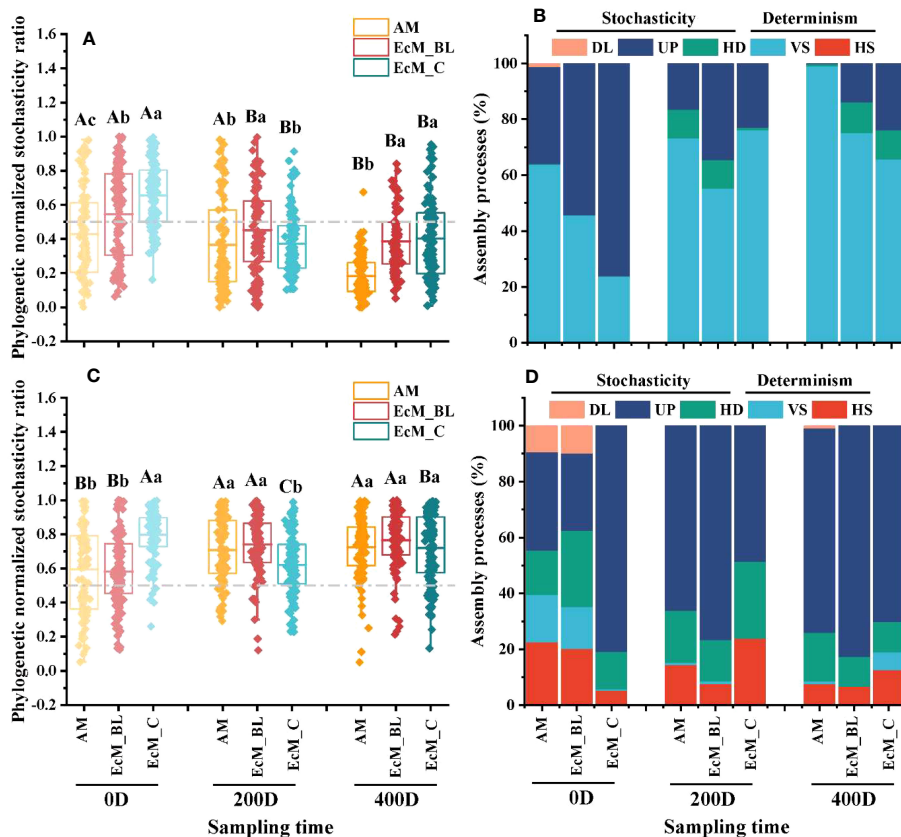


FIGURE 3

The ecological stochasticity in the potentially litter-associated bacterial (A) and fungal (C) community assembly estimated by the phylogenetic normalized stochasticity ratio (pNST). The value of 0.5 represents the boundary between the more deterministic (<0.5) and more stochastic (>0.5) assemblies. Data with different capital letters indicate significant differences at the 5% level between different sampling times in the same mycorrhizal type ($P < 0.05$), while different lowercase letters indicate significant differences between different mycorrhizal types in the same sampling time ($P < 0.05$). The relative contributions (%) of the community assembly processes based on pNST in shaping the litter-associated bacterial (B) and fungal (D) communities. HS, homogeneous selection; VS, variable selection; HD, homogenizing dispersal; UP, undominated process; DL, dispersal limitation; AM_BL, broadleaved arbuscular mycorrhizal trees; EcM_BL, broadleaved ectomycorrhizal trees; EcM_C, coniferous ectomycorrhizal trees.

understanding this process (Purahong et al., 2016). In the present study, the leaf-associated microbial community members colonizing broadleaved trees were more sensitive to environmental variation than those colonizing conifers, and there was less cross-kingdom competition in the EcM_C group (Figure 3). Broadleaved trees tend to have more “opportunistic” strategies and longer leaf lives than evergreens (Reich, 1995; Wright et al., 2004). AM litter is more readily decomposed than EcM litter due to its higher nutrient and polyphenol content, which is conducive to the growth of fungal pathogens and saprotrophs that rely on C and energy from the plant litter (Averill et al., 2019; Keller and Phillips, 2019). Fang et al. (2020) demonstrated that a higher abundance of saprotrophic fungi in the soil around AM trees results in a faster decomposition rate for AM leaf litter compared with EcM leaf litter.

More importantly, the average clustering coefficient was relatively higher at 0 days than at 200 and 400 days (Figure 4; Table S7), suggesting that the bacterial–fungal network is less connected at later stages and may be more susceptible to external perturbations such as environmental influences. The theory of priority effects suggests that in the early stages of colonization, an

early colonist can preempt niches and exclude later-arriving species by competing with them for resources (Cline and Zak, 2015). To the best of our knowledge, fungi have the potential to compete with bacteria for resources and expel them from their territories during the early decomposition phase (Tsujiyama and Minami, 2005; Purahong et al., 2016). In this study, we found that the percentage of links and negative links increased at 200 days and then decreased at 400 days, suggesting that more competitive and antagonistic relationships were present at the early stage of litter decomposition. We inferred that the competition potential of the cross-kingdom varied during the decomposition process due to niche differentiation. Cline and Zak (2015) showed that bacterial communities were decoupled from environmental changes and relatively stable despite different decomposition phases, mainly benefiting from readily available substances formed by fungal exoenzymes. Taken together, our network analyses (Figure 4) revealed that microbial interactions changed with the succession of litter decomposition and showed a contrasting pattern between mycorrhizal types.

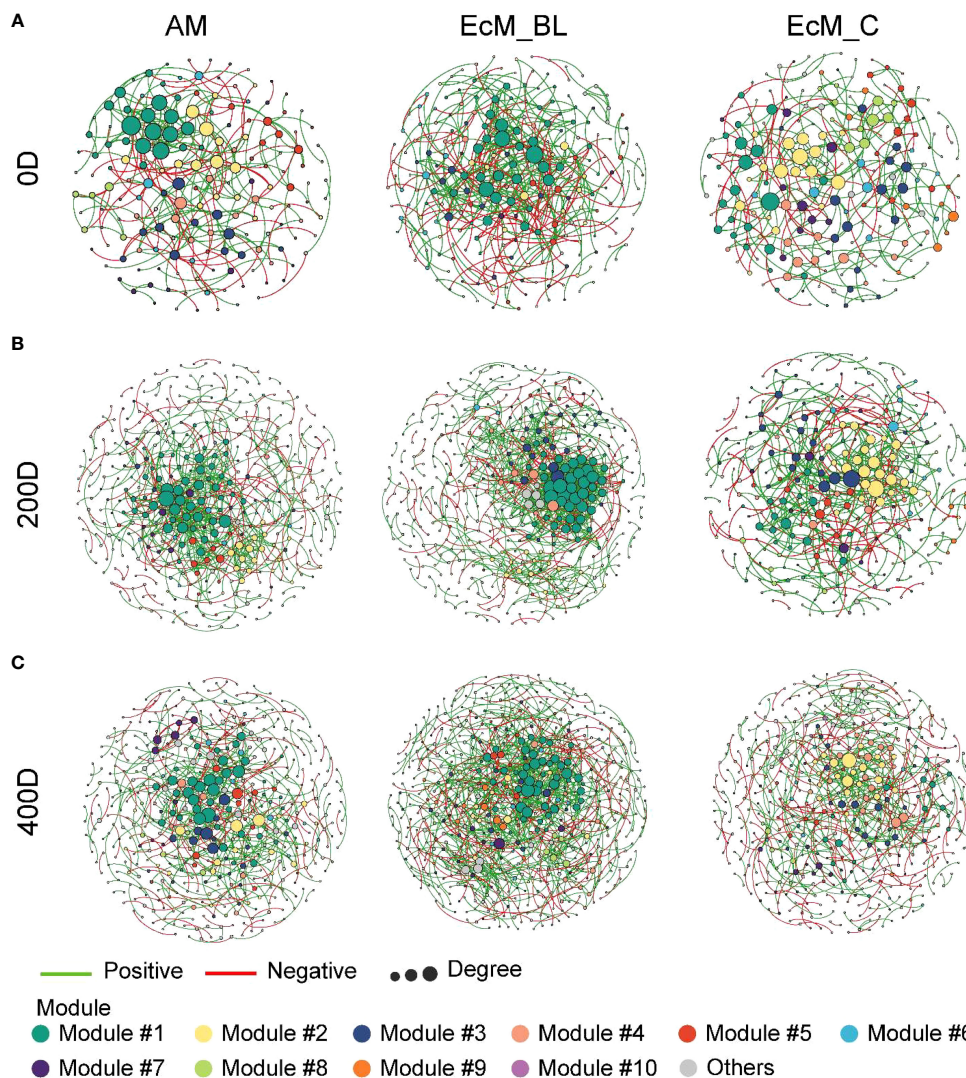


FIGURE 4

Modular networks of interkingdom among mycorrhizal types and sampling times. The node colors represent different modules. (A) Initial litter phase (0 days); (B) 200 days litter decomposition phase; (C) 400 days litter decomposition phase. The connections denote a strong (Spearman's $\rho > 0.6$) and significant ($P < 0.01$) correlations. AM_BL, broadleaved arbuscular mycorrhizal trees; EcM_BL, broadleaved ectomycorrhizal trees; EcM_C, coniferous ectomycorrhizal trees.

Variable selection and drift play important roles in regulating community assembly of leaf-associated microbiota

The proportion of determinisms and stochasticity that govern microbial communities change differently depending on the tree mycorrhizal type throughout the course of litter decomposition. Accumulating evidence suggests that plant-associated microbial communities are not random assemblages but rather are characterized by general rules for assembly and have well-defined phylogenetic relationships (Carlström et al., 2019). Assessing the ecological processes that govern the community assembly of leaf-associated microbiota provides a future avenue for advancing our understanding of litter decomposition (Carlström et al., 2019). In this study, the community assembly of leaf-associated bacteria was dominated by variable selection with a striking increase in the

proportion of deterministic processes over time. This selective filtering and recruitment of different microorganisms can be attributed to niche adaptation and modification (Maignien et al., 2014; Hamonts et al., 2018). Several successful colonizers inhabiting litter niches either compete for resources or cooperate to maintain stable coexistence (Trivedi et al., 2020). Cline and Zak (2015) demonstrated that deviations in community assembly are significantly influenced by the respiration of early colonizers in the early stages. In addition, we found that stochastic processes (mainly drift) governed the assembly of fungal communities inhabiting the EcM leaves and needles (Figure 3). Vellend (2010) and Chase and Myers (2011) reported that drift is more prominent under conditions of reduced biodiversity (e.g., smaller populations and/or lower species richness). It has also been reported that a smaller habitat space and a lower dispersal rate, which are characteristic of needles, can increase stochasticity, especially

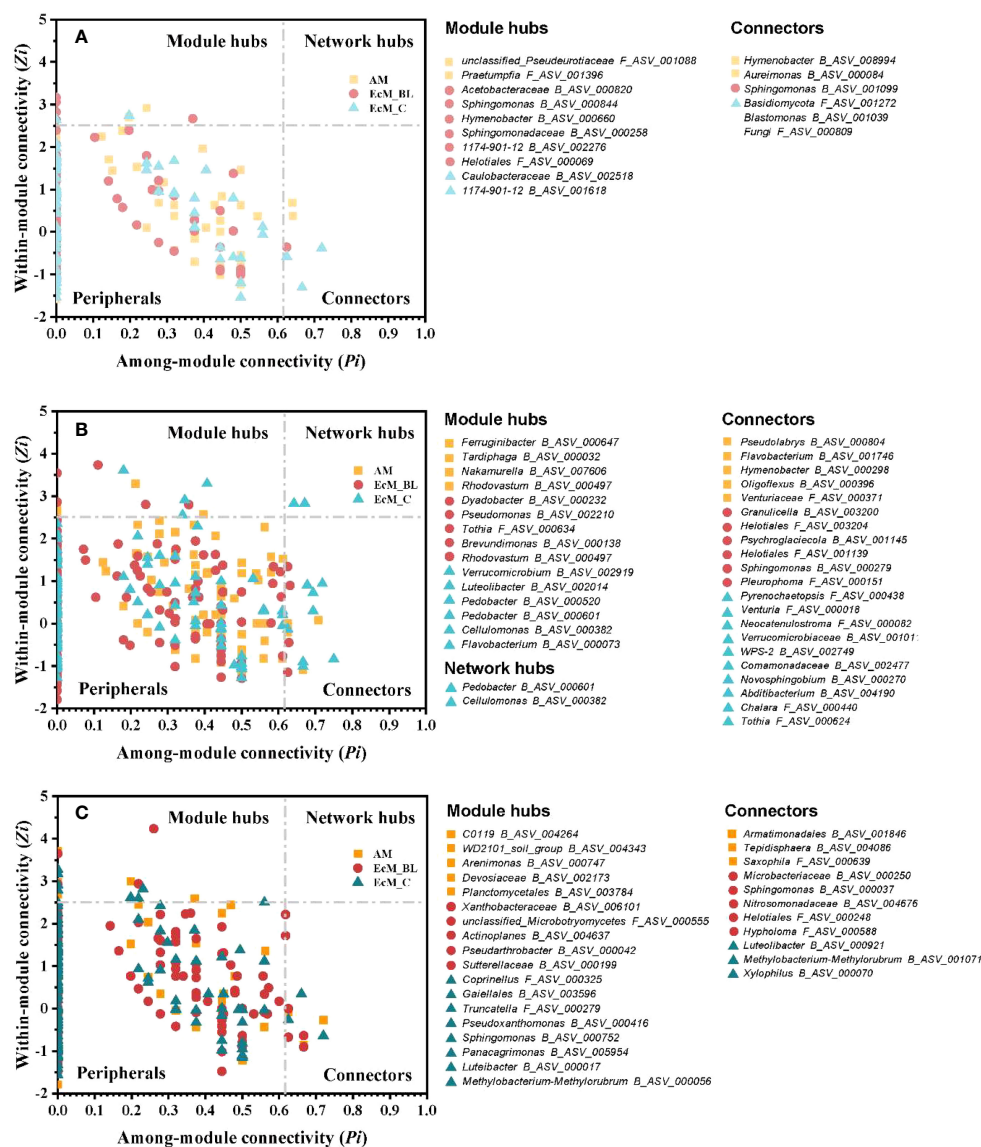


FIGURE 5

Topological roles of ASVs at 0 days (A), 200 days (B), and 400 days (C) decayed phase networks, as displayed by the Z_i - P_i plot. AM_BL, broadleaved arbuscular mycorrhizal trees; EcM_BL, broadleaved ectomycorrhizal trees; EcM_C, coniferous ectomycorrhizal trees.

ecological drift (Hanson et al., 2012; Evans et al., 2017). We observed an increasing trend in stochasticity in broadleaved trees (AM_BL and EcM_BL groups) during litter decomposition (Figure 3). Previous studies have suggested that initial plant colonization is favored by high-resource conditions, resulting in strong priority effects and divergent community assembly trajectories (Ejrnæs et al., 2006; Kardol et al., 2013). There is increasing evidence that the decomposition of N-rich, labile AM leaf litter results in increased mineral N availability and SOM content relative to EcM soil (Phillips et al., 2013; Keller and Phillips, 2019). Overall, community assemblages of leaf-associated microbiota are a multistep process that depends on species interactions, drift, and environmental selection.

Link between enzyme activities and microbial communities

In this study, we found a correlation between enzyme activity and bacterial and fungal communities. Although fungi are known for their important role in decomposing complex biopolymers, bacteria can play direct and indirect roles in degrading complex leaf litter (de Gonzalo et al., 2016; Purahong et al., 2016). We found that the mass loss of different tree mycorrhizal types was directly related to the presence of some bacterial functional groups, especially N-fixing bacteria. We observed that the mass loss of needles from the EcM_C tree after 200 days of decomposition was significantly lower than that of the leaves from AM_BL and EcM_BL trees (Figure 2). Brown rot and ascomycetous fungi dominate the fungal community composition in mature (0 days)

and decomposing leaves and needles at 200 days. We further found that at 0 days (mature leaves and needles), N-fixing bacteria, *Massilia*, *Methylobacterium-Methylorubrum*, *Pseudomonas*, and *Sphingomonas* were highly abundant in senescing leaves of AM_BL and EcM_BL trees, whereas only *Sphingomonas* was abundant in the senescing needles of the EcM_C tree (Figure S2). *Pseudomonas* dominated the bacterial community composition after 200 days of decomposition, whereas *Sphingomonas* co-dominated. *Pseudomonas* has been reported to be both an N-fixing bacterium and to produce a different type of peroxidase, bacterial DyP-type peroxidase, that modifies lignin (de Gonzalo et al., 2016; Desnoues et al., n.d.). Saprotrophic fungi require available N to produce exoenzymes for leaf litter decomposition (Hoppe et al., 2014; Purahong et al., 2016). Thus, N availability may be the rate-limiting step in leaf litter decomposition (Osono and Takeda, 2005). The high mass loss at 400 days (up to 89%) was associated with an increase in enzyme activity, especially oxidative enzyme activity. This is consistent with the enrichment of *Mycena*, which has been reported to decompose lignin (Miyamoto et al., 2000; Kellner et al., 2014; Purahong et al., 2016). Furthermore, we found a link between oxidative enzyme activity and the bacterial community at 400 days (Figure S5). Bacteria may not directly secrete the measured oxidative enzymes; however, some bacteria (such as *Sphingobium* and *Novosphingobium*) have been reported to secrete glutathione-dependent enzymes (β -etherases and lyases) that act on the lignin degradation process (de Gonzalo et al., 2016). A full discussion of the relationship between enzyme activity and the microbial community is provided in the Supplementary Material.

Conclusion

The fungal and bacterial community compositions of AM and EcM broadleaved trees as well as EcM conifer trees have only been studied for a few tree species. In this comprehensive study, we demonstrated for the first time that tree mycorrhizal types are critical for nutrient status, molar mass loss, and hydrolytic and oxidative enzyme activities of the microbial community and, thus, for the ecosystem service of leaf/needle decomposition. Moreover, each tree mycorrhizal type showed a specific community assembly process, and the microbial network architecture of broadleaved AM and EcM trees was more similar to each other than that of conifer EcM trees. Future research should use manipulation experiments to investigate the interactions of the community members, which were very abundant in our study, to decipher their respective roles in the leaf or needle decomposition process.

Data availability statement

The datasets presented in this study can be found in online repositories. The names of the repository/repositories and accession number(s) can be found in the article/Supplementary Material.

Author contributions

WP and E-DS conceived of and designed the study. BT, WP, SW, and E-DS led the experimental setup. BT, LJ, WP, SW, and E-DS collected the samples and metadata. WP, MN, and FB contributed the reagents and laboratory equipment. BT, KT, and WP performed the DNA analysis. SW led the bioinformatics analysis. BT, LJ, and WP led the microbial taxonomy and data analyses. LJ led the microbial network and community assembly analyses. SS, IH, GG, ASL, and EGA led the physicochemical analyses. BT, LJ, and WP drafted the manuscript. MN and WP supervised BT. MN, AG, E-DS, and FB reviewed the manuscript and provided comments and suggestions. All authors contributed to the article and approved the submitted version.

Funding

The author(s) declare financial support was received for the research, authorship, and/or publication of this article. This work was partially funded by the internal research budget of WP, Department of Soil Ecology, UFZ-Helmholtz Centre for Environmental Research.

Acknowledgments

The community composition data were computed at the High-Performance Computing (HPC) Cluster EVE, a joint effort of both the Helmholtz Centre for Environmental Research (UFZ) and the German Centre for Integrative Biodiversity Research (iDiv) Halle-Jena-Leipzig. We thank Beatrix Schnabel and Melanie Günther for their help with the Illumina sequencing. We thank the Helmholtz Association, the Federal Ministry of Education and Research, the State Ministry of Science and Economy of Saxony-Anhalt, and the State Ministry for Higher Education, Research, and the Arts Saxony. Benjawan Tanunchai acknowledges the Peter and Traudl Engelhorn Foundation for their financial support through her postdoc scholarship.

Conflict of interest

The authors declare that the research was conducted in the absence of any commercial or financial relationships that could be construed as a potential conflict of interest.

Publisher's note

All claims expressed in this article are solely those of the authors and do not necessarily represent those of their affiliated organizations, or those of the publisher, the editors and the reviewers. Any product that may be evaluated in this article, or

claim that may be made by its manufacturer, is not guaranteed or endorsed by the publisher.

Supplementary material

Q24

The Supplementary Material for this article can be found online at: <https://www.frontiersin.org/articles/10.3389/fpls.2023.1239600/full#supplementary-material>

References

- Abrego, N. (2021). Wood-inhabiting fungal communities: Opportunities for integration of empirical and theoretical community ecology. *Fungal Ecol.* 101112. doi: 10.1016/j.funeco.2021.101112
- Aerts, R., and de Caluwe, H. (1997). Nutritional and plant-mediated controls on leaf litter decomposition of *Carex* Species. *Ecology* 78, 244. doi: 10.2307/2265993
- Averill, C., Bhatnagar, J. M., Dietze, M. C., Pearse, W. D., and Kivlin, S. N. (2019). Global imprint of mycorrhizal fungi on whole-plant nutrient economics. *Proc. Natl. Acad. Sci.* 116, 23163–23168. doi: 10.1073/pnas.1906655116
- Barranca, V. J., Zhou, D., and Cai, D. (2015). Low-rank network decomposition reveals structural characteristics of small-world networks. *Phys. Rev. E* 92, 62822. doi: 10.1103/PhysRevE.92.062822
- Berg, B. (2000). Litter decomposition and organic matter turnover in northern forest soils. *For. Ecol. Manage.* 133, 13–22. doi: 10.1016/S0378-1127(99)00294-7
- Bonfante, P., and Genre, A. (2010). Mechanisms underlying beneficial plant–fungus interactions in mycorrhizal symbiosis. *Nat. Commun.* 1, 48. doi: 10.1038/ncomms1046
- Callahan, B. J., McMurdie, P. J., Rosen, M. J., Han, A. W., Johnson, A. J. A., and Holmes, S. P. (2016). DADA2: High-resolution sample inference from Illumina amplicon data. *Nat. Methods* 13, 581–583. doi: 10.1038/nmeth.3869
- Carlström, C. I., Field, C. M., Bortfeld-Miller, M., Müller, B., Sunagawa, S., and Vorholt, J. A. (2019). Synthetic microbiota reveal priority effects and keystone strains in the *Arabidopsis* phyllosphere. *Nat. Ecol. Evol.* 3, 1445–1454. doi: 10.1038/s41559-019-0994-z
- Cline, L. C., and Zak, D. R. (2015). Initial colonization, community assembly and ecosystem function: fungal colonist traits and litter biochemistry mediate decay rate. *Mol. Ecol.* 24, 5045–5058. doi: 10.1111/mec.13361
- de Gonzalo, G., Colpa, D. I., Habib, M. H. M., and Fraaije, M. W. (2016). Bacterial enzymes involved in lignin degradation. *J. Biotechnol.* 236, 110–119. doi: 10.1016/j.jbiotec.2016.08.011
- Deng, Y., Jiang, Y.-H., Yang, Y., He, Z., Luo, F., and Zhou, J. (2012). Molecular ecological network analyses. *BMC Bioinf.* 13, 113. doi: 10.1186/1471-2105-13-113
- Desnoues, N., Lin, M., Guo, X., Ma, L., Carreño-Lopez, R., and Elmerich, C. (2003). Nitrogen fixation genetics and regulation in a *Pseudomonas stutzeri* strain associated with rice. *Microbiology* 149, 2251–2262. doi: 10.1099/mic.0.26270-0
- Ejrnæs, R., Bruun, H. H., and Graae, B. J. (2006). Community assembly in experimental grasslands: Suitable environment or timely arrival? *Ecology* 87, 1225–1233.
- Evans, S., Martiny, J. B. H., and Allison, S. D. (2017). Effects of dispersal and selection on stochastic assembly in microbial communities. *ISME J.* 11, 176–185. doi: 10.1038/ismej.2016.96
- Fang, M., Liang, M., Liu, X., Li, W., Huang, E., and Yu, S. (2020). Abundance of saprotrophic fungi determines decomposition rates of leaf litter from arbuscular mycorrhizal and ectomycorrhizal trees in a subtropical forest. *Soil Biol. Biochem.* 149, 107966. doi: 10.1016/j.soilbio.2020.107966
- Hamonts, K., Trivedi, P., Garg, A., Janitz, C., Grinyer, J., Holford, P., et al. (2018). Field study reveals core plant microbiota and relative importance of their drivers. *Environ. Microbiol.* 20, 124–140. doi: 10.1111/1462-2920.14031
- Hanson, C. A., Fuhrman, J. A., Horner-Devine, M. C., and Martiny, J. B. H. (2012). Beyond biogeographic patterns: processes shaping the microbial landscape. *Nat. Rev. Microbiol.* 10, 497–506. doi: 10.1038/nrmicro2795
- Harrison, J. G., Calder, W. J., Shuman, B., and Buerkleet, C. A. (2021). The quest for absolute abundance: The use of internal standards for DNA-based community ecology. *Mol. Ecol. Resour.* 21, 30–43. doi: 10.1111/1755-0998.13247
- Hobbie, S. E. (2015). Plant species effects on nutrient cycling: revisiting litter feedbacks. *Trends Ecol. Evol.* 30, 357–363. doi: 10.1016/j.tree.2015.03.015
- Hoppe, B., Kahl, T., Karasch, P., Wubet, T., Bauhus, J., Buscot, F., et al. (2014). Network analysis reveals ecological links between N-fixing bacteria and wood-decaying fungi. *PLoS One* 9, e88141. doi: 10.1371/journal.pone.0088141
- Ihrmark, K., Bodeker, I. T. M., Cruz-Martinez, K., Friberg, H., Kubartova, A., Schenck, J., et al. (2012). New primers to amplify the fungal ITS2 region – evaluation by 454-sequencing of artificial and natural communities. *FEMS Microbiol. Ecol.* 82, 666–677. doi: 10.1111/j.1574-6941.2012.01437.x
- Jacobs, L. M., Sulman, B. N., Brzostek, E. R., Feighery, J. J., and Phillips, R. P. (2018). Interactions among decaying leaf litter, root litter and soil organic matter vary with mycorrhizal type. *J. Ecol.* 106, 502–513. doi: 10.1111/1365-2745.12921
- Kardol, P., Souza, L., and Classen, A. T. (2013). Resource availability mediates the importance of priority effects in plant community assembly and ecosystem function. *Oikos* 122, 84–94. doi: 10.1111/j.1600-0706.2012.20546.x
- Keller, A. B., and Phillips, R. P. (2019). Leaf litter decay rates differ between mycorrhizal groups in temperate, but not tropical, forests. *New Phytol.* 222, 556–564. doi: 10.1111/nph.15524
- Kellner, H., Luis, P., Pecyna, M. J., Barbi, F., Kapturska, D., Krüger, D., et al. (2014). Widespread occurrence of expressed fungal secretory peroxidases in forest soils. *PLoS One* 9, e95557. doi: 10.1371/journal.pone.0095557
- Ma, X., Razavi, B. S., Holz, M., Blagodatskaya, E., and Kuzyakov, Y. (2017). Warming increases hotspot areas of enzyme activity and shortens the duration of hot moments in the root-detritusphere. *Soil Biol. Biochem.* 107, 226–233. doi: 10.1016/j.soilbio.2017.01.009
- Maignien, L., DeForce, E. A., Chafee, M. E., Eren, A. M., and Simmons, S. L. (2014). Ecological succession and stochastic variation in the assembly of *Arabidopsis thaliana* phyllosphere communities. *mBio* 5, e00682–e00613. doi: 10.1128/mBio.00682-13
- Martin, M. (2011). Cutadapt removes adapter sequences from high-throughput sequencing reads. *EMBnet journal* 17, 10–12. doi: 10.14806/ej.17.1.200
- Mieszkina, S., Richet, P., Bach, C., Lambrot, C., Augusto, L., Buée, M., et al. (2021). Oak decaying wood harbors taxonomically and functionally different bacterial communities in sapwood and heartwood. *Soil Biol. Biochem.* 155, 108160. doi: 10.1016/j.soilbio.2021.108160
- Miyamoto, T., Igarashi, T., and Takahashi, K. (2000). Lignin-degrading ability of litter-decomposing basidiomycetes from *Picea* forests of Hokkaido. *Mycoscience* 41, 105–110. doi: 10.1007/BF02464317
- Montoya, J. M., Pimm, S. L., and Solé, R. V. (2006). Ecological networks and their fragility. *Nature* 442, 259–264. doi: 10.1038/nature04927
- Ning, D., Yuan, M., Wu, L., Zhang, Y., Guo, X., Zhou, X., et al. (2020). A quantitative framework reveals ecological drivers of grassland microbial community assembly in response to warming. *Nat. Commun.* 11. doi: 10.1038/s41467-020-18560-z
- Osburn, E. D., Aylward, F. O., and Barrett, J. E. (2021). Historical land use has long-term effects on microbial community assembly processes in forest soils. *ISME Commun.* 1, 1–4. doi: 10.1038/s43705-021-00051-x
- Osono, T., and Takeda, H. (2005). Decomposition of organic chemical components in relation to nitrogen dynamics in leaf litter of 14 tree species in a cool temperate forest. *Ecol. Res.* 20, 41–49. doi: 10.1007/s11284-004-0002-0
- Phillips, R. P., Brzostek, E., and Midgley, M. G. (2013). The mycorrhizal-associated nutrient economy: a new framework for predicting carbon–nutrient couplings in temperate forests. *New Phytol.* 199, 41–51. doi: 10.1111/nph.12221
- Pölme, S., Abarenkov, K., Henrik Nilsson, R., Lindahl, B. D., Clemmensen, K. E., Kauterud, H., et al. (2020). FungalTraits: a user-friendly traits database of fungi and fungus-like stramenopiles. *Fungal Diversity* 105, 1–16. doi: 10.1007/s13225-020-00466-2
- Purahong, W., Tanunchai, B., Muszynski, S., Maurer, F., Wahdan, S. F. M., Malter, J., et al. (2022). Cross-kingdom interactions and functional patterns of active microbiota matter in governing deadwood decay. *Proc. R. Soc. B: Biol. Sci.* 289, 20220130. doi: 10.1098/rspb.2022.0130
- Purahong, W., Wubet, T., Lentendu, G., Schloter, M., Pecyna, M. J., Kapturska, D., et al. (2016). Life in leaf litter: novel insights into community dynamics of bacteria and fungi during litter decomposition. *Mol. Ecol.* 25, 4059–4074. doi: 10.1111/mec.13739
- Reich, P. B. (1995). Phenology of tropical forests: patterns, causes, and consequences. *Can. J. Bot.* 73, 164–174. doi: 10.1139/b95-020
- Schloss, P. D., Westcott, S. L., Ryabin, T., Hall, J. R., Hartmann, M., Hollister, E. B., et al. (2009). Introducing mothur: open source, platform-independent, community-supported software for describing and comparing microbial communities. *Appl. Environ. Microbiol.* 75, 7537–7541. doi: 10.1128/AEM.01541-09
- Seyfried, G. S., Dalling, J. W., and Yang, W. H. (2021). Mycorrhizal type effects on leaf litter decomposition depend on litter quality and environmental context. *Biogeochemistry* 155, 21–38. doi: 10.1007/s10533-021-00810-x
- Singavarapu, B., Beugnon, R., Bruelheide, H., Cesarz, S., Du, J., Eisenhauer, N., et al. (2021). Tree mycorrhizal type and tree diversity shape the forest soil microbiota. *Environ. Microbiol.* doi: 10.1111/1462-2920.15690
- Strickland, M. S., Osburn, E., Lauber, C., Fierer, N., and Bradford, M. A. (2009). Litter quality is in the eye of the beholder: initial decomposition rates as a function of

- 1457 inoculum characteristics. *Funct. Ecol.* 23, 627–636. doi: 10.1111/j.1365-
1458 2435.2008.01515.x
- 1459 Tanunchai, B., Ji, L., Schröder, O., Gawol, S. J., Geissler, A., Wahdan, S. F. M., et al.
1460 (2023). Fate of a biodegradable plastic in forest soil: Dominant tree species and forest
1461 types drive changes in microbial community assembly, influence the composition of
1462 plastisphere, and affect poly(butylene succinate-co-adipate) degradation. *Sci. Total
1463 Environment.* 873, 162230. doi: 10.1016/j.scitotenv.2023.162230
- 1464 Tanunchai, B., Ji, L., Schroeter, S. A., Wahdan, S. F. M., Hossen, S., Deleegn, Y., et al.
1465 (2022a). FungalTraits vs. FUNGuild: comparison of ecological functional assignments
1466 of leaf- and needle-associated fungi across 12 temperate tree species. *Microb. Ecol.*
1467 doi: 10.1007/s00248-022-01973-2
- 1468 Tanunchai, B., Ji, L., Schroeter, S. A., Wahdan, S. F. M., Larpkern, P., Lehnert, A.-S.,
1469 et al. (2022b). A poisoned apple: First insights into community assembly and networks
1470 of the fungal pathobiome of healthy-looking senescing leaves of temperate trees in
1471 mixed forest ecosystem. *Front. Plant Sci.* 13. doi: 10.3389/fpls.2022.968218
- 1472 Tláškal, V., Voříšková, J., and Baldrian, P. (2016). Bacterial succession on
1473 decomposing leaf litter exhibits a specific occurrence pattern of cellulolytic taxa and
1474 potential decomposers of fungal mycelia. *FEMS Microbiol. Ecol.* 92. doi: 10.1093/
1475 femsec/fw177
- 1476 Trivedi, P., Leach, J. E., Tringe, S. G., Sa, T., and Singh, B. K. (2020). Plant-
1477 microbiome interactions: from community assembly to plant health. *Nat. Rev.
1478 Microbiol.* 18, 607–621. doi: 10.1038/s41579-020-0412-1
- 1479 Tsujiyama, S., and Minami, M. (2005). Production of phenol-oxidizing enzymes in
1480 the interaction between white-rot fungi. *Mycoscience* 46, 268–271. doi: 10.1007/s10267-
1481 005-0243-y
- 1482 Weißbecker, C., Schnabel, B., and Heintz-Buschart, A. (2020). Dadasnake, a
1483 Snakemake implementation of DADA2 to process amplicon sequencing data for
1484 microbial ecology. *GigaScience* 9. doi: 10.1093/gigascience/giaa135
- 1485 Wemheuer, F., Taylor, J. A., Daniel, R., Johnston, E., Meinicke, P., Thomas, T., et al.
1486 (2020). Tax4Fun2: prediction of habitat-specific functional profiles and functional
1487 redundancy based on 16S rRNA gene sequences. *Environ. Microbiome* 15, 11.
1488 doi: 10.1186/s40793-020-00358-7
- 1489 White, T. J., Bruns, T. D., Lee, S., and Taylor, J. (1990). ““Amplification and Direct
1490 Sequencing of Fungal Ribosomal RNA Genes for Phylogenetics,”” in *PCR Protocols: A
1491 Guide to Methods and Applications*. Eds. M. A. Innis, D. H. Gelfand, J. J. Sninsky and T.
1492 J. White (San Diego: Academic Press), 315–322.
- 1493 Wintzingerode, F. V., Göbel, U., and Stackebrandt, E. (1997). Determination of
1494 microbial diversity in environmental samples: pitfalls of PCR-based rRNA analysis.
1495 *FEMS Microbiol. Rev.* 21, 213–229. doi: 10.1111/j.1574-6976.1997.tb00351.x
- 1496 Wright, I. J., Reich, P. B., Westoby, M., Ackerly, D. D., Baruch, Z., Bongers, F., et al.
1497 (2004). The worldwide leaf economics spectrum. *Nature* 428, 821–827. doi: 10.1038/
1498 nature02403
- 1499 Zhang, P., Guan, P., Hao, C., Yang, J., Xie, Z., and Wu, D. (2022). Changes in
1500 assembly processes of soil microbial communities in forest-to-cropland conversion in
1501 Changbai Mountains, northeastern China. *Sci. Total Environ.* 818, 151738.
1502 doi: 10.1016/j.scitotenv.2021.151738
- 1503 Zhou, J., Deng, Y., Luo, F., He, Z., and Yang, Y. (2011). Phylogenetic molecular
1504 ecological network of soil microbial communities in response to elevated CO₂. *mBio* 2,
1505 e00122–e00111. doi: 10.1128/mBio.00122-11

Litter 4 – Supplementary Information

Tree mycorrhizal type regulates leaf and needle microbial communities, affects microbial assembly and co-occurrence network patterns, and influences litter decomposition rates in temperate forest

Author: Benjawan Tanunchai*, Li Ji*, Simon Andreas Schroeter, Sara Fareed Mohamed Wahdan, Katikarn Thongsuk, Ann-Sophie Lehnert, Eliane Gomes Alves, Ines Hilke, Gerd Gleixner, François Buscot, Ernst-Detlef Schulze, Matthias Noll, Witoon Purahong.

*These authors contributed equally to this work.

Status: In press, *Frontiers in Plant Science*

Please see separate attachments

Research



Cite this article: Purahong W, Tanunchai B, Muszynski S, Maurer F, Wahdan SFM, Malter J, Buscot F, Noll M. 2022 Cross-kingdom interactions and functional patterns of active microbiota matter in governing deadwood decay. *Proc. R. Soc. B* **289**: 20220130. <https://doi.org/10.1098/rspb.2022.0130>

Received: 24 February 2022

Accepted: 8 April 2022

Subject Category:

Ecology

Subject Areas:

ecology, microbiology, environmental science

Keywords:

beech, bromodeoxyuridine, diazotrophs, deadwood decay, enzyme activity, microbiome, spruce

Authors for correspondence:

Witoon Purahong

e-mail: witoon.purahong@ufz.de

Matthias Noll

e-mail: matthias.noll@hs-coburg.de

[†]These authors contributed equally to this study.

Electronic supplementary material is available online at <https://doi.org/10.6084/m9.figshare.c.5958617>.

Cross-kingdom interactions and functional patterns of active microbiota matter in governing deadwood decay

Witoon Purahong^{1,†}, Benjawan Tanunchai^{1,2,†}, Sarah Muszynski^{3,†}, Florian Maurer³, Sara Fareed Mohamed Wahdan^{1,4}, Jonas Malter³, François Buscot^{1,5} and Matthias Noll^{2,3}

¹Department of Soil Ecology, UFZ-Helmholtz Centre for Environmental Research, Theodor-Lieser-Str. 4, D-06120 Halle (Saale), Germany

²Bayreuth Center of Ecology and Environmental Research (BayCEER), University of Bayreuth, 95440, Bayreuth, Germany

³Institute for Bioanalysis, Coburg University of Applied Sciences and Arts, 96450 Coburg, Germany

⁴Department of Botany, Faculty of Science, Suez Canal University, Ismailia 41522, Egypt

⁵German Centre for Integrative Biodiversity Research (iDiv) Halle-Jena-Leipzig, Deutscher Platz 5e, D-04103 Leipzig, Germany

WP, 0000-0002-4113-6428; BT, 0000-0002-6543-3574; JM, 0000-0003-1053-9416; FB, 0000-0002-2364-0006; MN, 0000-0002-9981-5968

Microbial community members are the primary microbial colonizers and active decomposers of deadwood. This study placed sterilized standardized beech and spruce sapwood specimens on the forest ground of 8 beech- and 8 spruce-dominated forest sites. After 370 days, specimens were assessed for mass loss, nitrogen (N) content and ¹⁵N isotopic signature, hydrolytic and lignin-modifying enzyme activities. Each specimen was incubated with bromodeoxyuridine (BrdU) to label metabolically active fungal and bacterial community members, which were assessed using amplicon sequencing. Fungal saprotrophs colonized the deadwood accompanied by a distinct bacterial community that was capable of cellulose degradation, aromatic depolymerization, and N₂ fixation. The latter were governed by the genus *Sphingomonas*, which was co-present with the majority of saprotrophic fungi regardless of whether beech or spruce specimens were decayed. Moreover, the richness of the diazotrophic *Allorhizobium-Neorhizobium-Pararhizobium-Rhizobium* group was significantly correlated with mass loss, N content and ¹⁵N isotopic signature. By contrast, presence of obligate predator *Bdellovibrio* spp. shifted bacterial community composition and were linked to decreased beech deadwood decay rates. Our study provides the first account of the composition and function of metabolically active wood-colonizing bacterial and fungal communities, highlighting cross-kingdom interactions during the early and intermediate stages of wood decay.

1. Introduction

Deadwood is a major reservoir of photosynthetically fixed carbon (C) and nutrients in forest ecosystems that are highly resistant to decay [1]. The contribution of wood to total current C stock in the world's forests is estimated to reach 73 Pg C or 8% of the global C pool [2]. Mineralization of deadwood into simple compounds is carried out by a broad range of saprotrophs, including insects, fungi and bacteria, which can share such compounds with other heterotrophic organisms [3–5]. For instance, saprotrophic fungi are supported during wood decay by bacterial community members that provide bio-available nitrogen (N) sources [3,4,6,7]. Atmospheric N₂ fixing microorganisms (diazotrophs) from the bacterial orders *Burkholderiales* and *Rhizobiales* were strongly correlated with principal fungal deadwood decomposers, especially at the initial stage

of decomposition [7]. N-rich fungal enzymes and fruiting bodies were also found to be positively correlated by the presence of diazotrophs [6].

Different abiotic factors shape the deadwood microbiota in forest ecosystems. At plot level, deadwood quantity and quality on forest floor, dominant tree species, forest structure and age, soil physico-chemical variables, soil pH, temperature, humidity, elevation, plot location, slope and micro-climate were correlated with richness and distribution patterns of wood associated fungi [8,9]. However, only micro-climatic conditions and forest age were significantly correlated to wood-associated bacterial community composition [7,10]. In addition, the dominant tree species in forests supported deadwood decomposition of the same dominant tree species, which was mediated by a defined fungal community without significant impact on bacterial community composition [11]. At the individual wood piece level, wood species and anatomy (deciduous versus conifer), wood compartments (sapwood versus heartwood), wood physico-chemical properties such as wood density, size, water content, pH, C and N content, C:N ratio, lignin content explained the fungal and bacterial community patterns [9,12,14]. While these wood physico-chemical variables are tree-species-specific, they also change along the succession of decomposition [15]. Biotic factors such as fungal-fungal, bacterial-bacterial and fungal-bacterial interactions affect deadwood microbiota and their functional patterns along the decomposition process [16–18].

Although a significant amount of data and knowledge of wood-associated microbiota with Next-Generation Sequencing (NGS) were gathered, the majority of such studies to date are based on total genomic DNA [19,20]. The total genomic DNA pool consists of both intracellular DNA (represents the intact potentially living cells, including both active and dormant cells) and extracellular DNA (represents the DNA originates from both cell lysis and active secretion) [21]. Thus, the present microbial community datasets derived from total DNA represent both active and inactive (dead or dormant) microbes [12,21] of historic and present microbial community compositions [12], including those community members that used to live within the trees before tree death such as endophytes, ectomycorrhizal and arbuscular mycorrhizal fungi, animal parasite and lichens [8]. Diverse saprotrophic fungal communities were frequently detected in deadwood but mostly without addressing their activity status [22]. In addition, bacterial community compositions (including diazotrophs) in deadwood were correlated to biological N₂ fixation, however without information as to which part of the microbial community was active during N₂ fixation [6,7,23]. The wood degrading enzymes are known to have a complex structure and require a large amount of resources [1,8,24], thus microbes have to be very active and capable of translocating many resources to produce such enzymes. Community-level analyses of metabolically active microbial communities on a nucleic acid-based level are well established and can be performed by extractions of RNA [9] and also newly synthesized DNA (obtaining by Bromodeoxyuridine (BrdU) labelling and immunocapture assay) [25]. Shifts in microbial community composition to environmental parameters were much faster on RNA than on DNA level [19], but concentration of rRNA and microbial growth attributes are not simply correlated, intracellular rRNA turnover is specific to strain and environmental conditions, and dormant cells may also contain rRNA [20].

In turn, BrdU-based approaches are long-term established in mammalian cell biology and medicine [26] and can clearly elucidate proliferating microorganisms substrate-independently in various environments [25,27]. However, a few bacteria are not capable of BrdU uptake or DNA incorporation [26].

In this experiment, BrdU labelling and immunocapture assay coupled with a NGS approach [28] was employed to investigate the colonization of active microbiota on gamma sterilized Norway spruce and European beech specimens after 1 year of exposure. Gamma sterilization was applied to inactivate the wood-inhabiting communities and thereby to remove potential priming effects [16,29]. Therefore, the colonization from surrounding environments was envisaged.

We aimed to (i) describe and compare the richness and community composition of metabolically active wood microbiota (including both bacteria and fungi), (ii) disentangle the ecological and environmental factors that correlate with richness and community composition of the metabolically active deadwood microbiome, (iii) investigate the general relationships between the active bacteria and fungi as well as their co-occurrence network patterns, and (iv) link microbiome richness, taxonomically resolved identity and microbiome composition with microbial-mediated ecosystem functions such as C, N and phosphorus (P) contents, acquisition of hydrolytic enzyme activities and lignin-modifying enzyme activities and mass loss. Wood tree species and forest type played a significant role in shaping richness and community compositions of overall genomic DNA approach, and we hypothesize that holds also true for metabolically active wood microbiota. We expected that especially diverse diazotrophs and co-occurring fungal saprotrophs are highly active in both spruce and beech wood. We also hypothesized that high hydrolytic enzyme activities are linked to accelerated wood decomposition rates, which are related to the active fraction of both bacteria and fungi. By contrast, we assumed that lignin-modifying enzymes, especially general peroxidase and manganese peroxidase, are more related to active fungal community members.

2. Material and methods

(a) Exploration sites, experimental design and sample preparation

Investigated forest plots were part of the German Biodiversity Exploratories [30] and located in the UNESCO Biosphere Reserve Swabian Alb in the southwest of Germany. The field experiment was conducted on 16 forest plots (each one hectare) of the exploratory of which eight plots are located in a *Fagus sylvatica* and eight plots in a *Picea abies* dominated forest site. Furthermore, investigated plots differed in forest management intensity (ForMI) as introduced earlier [31]. We excluded the results from Norway spruce and European beech specimens in some plots due to low DNA quality and quantity. The final experimental design consisted of specimens of two tree species \times 2 forest types \times 6 independent replicate plots.

Sapwood deadwood specimens of one *F. sylvatica* and one *P. abies* tree trunk were cut in 50 \times 25 \times 15 mm. Each specimen was gamma sterilized at 70 kGy by Synergy Health Radeberg GmbH (Radeberg, Germany) to inactivate endophytes as explained earlier [32]. Afterward specimens were dried at 103 \pm 2°C for 48 h, and dry weight was determined precisely under kiln-dried conditions.

In May 2017, both of two *F. sylvatica* and two *P. abies* deadwood specimens were placed in mesh bags on top of the forest ground of

each forest plot with 10 cm distance between each specimen to obtain the same environmental conditions, and after 370 days of exposure specimens were collected. One specimen was directly treated with 0.1 ml of 10 mM BrdU on top for 48 h at room temperature as explained earlier [25], while the other specimen was shock frozen with liquid N at the field site to measure mass loss, wood pH, enzyme activities, C and N content and its isotopic signatures. After BrdU treatment, specimens were shock frozen with liquid nitrogen and stored at -80°C until further use.

Mass loss and wood pH measurement was carried out as explained recently [32]. Enzyme activities such as acid phosphatase, β -glucosidase, cellobiohydrolase, manganese peroxidase, N-acetylglucosaminidase, laccase, peroxidase and xylosidase were assessed to differentiate C, N and P acquisition as explained earlier [24,28]. Content of C and N and its isotopic signatures was measured from milled sub-samples by a vario EL III element analyser combined with an Isoprime 100 stable isotope ratio mass spectrometer (EA-IRMS) (Elementar Analysensysteme GmbH, Langensfeld, Germany).

(b) Analyses of metabolically active wood microbiota using BrdU labelling technique, Illumina sequencing and statistics

DNA was extracted from the BrdU-treated specimens using Quick-DNA Fecal/Soil Microbe Miniprep Kit (Zymo, California, USA). BrdU-labelled DNA from the metabolically active microbial cells was isolated from each total DNA extract by a BrdU immune-capture approach as described previously [25,28] and in the electronic supplementary material. Details of the construction of the bacterial and fungal amplicon libraries, Illumina sequencing and sequence data processing can be found in the supplementary material.

The effects of tree species of specimen on bacterial and fungal ASV richness and community composition were analysed using *t*-test and permutational multivariate analysis of variance (PERMANOVA), based on Jaccard distance measure. Correlations between various factors and the co-occurrence network patterns of the microbial communities were analysed using Spearman's rank correlation. The correlation matrix was visualized and the networks were extracted using Cytoscape v. 3.8.0. For full details of material and methods, and statistical analyses, see electronic supplementary material.

3. Results

(a) Active community composition and richness in deadwood

High diversity (bacterial: 16 phyla (44 classes); fungi: 15 classes) with moderate number of functions (nine functional groups for both bacteria and fungi) were detected with uneven distribution in beech and spruce deadwood (figures 1 and 2). *Gammaproteobacteria* (highly contributed by *Stenotrophomonas*, *Massilia*, *Rhodanobacter*, *Luteibacter*) and *Alphaproteobacteria* (highly contributed by *Sphingomonas*, *Allorhizobium-Neorhizobium-Pararhizobium-Rhizobium* (ANPR)) highly dominated the bacterial communities in both tree species whereas *Acidobacteriae*, *Actinobacteria*, *Bacteroidota* and *Mollicutes* were frequently detected bacterial classes (electronic supplementary material, figure S1; genus level in figure 1a). These phyla except *Mollicutes* were observed very frequently (electronic supplementary material, figure S1). Chemoheterotrophic bacteria (saprotrophs) were the most dominant functional group, followed by bacteria involved with N cycling (ureolysis, diazotrophs, nitrate respiration and reduction) (figure 1b). Diazotrophic bacteria

were detected in all specimens and they even dominate/co-dominant the majority of bacterial functions in both tree species (beech = average $34.3 \pm 6.0\%$ (mean \pm s.e.), spruce = average $18.5 \pm 1.4\%$ (mean \pm s.e.)) (electronic supplementary material, figure S2a). This dominance of potential diazotrophic bacteria was reflected by a diverse average species richness of 28.5 ± 2.4 and 35.8 ± 2.5 (mean \pm s.e.) ASVs in beech and spruce deadwood, respectively (electronic supplementary material, figure S2b). Members of the genus *Sphingomonas* were the most frequent detected diazotrophic bacteria in beech ($7.8 \pm 2.0\%$) and spruce ($10.3 \pm 1.1\%$) (mean \pm s.e.) deadwood blocks. In addition, ANPR were detected in average 1.9% both in spruce and beech wood blocks (electronic supplementary material, figure S2c).

Agaricomycetes (mainly *Mycena* spp.) highly dominated the fungal communities in specimens of both tree species (average relative abundances = $60 \pm 11\%$ (beech) and $69 \pm 10\%$ (spruce) (mean \pm s.e.)) followed by *Sordariomycetes* (average relative abundances = $19 \pm 7\%$ beech and $19 \pm 7\%$ spruce (mean \pm s.e.)) (electronic supplementary material, figure S3, genus level in figure 2a). Fungal saprotrophs were the most dominant functional groups while other functional groups were rarely detected in the metabolically active fungal communities (figure 2b). There were 26 plant pathogenic fungal ASVs detected with low relative abundances (average $0.6 \pm 0.3\%$ (mean \pm s.e.), ranging from 0–6.5%) (figure 2b; electronic supplementary material, table S1).

(b) Comparison of the richness and community composition of metabolically active microbiota

Tree species did not significantly impact on richness of the active bacterial and fungal communities (figure 3a,b). Bacterial and fungal richness varied greatly, especially fungal richness (ranging from 3 to maximum 110 ASVs). Bacterial and fungal community compositions also strongly differed among all samples (electronic supplementary material, figures S1d and S3d). The similarity among all the samples was below 30% and 20% for bacteria and fungi. The majority of the deadwood samples were composed each of one to three ASVs that contributed to more than 80% of the relative sequence read abundances (figure 2a). Nevertheless, we found that bacterial community composition in beech specimens was significantly different from those in spruce specimens (electronic supplementary material, figure S1d). The effect of tree species on bacterial community composition was consistent in both beech and spruce forests ($F = 1.08\text{--}1.12$, $p = 0.023\text{--}0.026$). The bacterial genera *Sphingomonas*, *Mucilagibacter*, *Rhodanobacter* and *Halomonas* were frequently detected in both tree species. *Stenotrophomonas* and *Luteibacter* were enriched in beech specimens, whereas *Massilia* and *Puia* were significantly enriched in spruce specimens. Fungal community compositions differed only for spruce specimens incubated in beech and spruce forest (electronic supplementary material, figure S3d). Members of the genus *Mycena* were the most dominant in the active fungal community compositions (figure 2a).

(c) Factors corresponding with community composition of metabolically active deadwood microbiota

C and N contents were significantly correlated to both bacterial and fungal community compositions associated with beech specimens (electronic supplementary material, table S2). Furthermore, the plot factors such as soil temperature and ForMI also significantly contributed to effect both

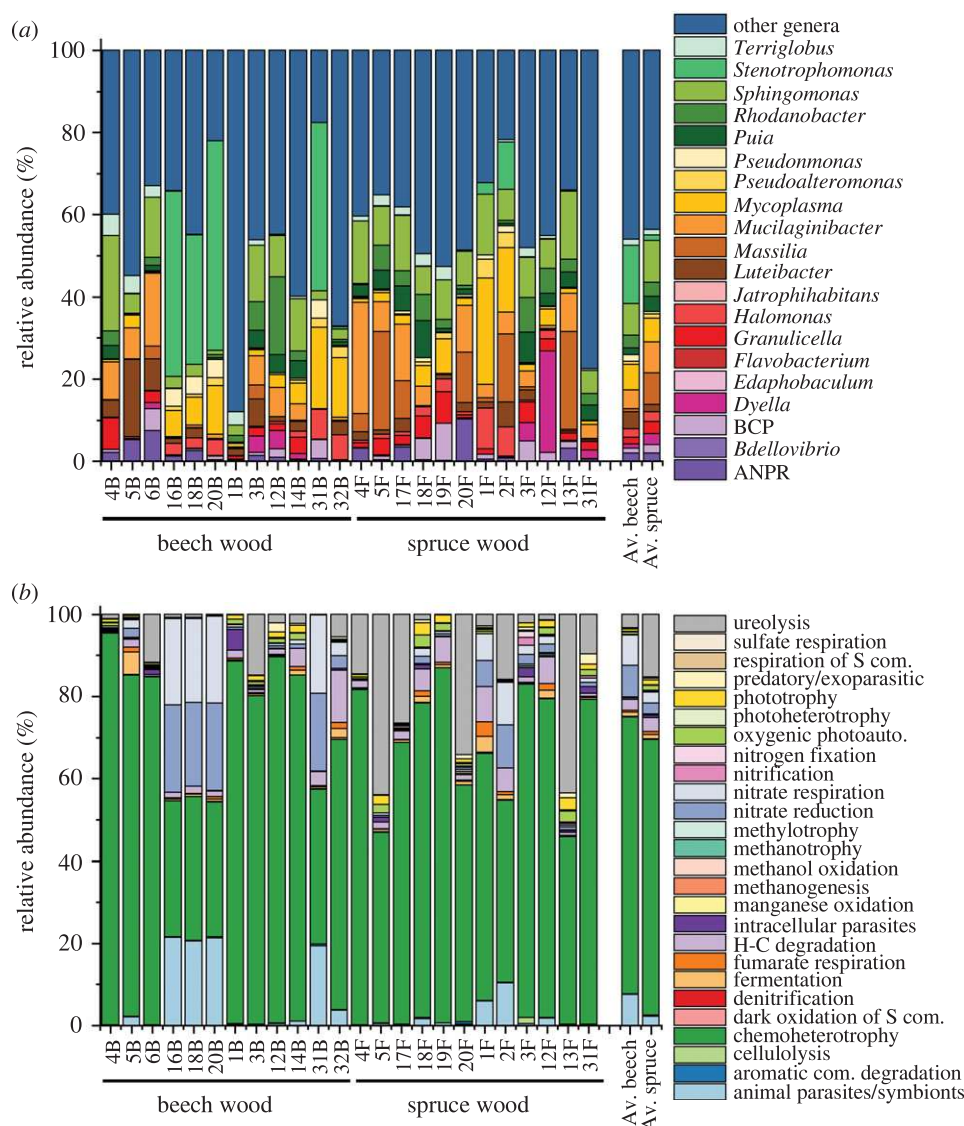


Figure 1. Active bacterial community composition at genus level retrieved from decayed beech and spruce deadwood in relative sequence read abundances (a), and their assigned metabolic functions (b). Av = average, B = beech wood, F = spruce wood, BCP = *Burkholderia-Caballeronia-Paraburkholderia*. The relative sequence read abundances of ASVs assigned to N fixing bacteria, and their richness as well as the relative sequence read abundances of ASVs assigned to the *Allorhizobium-Neorhizobium-Pararhizobium-Rhizobium* complex (ANPR) are presented in electronic supplementary material, figure S2. Details on class level and presence/absence data can be found in electronic supplementary material, figure S1. (Online version in colour.)

community compositions. Bacterial and fungal community compositions in spruce specimens were only significantly correlated to soil pH for bacteria and ForMI for fungi (electronic supplementary material, table S2).

(d) Relationships and co-occurrence network patterns of the active microbiota

Richness of active bacterial and fungal ASVs was correlated when both beech and spruce specimens were considered together ($R = 0.64$, $p < 0.001$). However, richness of active bacteria and fungi present in spruce specimens was significantly correlated ($R = 0.84$, $p < 0.001$) whereas such correlation in beech specimens was not significant. Relationships between fungi and bacteria strongly differed between both tree species (figure 3c,d). The same fungal genera mostly co-occurred with different bacterial taxa. Nevertheless, we observed that diazotrophic bacteria were associated with most fungal saprotrophs, including the main fungal decomposers in this study (*Mycena* spp.) (compare figure 3c,d with figure 2b).

(e) Link between microbiome richness, composition and microbial-mediated ecosystem functions and processes

Even with similar decomposition time and environmental frame, deadwood samples showed a high variance in mass loss reflecting different decay stages. Beech specimens had average mass loss of $25 \pm 4\%$ (mean \pm s.e.) whereas spruce specimens had average mass loss of $9 \pm 2\%$ (mean \pm s.e.) (electronic supplementary material, table S3). Significant correlations between mass loss and enzyme activities were observed in specimens of both tree species. High beech mass loss was significantly correlated to high cellobiohydrolase, β -glucosidase and peroxidase activity, while in spruce mass loss was only positively correlated with cellobiohydrolase (electronic supplementary material, table S4). In addition, patterns of wood degrading enzyme activities in both tree species were highly correlated with wood-physiochemical properties, species richness and relative abundances of specific microbial taxa (electronic supplementary material, table S5). N content in beech specimens was significantly correlated with enzyme

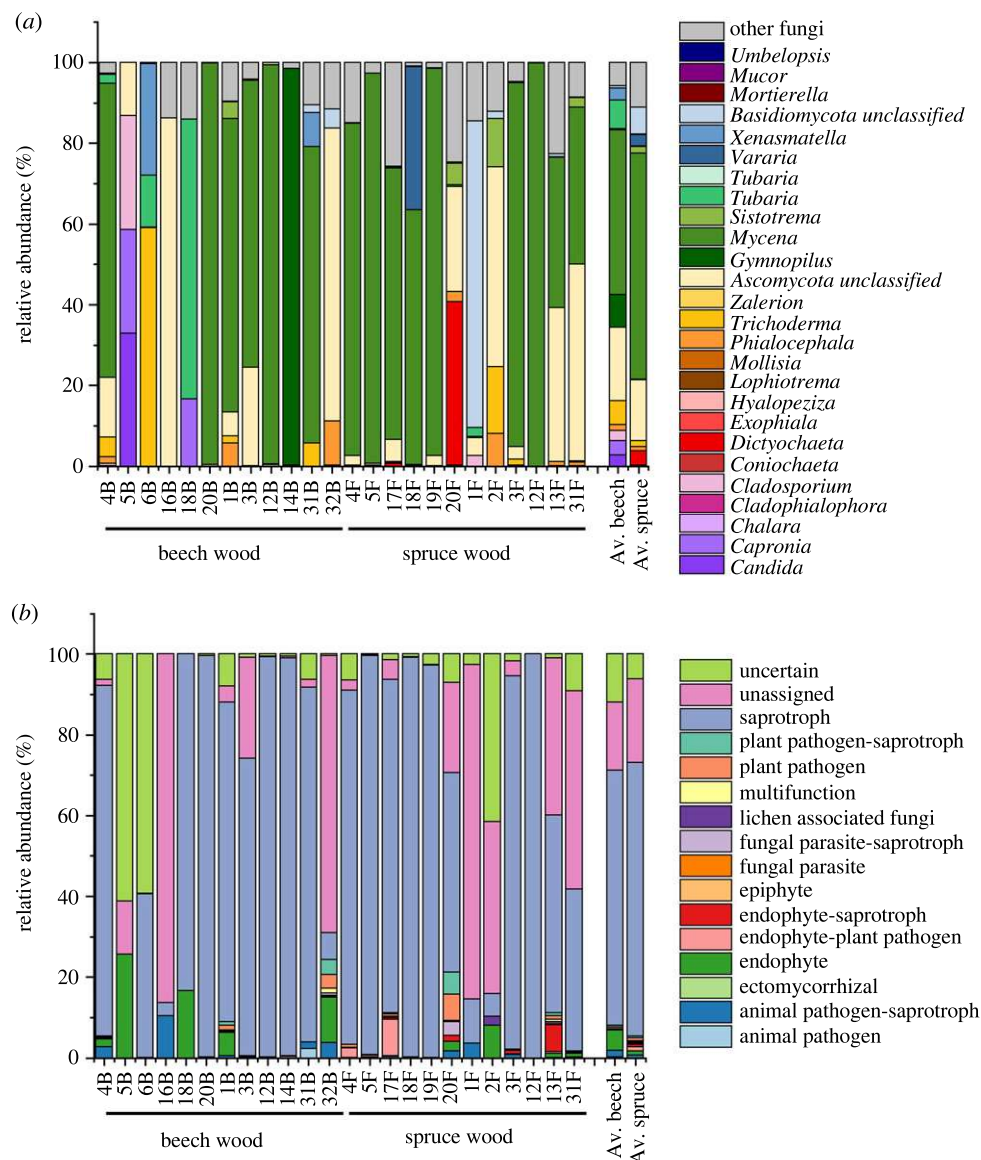


Figure 2. Active fungal community composition at genus level retrieved from decayed beech and spruce deadwood in relative sequence read abundances (a), and their assigned ecological functions (b). Av = average, B = beech wood, F = spruce wood. Details on class level and presence/absence data can be found in electronic supplementary material, figure S3. (Online version in colour.)

activity patterns whereas spruce specimens were significantly correlated to C content (electronic supplementary material, table S5). *Mucilaginibacter*, ANPR, *Hypocreaceae*, *Trichoderma*, *Halomonas*, *Gammaproteobacteria* and *Bacteroidota* were significantly correlated with enzyme activity patterns in beech while *Mucilaginibacter*, *Sphingomonas*, *Umbelopsis* and *Umbelopsisidaceae* in spruce specimens. Among these bacterial taxa, *Mucilaginibacter* is the only genus significantly correlated with enzyme activity patterns in both deadwood species and the diazotrophic bacteria from ANPR were strongly correlated with enzyme activity patterns only in beech specimens (electronic supplementary material, table S5).

Individual enzyme activities were mostly negatively correlated with richness and/or relative abundances of the majority of bacterial taxa but positively with fungal taxa in beech specimens (figure 4a). Especially *Bdellovibrio* known as bacterial predators were highly negatively correlated to enzyme activities (5 out of 8 enzymes) in beech specimens (figure 4a). Furthermore, richness of *Bdellovibrio* spp. significantly corresponding with the bacterial community composition in beech specimens ($r^2 = 0.43$, $p < 0.05$). Xylosidase and N-acetyl-glucosaminidase activities were positively

correlated in spruce specimens with richness/relative abundances of *Acidobacteria* (including *Granulicella*) and fungi. All correlated taxa were different between both tree species, and only the relative abundances of *Strophariaceae* (*Tubaria* and *Hypholoma*) and peroxidase activity was similar (figure 4a). The majority of plot factors and wood physico-chemical properties were negatively correlated with individual enzyme activities (figure 4b). However, higher N contents had the most prominent positive correlations to acid phosphatase and mass loss both in beech wood and Xylosidase and N-acetyl-glucosaminidase in spruce wood. Overall, hydrolytic enzyme activities were correlated to active bacteria and fungi whereas lignin-modifying enzyme were positively correlated to active fungi (*Strophariaceae*).

Mass loss of beech specimens was positively correlated to richness/relative abundances of ANPR ($\rho = 0.81$, $p < 0.001$), fungi (*Strophariaceae* and *Herpotrichiellaceae*) as well as C and N content but negatively to *Bdellovibrio* ($\rho = -0.65$, $p < 0.05$) (figure 4a; electronic supplementary material, figure S4). N content in beech specimens was positively correlated with ANPR and $\delta^{15}\text{N}$ signature (electronic supplementary material, figure S4). In spruce specimens, mass loss was positively linked

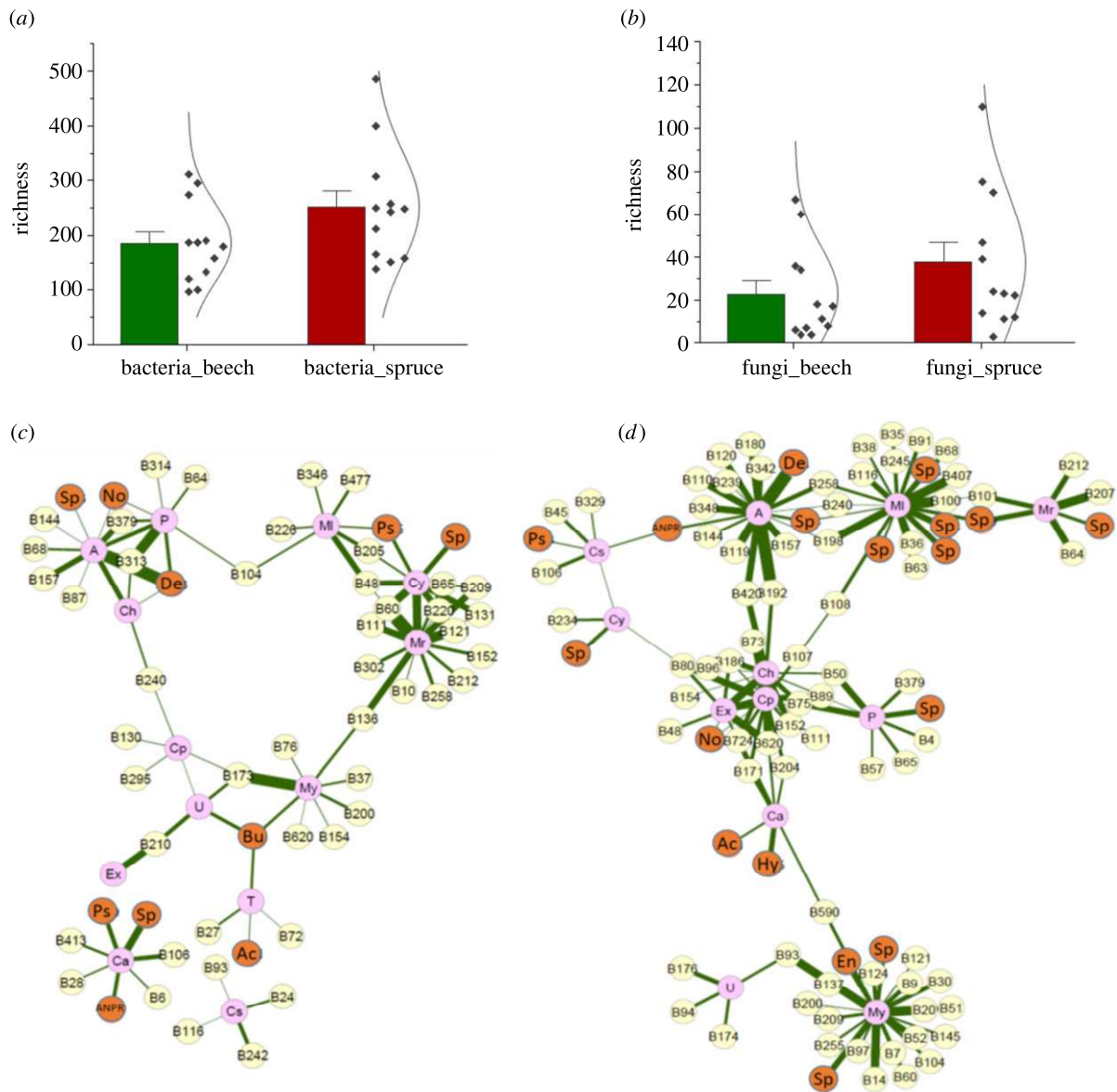


Figure 3. Active bacterial (a) and fungal richness (b) and networks retrieved from decayed beech (c) and spruce deadwood (d). Fungi (pink nodes; *Angustimasarina* (A), *Capronia* (Ca), *Chaetosphaeria* (Ch), *Cladophialophora* (Cp), *Cladosporium* (Cs), *Cyphellophora* (Cy), *Exophiala* (Ex), *Trichoderma* (T), *Mollisia* (Ml), *Mortierella* (Mr), *Mycena* (My), *Phialocephala* (P), *Umbelopsis* (U)), general bacteria (yellow nodes) and diazotrophic bacteria (orange node; *Acidiphilium* (Ac), *Allorhizobium-Neorhizobium-Pararhizobium-Rhizobium* (ANPR), *Burkholderia* (Bu), *Dexia* (De), *Enterobacterales* (En), *Hyphomicrobium* (Hy), *Novosphingobium* (No), *Sphingomonas* (Sp), *Pseudomonas* (Ps)) are indicated. Additional information to respective ASV numbers of selected ASVs can be found in electronic supplementary material, table S1.

to richness/relative abundances of *Gammaproteobacteria* and negatively to *Actinobacteria* and wood pH (figure 4a).

4. Discussion

Recent studies based on DNA sequencing demonstrated that total bacterial communities in beech and spruce specimens are co-dominated by diverse bacterial phyla including, members of the classes *Alphaproteobacteria*, *Betaproteobacteria*, *Gammaproteobacteria*, *Acidobacteria*, *Actinobacteria* and *Bacteroidota* [10,13,14]. However, our results based on active bacterial fraction revealed that only *Gammaproteobacteria*, *Alphaproteobacteria* and *Bacteroidetes* governed the deadwood communities. Moreover, the dominant members of the *Gammaproteobacteria* and *Alphaproteobacteria* were also consistent during decay of spruce and beech specimens of our study, regardless of respective decay stage. Although other dominant bacterial phyla, which were

previously detected with DNA sequencing approaches, were not dominant in the active bacterial communities, but they were still frequently detected [10,13,14]. Members of the genera *Stenotrophomonas*, *Massilia*, *Rhodanobacter*, *Luteibacter*, *Sphingomonas* and ANPR were highly represented in the active bacterial communities. While the majority of these dominant bacteria genera are known for their potential function in C cycle such as cellulose degraders (*Stenotrophomonas*, *Massilia*, *Luteibacter*) [33–35] and catabolizing aromatic lignin depolymerization (*Sphingomonas*) [36], some of them are also known to potentially play important roles in N cycling. Majority of members of *Sphingomonas* and ANPR are able to fix atmospheric N_2 [37], *Rhodanobacter* spp. show denitrification capabilities [38] and *Luteibacter* spp. are efficient chitin degraders [39]. Moreover, ANPR was dominant bacterial fraction in the fruiting bodies of saprotrophic *Cantharellales* indicating a close relationship between both [40]. Thus, our results demonstrate that apart from bacteria involved in C cycling, the bacteria involved in N

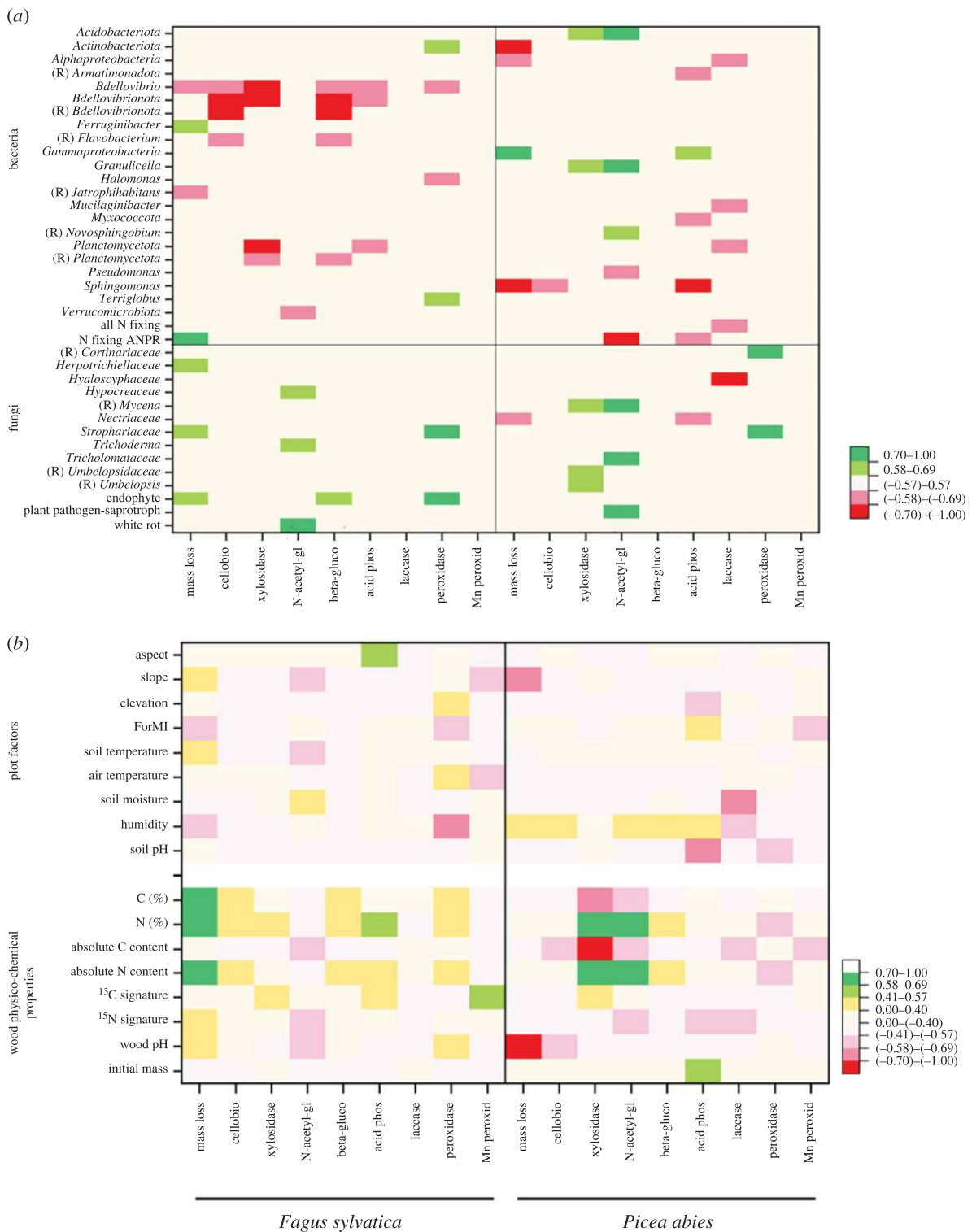


Figure 4. Heat map of Spearman's rank correlations between richness versus relative abundance of microbial taxa (a), wood physico-chemical properties and plot factors (b) on wood mass loss versus enzyme activities in *Fagus sylvatica* or *Picea abies*. Light and dark green colours of the heat map indicate significant positive correlations ($p < 0.05$) and pink and red colours indicate significant negative correlations ($p < 0.05$). Full enzymatic names are presented in the Material and methods section.

cycling are highly active in deadwood. In fact, based on bacterial functional analyses, we showed that these N cycling bacteria were potentially drivers for C and N cycling during deadwood decay, including N fixation, ureolysis, nitrate respiration and reduction, and N respiration. It is noteworthy that potential diazotrophic bacteria represent in average 18.5% and 34% of total detected bacterial sequences in spruce and beech specimens, respectively. Moreover, *Acidobacteriae* (*Granulicella*) and *Bacteroidota* (*Mucilaginibacter*) may also highly contribute in the decomposition of specimens as members of both genera are

known as efficient cellulose degraders [39]. The relative abundance of *Mucilaginibacter* was highly correlated with enzyme activity patterns in both beech and spruce specimens (electronic supplementary material, table S5), indicating that released cellulose from the wood fibres was metabolized by these bacteria. However, such correlations should be carefully interpreted as bacterial occurrence is not always linked to environmental enzyme activities. Interestingly, in our work we also detected relatively high richness of obligate predatory bacteria *Bdellovibrio* spp. and found that their high richness and increased relative

abundances negatively impacted both enzyme activities and decomposition rates in beech specimens. Prey range of *Bdellovibrio* spp. is relatively narrowly specific to gram-negative bacteria [41]. Frequently detected gram-negative bacteria genera (*Pseudomonas*, *Rhizobium*) detected in our study that were classified as potential diazotrophic bacteria are known to be among the potential preys of *Bdellovibrio* spp. An indirect study showed that predator–prey interactions were known in some ecosystems to impact on microbial ecosystem processes and services [42], but this is the first time we detected such phenomenon during deadwood decay. Direct consequences of the obligate predator *Bdellovibrio* spp. could shift the bacterial community composition (figure 1), which leads to decreased deadwood decay rates. Deadwood has a high bacterial biomass (2×10^{12} gene copy numbers g^{-1}) [43,44], which is more than enough to enable predatory lifestyle of *Bdellovibrio* spp. with need of a minimal concentration of 7×10^5 prey cells ml^{-1} [45,46]. Future studies should address the prey turnover and its consequences for the microbial part in ecosystem services of deadwood decay.

The early decomposition process of deadwood is mediated by fungal endophytes which used to live within the trees before tree death [29]. On the one hand, these fungal endophytes play a direct role as early decomposers to decompose the wood. This aspect has been demonstrated in both beech and spruce wood, which endophytes (beech: *Xylaria* and spruce: *Phialocephala*) change their functionality from endophytes to saprotrophs (soft-rot fungi) [8,12]. On the other hand, the endophytes indirectly regulate the wood decomposition rate through the priority effects as initial community determines the subsequent community successions [16,29]. We demonstrated in this study that eliminating the endophytes from specimens can cancel the priority effects of endophytes, thereby enabling opportunities for diverse fungi to colonize deadwood. Despite similar deadwood physico-chemical properties, surrounding environment conditions (including ForMI) and decomposition time, each specimen from each tree species used in this study colonized by different active fungal and bacterial community compositions and their decomposition rates differed greatly. Some wood blocks have reached the late stage of decomposition whereas some wood blocks are still at the very early phase. In addition, ForMI also significantly affected active fungal community composition (electronic supplementary material, table S2), which was already shown in a previous study from the same sites [47]. However, we could show that this shift in the active fungal community composition was correlated with a lower mass loss, lower peroxidase and manganese dependent peroxidase activities compared to forest sites with low ForMI (figure 4). This phenomenon is strongly different from deadwood that contains initial endophytes, which often resulting in homogenization of the subsequent communities depending on the dominant endophytic taxa [8,16,29].

Our study demonstrates that saprotrophs are the most active fungal functional group in specimens whereas other functional groups are also active but their contributions were relatively minor. This can be explained by two observations: (i) fungal saprotrophs gain competitive advantage in specimens as compared with other functional groups due to the sufficient nutrient source availability and their abilities to produce wood-degrading enzymes; and (ii) other fungal functional groups, especially mycorrhizal fungi, plant pathogens and animal pathogens, are slow growing or partly in dormant phase to conserve their energy and waiting for their suitable hosts [48,49]. Fungal endophyte is the only functional group that can substantially

compete for deadwood substrate resources with fungal saprotrophs. Although they are eliminated from the initial community, our work showed that endophytes from surrounding environments can re-colonize and proliferate into deadwood. This again demonstrates the ability of fungal endophytes to switch their lifestyle as saprotrophs (commonly as soft rot) [8,29].

The presence of diazotrophs in deadwood logs of spruce [6,50] and beech [6,22] has been previously shown, and the overall majority of these diazotrophs in deadwood were characterized as asymbiotic and free-living diazotrophs. The cleavage and reduction of atmospheric N_2 molecule by the nitrogenase system is a very energy-consuming process of the diazotrophs [3]. In our beech specimens, we observed not only a decrease in the C/N ratio based on the removal of the absolute C content but also an increase in absolute N content, indicating an active input of N into the specimen. N in wood is among the most important macronutrients required for fungi to produce enzyme to degrade wood [3,7]. Indeed, we found in our study that N content was highly correlated with mass loss in beech wood. Moreover, there were strong linear relationships of $\delta^{15}N$ signature increase and total N content of beech specimens as well as $\delta^{15}N$ signature increase and sequent abundances of diazotrophs (ANPR) (electronic supplementary material, figure S4), indicating a linear relationship. As the $\delta^{15}N$ signature was getting less negative and more close to $\delta^{15}N$ (0‰) of atmospheric N_2 [51], a higher proportion of microbial fixed atmospheric N_2 was present in deadwood and therefore other sources to enrich absolute N content were less likely. A very recent study showed by metagenomics and metatranscriptomics linked to the N-cycling genes that old and young beech deadwood were dominated by transcripts of N fixation [22], which supports our findings of a very active N fixing bacterial community during beech deadwood decay. Interestingly, the richness of the diazotrophic part of the bacterial community composition, at 20–30% (electronic supplementary material, figure S2a), was very high compared with recent transcriptomic analyses [22], however both analysis types has its drawbacks in over- and underestimating present status. Network analyses showed a clear link between the diazotrophic taxa and fungi (figure 3c and d). The majority of the 13 active mainly saprotrophic fungal taxa were linked to members of the diazotrophic genus *Sphingomonas*. A cross-kingdom association between ectomycorrhizal and arbuscular mycorrhizal fungi and *Sphingomonas* was shown several times [52,53], and the presence of *Sphingomonas* enriched the system with additional N [52]. Moreover, *Sphingomonas* were mainly found in the early stage of deadwood decay [54], indicating that they are of high importance to initiate accelerated deadwood decay by atmospheric N addition like in our study. The wood-rotting fungal taxa *Mollisia* was linked to five ASVs, which were all assigned to *Sphingomonas* (figure 3c). Furthermore, *Angustimassarina* was linked to *Sphingomonas* in both spruce and beech deadwood decay, indicating a tree-species-independent partnership between both cross-kingdom taxa (compare figure 3c,d). However, some diazotrophic genera share co-presence with more than one fungal taxa. For instance, *Derxia* was associated in the co-occurrence network with both endophytic *Phialocephala* and saprotrophic *Chaetosphaeria* or *Burkholderia* with three saprotrophic fungal taxa *Trichoderma*, *Mycena* and *Umbelopsis* (figure 3), indicating a free diazotrophic life style with changing partners. The mass loss of spruce specimens involved a greater richness and diversity of diazotrophic bacteria, indicating that the initial deadwood decay just started and superior taxa will outcompete

others in a later decay stage. Moreover, there was no such correlation between increase of $\delta^{15}\text{N}$ signature and mass loss in spruce deadwood decay, indicating that N acquisition was not high enough to accelerate deadwood decay.

5. Conclusion

The spotlight on the metabolic active fraction during beech and spruce deadwood decay discovered a less diverse fungal and bacterial taskforce with clearly defined functional assignments. Similar biological patterns of colonizers were found between beech and spruce, but different patterns of microbial interactions and functions. Mass loss of deadwood was conducted by saprotrophic fungi and their respective hydrolytic and lignin-modifying enzyme activities. So few active fungi were accompanied by a selected bacterial community that is capable for cellulose degradation, aromatic depolymerization and N cycling including diazotrophs. The latter diazotrophic activity is underlined by N enrichment in the deadwood and an increase of the $\delta^{15}\text{N}$ signature, which was closely linked to the abundance of ANPR. Moreover, members of the genus *Sphingomonas* were co-present with most saprotrophic fungi regardless of whether beech or spruce specimens were decayed, highlighting their importance in ecological functioning in the early stage of deadwood decomposition. Further research should employ proteome analyses, ideally in deadwood decay stages, to get more insight into the interaction patterns of the deadwood decaying community.

References

- Floudas D *et al.* 2012 The Paleozoic origin of enzymatic lignin decomposition reconstructed from 31 fungal genomes. *Science* **336**, 1715–1719. (doi:10.1126/science.1221748)
- Pan Y *et al.* 2011 A large and persistent carbon sink in the world's forests. *Science* **333**, 988–993. (doi:10.1126/science.1201609)
- Weißhaupt P, Pritzkow W, Noll M. 2011 Nitrogen metabolism of wood decomposing basidiomycetes and their interaction with diazotrophs as revealed by IRMS. *Int. J. of Mass Spectrom.* **307**, 225–231. (doi:10.1016/j.ijms.2010.12.011)
- Hobbie EA, Grandy AS, Harmon ME. 2020 Isotopic and compositional evidence for carbon and nitrogen dynamics during wood decomposition by saprotrophic fungi. *Fungal Ecol.* **45**, 100915. (doi:10.1016/j.funeco.2020.100915)
- Palin OF, Eggleton P, Malhi Y, Girardin CAJ, Rozas-Dávila A, Parr CL. 2011 Termite diversity along an Amazon–Andes elevation gradient, Peru. *Biotropica* **43**, 100–107. (doi:10.1111/j.1744-7429.2010.00650.x)
- Hoppe B, Kahl T, Karasch P, Wubet T, Bauhus J, Buscot F, Krüger D. 2014 Network analysis reveals ecological links between N-fixing bacteria and wood-decaying fungi. *PLoS ONE* **9**, e88141. (doi:10.1371/journal.pone.0088141)
- Gómez-Brandón M, Probst M, Siles JA, Peintner U, Bardelli T, Egli M, Insam H, Ascher-Jenull J. 2020 Fungal communities and their association with nitrogen-fixing bacteria affect early decomposition of Norway spruce deadwood. *Sci. Rep.* **10**, 8025. (doi:10.1038/s41598-020-64808-5)
- Purahong W, Pietsch KA, Lentendu G, Schöps R, Bruelheide H, Wirth C, Buscot F, Wubet T. 2017 Characterization of unexplored deadwood mycobiome in highly diverse subtropical forests using culture-independent molecular technique. *Front. Microbiol.* **8**, 574. (doi:10.3389/fmicb.2017.00574)
- Rajala T, Peltoniemi M, Pennanen T, Mäkipää R. 2012 Fungal community dynamics in relation to substrate quality of decaying Norway spruce (*Picea abies* [L.] Karst.) logs in boreal forests. *FEMS Microbiol. Ecol.* **81**, 494–505. (doi:10.1111/j.1574-6941.2012.01376.x)
- Tláškal V, Voříšková J, Baldrian P. 2016 Bacterial succession on decomposing leaf litter exhibits a specific occurrence pattern of cellulolytic taxa and potential decomposers of fungal mycelia. *FEMS Microbiol. Ecol.* **92**, fiw177. (doi:10.1093/femsec/fiw177)
- Purahong W, Kahl T, Krüger D, Buscot F, Hoppe B. 2019 Home-field advantage in wood decomposition is mainly mediated by fungal community shifts at 'home' versus 'away'. *Microb. Ecol.* **78**, 725–736. (doi:10.1007/s00248-019-01334-6)
- Rajala T, Peltoniemi M, Hantula J, Mäkipää R, Pennanen T. 2011 RNA reveals a succession of active fungi during the decay of Norway spruce logs. *Fungal Ecol.* **4**, 437–448. (doi:10.1016/j.funeco.2011.05.005)
- Hoppe B, Krüger K, Kahl T, Armstadt T, Buscot F, Bauhus J, Wubet T. 2015 A pyrosequencing insight into sprawling bacterial diversity and community dynamics in decaying deadwood logs of *Fagus sylvatica* and *Picea abies*. *Sci. Rep.* **5**, 9456. (doi:10.1038/srep09456)
- Moll J, Kellner H, Leonhardt S, Stengel E, Dahl A, Bässler C, Buscot F, Hofrichter M, Hoppe B. 2018 Bacteria inhabiting deadwood of 13 tree species are heterogeneously distributed between sapwood and heartwood. *Environ. Microbiol.* **20**, 3744–3756. (doi:10.1111/1462-2920.14376)
- Baldrian P, Zrůstová P, Tláškal V, Davidová A, Merhautová V, Vrška T. 2016 Fungi associated with decomposing deadwood in a natural beech-dominated forest. *Fungal Ecol.* **23**, 109–122. (doi:10.1016/j.funeco.2016.07.001)
- Hiscox J, Savoury M, Müller CT, Lindahl BD, Rogers HJ, Boddy L. 2015 Priority effects during fungal community establishment in beech wood. *ISME J.* **9**, 2246–2260. (doi:10.1038/ismej.2015.38)
- Moll J, Heintz-Buschart A, Bässler C, Hofrichter M, Kellner H, Buscot F, Hoppe B. 2021 Amplicon sequencing-based bipartite network analysis confirms a high degree of specialization and modularity for fungi and prokaryotes in deadwood. *mSphere* **6**, e00856-20. (doi:10.1128/mSphere.00856-20)
- Odrozola I, Abrego N, Tláškal V, Zrůstová P, Morais D, Větrovský T, Ovaskainen O, Baldrian P. 2021 Fungal communities are important determinants of bacterial community composition in deadwood. *mSystems* **6**, e01017-20. (doi:10.1128/mSystems.01017-20)

19. Noll M, Matthies D, Frenzel P, Derakshani M, Liesack W. 2005 Succession of bacterial community structure and diversity in a paddy soil oxygen gradient. *Environ. Microbiol.* **7**, 382–395. (doi:10.1111/j.1462-2920.2005.00700.x)
20. Blazewicz SJ, Barnard RL, Daly RA, Firestone MK. 2013 Evaluating rRNA as an indicator of microbial activity in environmental communities: limitations and uses. *ISME J.* **7**, 2061–2068. (doi:10.1038/ismej.2013.102)
21. Probst M, Ascher-Jenull J, Insam H, Gómez-Brandón M. 2021 The molecular information about deadwood bacteriomes partly depends on the targeted environmental DNA. *Front. Microbiol.* **12**, 825. (doi:10.3389/fmicb.2021.640386)
22. Tláškal V *et al.* 2021 Complementary roles of wood-inhabiting fungi and bacteria facilitate deadwood decomposition. *mSystems* **6**, e01078-20. (doi:10.1128/mSystems.01078-20)
23. Rinne KT, Rajala T, Peltoniemi K, Chen J, Smolander A, Mäkipää R. 2017 Accumulation rates and sources of external nitrogen in decaying wood in a Norway spruce dominated forest. *Funct. Ecol.* **31**, 530–541. (doi:10.1111/1365-2435.12734)
24. Kellner H *et al.* 2014 Widespread occurrence of expressed fungal secretory peroxidases in forest soils. *PLoS ONE* **9**, e95557. (doi:10.1371/journal.pone.0095557)
25. Allison SD, Hanson CA, Treseder KK. 2007 Nitrogen fertilization reduces diversity and alters community structure of active fungi in boreal ecosystems. *Soil Biol. Biochem.* **39**, 1878–1887. (doi:10.1016/j.soilbio.2007.02.001)
26. Urbach E, Vergin KL, Giovannoni SJ. 1999 Immunochemical detection and isolation of DNA from metabolically active bacteria. *Appl. Environ. Microbiol.* **65**, 1207–1213.
27. McMahon SK, Wallenstein MD, Schimel JP. 2011 A cross-seasonal comparison of active and total bacterial community composition in Arctic tundra soil using bromodeoxyuridine labeling. *Soil Biol. Biochem.* **43**, 287–295. (doi:10.1016/j.soilbio.2010.10.013)
28. Wahdan SFM, Heintz-Buschart A, Sansupa C, Tanunchai B, Wu Y-T, Schädler M, Noll M, Purahong W, Buscot F. 2021 Targeting the active rhizosphere microbiome of *Trifolium pratense* in grassland evidences a stronger-than-expected belowground biodiversity-ecosystem functioning link. *Front. Microbiol.* **12**, 629169. (doi:10.3389/fmicb.2021.629169)
29. Song Z, Kennedy PG, Liew FJ, Schilling JS. 2017 Fungal endophytes as priority colonizers initiating wood decomposition. *Funct. Ecol.* **31**, 407–418. (doi:10.1111/1365-2435.12735)
30. Fischer M *et al.* 2010 Implementing large-scale and long-term functional biodiversity research: the biodiversity exploratories. *Basic Appl. Ecol.* **11**, 473–485. (doi:10.1016/j.baae.2010.07.009)
31. Kahl T, Bauhus J. 2014 An index of forest management intensity based on assessment of harvested tree volume, tree species composition and dead wood origin. *Nat. Conserv.* **7**, 15–27. (doi:10.3897/natureconservation.7.7281)
32. Muszynski S, Maurer F, Henjes S, Horn MA, Noll M. 2021 Fungal and bacterial diversity patterns of two diversity levels retrieved from a late decaying *Fagus sylvatica* under two temperature regimes. *Front. Microbiol.* **11**, 548793. (doi:10.3389/fmicb.2020.548793)
33. Dantur KI, Enrique R, Welin B, Castagnaro AP. 2015 Isolation of cellulolytic bacteria from the intestine of *Diatraea saccharalis* larvae and evaluation of their capacity to degrade sugarcane biomass. *AMB Express* **5**, 15. (doi:10.1186/s13568-015-0101-z)
34. Hryniewicz K, Baum C, Leinweber P. 2010 Density, metabolic activity, and identity of cultivable rhizosphere bacteria on *Salix viminalis* in disturbed arable and landfill soils. *J. Plant Nut. Soil Sci.* **173**, 747–756. (doi:10.1002/jpln.200900286)
35. Tláškal V, Baldrian P. 2021 Deadwood-inhabiting bacteria show adaptations to changing carbon and nitrogen availability during decomposition. *Front. Microbiol.* **12**, Article 685303. (doi:10.3389/fmicb.2021.685303)
36. Wilhelm RC, Singh R, Eltis LD, Mohn WW. 2019 Bacterial contributions to delignification and lignocellulose degradation in forest soils with metagenomic and quantitative stable isotope probing. *ISME J.* **13**, 413–429. (doi:10.1038/s41396-018-0279-6)
37. Xie C-H, Yokota A. 2006 *Sphingomonas azotifigens* sp. nov., a nitrogen-fixing bacterium isolated from the roots of *Oryza sativa*. *Int. J. Syst. Evol. Microbiol.* **56**, 889–893. (doi:10.1099/ijs.0.64056-0)
38. Kostka JE *et al.* 2012 Genome sequences for six *Rhodanobacter* strains, isolated from soils and the terrestrial subsurface, with variable denitrification capabilities. *J. Bacteriol.* **194**, 4461–4462. (doi:10.1128/JB.00871-12)
39. Mieszkin S, Richet P, Bach C, Lambrot C, Augusto L, Buée M, Uroz S. 2021 Oak decaying wood harbors taxonomically and functionally different bacterial communities in sapwood and heartwood. *Soil Biol. Biochem.* **155**, 108160. (doi:10.1016/j.soilbio.2021.108160)
40. Gohar D, Pent M, Pöldmaa K, Bahram M. 2020 Bacterial community dynamics across developmental stages of fungal fruiting bodies. *FEMS Microbiol. Ecol.* **96**, fiaa175. (doi:10.1093/femsec/fiaa175)
41. Jurkevitch E, Minz D, Ramati B, Barel G. 2000 Prey range characterization, ribotyping, and diversity of soil and rhizosphere *Bdellovibrio* spp. isolated on phytopathogenic bacteria. *Appl. Environ. Microbiol.* **66**, 2365–2371.
42. Saleem M, Fetzter I, Harms H, Chatzinotas A. 2013 Diversity of protists and bacteria determines predation performance and stability. *ISME J.* **7**, 1912–1921. (doi:10.1038/ismej.2013.95)
43. Lasota S, Stephan I, Horn MA, Otto W, Noll M. 2018 Copper in wood preservatives delayed wood decomposition and shifted soil fungal but not bacterial community composition. *Appl. Environ. Microbiol.* **85**, e02391-18. (doi:10.1128/AEM.02391-18)
44. Noll M, Buettner C, Lasota S. 2019 Copper containing wood preservatives shifted bacterial and fungal community compositions in pine sapwood in two field sites. *Int. Biodeterior. Biodegradation* **142**, 26–35. (doi:10.1016/j.ibiod.2019.04.007)
45. Varon M, Fine M, Stein A. 1984 The maintenance of *Bdellovibrio* at low prey density. *Microb. Ecol.* **10**, 95–98.
46. Varon M, Zeigler BP. 1978 Bacterial predator-prey interaction at low prey density. *Appl. Environ. Microbiol.* **36**, 11–17.
47. Blaser S, Prati D, Senn-Irlet B, Fischer M. 2013 Effects of forest management on the diversity of deadwood-inhabiting fungi in Central European forests. *Forest Ecol. Manag.* **304**, 42–48. (doi:10.1016/j.foreco.2013.04.043)
48. Bödeker ITM, Lindahl BD, Olson Å, Clemmensen KE. 2016 Mycorrhizal and saprotrophic fungal guilds compete for the same organic substrates but affect decomposition differently. *Funct. Ecol.* **30**, 1967–1978. (doi:10.1111/1365-2435.12677)
49. Krah F-S, Bässler C, Heibl C, Soghigian J, Schaefer H, Hibbett DS. 2018 Evolutionary dynamics of host specialization in wood-decay fungi. *BMC Evol. Biol.* **18**, 119. (doi:10.1186/s12862-018-1229-7)
50. Mäkipää R, Leppänen SM, Sanz Munoz S, Smolander A, Tirola M, Tuomivirta T, Fritze H. 2018 Methanotrophs are core members of the diazotroph community in decaying Norway spruce logs. *Soil Biol. Biochem.* **120**, 230–232. (doi:10.1016/j.soilbio.2018.02.012)
51. Yamamuro M, Kayanne H, Minagawao M. 1995 Carbon and nitrogen stable isotopes of primary producers in coral reef ecosystems. *Limnol. Oceanogr.* **40**, 617–621. (doi:10.4319/lo.1995.40.3.0617)
52. Hryniewicz K, Baum C, Niedojadło J, Dahm H. 2009 Promotion of mycorrhiza formation and growth of willows by the bacterial strain *Sphingomonas* sp. 23 L on fly ash. *Biol. Fertil. Soils* **45**, 385–394. (doi:10.1007/s00374-008-0346-7)
53. Akyol TY *et al.* 2019 Impact of introduction of arbuscular mycorrhizal fungi on the root microbial community in agricultural fields. *Microbes Environ.* **34**, 23–32. (doi:10.1264/jmsme2.ME18109)
54. Tláškal V, Zrustová P, Vrška T, Baldrian P. 2017 Bacteria associated with decomposing dead wood in a natural temperate forest. *FEMS Microbiol. Ecol.* **93**, fix157. (doi:10.1093/femsec/fix157)
55. Purahong W *et al.* 2022 Data from: cross-kingdom interactions and functional patterns of active microbiota matter in governing deadwood decay. Dryad Digital Repository. (doi:10.5061/dryad.g79cnp5rs)
56. Purahong W, Tanunchai B, Muszynski S, Maurer F, Mohamed Wahdan SF, Malter J, Buscot F, Noll M. 2022 Cross-kingdom interactions and functional patterns of active microbiota matter in governing deadwood decay. FigShare. (<https://doi.org/10.6084/m9.figshare.c.5958617>)

Deadwood 1 – Supplementary Information

Cross-kingdom interactions and functional patterns of active microbiota matter in governing deadwood decay.

Author: Witoon Purahong*, **Benjawan Tanunchai***, Sarah Muszynski*, Florian Maurer, Sara Fareed Mohamed Wahdan, Jonas Malter, François Buscot and Matthias Noll

*These authors contributed equally to this work.

Status: Published

Publication: Proceedings of the Royal Society B: Biological Sciences

Publisher: ROYAL SOCIETY

Date: 8 April 2022

Proceedings of the Royal Society B: Biological Sciences 289, 20220130.

© 2022 The Royal Society

Reprinted with permission from ROYAL SOCIETY.

Available online at: <https://doi.org/10.6084/m9.figshare.c.5958617.v2>

Or please see separate attachments



Fate of a biodegradable plastic in forest soil: Dominant tree species and forest types drive changes in microbial community assembly, influence the composition of plastisphere, and affect poly(butylene succinate-co-adipate) degradation

Benjawan Tanunchai^{a,b,c,1}, Li Ji^{a,d,1}, Olaf Schröder^b, Susanne Julia Gawol^b, Andreas Geissler^e, Sara Fareed Mohamed Wahdan^{a,f}, François Buscot^{a,g}, Stefan Kalkhof^{b,h}, Ernst-Detlef Schulzeⁱ, Matthias Noll^{b,c,*}, Witoon Purahong^{a,**}

^a UFZ-Helmholtz Centre for Environmental Research, Department of Soil Ecology, Theodor-Lieser-Str. 4, 06120 Halle (Saale), Germany

^b Institute of Bioanalysis, Coburg University of Applied Sciences and Arts, 96450 Coburg, Germany

^c Bayreuth Center of Ecology and Environmental Research (BayCEER), University of Bayreuth, 95440 Bayreuth, Germany

^d School of Forestry, Central South of Forestry and Technology, 410004 Changsha, PR China

^e Department of Macromolecular Chemistry and Paper Chemistry, Technical University of Darmstadt, Darmstadt D-64287, Germany

^f Department of Botany and Microbiology, Faculty of Science, Suez Canal University, 41522 Ismailia, Egypt

^g German Centre for Integrative Biodiversity Research (iDiv) Halle-Jena-Leipzig, Puschstraße 4, 04103 Leipzig, Germany

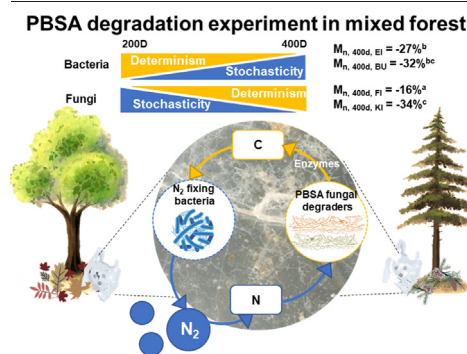
^h Department of Preclinical Development and Validation, Fraunhofer Institute for Cell Therapy and Immunology, 04103 Leipzig, Germany

ⁱ Max Planck Institute for Biogeochemistry, Biogeochemical Processes Department, Hans-Knöll-Str. 10, 07745 Jena, Germany

HIGHLIGHTS

- Dominate trees affected the degradation of PBSA film (16–34 % molar mass loss).
- Fungal PBSA decomposers and N₂-fixing bacteria were identified as keystone taxa.
- The microbial community was governed by both stochastic and deterministic processes.
- Forest types impact microbial richness, fungal community, but not microbial abundance.
- Relationship and uncoupling of microbial community structure–function was observed.

GRAPHICAL ABSTRACT



ARTICLE INFO

Editor: Manuel Esteban Lucas-Borja

Keywords:

Plastisphere microbiome
 Homogenizing dispersal
 Ecological drift
 Homogeneous selection

ABSTRACT

Poly(butylene succinate-co-adipate) (PBSA) degradation and its plastisphere microbiome in cropland soils have been studied; however, such knowledge is limited in the case of forest ecosystems. In this context, we investigated: i) the impact of forest types (conifer and broadleaved forests) on the plastisphere microbiome and its community assembly, ii) their link to PBSA degradation, and iii) the identities of potential microbial keystone taxa. We determined that forest type significantly affected microbial richness ($F = 5.26\text{--}9.88$, $P = 0.034$ to 0.006) and fungal community composition ($R^2 = 0.38$, $P = 0.001$) of the plastisphere microbiome, whereas its effects on microbial abundance and bacterial community composition were not significant. The bacterial community was governed by stochastic processes (mainly

* Correspondence to: M. Noll, Institute of Bioanalysis, Coburg University of Applied Sciences and Arts, 96450 Coburg, Germany.

** Corresponding author.

E-mail addresses: matthias.noll@hs-coburg.de (M. Noll), witoon.purahong@ufz.de (W. Purahong).

¹ These authors contribute equally.

<http://dx.doi.org/10.1016/j.scitotenv.2023.162230>

Received 26 October 2022; Received in revised form 6 February 2023; Accepted 9 February 2023

Available online 14 February 2023

0048-9697/© 2023 Elsevier B.V. All rights reserved.

Atmospheric dinitrogen fixing bacteria
Microbial keystone taxa

homogenizing dispersal), whereas the fungal community was driven by both stochastic and deterministic processes (drift and homogeneous selection). The highest molar mass loss was found for PBSA degraded under *Pinus sylvestris* (26.6 ± 2.6 to 33.9 ± 1.8 % (mean \pm SE) at 200 and 400 days, respectively), and the lowest molar mass loss was found under *Picea abies* (12.0 ± 1.6 to 16.0 ± 0.5 % (mean \pm SE) at 200 and 400 days, respectively). Important fungal PBSA decomposers (*Tetracladium*) and atmospheric dinitrogen (N₂)-fixing bacteria (symbiotic: *Allorhizobium-Neorhizobium-Pararhizobium-Rhizobium* and *Methylobacterium* and non-symbiotic: *Mycobacterium*) were identified as potential keystone taxa. The present study is among the first to determine the plastisphere microbiome and its community assembly processes associated with PBSA in forest ecosystems. We detected consistent biological patterns in the forest and cropland ecosystems, indicating a potential mechanistic interaction between N₂-fixing bacteria and *Tetracladium* during PBSA biodegradation.

1. Introduction

Plastic pollution is a major environmental concern because nano- and micro-plastics have been detected in every crevice on Earth (Jamieson et al., 2019; Napper et al., 2020). Such plastics have moved into all land cover types and ecosystems, ranging from the deepest reaches of the oceans (>7000 m) (Jamieson et al., 2019) to low- and high-land grassland, cropland, settlements, and forestland, even to the top of Mount Everest (height up to 8440 m) (Napper et al., 2020). Potentially, they can be horizontally transferred through food webs and vertically transferred from adult organisms and their offspring (D'Souza et al., 2020). Major plastic pollution is caused by non-biodegradable plastics (such as polyethylene, polypropylene, and polyvinyl chloride), which accumulate over time (Liu et al., 2014). For approximately half a century, biodegradable plastics have been developed and introduced into the market. Biodegradable plastics can be produced from both renewable (i.e., plant biomass) and nonrenewable (i.e., petroleum) resources (Emadian et al., 2017; Tanunchai et al., 2021). Poly(butylene succinate) (PBS) and its copolymer, poly(butylene succinate-co-adipate) (PBSA), are among the most promising aliphatic polyesters for degradation in natural environments and are commercially available (Gigli et al., 2012). PBS and its common copolymer PBSA can be produced from both non-renewable (e.g., fossil fuels) and renewable resources (e.g., plant biomass) (Jiang et al., 2015; Tanunchai et al., 2021; Xu and Guo, 2010). However, they tend to be produced from renewable resources owing to the awareness of global climate change. They have been proven to decompose in soils under both laboratory and natural field conditions (Huang et al., 2018; Puchalski et al., 2018; Purahong et al., 2021). Their wide range of applications, for example, in the packaging industry and agriculture as mulching films, can be attributed to their comparable mechanical properties to petroleum-based low-density polyethylene (LDPE) (Polymer properties database, 2021). Packaging and agricultural applications have been one of the major sources of plastic pollution to date (Liu et al., 2014). Plastic wastes can be transported by wind, water, and animals many kilometers away from different land uses and ecosystems, in terrestrial and aquatic environments. Bio-based and biodegradable plastics, which can be produced by means of plants and microbial fermentation, have received much attention as they offer opportunities for degradation in various environments with potentially lower adverse and/or ecotoxicological effects than conventional petroleum-based plastics (Haider et al., 2019). Nevertheless, some bio-based and biodegradable plastics may produce more microplastics, which are potentially more toxic to organisms and plants than petroleum-based plastics (Qi et al., 2018, 2020). Furthermore, diverse fungal plant pathogens have been reported to hitchhike, colonize, and/or metabolize bio-based and biodegradable plastics (Abe et al., 2010; Tanunchai et al., 2021). Although the bio-based and biodegradable plastic itself may not be harmful to plants and microorganisms, its residues can interact with other factors, such as nitrogen (N) fertilization, which can have negative effects on plant health and microbial diversity (Scheid et al., 2022; Tanunchai et al., 2021).

Cropland is considered to be a source and sink of plastic pollution after plastic mulching films are used to conserve water, increase water content, soil temperature, and nutrient-use efficiency, to finally enhance crop yield (Huang et al., 2020; Liu et al., 2014). However, nano-, micro-, and macro-

plastics from croplands can be transported to other terrestrial and aquatic ecosystems in the vicinity or even deeper soil horizons (Lwanga et al., 2022). Bio-based and biodegradable plastics have been identified as potential solutions to plastic pollution and have already been recommended by the Food and Agriculture Organization (FAO) instead of non-biodegradable petroleum-based plastics (FAO, 2021; Liu et al., 2022). Thus, bio-based and biodegradable plastics are expected to contribute substantially to plastic pollution in croplands and other terrestrial and aquatic ecosystems (Huang et al., 2020; Lwanga et al., 2022). Recently, the degradation rates of bio-based and biodegradable plastics, as well as their plastisphere microbiome in cropland ecosystems, have been studied in detail using high-resolution molecular biological approaches (Purahong et al., 2021). The results showed that fungi and bacteria contribute substantially to the degradation of bio-based and biodegradable plastics (Purahong et al., 2021; Tanunchai et al., 2021). Although fungi (commonly, Ascomycota, i.e., *Cladosporium* spp., *Tetracladium* spp., *Exophiala* spp., and *Fusarium* spp.) are considered the main plastic decomposers (Purahong et al., 2021; Tanunchai et al., 2021; Yamamoto-Tamura et al., 2020), bacteria also play very important roles as facilitators, especially in relation to the accumulation of N in bio-based- and biodegradable plastics, which results in an increase in fungal abundance (Tanunchai et al., 2022c). Specifically, *nifH* gene abundance, which encodes nitrogenase essential for atmospheric N₂-fixation, was found to be positively linked to fungal abundance. The accumulation of N in bio-based and biodegradable plastics by N₂-fixing bacteria is a critical step in determining the rate of plastic degradation (Tanunchai et al., 2022c). Some bacterial taxa capable of N₂-fixation, including Burkholderiaceae and *Devosia*, have been identified as potential keystone taxa that are important for potential microbial interactions in plastic co-occurrence networks (Ji et al., 2022; Purahong et al., 2021; Tanunchai et al., 2022c). In addition to its facilitating roles, a recent study detected plastic degradation genes within the bacterial genome of *Bradyrhizobium* sp. (Han et al., 2021). These results demonstrate that bacteria can degrade bio-based and biodegradable plastics, both directly and indirectly, as facilitators (Tanunchai et al., 2022c).

Various environmental factors, including soil type, temperature, and pH, influence the plastisphere microbiome of bio-based and biodegradable plastics that decompose in cropland soils (Han et al., 2021; Purahong et al., 2021; Tanunchai et al., 2021). Although the degradation processes of bio-based and biodegradable plastics, plastisphere microbiomes, and their regulating factors are relatively well known in cropland soils (Han et al., 2021; Purahong et al., 2021; Tanunchai et al., 2021), such knowledge in forest ecosystems is almost completely absent. The responses and resilience levels of forest ecosystems to bio-based and biodegradable plastics are also unexplored and cannot be estimated based on current literature (Purahong et al., 2021). Forest ecosystems have a lower organic C turnover (Herold et al., 2014), but a higher mass loss of complex C sources, such as deadwood, compared to grasslands of the same soil type (Kipping et al., 2022). Therefore, it is unclear whether the current knowledge from cropland ecosystems can be transferred to other ecosystems (Purahong et al., 2021; Tanunchai et al., 2022c).

Although the microbial co-occurrence network and community assembly processes of plastisphere microbiota in aquatic ecosystems have been extensively investigated (Bhagwat et al., 2021; Yang et al., 2020), such

knowledge in terrestrial ecosystems is largely absent (Ji et al., 2022). The microbial community and assembly processes of plastispheres may vary substantially in different environments and may have different impacts on environmental safety and sustainability (Agathokleous et al., 2021; Zang et al., 2020). Thus, investigating the potential microbial interactions and community assembly processes of the plastisphere microbiome is crucial for a deeper, mechanistic understanding of the degradation of bio-based and biodegradable plastics in soils and in evaluating their impact on the environment. Understanding community assembly is crucial for a deeper understanding of community ecology. Deterministic processes such as substrate competition are common within and between plastic-degrading fungi (Hiscox et al., 2018) and bacterial community members (Wilhelm et al., 2019), although the bacterial community structure is governed by the fungal community composition during plastic decay (Odriozola et al., 2021). Stochastic processes, such as microbial immigration and emigration (also termed dispersal) and random microbial proliferation and death (also termed drift), are addressed by neutral-based theory, which postulates that community structures are independent of species characteristics and assemble randomly (Zhou and Ning, 2017). Deterministic and stochastic processes can occur simultaneously during the assembly and maintenance of local communities (Chase and Myers, 2011). However, the contribution of deterministic and stochastic processes to plastic-decaying communities remains unclear. Stochastic processes, especially ecological drift, play a very important role in the assembly of the plastisphere microbiome in agricultural soils (Ji et al., 2022; Purahong et al., 2021). However, the assembly mechanisms of plastic-associated microbial communities in temperate forests have not yet been studied.

In forest ecosystems, forest types, as determined by different dominant tree species and tree species community composition, significantly affect the soil microbial community (Goldmann et al., 2015), which may potentially impact microbial community members capable of colonizing plastics. Slow degradation of coniferous litter and its accumulation on the forest floor also affect litter layer pH, soil water content, and other environmental parameters (Burgess-Conforti et al., 2019; Wang et al., 2016). Soil water content, pH, and nutrients are among the main drivers that determine microbial community composition in forest ecosystems (Kaiser et al., 2016), and they are known to affect the degradation of biodegradable plastics in cropland ecosystems (Hoshino et al., 2001). Although there is a high potential for forest types to substantially impact the plastisphere microbial community and degradation rate of biodegradable plastics, no experiment to date has addressed this issue. In general, ecosystem function is believed to be determined by the structure of the microbial community (structure–function relationship) (Purahong et al., 2014). However, owing to functional redundancy within the microbial community composition (different microbial taxa or microbial sub-communities are able to perform similar ecosystem functions), changes in the composition of the plastisphere microbiome arising from different forest types do not necessarily result in different rates of plastic degradation (Purahong et al., 2014). However, information on the plastisphere microbiome is required to evaluate the degree of functional redundancy (Purahong et al., 2021). The functional redundancy level is positively linked to ecosystem resilience, as redundant microbial taxa can work as “back-up” to buffer the changes in ecological conditions when ecosystems are under stress or faced with environmental changes (Biggs et al., 2020).

This study aimed to investigate (i) the impact of forest type (conifer- and broadleaf-dominated forests) on microbial richness, community assembly, and community composition; (ii) their link to the degradation of a bio-based and biodegradable plastic, poly(butylene succinate-co-adipate) (PBSA); and (iii) the potential microbial keystone taxa important for PBSA degradation. We hypothesized that forest type affects microbial attributes and community assembly, which in turn affects the degradation rate of PBSA. We expected more complex assembly processes, including stochastic and deterministic processes, to control the assembly of the plastisphere microbiome in these forest ecosystems, which differ from processes in cropland ecosystems (where mainly stochastic processes are found). We also expected that N_2 -fixing bacteria would be potential

microbial keystone taxa for PBSA degradation in forest ecosystems, and *nifH* gene abundance would be positively correlated with fungal abundance.

2. Material and methods

2.1. Study site, experimental setup, designs and environmental parameters

The study site is located in a managed mixed forest in Thuringia, Germany (51°12'N 10°18'E) and is characterized by mean annual precipitations of 600 to 800 mm, mean annual temperatures of 6 to 7.5 °C, and elevations of 100 to 494 m above sea level. The main soil type is Cambisol on limestone as bed-rock. The soil pH is weakly acidic (5.1 ± 1.1 ; mean \pm SD). PBSA films (BioPBS FD92) as a double-layer thin film (21 cm \times 30 cm) with 50 μ m thickness and 35 % bio-based carbon (from corn) were provided from PTT MCC Biochem Company Limited, Thailand. In November 2019, PBSA film were placed on top of the litter layer under the canopy of five individual trees (five independent biological replicates) in a forest dominated by beech (*Fagus sylvatica*, BU), by oak (*Quercus robur*, EI), by spruce (*Picea abies*, FI) or by pine (*Pinus sylvestris*, KI). After 200 and 400 days of PBSA incubation in each forest site, PBSA films and soil samples were collected from under the PBSA films in a separate sterile plastic bag and with new gloves. PBSA films and soil samples were transported on ice to the laboratory within 3 h and stored at -80 °C for further analysis. Soil pH and soil water content were investigated along with microbial diversity and community composition and was used as an explanatory variable for microbial responses. More details on study site, experimental setup, designs and environmental parameters are provided in Supplementary Information.

2.2. Measurement of PBSA degradation

The procedure for sample preparation for molar mass loss measurements has been published elsewhere (Purahong et al., 2021). Briefly, PBSA films were cleaned of attached debris by vortexing for 5 min in sterile phosphate-buffered saline (0.01 M) and subsequently by rinsing three times with sterile Tween®20 (0.1 % vol/vol). Thereafter, PBSA films were washed seven times using sterile water to remove all chemical residues. Molar mass was then determined by gel permeation chromatography (GPC) (SECcurity, GPCSystem PSS 1260 Infinity, Agilent Technologies) as described previously (Valainis et al., 2019). To determine specific gravimetric weight of PBSA, each PBSA film was cut into 12.5 cm². The cleaned PBSA films were oven-dried at 60 °C for 72 h or until constant weight. The specific gravimetric mass loss of each PBSA film was determined using a five-digit balance (Mewes Wägetechnik, Haldensleben, Germany).

2.3. Investigation of PBSA films by scanning electron microscopy

The procedure for sample preparation for scanning electron microscopy (SEM) has been published elsewhere (Purahong et al., 2021). Briefly, A subset of PBSA films of each forest were subjected to SEM. The samples were cleaned with the same procedure as described above and lyophilized (Lee and Chow, 2012). The PBSA films were placed on C conductive tapes and coated by sputtering with a 10 nm platinum/palladium 80/20 (w/w) alloy. A sputter coater “208 HR” with the associated thickness gauge “mtm 20” from Cressington (Cressington Scientific Instruments Ltd., Watford, England) was used. SEM images were acquired using a Philips XL30 FEG device (Philips, Amsterdam, NL) at an acceleration voltage of 5 kV.

2.4. Characterization of the plastisphere

The procedure for plastisphere analysis using Illumina Sequencing has been published elsewhere (Purahong et al., 2021; Tanunchai et al., 2021). Briefly, we randomly cut 12.5 cm² from the PBSA film and cleaned the surface as described above. Microbial biomass attached firmly to the PBSA film was subjected to DNA extraction using the DNeasy PowerSoil Kit (Qiagen,

Hilden, Germany) according to manufacturer's instructions. The 16S rRNA gene V4 region and fungal internal transcribed spacer 2 (ITS2) gene was amplified from the nucleic acid extracts using the bacteria primer pair 515F (5'-GTGCCAGCMGCCGCGGTAA-3') and 806R (5'-GGAC TACHVGGTWTCTAAT-3') (Caporaso et al., 2011) or the fungal universal primer pair fITS7 (5'-GTGARTCATCGAATCTTTG-3') (Ihmark et al., 2012) and ITS4 (5'-TCCTCCGCTATTGATATGC-3') (White et al., 1990), both with Illumina adapter sequences. Amplifications were performed in 20 μ L reactions with 5 \times HOT FIRE Pol Blend Master Mix (Solis BioDyne, Tartu, Estonia). Paired-end sequencing of 2 \times 300 nucleotides of this pool (three technical replicates) was performed using a MiSeq Reagent kit v3 on an Illumina MiSeq system (Illumina Inc., San Diego, CA, United States) at the Department of Soil Ecology, Helmholtz Centre for Environmental Research. The 16S and ITS rRNA gene sequences were then processed for bioinformatics. More details on bioinformatics are provided in Supplementary Information. Rare ASVs (singletons or sequences that was observed in only one sample), which potentially represent artificial sequences, were removed. The read counts were rarefied to 41,246 and 71,330 reads for bacteria and fungi, respectively. Finally, we obtained 9681 and 2683 rarefied bacterial and fungal ASVs, respectively. Rarefaction curves obtained from the reads of each PBSA film indicated a sufficient sampling effort (Fig. S1). Thus, we used the observed richness as a measure of microbial diversity associated with PBSA degradation. Ecological functions of fungi were determined for each ASV using FungalTraits (Pöhlme et al., 2020; Tanunchai et al., 2022a). The same nucleic acid extracts were used for quantitative PCR by using the same ITS primer set as mentioned above, the bacterial 16S rRNA gene based primer pair BAC341f (5'-CCTACGGG NGGCWGCAG-3') and BAC785R (5'-GACTACHVGGGTATCTAAKCC-3') (Klindworth et al., 2013), and the *nifH* gene based primer pair *PoIf* (5'-TGCGAYCCSAARGCBGACTC-3') and *PoIR* (5'-ATSGCCATCAT YTCRCGGA-3') (Poly et al., 2001). More details on characterization of the plastisphere are provided in Supplementary Information.

Furthermore, we preliminarily investigated the selectivity of the plastisphere microbiome by comparing the plastisphere microbiomes with those of leaf litter at 200 and 400 days of decomposition. Method details for investigation of the selectivity of the plastisphere microbiome as well as physicochemical analyses of litter layer are provided in Supplementary Information.

2.5. Network analysis

The bacterial and fungal network analysis was constructed based on Random Matrix Theory using the molecular ecological network analysis pipeline (<http://ieg4.rccc.ou.edu/mena/>, Deng et al., 2012). Spearman's rank correlation coefficients were analyzed for any pair of ASVs based on the sequencing reads. Network analysis may not provide a direct way to quantify biotic interactions or discern the interactions (competition and facilitation), which depend on the microbial member or environmentally-induced variations. Nonetheless, we focused more on the relative changes in microbial interactions among the tree types (or decayed phases). For detailed information regarding theories, algorithms, and procedures, please refer to (Deng et al., 2012) and (Zhou et al., 2011). All networks were visualized using Gephi version 0.9.2. (Bastian et al., 2009). Method details for network analysis are provided in Supplementary Information.

2.6. Community assembly analysis

To quantify the relative proportion of deterministic and stochastic processes in community assembly, the phylogenetic normalized stochasticity ratio (pNST) and beta nearest taxon indices (β NTI) based on the null model theory were calculated using 'iCAMP' package in R (Ning et al., 2020; Stegen et al., 2013). To construct a phylogenetic tree, the alignment was filtered to remove common gaps using PASTA (<https://github.com/smirarab/pasta>; Mirarab et al., 2015) and a phylogenetic tree was constructed de novo using Molecular Evolutionary Genetics Analysis software (MEGA, version 7.0) with the "maximum-likelihood" approach to support

phylogenetic tree inference (Hall, 2013). In addition to β NTI, the Raup-Crick (RC_{bray}) null model based on Bray-Curtis dissimilarity was also calculated to quantify the dispersal-based stochastic ecological processes generating the turnover of community composition (Stegen et al., 2015). Briefly, for pNST index, deterministic and stochastic assemblies were determined when pNST < 50 % and pNST > 50 %, respectively. For β NTI, homogeneous and variable selections were indicated by β NTI < -2 and β NTI > +2, respectively. The relative importance of dispersal limitation and homogenizing dispersal processes was assessed using $|\beta$ NTI| < 2, but RC_{bray} > +0.95 and RC_{bray} < -0.95, respectively, and the undominated process was estimated using $|\beta$ NTI| < 2 and $|RC_{bray}| < 0.95$ (Stegen et al., 2015). We verified the phylogenetic conservatism of the communities in each dataset by testing the correlation coefficient between ASV phylogenetic distances and ASV niche distances. Mantel correlogram analyses revealed a significant positive phylogenetic signal across short phylogenetic distances for both bacterial and fungal communities in all plastic samples (Mantel correlograms, 999 randomizations, using "microeco" package) (Liu et al., 2021) (Fig. S2). To date, there is still no certain threshold for the minimum replicates needed to detect robust correlations and construct stable networks, or for community assembly analysis. Smaller sample sizes presumably negatively affect the validation and robustness of the results. However, when the focus of the studies is placed on a small niche at the local scale, such results can still be relevant and provide useful information on the potential interactions of microbes and their community assembly (Ju et al., 2021; Sansupa et al., 2022; Tanunchai et al., 2022b; Wahdan et al., 2022). Nevertheless, these results should be carefully interpreted. Details about community assembly analyses and statistics are provided in Supplementary Information.

3. Results

3.1. Overview of the of plastisphere microbiome in forest ecosystems

PBSA was colonized by diverse microbial communities, including 9681 bacterial and 2683 fungal ASVs, which were classified into 465 and 407 bacterial and fungal genera, respectively (Figs. 1 and 2; Tables S1 and S2). The numbers of bacterial and fungal ASVs detected in all tree species at 200 and 400 days are presented in Fig. S3. Gammaproteobacteria (represented by *Rhizobacter* spp., *Variovorax* spp., *Massilia* spp., and *Pseudomonas* spp.), Alphaproteobacteria (represented by *Sphingomonas* spp., *Bradyrhizobium* spp., *Brevundimonas* spp., *Methylobacterium-Methylorubrum* spp., and *Allorhizobium-Neorhizobium-Pararhizobium-Rhizobium* spp., ANPR), Actinobacteria (represented by *Pseudonocardia* spp., *Nakamurella* spp., *Pseudonocardia* spp., and *Mycobacterium* spp.), and Bacteroidia (represented by *Pedobacter* spp., *Ferruginibacter* spp., and *Hymenobacter* spp.) formed the backbone of the bacterial PBSA microbiome across different forest types and incubation times with a cumulative relative abundance of over 84 % (Figs. 1, S4, and S5). Interestingly, members of *Polyangia* were also frequently detected on PBSA incubated in coniferous forests, but they were almost absent in broadleaved forests. Many bacterial genera that degrade PBS-based plastics (i.e., *Amycolatopsis*, *Acidovorax*, *Burkholderia*, *Streptomyces*, *Paenibacillus*, and *Roseateles* (Ahmad et al., 2019; Emadian et al., 2017; Uchida et al., 2000)) were detected in our study. Among these bacterial genera, *Roseateles* ASV 157 (closest hit, 100 % to *Roseateles depolymerans*) and *Burkholderia-Caballeronia-Paraburkholderia* ASV107 were frequently detected (Fig. S5). Interestingly, different N_2 -fixing bacterial genera, including ANPR, *Bradyrhizobium*, *Mycobacterium*, *Methylobacterium*, *Rhodopseudomonas*, and *Sphingomonas* were among the frequently detected bacterial genera in this study.

For the fungal microbiome, members of the Ascomycota classes, Dothideomycetes (represented by *Venturia* spp., *Cladosporium* spp., *Phoma* spp., *Plenodomus* spp., *Chaetosphaeronema* spp., and *Paraphoma* spp.), Leotiomycetes (represented by *Tetracladium* spp., *Mollisia* spp., *Xenopolyscytium* spp., and *Collophora* spp.) and Eurotiomycetes (represented by *Cyphellophora* spp., *Knufia* spp., *Exophiala* spp., and *Cladophialophora* spp.) built the backbone across different forest types and incubation times

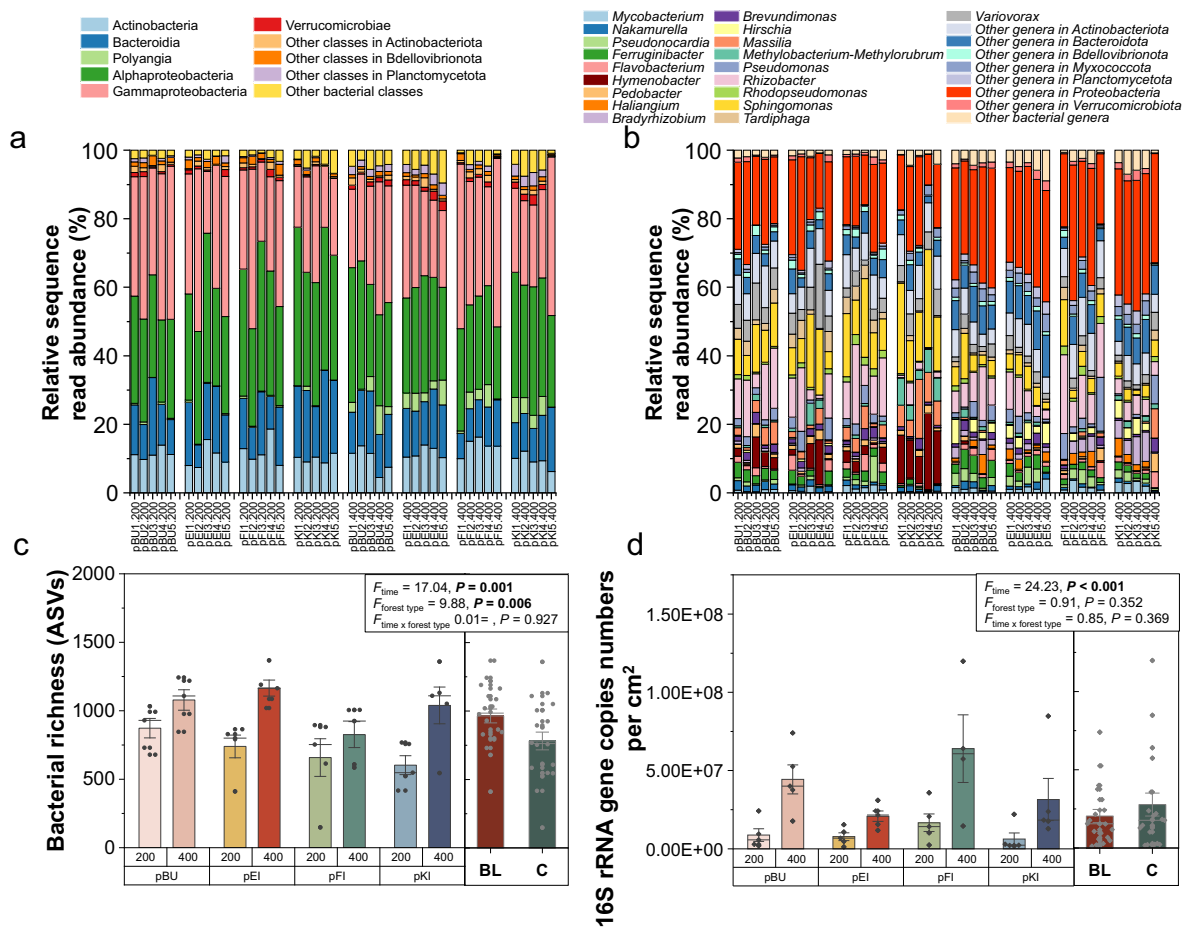


Fig. 1. Composition of the bacterial communities, richness, and gene copy numbers. Composition of the bacterial communities [class-level (a) and genus-level (b), considering only classes or genera with sequence read relative abundances $\geq 1\%$; the rest of the bacterial classes and genera were pooled as “others”] associated with the degradation of bio-based and biodegradable poly(butylene succinate-co-adipate) (PBSA), based on relative sequence read abundance. A bar chart with a standard error and median line displays the variation in bacterial richness (amplicon sequence variants; ASVs, c) and 16S rRNA gene-based copy numbers per cm^2 (d) in PBSA samples under different tree species at the sampling times (200 and 400 days). Data are presented for PBSA samples under *Fagus sylvatica* (pBU), *Quercus robur* (pEI), *Picea abies* (pFI), *Pinus sylvestris* (pKI), all-broadleaved (BL), and all-coniferous tree species (C); rose-red tones and blue tones represent broadleaved and coniferous tree species, respectively. (For interpretation of the references to colour in this figure legend, the reader is referred to the web version of this article.)

with a cumulative relative abundance of over 75 % (Figs. 2, S6, and S7). Interestingly, members of Basidiomycota, including Tremellomycetes (represented by *Vishniacozyma* spp.) and Microbotryomycetes (represented by *Fellozyma* spp.), were frequently detected (relative abundances 4.2–7.8 %) in both broadleaved and coniferous forests at 200 days, and they disappeared almost completely after 400 days of exposure. At 400 days, Sordariomycetes (represented by *Fusidium* spp.) were frequently detected in broadleaved forests, whereas Orbiliomycetes (represented by *Dactylellina* spp.) were frequently detected in coniferous forests.

3.2. Impact of forest types on microbial richness, abundance, and community composition of plastsphere microbiome

The forest type significantly affected the microbial richness ($F = 5.26\text{--}9.88, P = 0.034\text{ to }0.006$) and fungal community composition ($R^2 = 0.38, P = 0.001$) of plastsphere microbiome, whereas its effects on microbial sequence read abundances and bacterial community composition were similar ($P > 0.05$) (Tables S3 and S4). Specifically, PBSA incubated in coniferous forests harbored significantly lower bacterial and fungal richness than broadleaved forests. Incubation time also significantly affected both bacterial and fungal richness. Bacterial richness significantly decreased at day 200, whereas fungal richness significantly decreased at day 400 (Figs. 1c and 2c). Tree species also significantly affected the richness of the PBSA microbiome, as PBSA incubated under *P. abies* harbored

significantly less bacterial and fungal richness than PBSA incubated under broadleaved tree species. Fungal community compositions on PBSA and their dynamics at 200 and 400 days of exposure differed significantly across the different forest types (Fig. 3). Specifically, the PBSA microbiome at 200 days in broadleaved forests was dominated by *Tetracladium* spp., *Mollisia* spp., and *Cladosporium* spp., whereas in coniferous forests, the PBSA microbiome was dominated by *Venturia* spp., *Phoma* spp., *Vishniacozyma* spp., and *Cladosporium* spp. (Figs. 2, S6, and S7). At 400 days, *Tetracladium* spp. and *Cyphellophora* spp. *Exophiala* spp. and *Plenodomus* spp. were the dominant taxa in both forest types; however, in coniferous forests, they were co-dominated by *Kruefia* spp., *Venturia* spp., *Cladophialophora* spp., *Paraphoma* spp. (mainly detected under *P. sylvestris*), and *Dactylellina* spp. (mainly detected under *P. abies*). Bacterial and fungal gene copy number significantly increased with incubation time, regardless of the land cover type and tree species (Figs. 1d and 2d).

3.3. Factors determining the microbial community composition of the plastsphere

In addition to sampling times (decomposition times, $R^2 = 0.62\text{--}0.88, P < 0.001$), plot factors (including soil water content, pH, and coordinates) and the physicochemical properties of the litter layer (including leaf water content, pH, and nutrients) also significantly affected the microbial community composition in both forest types (Table 1). In broadleaved tree species, the plastsphere microbiome was also significantly correlated to soil and

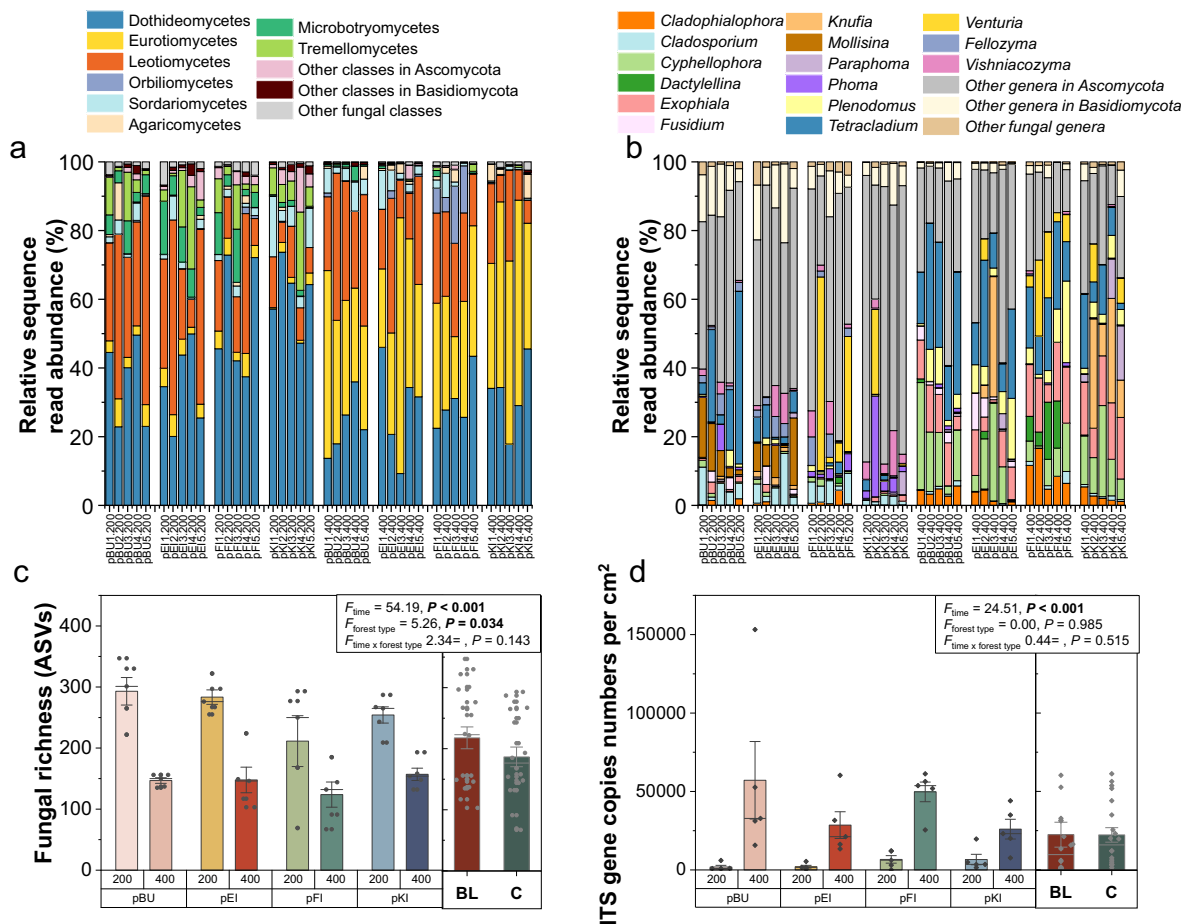


Fig. 2. Composition of the fungal communities, richness, and gene copy numbers. Composition of the fungal communities [class-level (a) and genus-level (b), considering only classes and genera with relative sequence read abundances $\geq 1\%$; the rest of the fungal classes and genera were pooled as “others”] associated with the degradation of bio-based and biodegradable poly(butylene succinate-co-adipate) (PBSA), based on relative sequence read abundance. A bar chart with a standard error and median line displays the variation in fungal richness (amplicon sequence variants; ASVs, c) and ITS based gene copy numbers per cm^2 (d) in PBSA samples under different tree species at the sampling times (200 and 400 days). Data are presented for PBSA samples under *Fagus sylvatica* (pBU), *Quercus robur* (pEI), *Picea abies* (pFI), *Pinus sylvestris* (pKI), all-broadleaved (BL), and all-coniferous tree species (C); rose-red tones and blue tones represent broadleaved and coniferous tree species, respectively. (For interpretation of the references to colour in this figure legend, the reader is referred to the web version of this article.)

leaf water content, leaf pH, N: P ratio, Fe and Mg content ($R^2 = 0.34\text{--}0.79$, $P < 0.05\text{--}0.001$, Table 1). P content was also correlated with the fungal community of the plastisphere under broadleaved tree species ($R^2 = 0.33$, $P < 0.05$, Table 1). The plastisphere microbiome under coniferous tree species ($R^2 = 0.30\text{--}0.33$, $P < 0.01\text{--}0.001$, Table 1) significantly corresponded to tree species along the sampling times. Plot factors (including soil water content, pH, and coordinates) and physicochemical properties of the litter layer (including leaf water content, pH, and most nutrient contents, except Fe and P contents) also significantly shaped the bacterial and/or fungal community composition of the plastisphere under coniferous tree species ($R^2 = 0.34\text{--}0.88$, $P < 0.05\text{--}0.001$, Table 1).

3.4. Impact of forest type on community assembly of the plastisphere

Based on the null model, the relative importance of ecological processes in the microbial community assembly was calculated (Table S5). The pNST values of the bacterial communities in both broadleaved and coniferous forests at 200 days were lower than those at 400 days (Fig. 4, $P < 0.05$). For fungi, there was a higher pNST value at day 200 for both forest types (Fig. 4, $P < 0.05$). The plastic-associated bacterial and fungal communities at 200 days in all samples were governed by stochastic processes, but the fungal community inhabiting plastic at 400 days was predominantly mediated by both stochastic and deterministic processes (Figs. 4b and 4e). More importantly, the community assembly of the plastic-associated bacterial

community was mainly controlled by homogenizing dispersal processes, whereas the fungal community was governed by drift and homogeneous selection at 200 and 400 days, respectively (Figs. 4e and 4f). At 200 and 400 days, the proportions of homogenizing dispersal of the bacterial community in broadleaved trees (91.1 % and 73.3 %) were higher than those in coniferous trees (89.3 % and 60.0 %). At 400 days, fungal community exhibited a higher percentage of homogeneous selection in broadleaved forests (57.8 %) than in coniferous forests (28.9 %), but a lower proportion of drift (broadleaf forest = 9.4 % and coniferous forest = 39.5 %). These results clearly demonstrate the impact of forest type on the community assembly of plastispheres.

3.5. Microbial co-occurrence network and the potential keystone taxa for PBSA degradation

Modular networks of bacteria and fungi varied between forest types and incubation times (Fig. 5). The divergent network topology showed a shift between the broadleaved and coniferous forests (Fig. 5). Compared to the broadleaved forest, the plastic-associated bacteria in the coniferous forest had fewer nodes, a higher average degree, and a shorter average path distance, which suggests more complex and closer relationships (Table S6). The higher average clustering coefficient and lower percentage of negative links indicated that the bacterial network in coniferous forests was more connected, as well as less competitive than in broadleaved forests

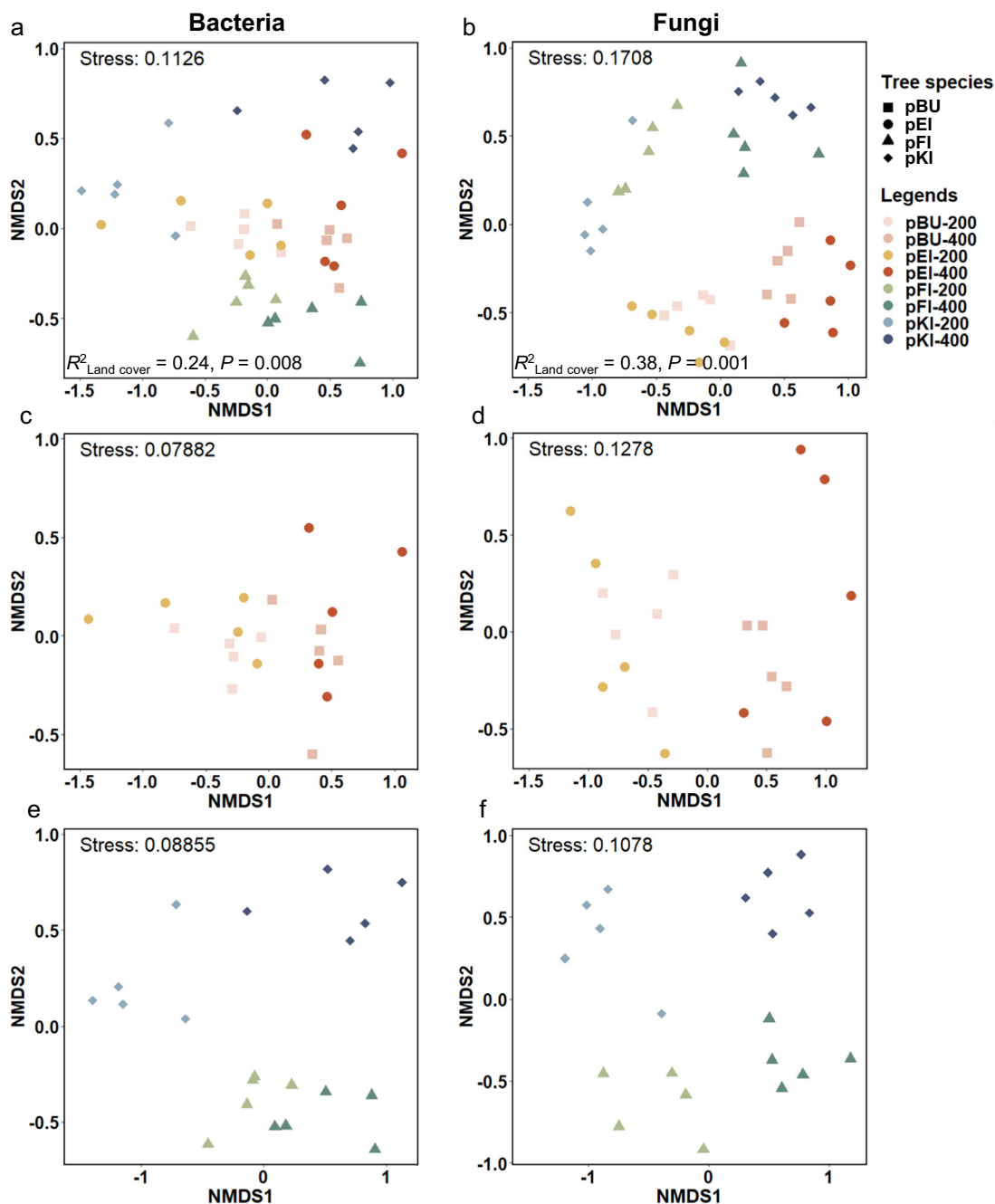


Fig. 3. Non-metric multidimensional scaling (NMDS) ordinations of bacterial (left panel) and fungal community composition (right panel) in poly(butylene succinate-co-adipate) (PBSA) under all tree species (a–b), broadleaved (c–d), and coniferous tree species (e–f), based on relative sequence abundance data and Bray–Curtis distance measures. Rose-red tones: broadleaved trees; blue tones: coniferous trees. Data are presented for PBSA samples under *Fagus sylvatica* (pBU), *Quercus robur* (pEI), *Picea abies* (pFI), *Pinus sylvestris* (pKI). (For interpretation of the references to colour in this figure legend, the reader is referred to the web version of this article.)

(Table S6). Interestingly, the potential interaction patterns of bacterial community members in coniferous forests showed a dramatic decrease at 400 days, compared to 200 days, of exposure (Fig. 5a). Notably, in contrast to bacteria, the complexity of the fungal network exhibited a striking increase at 400 days compared to that at 200 days of exposure (Fig. 5b and Table S6). The total links and proportion of mutual exclusions (negative links) in both forest types were higher at 400 days than at 200 days, indicating that potentially more competition occurred in the forests at a later stage of plastic decomposition (Table S6).

Based on the co-occurrence networks, potential keystone taxa were identified as module hubs and connectors (Fig. 6). We found that important fungal PBSA decomposers (*Tetracladium* spp.) as well as N_2 -fixing bacteria (symbiotic N_2 -fixing bacteria: ANPR and *Methylobacterium* and non-

symbiotic N_2 -fixing aerobic bacteria: *Mycobacterium*) were identified as potential keystone taxa. Among the N_2 -fixing bacteria, *Methylobacterium* spp. were consistently detected as potential keystone taxa in most of the co-occurrence networks, regardless of forest type and incubation time (except for 400 days in coniferous forest).

3.6. Links of microbial attributes and forest types to PBSA degradation

We determined the link between microbial attributes (*nifH* and fungal gene copy numbers) and PBSA degradation in different forest types. Scanning electron microscopy images showed that fungal hyphae were omnipresent, indicating that fungi were the main decomposers of PBSA at both 200 and 400 days in both forest types (Fig. 7). At 400 days, we observed

Table 1
Goodness-of-fit statistics (R^2) of environmental variables fitted to the nonmetric multidimensional scaling (NMDS) ordination of bacterial and fungal community based on relative abundance data and Bray–Curtis distance measure. Bold letter indicates statistical significances with the $R^2 \geq 0.70$.

Factors	Broadleaved tree		Coniferous tree	
	Bac	Fun	Bac	Fun
Tree factors				
Tree species	0.03	0.01	0.30**	0.33***
Sampling times	0.64***	0.85***	0.62***	0.88***
Plot factors				
Soil water content	0.55***	0.46**	0.18	0.42**
Soil pH	0.16	0.14	0.82***	0.74***
Latitude	0.11	0.00	0.88***	0.86***
Longitude	0.08	0.15	0.88***	0.86***
Factors from litter layer				
Leaf water content	0.68***	0.62***	0.67**	0.75***
Leaf pH	0.64***	0.79***	0.26	0.56***
C	0.20	0.31	0.53**	0.55**
N	0.06	0.02	0.63***	0.71***
C: N ratio	0.07	0.08	0.54**	0.68***
C: P ratio	0.27	0.26	0.15	0.34*
N: P ratio	0.34*	0.47**	0.44	0.64**
Ca	0.06	0.05	0.51**	0.50**
Fe	0.38*	0.55***	0.17	0.18
K	0.12	0.18	0.63***	0.49**
Mg	0.50***	0.42**	0.53***	0.44**
P	0.25	0.33*	0.15	0.29

* $P < 0.05$.
** $P < 0.01$.
*** $P < 0.001$.

that localized bio-corrosion/degradation often originated in the immediate proximity of hyphae. We detected bacterial, *nifH*, and fungal gene copy numbers in PBSA films from different tree species (Figs. 1d, 2d, and 8a).

The microbial gene copy numbers were significantly higher after 400 days of exposure than after 200 days of exposure (Figs. 1d, 2d, 8a, and Table S3). No effects of tree species or tree type on the microbial gene copy number were detected (Figs. 1d, 2d, 8a, and Table S3). The *nifH* gene copy numbers were strongly positively correlated with the fungal gene copy numbers in both forest types ($\rho = 0.86\text{--}0.87$, $P < 0.001$) (Fig. 8b and 8c).

The molar mass loss of PBSA in the forest ecosystem followed an exponential degradation curve (Fig. 9). The molar mass loss of PBSA degraded under *P. abies* was significantly lower (12.0 ± 1.6 to $16.0 \pm 0.5\%$ (mean \pm SE) at 200 and 400 days) compared to those under *P. sylvestris* and broadleaved tree species (Fig. 9). The highest molar mass loss was found for PBSA degraded under *P. sylvestris* (26.6 ± 2.6 to $33.9 \pm 1.8\%$ (mean \pm SE) at 200 and 400 days, respectively). The specific mass loss values ranged from 9.9 ± 8.9 to $19.3 \pm 6.7\%$ (mean \pm SE) and 19.7 ± 6.3 to $30.0 \pm 9.3\%$ (mean \pm SE) at 200 and 400 days (Fig. S8), respectively.

4. Discussion

4.1. Bio-based and biodegradable PBSA selects the microbiome across forest types and land uses: “We belong together”

Our results showed that fungal community members were the primary PBSA decomposers in these two forest ecosystems, whereas bacteria could directly and indirectly (facilitators) decompose PBSA, which is consistent with other PBSA experiments in different land-uses and locations (Abe et al., 2010; Purahong et al., 2021; Yamamoto-Tamura et al., 2020). We observed localized biocorrosion/degradation on the PBSA film surface in the immediate proximity of hyphae (Fig. 7), which suggests the action of extracellular enzymes released from fungal hyphae (Purahong et al., 2021). Some dominant PBSA bacteria (*Burkholderia* (Emadian et al., 2017) and *Roseateles* (Ahmad et al., 2019)) and fungi (i.e., *Tetracladium* spp.

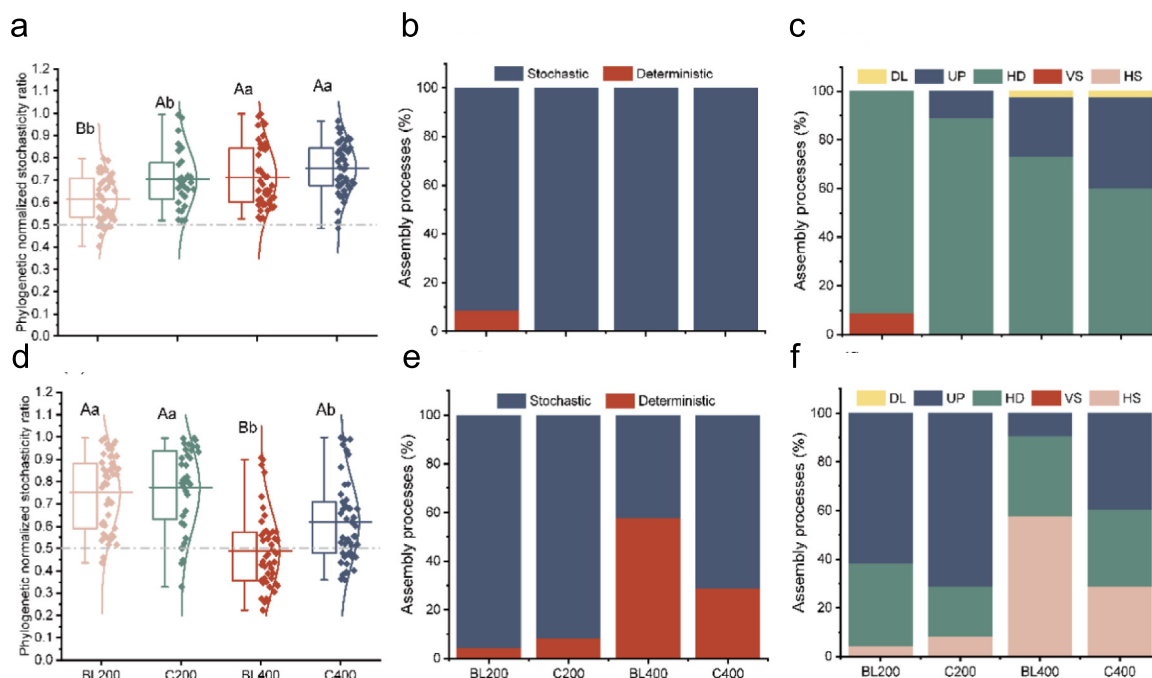


Fig. 4. The ecological stochasticity and relative contributions (%) of community assembly processes, based on the phylogenetic normalized stochasticity ratio (pNST). The ecological stochasticity in the poly(butylene succinate-co-adipate) (PBSA)-associated bacterial (a–c) and fungal (d–f) community assembly estimated using pNST. The value of 0.5 was the boundary point between more deterministic (< 0.5) and more stochastic (> 0.5) assemblies. Data with different uppercase letters are significantly different at the 5% level between the tree types at the same decay stage ($P < 0.05$), while different lowercase letters are significantly different at different decay stages (200 days vs. 400 days) in the same tree type ($P < 0.05$) (a, d). Relative contributions (%) of the community assembly processes, based on the pNST, in shaping PBSA-associated bacterial (b, c) and fungal (e, f) communities. Data are presented for PBSA under broadleaved (BL) and coniferous tree species (C) at two sampling time points (200 and 400 days). HS, homogeneous selection; VS, variable selection; HD, homogenizing dispersal; UP, undominated process; DL, dispersal limitation, defined by Ning et al. (2020), Stegen et al. (2015).

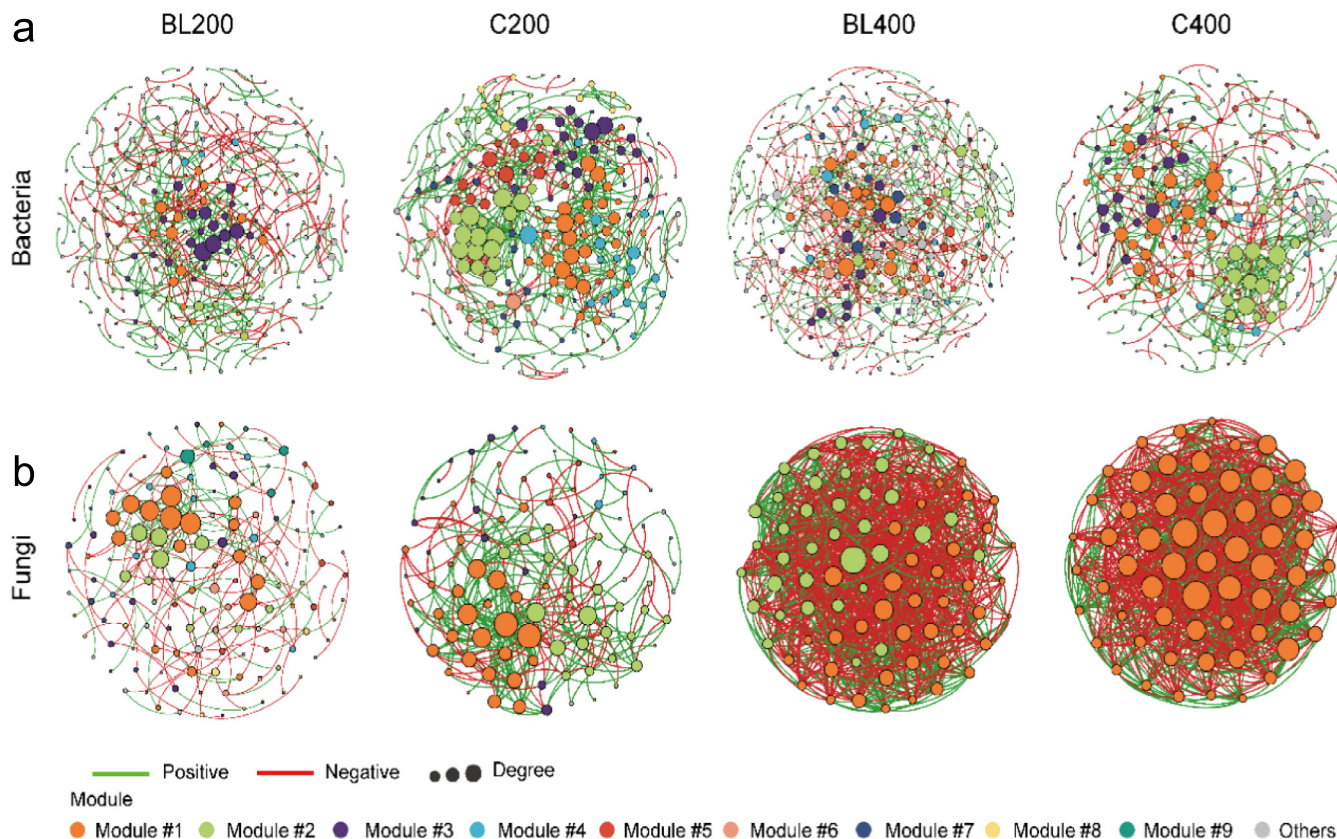


Fig. 5. Comparison of modular networks of bacteria (a) and fungi (b) between tree types and two sampling time points (200 and 400 days). Node colors represent different modules. Connections denote strong (Spearman's $\rho > 0.6$) and significant ($P < 0.01$) correlations.

(Carrasco et al., 2017, 2019; Purahong et al., 2021), *Cladosporium* spp. (Emadian et al., 2017; Purahong et al., 2021), and *Exophiala* spp. (Tanunchai et al., 2021)) decomposers/colonizers have been detected across different forest types, regardless of the dominant tree species. However, we also found that some known PBSA colonizers/decomposers are often detected in certain tree species (i.e., *Paraphoma* spp. and *Dactylellina* spp.) (Sato et al., 2017; Tanunchai et al., 2021). *Tetracladium* spp., *Cladosporium* spp., *Exophiala* spp., and *Dactylellina* spp. have been reported as the dominant PBSA colonizers in croplands (conventional farming of winter wheat, barley, and rapeseed) located >100 km away (Purahong et al., 2021). Besides the role in PBSA decomposition, some of dominant genera such as *Cladosporium* and *Exophiala* can also act as plant pathogen for economic-important fruit (Juncheed et al., 2022; Nam et al., 2015) and opportunistic pathogen (Song et al., 2017; Tanunchai et al., 2021), respectively. Indeed, diverse fungal plant pathogens are detected in PBSA in forest ecosystems (Table S7 and Supplementary Information). *Amycolatopsis*, *Burkholderia*, *Streptomyces*, *Paenibacillus*, and *Roseateles* have also been detected in PBSA incubated in cropland fields (Purahong et al., 2021). There are strong differences in soil characteristics, such as soil type, soil physicochemical properties, soil management, soil microbial communities, and dominant plant species among cropland, broadleaved forests, and coniferous forests (Purahong et al., 2021; Tanunchai et al., 2022a). These fungi and bacteria were relatively rare or very rare in the soil or litter layers of cropland and the two forest ecosystems, but they were enriched in PBSA films (Purahong et al., 2021; Tanunchai et al., 2022a). When plastics decompose in forest ecosystems, they decompose in the respective litter layer. Thus, we preliminarily investigated the selectivity of the plastisphere microbiome by comparing the microbial ASVs detected in PBSA with those in leaves and needles decomposed in the vicinity of PBSA in the same plot (Table S8, S9, and Supplementary Information). We found that the majority of microbial ASVs detected in the PBSA plastisphere were absent from decomposing leaves and needles, indicating

the specificity of the plastisphere microbiome (Supplementary Information). The selective influence of the plastic may due to the fact that many taxa will simply not be able to colonize and utilize the plastic substrate (Tanunchai et al., 2021). Nevertheless, further studies are needed to understand the selectivity of environmental factors and the composition of nearby microbial diversities that facilitate colonization and establishment of the plastisphere microbiome.

4.2. Potentially novel PBSA decomposers detected in forest ecosystems

This study is the first to investigate the effects of forest type on bio-based and biodegradable plastispheres using a high-resolution molecular approach (i.e., next-generation sequencing). The results revealed many potentially novel PBSA colonizers/decomposers that have not yet been included in the recent database of PBS/PBSA colonizers. These include different bacteria (*Brevundimonas*, *Ferruginibacter*, *Flavobacterium*, *Haliangium*, *Hirschia*, *Massilia*, *Pseudonocardia*, *Rhizobacter*, *Sphingomonas*, *Tardiphaga*, and *Variovorax*) and fungal genera (*Cladophialophora*, *Cyphellophora*, *Fellozoma*, *Fusidium*, *Knufia*, *Mollisia*, *Phoma*, *Plenodomus*, *Venturia*, and *Vishniacozyma*), which were frequently detected in PBSA exposed in our forest sites. Their representative sequences, as well as those of other bacteria and fungi, are shown in Tables S1 and S2, and they can be used for in-depth analysis of their taxonomic identification. Among these bacterial and fungal genera, members of *Flavobacterium* (Labuschagne et al., 1997), *Haliangium* (Kang et al., 2011), *Massilia* (Sedláček et al., 2022), *Pseudonocardia* (Parra et al., 2021), *Variovorax* (Natsagdorj et al., 2019), *Cladophialophora* (Corbellini et al., 2009), *Knufia* (Tesei et al., 2020), *Phoma* (Pollero et al., 2001), *Venturia* (Deng et al., 2017; Müller and Ishir, 1997), and *Vishniacozyma* (Da Silva et al., 2022) have already been tested for lipase/esterase activity. Thus, we propose that they can be listed as candidates for potential PBSA degraders, which should be further verified for their PBSA degradation potential.

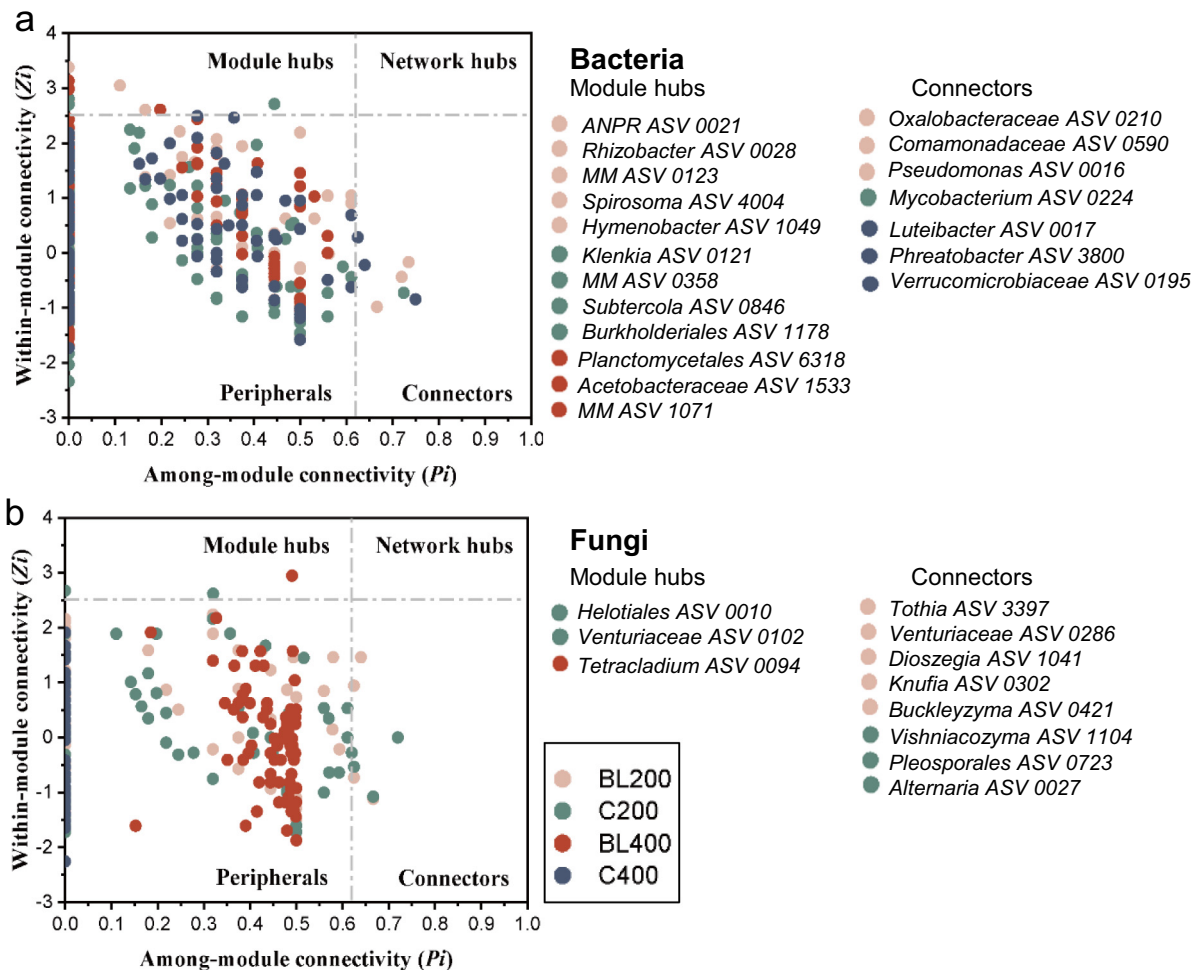


Fig. 6. Topological roles of bacterial and fungal ASVs in PBSA-associated bacterial (a) and fungal (b) networks are displayed by the Z_i - P_i plot. The intra-module connectivity value (Z_i) and inter-module connectivity value (P_i) identify the keystone taxa in the network, classified by Deng et al. (2012), Ji et al. (2022), Zhou et al. (2011) as following: peripheral nodes ($Z_i < 2.5$, $P_i < 0.62$); connectors ($Z_i < 2.5$, $P_i > 0.62$); module hubs ($Z_i > 2.5$, $P_i < 0.62$); and network hubs ($Z_i > 2.5$, $P_i > 0.62$). Data are presented for PBSA under broadleaved (BL) and coniferous tree species (C).

4.3. Involvement of N_2 -fixing bacteria in PBSA degradation: a consistent pattern between cropland and forestland

In this study, we obtained results consistent with our previous experiments in cropland and cropland soils, which emphasize the presence and involvement of N_2 -fixing bacteria in the PBSA degradation process (Purahong et al., 2021; Tanunchai et al., 2021, 2022c). First, our current results showed that diverse functional groups of N_2 -fixing bacteria, including both symbiotic (i.e., ANPR, *Bradyrhizobium*, *Burkholderia-Caballeronia-Paraburkholderia*, *Devosia*, and *Methylobacterium*) and non-symbiotic (i.e., *Rhodopseudomonas* and *Mycobacterium*) N_2 -fixing bacteria were detected or even enriched on PBSA incubated in forest ecosystems. Such bacterial genera have also been enriched in PBSA in cropland ecosystems in our previous experiment (Tanunchai et al., 2022c), suggesting that the taxonomic composition of N_2 -fixing bacteria colonizing PBSA may be conserved and specific to the PBSA degradation process. Second, *Bradyrhizobium* spp., which may play direct and indirect roles in PBSA degradation, are dominant in both forest and cropland ecosystems (Han et al., 2021; Tanunchai et al., 2022c). Third, similar N_2 -fixing bacterial genera, including ANPR, *Methylobacterium*, and *Mycobacterium* were identified as potential keystone taxa in both forest and cropland ecosystems (Ji et al., 2022; Purahong et al., 2021; Tanunchai et al., 2022c). Fourth, we detected strong, positive correlations between *nifH* and fungal ITS-based gene copy numbers in both the forest and cropland ecosystems. These findings highlight the facilitation roles of N_2 -fixing bacterial community members and fungal PBSA

decomposers, as already found in our previous study on cropland ecosystems (Tanunchai et al., 2022c).

4.4. Co-occurrence network and community assembly of plastisphere microbiome in forest soils

The present study is among the first to show the microbial co-occurrence network in the plastisphere microbiome degraded in temperate forest ecosystems. The co-occurrence network showed an increase in potential competitive interactions between bacteria and fungi at the later stages of PBSA degradation in both forest ecosystems. Furthermore, the complexity of the fungal co-occurrence network increased after 400 days of PBSA degradation. Network analysis reveals statistical associations and may not necessarily provide direct evidence of biological interactions or influences. Nevertheless, microorganisms assemble together within complex networks through various types of interactions, either negative (e.g., competition) or positive (e.g., mutualism) (Faust et al., 2012). Positive correlations may indicate potential cooperative or mutualistic associations, such as cross-feeding and/or syntrophic relationships, whereas negative correlations can be used to infer potential antagonistic associations among species, such as predation and/or competition for a limiting resource (Faust and Raes, 2012; Li et al., 2020; Lin et al., 2019). Negative feedback tends to potentially stabilize processes, whereas positive feedback conversely enhances ecosystem changes and destabilizes the status quo (Simard et al., 2012). The increased positive links of the networks indicated that the

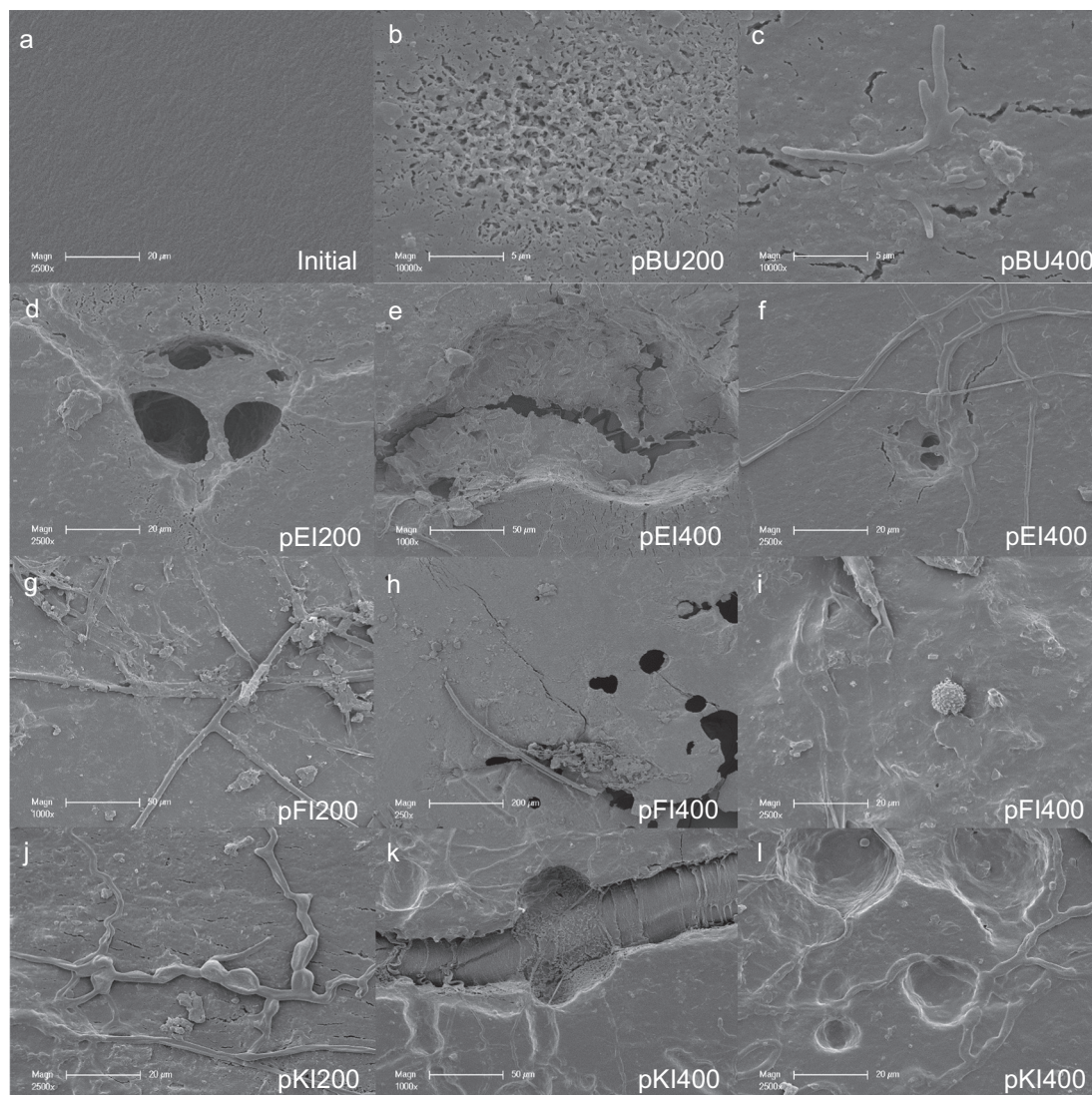


Fig. 7. SEM images of non-exposed (a) and degraded poly(butylene succinate-co-adipate) PBSA surfaces (b–l) after 200 (b, d, g, j) and 400 (c, e–f, h–i, and k–l) days of exposure. Data are presented for PBSA samples under *Fagus sylvatica* (pBU, b–c), *Quercus robur* (pEI, d–f), *Picea abies* (pFI, g–i), and *Pinus sylvestris* (pKI, j–l).

majority of the microorganisms tended to co-occur rather than co-exclude, and vice versa.

The present study showed that the bacterial community assembly processes were not significantly different between forest types. We demonstrated that the bacterial community assembly of bio-based and biodegradable plastics is governed by stochastic processes (Fig. 4), which is consistent with the results of bacterial community assembly in biodegradable and non-biodegradable plastics in aquatic and terrestrial (cropland soil) ecosystems (Ju et al., 2021; Zhang et al., 2022). However, we further identified that homogenizing dispersal was the most important stochastic process governing the bacterial community assembly on PBSA, which differed from the mechanisms of bacterial community assembly in the plastisphere of aquatic (dispersal limitation) (Zhang et al., 2022) and terrestrial (both drift and dispersal) (Ju et al., 2021) ecosystems. Therefore, for the bacterial community assembly on PBSA in forest ecosystems, the dispersal rates of bacteria are high, so bacteria can colonize PBSA even though PBSA may not be their preferred habitat (Wang et al., 2020).

We revealed that the community assembly processes differed between fungi and bacteria, and between both forest types. The fungal community assembly processes in the early stage of PBSA degradation (200 days) were dominated by stochastic processes (mainly drift and homogenizing dispersal), but at the later stage (400 days), they were governed by both

stochastic and deterministic processes (Fig. 4). Forest type played a role in the later stages of PBSA decomposition when we found that in broadleaved forests, the fungal community assembly was strongly controlled by homogeneous selection (deterministic process), followed by homogenizing dispersal (stochastic process). However, in coniferous forests, three processes (stochastic processes: drift and homogenizing dispersal, and deterministic process: homogeneous selection) contributed almost equally. Owing to the contributions of deterministic processes (homogeneous selection), we suggest that PBSA films can be considered as a filter, which selects part of its fungal microbiome from the nearby environment. This may partly explain why rare fungal community members in the litter layers or soils, such as *Tetracladium* spp. and *Exophiala* spp., can be dominant colonizers in the plastisphere of PBSA (Purahong et al., 2021; Tanunchai et al., 2021).

4.5. Similar but distinct: functional redundancy of the PBSA plastisphere between forest types and across different tree species

Although we could clearly demonstrate that the richness and community composition of fungi were significantly different between broadleaved and coniferous forests, the fungal and bacterial gene copy numbers were similar (Figs. 1 and 2). Decomposition of dead plant materials and plastics

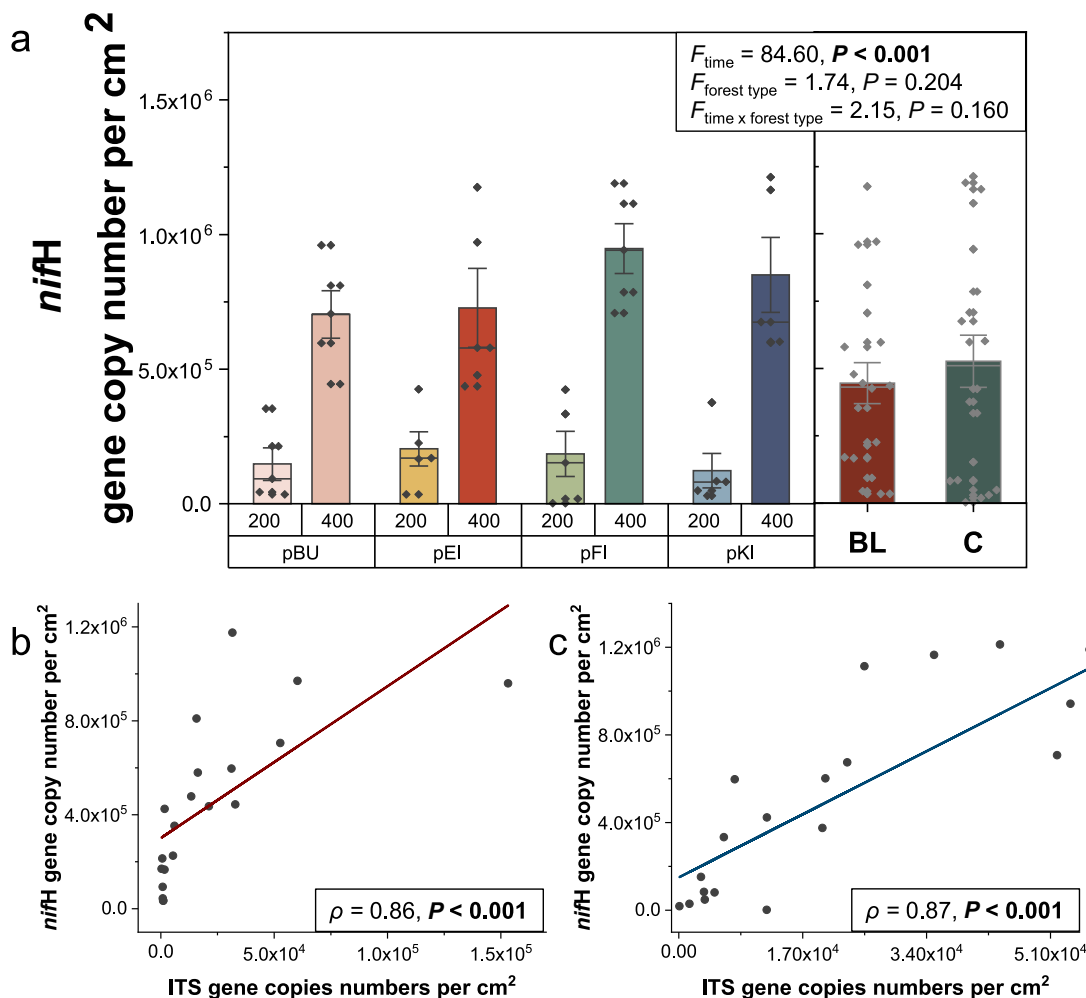


Fig. 8. The *nifH* gene copy numbers (a) and the Spearman's rank correlation between *nifH* gene copy numbers and fungal ITS based gene copy numbers in poly(butylene succinate-co-adipate) PBSA samples under broadleaved (b) and coniferous forests (c). Data are presented for PBSA samples under *Fagus sylvatica* (pBU), *Quercus robur* (pEI), *Picea abies* (pFI), *Pinus sylvestris* (pKI), all-broadleaved (BL), and all-coniferous tree species (C); rose-red tones and blue tones represent broadleaved and coniferous tree species, respectively. (For interpretation of the references to colour in this figure legend, the reader is referred to the web version of this article.)

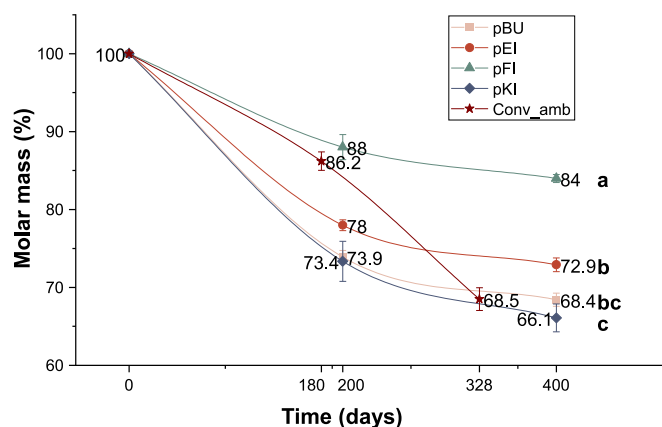


Fig. 9. Molar mass losses of bio-based and biodegradable poly(butylene succinate-co-adipate) (PBSA) at 200 and 400 days of exposure. Data points are presented for PBSA samples under *Fagus sylvatica* (pBU), *Quercus robur* (pEI), *Picea abies* (pFI), and *Pinus sylvestris* (pKI) in forest ecosystems as well as for PBSA samples under conventional farming in ambient conditions (Conv_amb) obtained in our previous study (Purahong et al., 2021). The line between the points indicates the degradation trends. Statistical differences (indicated by different lowercase letters) between molar mass losses among different tree species were tested using repeated measures analysis of variance (ANOVA) with Fisher's least significant difference (LSD) post-hoc test.

is determined by both biotic (e.g., microorganisms and soil organisms) and abiotic factors (e.g., temperature, pH, water content, and nutrients) (Haider et al., 2019; Hoppe et al., 2016). Environmental factors might influence community–function relationships in both direct and indirect ways. On the one hand, environmental conditions under some tree species may constrain microbial activity and influence decomposition abiotically, regardless of the organisms present. On the other hand, some key environmental factors may shape the microbial community, which in turn affects decomposition (Rajala et al., 2012). In this study, we observed both the microbial community structure–function relationship and the uncoupling of microbial community structure and function between the plastisphere of PBSA incubated under different tree species. The uncoupling of microbial community structure and function may be due to functional redundancy (different microbial communities can decompose PBSA at a similar rate). For the first case of the microbial community structure–function relationship, we found that similar fungal community composition among the broadleaved tree species resulted in similar degradation rates of PBSA under both broadleaved tree species. The potential lipase producers, *Tetracladium* (Anderson and Marvanová, 2020; Purahong et al., 2021) and *Mollisina* (Sedláček et al., 2022) were hyperdominant in the plastisphere under both broadleaved tree species. The degradation rate of PBSA in *P. abies* was significantly lower than that in other tree species, where *Tetracladium* and *Mollisina* were almost absent at 200 days. These findings suggest that different microbial community structures in the plastisphere determine the degradation rate of PBSA. Different microbial community

structures in coniferous tree species are derived from many factors, including tree species, plot factors (mainly soil pH and coordinates), and physicochemical properties of the litter layer (e.g., leaf water content and nutrients; Table 1). In the case of uncoupling of microbial community structure and function, we found that PBSA degradation rates under *P. sylvestris* and *F. sylvatica* were similar, even though the plastispheres under both tree species were completely different. In plastispheres under *P. sylvestris*, other important lipase producers, *Phoma* (Pollero et al., 2001) and *Knufia* (Tesei et al., 2020) were detected at 200 and 400 days, respectively. We propose that functional redundancy may occur between the plastisphere of PBSA to maintain ecosystem functioning in *P. sylvestris* and *F. sylvatica* (Biggs et al., 2020; Louca et al., 2018). In addition, the core PBSA decomposers detected in both tree species could also decompose PBSA at a similar rate. A similar phenomenon was reported in the PBSA decomposition experiment in cropland ecosystems subjected to ambient and future climate conditions, where the rate of PBSA degradation was not significantly different between the two climates owing to the core climate PBSA microbiome (Purahong et al., 2021).

5. Conclusions

The current study is among the first to explore the plastisphere microbiome and its community assembly processes associated with PBSA in forest ecosystems. The bacterial community was governed by stochastic processes (mainly homogenizing dispersal), whereas the fungal community was driven by both stochastic and deterministic processes (drift and homogeneous selection). We determined the transferability of mechanisms of PBSA biodegradation from cropland to forest ecosystems, explaining i) the functional redundancy that may occur between the plastisphere of PBSA incubated under *P. sylvestris* and *F. sylvatica* (however, in forest ecosystems, we observed microbial community structure–function relationships that differed between both forest types), and ii) how N₂-fixing bacteria participated in PBSA degradation, indicating that the accumulation of N is important for microbial degradation in N-poor substrates. Notably, our previous study on cropland and the current study on forest ecosystems have been conducted only in cold temperate climates. Transferability to other climates (such as tropical, subtropical, and boreal climates) should be addressed in future studies.

CRedit authorship contribution statement

WP and EDS conceived and designed the study. BT, WP, SW and EDS led the experimental set-up. BT, LJ, WP, SW, and EDS collected the samples and metadata. WP, MN, and FB contributed reagents and laboratory equipment. BT and WP led the DNA analysis. EDS led the physicochemical analyses of litter layer. SW led bioinformatics. BT, and WP led the microbial taxonomy, and data analyses. LJ led microbial network and community assembly analyses. AG performed SEM. MN led quantitative PCR. OS, SJG, and SK led GPC. BT, LJ and WP wrote the manuscript. MN and WP supervised BT. MN, AG, EDS, and FB reviewed and gave comments and suggestions for manuscript. All of the authors gave final approval for manuscript submission.

Data availability

The Illumina sequencing of bacterial and fungal datasets are deposited in The National Center for Biotechnology Information (NCBI) database under BioProject ID: PRJNA890592. Microbial taxonomic and relative abundance information is provided in Supporting Information Table S1 and S2.

Declaration of competing interest

The authors declare that they have no competing interests. The authors declare that they have no known competing financial interests or personal relationships that could have appeared to influence the work reported in this paper.

Acknowledgements

The community composition data have been computed at the High-Performance Computing (HPC) Cluster EVE, a joint effort of both the Helmholtz Centre for Environmental Research - UFZ and the German Centre for Integrative Biodiversity Research (iDiv) Halle-Jena-Leipzig. We thank Beatrix Schnabel and Melanie Günther for their help with Illumina sequencing, Dominik Stafp for assistance in the quantitative PCR laboratory, and Ines Hille for her help analysing physicochemical properties of litter layer. We thank the Helmholtz Association, the Federal Ministry of Education and Research, the State Ministry of Science and Economy of Saxony-Anhalt, and the State Ministry for Higher Education, Research and the Arts Saxony. We thank PTT MCC Biochem, Thailand, for providing the BioPBS (PBSA) films. PTT MCC Biochem did not contribute or influence on the experimental design, experiment, data analysis, and results of this study. Benjawan Tanunchai acknowledges the Peter and Traudl Engelhorn Foundation for the financial support through her PostDoc scholarship. Li Ji appreciates the financial support by the China Scholarship Council (No. 201906600038). Stefan Kalkhof acknowledges the Federal Ministry of Education and Research, Germany (Bundesministerium für Bildung und Forschung, BMBF) [grant number 01ZX1910B].

Funding

This work has been partially funded by the internal research budget of Dr. Witoon Purahong, Department of Soil Ecology, UFZ-Helmholtz Centre for Environmental Research.

Ethics approval and consent to participate

Not applicable.

Consent for publication

Not applicable.

Appendix A. Supplementary data

Supplementary data to this article can be found online at <https://doi.org/10.1016/j.scitotenv.2023.162230>.

References

- Abe, M., Kobayashi, K., Honma, N., Nakasaki, K., 2010. Microbial degradation of poly(butylene succinate) by *Fusarium solani* in soil environments. *Polym. Degrad. Stab.* 95, 138–143. <https://doi.org/10.1016/j.polymdegradstab.2009.11.042>.
- Agathokleous, E., Iavicoli, I., Barceló, D., Calabrese, E.J., 2021. Ecological risks in a 'plastic' world: a threat to biological diversity? *J. Hazard. Mater.* 417, 126035. <https://doi.org/10.1016/j.jhazmat.2021.126035>.
- Ahmad, A., Tsutsui, A., Iijima, S., Suzuki, T., Shah, A.A., Nakajima-Kambe, T., 2019. Gene structure and comparative study of two different plastic-degrading esterases from *Roseateles depolymerans* strain TB-87. *Polym. Degrad. Stab.* 164, 109–117. <https://doi.org/10.1016/j.polymdegradstab.2019.04.003>.
- Anderson, J.L., Marvanová, L., 2020. Broad geographical and ecological diversity from similar genomic toolkits in the Ascomycete genus *Tetracladium*. <https://doi.org/10.1101/2020.04.06.027920> bioRxiv 2020.04.06.027920.
- Bastian, M., Heymann, S., Jacomy, M., 2009. Gephi: an open source software for exploring and manipulating networks. *Proceedings of the International AAAI Conference on Web and Social Media*, 3, pp. 361–362. <https://doi.org/10.1609/icwsm.v3i1.13937>.
- Bhagwat, G., Zhu, Q., O'Connor, W., Subashchandrabose, S., Grainge, I., Knight, R., Palanisami, T., 2021. Exploring the composition and functions of plastic microbiome using whole-genome sequencing. *Environ. Sci. Technol.* 55, 4899–4913. <https://doi.org/10.1021/acs.est.0c07952>.
- Biggs, C.R., Yeager, L.A., Bolser, D.G., Bonsell, C., Dichiera, A.M., Hou, Z., Keyser, S.R., Khursigara, A.J., Lu, K., Muth, A.F., Negrete Jr., B., Erisman, B.E., 2020. Does functional redundancy affect ecological stability and resilience? A review and meta-analysis. *Ecosphere* 11, e03184. <https://doi.org/10.1002/ecs2.3184>.
- Burgess-Conforti, J.R., Moore, P.A., Owens, P.R., Miller, D.M., Ashworth, A.J., Hays, P.D., Evans-White, M.A., Anderson, K.R., 2019. Are soils beneath coniferous tree stands more acidic than soils beneath deciduous tree stands? *Environ. Sci. Pollut. Res.* 26, 14920–14929. <https://doi.org/10.1007/s11356-019-04883-y>.

- Caporaso, J.G., Lauber, C.L., Walters, W.A., Berg-Lyons, D., Lozupone, C.A., Turnbaugh, P.J., Fierer, N., Knight, R., 2011. Global patterns of 16S rRNA diversity at a depth of millions of sequences per sample. *PNAS* 108, 4516–4522. <https://doi.org/10.1073/pnas.1000080107>.
- Carrasco, M., Alcaño, J., Cifuentes, V., Baeza, M., 2017. Purification and characterization of a novel cold adapted fungal glucoamylase. *Microb. Cell Factories* 16, 75. <https://doi.org/10.1186/s12934-017-0693-x>.
- Carrasco, M., Rozas, J.M., Alcaño, J., Cifuentes, V., Baeza, M., 2019. Pectinase secreted by psychrotolerant fungi: identification, molecular characterization and heterologous expression of a cold-active polygalacturonase from *Tetracladium* sp. *Microb. Cell Factories* 18, 45. <https://doi.org/10.1186/s12934-019-1092-2>.
- Chase, J.M., Myers, J.A., 2011. Disentangling the importance of ecological niches from stochastic processes across scales. *Philos. Trans. R. Soc. Lond., B Biol. Sci.* 366, 2351–2363. <https://doi.org/10.1098/rstb.2011.0063>.
- Corbellini, V.A., Scroferneker, M.L., Carissimi, M., da Costa, J.M., Ferrão, M.F., 2009. Lipolytic activity of chromoblastomycosis agents measured by infrared spectroscopy and chemometric methods. *Med. Mycol.* 47, 63–69. <https://doi.org/10.1080/13693780802566325>.
- Da Silva, M.K., Da Silva, A.V., Fernandez, P.M., Montone, R.C., Alves, R.P., De Queiroz, A.C., De Oliveira, V.M., Dos Santos, V.P., Putzke, J., Rosa, L.H., Duarte, A.W.F., 2022. Extracellular hydrolytic enzymes produced by yeasts from Antarctic lichens. *An. Acad. Bras. Ciênc.* 94. <https://doi.org/10.1590/0001-376520220210540>.
- Deng, Y., Jiang, Y.-H., Yang, Y., He, Z., Luo, F., Zhou, J., 2012. Molecular ecological network analyses. *BMC Bioinformatics* 13, 113. <https://doi.org/10.1186/1471-2105-13-113>.
- Deng, C.H., Plummer, K.M., Jones, D.A.B., Mesarich, C.H., Shiller, J., Taranto, A.P., Robinson, A.J., Kastner, P., Hall, N.E., Templeton, M.D., Bowen, J.K., 2017. Comparative analysis of the predicted secretomes of *Rosaceae* scab pathogens *Venturia inaequalis* and *V. pirina* reveals expanded effector families and putative determinants of host range. *BMC Genomics* 18, 339. <https://doi.org/10.1186/s12864-017-3699-1>.
- D'Souza, J.M., Windsor, F.M., Santillo, D., Ormerod, S.J., 2020. Food web transfer of plastics to an apex riverine predator. *Glob. Chang. Biol.* 26, 3846–3857. <https://doi.org/10.1111/gcb.15139>.
- Emadian, S.M., Onay, T.T., Demirel, B., 2017. Biodegradation of bioplastics in natural environments. *Waste Manag.* 59, 526–536. <https://doi.org/10.1016/j.wasman.2016.10.006>.
- FAO, 2021. Assessment of Agricultural Plastics and Their Sustainability: A Call for Action. FAO, Rome, Italy.
- Faust, K., Raes, J., 2012. Microbial interactions: from networks to models. *Nat. Rev. Microbiol.* 10, 538–550. <https://doi.org/10.1038/nrmicro2832>.
- Faust, K., Sathirapongasuti, J.F., Izard, J., Segata, N., Gevers, D., Raes, J., Huttenhower, C., 2012. Microbial co-occurrence relationships in the human microbiome. *PLoS Comput. Biol.* 8, e1002606. <https://doi.org/10.1371/journal.pcbi.1002606>.
- Gigli, M., Negroni, A., Soccio, M., Zanolli, G., Lotti, N., Fava, F., Munari, A., 2012. Influence of chemical and architectural modifications on the enzymatic hydrolysis of poly(butylene succinate). *Green Chem.* 14, 2885–2893. <https://doi.org/10.1039/C2GC35876j>.
- Goldmann, K., Schöning, I., Buscot, F., Wubet, T., 2015. Forest management type influences diversity and community composition of soil fungi across temperate forest ecosystems. *Front. Microbiol.* 1300. <https://doi.org/10.3389/fmicb.2015.01300>.
- Haider, T.P., Völker, C., Kramm, J., Landfester, K., Wurm, F.R., 2019. Plastics of the future? The impact of biodegradable polymers on the environment and on society. *Angew. Chem. Int. Ed.* 58, 50–62. <https://doi.org/10.1002/anie.201805766>.
- Hall, B.G., 2013. Building phylogenetic trees from molecular data with MEGA. *Mol. Biol. Evol.* 30, 1229–1235. <https://doi.org/10.1093/molbev/mst012>.
- Han, Y., Teng, Y., Wang, Xia, Ren, W., Wang, Xiaomi, Luo, Y., Zhang, H., Christie, P., 2021. Soil type driven change in microbial community affects poly(butylene adipate-co-terephthalate) degradation. *Potential. Environ. Sci. Technol.* <https://doi.org/10.1021/acs.est.0c04850>.
- Herold, N., Schöning, I., Michalzik, B., Trumbore, S., Schrumpp, M., 2014. Controls on soil carbon storage and turnover in German landscapes. *Biogeochemistry* 119, 435–451. <https://doi.org/10.1007/s10533-014-9978-x>.
- Hiscox, J., O'Leary, J., Boddy, L., 2018. Fungus wars: basidiomycete battles in wood decay. *Stud. Mycol.* 89, 117–124. <https://doi.org/10.1016/j.simyco.2018.02.003>.
- Hoppe, B., Purahong, W., Wubet, T., Kahl, T., Bauhus, J., Armstadt, T., Hofrichter, M., Buscot, F., Krüger, D., 2016. Linking molecular deadwood-inhabiting fungal diversity and community dynamics to ecosystem functions and processes in central European forests. *Fungal Divers.* 77, 367–379. <https://doi.org/10.1007/s13225-015-0341-x>.
- Hoshino, A., Sawada, H., Yokota, M., Tsuji, M., Fukuda, K., Kimura, M., 2001. Influence of weather conditions and soil properties on degradation of biodegradable plastics in soil. *Soil Sci. Plant Nutr.* 47, 35–43. <https://doi.org/10.1080/00380768.2001.10408366>.
- Huang, Z., Qian, L., Yin, Q., Yu, N., Liu, T., Tian, D., 2018. Biodegradability studies of poly(butylene succinate) composites filled with sugarcane rind fiber. *Polym. Test.* 66, 319–326. <https://doi.org/10.1016/j.polymertesting.2018.02.003>.
- Huang, Y., Liu, Q., Jia, W., Yan, C., Wang, J., 2020. Agricultural plastic mulching as a source of microplastics in the terrestrial environment. *Environ. Pollut.* 260, 114096. <https://doi.org/10.1016/j.envpol.2020.114096>.
- Ihrmark, K., Bodeker, I.T.M., Cruz-Martinez, K., Friberg, H., Kubartova, A., Schenck, J., Strid, Y., Stenlid, J., Brandström-Durling, M., Clemmensen, K.E., Lindahl, B.D., 2012. New primers to amplify the fungal ITS2 region – evaluation by 454-sequencing of artificial and natural communities. *FEMS Microbiol. Ecol.* 82, 666–677. <https://doi.org/10.1111/j.1574-6941.2012.01437.x>.
- Jamieson, A.J., Brooks, L.S.R., Reid, W.D.K., Piertney, S.B., Narayanaswamy, B.E., Linley, T.D., 2019. Microplastics and synthetic particles ingested by deep-sea amphipods in six of the deepest marine ecosystems on Earth. *R. Soc. Open Sci.* 6, 180667. <https://doi.org/10.1098/rsos.180667>.
- Ji, L., Tanunchai, B., Wahdan, S.F.M., Schädler, M., Purahong, W., 2022. Future climate change enhances the complexity of plastisphere microbial co-occurrence networks, but does not significantly affect the community assembly. *Sci. Total Environ.* 157016. <https://doi.org/10.1016/j.scitotenv.2022.157016>.
- Jiang, Y., Woortman, A.J.J., van Ekenstein, G.O.R.A., Loos, K., 2015. Environmentally benign synthesis of saturated and unsaturated aliphatic polyesters via enzymatic polymerization of biobased monomers derived from renewable resources. *Polym. Chem.* 6, 5451–5463. <https://doi.org/10.1039/C5PY00660K>.
- Ju, Z., Du, X., Feng, K., Li, S., Gu, S., Jin, D., Deng, Y., 2021. The succession of bacterial community attached on biodegradable plastic mulches during the degradation in soil. *Front. Microbiol.* 12. <https://doi.org/10.3389/fmicb.2021.785737>.
- Juncheed, K., Tanunchai, B., Wahdan, S.F.M., Thongsuk, K., Schädler, M., Noll, M., Purahong, W., 2022. Dark side of a bio-based and biodegradable plastic? Assessment of pathogenic microbes associated with poly(butylene succinate-co-adipate) under ambient and future climates using next-generation sequencing. *Front. Microbiol.* 13. <https://doi.org/10.3389/fpls.2022.966363>.
- Kaiser, K., Wemheuer, B., Korolkow, V., Wemheuer, F., Nacke, H., Schöning, I., Schrumpp, M., Daniel, R., 2016. Driving forces of soil bacterial community structure, diversity, and function in temperate grasslands and forests. *Sci. Rep.* 6, 33696. <https://doi.org/10.1038/srep33696>.
- Kang, C.-H., Oh, K.-H., Lee, M.-H., Oh, T.-K., Kim, B.H., Yoon, J.-H., 2011. A novel family VII esterase with industrial potential from compost metagenomic library. *Microb. Cell Factories* 10, 41. <https://doi.org/10.1186/1475-2859-10-41>.
- Kipping, L., Gossner, M.M., Koschorreck, M., Muszynski, S., Maurer, F., Weisser, W.W., Jehmlich, N., Noll, M., 2022. Emission of CO₂ and CH₄ from 13 deadwood tree species is linked to tree species identity and management intensity in forest and grassland habitats. *Glob. Biogeochem. Cycles* 36, e2021GB007143. <https://doi.org/10.1029/2021GB007143>.
- Klindworth, A., Pruesse, E., Schweer, T., Peplies, J., Quast, C., Horn, M., Glöckner, F.O., 2013. Evaluation of general 16S ribosomal RNA gene PCR primers for classical and next-generation sequencing-based diversity studies. *Nucleic Acids Res.* 41, e1. <https://doi.org/10.1093/nar/gks808>.
- Labuschagne, R.B., van Tonder, A., Lithauer, D., 1997. *Flavobacterium odoratum* lipase: isolation and characterization. *Enzym. Microb. Technol.* 21, 52–58. [https://doi.org/10.1016/S0141-0229\(96\)00226-8](https://doi.org/10.1016/S0141-0229(96)00226-8).
- Lee, J.T.Y., Chow, K.L., 2012. SEM sample preparation for cells on 3D scaffolds by freeze-drying and HMDS. *Scanning* 34, 12–25. <https://doi.org/10.1002/sca.20271>.
- Li, J., Li, C., Kou, Y., Yao, M., He, Z., Li, X., 2020. Distinct mechanisms shape soil bacterial and fungal co-occurrence networks in a mountain ecosystem. *FEMS Microbiol. Ecol.* 96, fiae030. <https://doi.org/10.1093/femsec/fiae030>.
- Lin, Y., Ye, G., Kuzyakov, Y., Liu, D., Fan, J., Ding, W., 2019. Long-term manure application increases soil organic matter and aggregation, and alters microbial community structure and keystone taxa. *Soil Biol. Biochem.* 134, 187–196. <https://doi.org/10.1016/j.soilbio.2019.03.030>.
- Liu, E.K., He, W.Q., Yan, C.R., 2014. 'White revolution' to 'white pollution'—agricultural plastic film mulch in China. *Environ. Res. Lett.* 9, 091001. <https://doi.org/10.1088/1748-9326/9/9/091001>.
- Liu, C., Cui, Y., Li, X., Yao, M., 2021. Microeco: an R package for data mining in microbial community ecology. *FEMS Microbiol. Ecol.* 97, fiae255. <https://doi.org/10.1093/femsec/fiae255>.
- Liu, L., Zou, G., Zuo, Q., Li, S., Bao, Z., Jin, T., Liu, D., Du, L., 2022. It is still too early to promote biodegradable mulch film on a large scale: a bibliometric analysis. *Environ. Technol. Innov.* 27, 102487. <https://doi.org/10.1016/j.eti.2022.102487>.
- Louca, S., Polz, M.F., Mazel, F., Albright, M.B.N., Huber, J.A., O'Connor, M.I., Ackermann, M., Hahn, A.S., Srivastava, D.S., Crowe, S.A., Doebeli, M., Parfrey, L.W., 2018. Function and functional redundancy in microbial systems. *Nat. Ecol. Evol.* 2, 936–943. <https://doi.org/10.1038/s41559-018-0519-1>.
- Lwanga, E.H., Beriot, N., Corradini, F., Silva, Y., Yang, X., Baartman, J., Rezaei, M., van Schaik, L., Riksen, M., Geissen, V., 2022. Review of microplastic sources, transport pathways and correlations with other soil stressors: a journey from agricultural sites into the environment. *Chem. Biol. Technol. Agric.* 9, 20. <https://doi.org/10.1186/s40538-021-00278-9>.
- Mirarab, S., Nguyen, N., Guo, S., Wang, L.-S., Kim, J., Warnow, T., 2015. PASTA: ultra-large multiple sequence alignment for nucleotide and amino-acid sequences. *J. Comput. Biol.* 22, 377–386. <https://doi.org/10.1089/cmb.2014.0156>.
- Müller, M.W., Ishir, H., 1997. Esterase activity from *Venturia nashicola*: histochemical detection and supposed involvement in the pathogenesis of scab on Japanese pear. *J. Phytopathol.* 145, 473–477. <https://doi.org/10.1111/j.1439-0434.1997.tb00353.x>.
- Nam, M.H., Park, M.S., Kim, H.S., Kim, T.I., Kim, H.G., 2015. *Cladosporium cladosporioides* and *C. tenuissimum* cause blossom blight in strawberry in Korea. *Mycobiology* 43, 354–359. <https://doi.org/10.5941/MYCO.2015.43.3.354>.
- Napper, I.E., Davies, B.F.R., Clifford, H., Elvin, S., Koldewey, H.J., Mayewski, P.A., Miner, K.R., Potocnik, M., Elmore, A.C., Gajurel, A.P., Thompson, R.C., 2020. Reaching new heights in plastic pollution—preliminary findings of microplastics on Mount Everest. *One Earth* 3, 621–630. <https://doi.org/10.1016/j.oneear.2020.10.020>.
- Natsagdorj, O., Sakamoto, H., Santiago, D.M.O., Santiago, C.D., Orikasa, Y., Okazaki, K., Ikeda, S., Ohwada, T., 2019. *Variovorax* sp. has an optimum cell density to fully function as a plant growth promoter. *Microorganisms* 7, 82. <https://doi.org/10.3390/microorganisms7030082>.
- Ning, D., Yuan, M., Wu, L., Zhang, Y., Guo, X., Zhou, X., Yang, Y., Arkin, A.P., Firestone, M.K., Zhou, J., 2020. A quantitative framework reveals ecological drivers of grassland microbial community assembly in response to warming. *Nat. Commun.* 11, 4717. <https://doi.org/10.1038/s41467-020-18560-z>.
- Odrizola, I., Abrego, N., Tláškal, V., Zrůstová, P., Morais, D., Větrovský, T., Ovaskainen, O., Baldrian, P., 2021. Fungal communities are important determinants of bacterial community composition in deadwood. *mSystems* 6, e01017-20. <https://doi.org/10.1128/mSystems.01017-20>.

- Parra, J., Soldatou, S., Rooney, L.M., Duncan, K.R., 2021. *Pseudonocardia abyssalis* sp. nov. and *Pseudonocardia oceanii* sp. nov., two novel actinomycetes isolated from the deep Southern Ocean. *Int. J. Syst. Evol. Microbiol.* 71. <https://doi.org/10.1099/ijsem.0.005032>.
- Pollero, R.J., Gaspar, M.L., Cabello, M., 2001. Extracellular lipolytic activity in *Phoma glomerata*. *World J. Microbiol. Biotechnol.* 17, 805–810. <https://doi.org/10.1023/A:1013517116198>.
- Pölme, S., Abarenkov, K., Henrik Nilsson, R., Lindahl, B.D., Clemmensen, K.E., Kauterud, H., Nguyen, N., Kjoller, R., Bates, S.T., Baldrian, P., Froslev, T.G., Adojaan, K., Vizzini, A., Suija, A., Pfister, D., Baral, H.-O., Järv, H., Madrid, H., Nordén, J., Liu, J.-K., Pawłowska, J., Pöldmaa, K., Pärtel, K., Runnel, K., Hansen, K., Larsson, K.-H., Hyde, K.D., Sandoval-Denis, M., Smith, M.E., Toome-Heller, M., Wijayawardene, N.N., Menolli, N., Reynolds, N.K., Drenkhan, R., Maharachchikumbura, S.S.N., Gibertoni, T.B., Læssøe, T., Davis, W., Tokarev, Y., Corrales, A., Soares, A.M., Agan, A., Machado, A.R., Argüelles-Moyao, A., Detheridge, A., de Meiras-Ottoni, A., Verbeken, A., Dutta, A.K., Cui, B.-K., Pradeep, C.K., Marin, C., Stanton, D., Gohar, D., Wanasinghe, D.N., Otsing, E., Aslani, F., Griffith, G.W., Lumbsch, T.H., Grossart, H.-P., Masigol, H., Timling, I., Hiiesalu, I., Oja, J., Kupagme, J.Y., Geml, J., Alvarez-Manjarrez, J., Ilves, K., Loit, K., Adamson, K., Nara, K., Küngas, K., Rojas-Jimenez, K., Bitenieks, K., Irinyi, L., Nagy, L.G., Soonvald, L., Zhou, L.-W., Wagner, L., Aime, M.C., Öpik, M., Mujica, M.L., Metsoja, M., Ryberg, M., Vasar, M., Murata, M., Nelsen, M.P., Cleary, M., Samarakoon, M.C., Doilom, M., Bahram, M., Hagh-Doust, N., Dulya, O., Johnston, P., Kohout, P., Chen, Q., Tian, Q., Nandi, R., Amiri, R., Perera, R.H., dos Santos Chikowski, R., Mendes-Alvarenga, R.L., Garibay-Orijel, R., Gielen, R., Phookamsak, R., Jayawardena, R.S., Rahimlou, S., Karunarathna, S.C., Tibpromma, S., Brown, S.P., Sepp, S.-K., Mundra, S., Luo, Z.-H., Bose, T., Vahter, T., Netherway, T., Yang, T., May, T., Varga, T., Li, W., Coimbra, V.R.M., de Oliveira, V.R.T., de Lima, V.X., Mikryukov, V.S., Lu, Y., Matsuda, Y., Miyamoto, Y., Kõljalg, U., Detsuroo, L., 2020. FungalTraits: a user-friendly traits database of fungi and fungus-like stramenopiles. *Fungal Divers.* 105, 1–16. <https://doi.org/10.1007/s13225-020-00466-2>.
- Poly, F., Monrozier, L.J., Bally, R., 2001. Improvement in the RFLP procedure for studying the diversity of *nifH* genes in communities of nitrogen fixers in soil. *Res. Microbiol.* 152, 95–103. [https://doi.org/10.1016/S0923-2508\(00\)01172-4](https://doi.org/10.1016/S0923-2508(00)01172-4).
- Polymer properties database, 2021. Polymer properties database. URL <https://polymerdatabase.com/Polymer%20Brands/PBS.html> (accessed 10.13.19).
- Puchalski, M., Szparaga, G., Biela, T., Gutowska, A., Sztajnowski, S., Krucińska, I., 2018. Molecular and supramolecular changes in polybutylene succinate (PBS) and polybutylene succinate adipate (PBSA) copolymer during degradation in various environmental conditions. *Polymers* 10, 251. <https://doi.org/10.3390/polym10030251>.
- Purahong, W., Schlotter, M., Pecyna, M.J., Kapturska, D., Däumlich, V., Mital, S., Buscot, F., Hofrichter, M., Gutknecht, J.L.M., Krüger, D., 2014. Uncoupling of microbial community structure and function in decomposing litter across beech forest ecosystems in Central Europe. *Sci. Rep.* 4. <https://doi.org/10.1038/srep07014>.
- Purahong, W., Wahdan, S.F.M., Heinz, D., Jariyavidyanont, K., Sungkapreecha, C., Tanunchai, B., Sansupa, C., Sadubsarn, D., Alaneed, R., Heintz-Buschart, A., Schädler, M., Geissler, A., Kressler, J., Buscot, F., 2021. Back to the future: decomposability of a biobased and biodegradable plastic in field soil environments and its microbiome under ambient and future climates. *Environ. Sci. Technol.* 55, 12337–12351. <https://doi.org/10.1021/acs.est.1c02695>.
- Qi, Y., Yang, X., Pelaez, A.M., Huerta Lwanga, E., Beriot, N., Gertsen, H., Garbeva, P., Geissen, V., 2018. Macro- and micro- plastics in soil-plant system: effects of plastic mulch film residues on wheat (*Triticum aestivum*) growth. *Sci. Total Environ.* 645, 1048–1056. <https://doi.org/10.1016/j.scitotenv.2018.07.229>.
- Qi, Y., Ossowicki, A., Yang, X., Huerta Lwanga, E., Dini-Andreote, F., Geissen, V., Garbeva, P., 2020. Effects of plastic mulch film residues on wheat rhizosphere and soil properties. *J. Hazard. Mater.* 387, 121711. <https://doi.org/10.1016/j.jhazmat.2019.121711>.
- Rajala, T., Peltoniemi, M., Pennanen, T., Mäkipää, R., 2012. Fungal community dynamics in relation to substrate quality of decaying Norway spruce (*Picea abies* [L.] Karst.) logs in boreal forests. *FEMS Microbiol. Ecol.* 81, 494–505. <https://doi.org/10.1111/j.1574-6941.2012.01376.x>.
- Sansupa, C., Purahong, W., Nawaz, A., Wubet, T., Suwannarach, N., Chantawannakul, P., Chairuangri, S., Disayathanooat, T., 2022. Living fungi in an opencast limestone mine: who are they and what can they do? *J. Fungi* 8, 987. <https://doi.org/10.3390/jof8100987>.
- Sato, S., Saika, A., Shinozaki, Y., Watanabe, T., Suzuki, K., Sameshima-Yamashita, Y., Fukuoka, T., Habe, H., Morita, T., Kitamoto, H., 2017. Degradation profiles of biodegradable plastic films by biodegradable plastic-degrading enzymes from the yeast *Pseudozyma antarctica* and the fungus *Paraphoma* sp. B47–9. *Polym. Degrad. Stab.* 141, 26–32. <https://doi.org/10.1016/j.polydegradstab.2017.05.007>.
- Scheid, S.-M., Juncheed, K., Tanunchai, B., Wahdan, S.F.M., Buscot, F., Noll, M., Purahong, W., 2022. Interactions between high load of a bio-based and biodegradable plastic and nitrogen fertilizer affect plant biomass and health: a case study with *Fusarium solani* and mung bean (*Vigna radiata* L.). *J. Polym. Environ.* 30, 3534–3544. <https://doi.org/10.1007/s10924-022-02435-z>.
- Sedláček, I., Holochová, P., Busse, H.-J., Koubová, V., Králová, S., Švec, P., Sobotka, R., Staňková, E., Pilný, J., Šedo, O., Smolíková, J., Sedlář, K., 2022. Characterisation of waterborne psychrophilic *Massilia* isolates with violacein production and description of *Massilia antarctica* sp. nov. *Microorganisms* 10, 704. <https://doi.org/10.3390/microorganisms10040704>.
- Simard, S.W., Beiler, K.J., Bingham, M.A., Deslippe, J.R., Philip, L.J., Teste, F.P., 2012. Mycorrhizal networks: mechanisms, ecology and modelling. *Fungal Biol. Rev.* 26, 39–60. <https://doi.org/10.1016/j.fbr.2012.01.001>.
- Song, Y., Laureijsen-van de Sande, W.W.J., Moreno, L.F., Gerrits van den Ende, B., Li, R., de Hoog, S., 2017. Comparative ecology of capsular *Exophiala* species causing disseminated infection in humans. *Front. Microbiol.* 8. <https://doi.org/10.3389/fmicb.2017.02514>.
- Stegen, J.C., Lin, X., Fredrickson, J.K., Chen, X., Kennedy, D.W., Murray, C.J., Rockhold, M.L., Konopka, A., 2013. Quantifying community assembly processes and identifying features that impose them. *ISME J.* 7, 2069–2079. <https://doi.org/10.1038/ismej.2013.93>.
- Stegen, J.C., Lin, X., Fredrickson, J.K., Konopka, A.E., 2015. Estimating and mapping ecological processes influencing microbial community assembly. *Front. Microbiol.* 6. <https://doi.org/10.3389/fmicb.2015.00370>.
- Tanunchai, B., Ji, L., Schroeter, S.A., Wahdan, S.F.M., Larperkern, P., Lehnert, A.-S., Alves, E.G., Gleixner, G., Schulze, E.-D., Noll, M., Buscot, F., Purahong, W., 2022b. A poisoned apple: first insights into community assembly and networks of the fungal pathobiome of healthy-looking senescing leaves of temperate trees in mixed forest ecosystem. *Front. Plant Sci.* 13. <https://doi.org/10.3389/fpls.2022.968218>.
- Tanunchai, B., Juncheed, K., Wahdan, S.F.M., Guliyev, V., Udovenko, M., Lehnert, A.-S., Alves, E.G., Glaser, B., Noll, M., Buscot, F., Blagodatskaya, E., Purahong, W., 2021. Analysis of microbial populations in plastic-soil systems after exposure to high poly(butylene succinate-co-adipate) load using high-resolution molecular technique. *Environ. Sci. Eur.* 33, 105. <https://doi.org/10.1186/s12302-021-00528-5>.
- Tanunchai, B., Ji, L., Schroeter, S.A., Wahdan, S.F.M., Hossen, S., Delelegn, Y., Buscot, F., Lehnert, A.-S., Alves, E.G., Hilke, I., Gleixner, G., Schulze, E.-D., Noll, M., Purahong, W., 2022a. FungalTraits vs. FUNGuild: comparison of ecological functional assignments of leaf- and needle-associated fungi across 12 temperate tree species. *Microb. Ecol.* 1–18. <https://doi.org/10.1007/s00248-022-01973-2>.
- Tanunchai, B., Kalkhof, S., Guliyev, V., Wahdan, S.F.M., Krstic, D., Schädler, M., Geissler, A., Glaser, B., Buscot, F., Blagodatskaya, E., Noll, M., Purahong, W., 2022c. Nitrogen fixing bacteria facilitate microbial biodegradation of a bio-based and biodegradable plastic in soils under ambient and future climatic conditions. *Environ. Sci.: Processes Impacts* <https://doi.org/10.1039/D1EM00426C>.
- Tesei, D., Quartanella, F., Guebitz, G.M., Ribitsch, D., Nöbauer, K., Razzazi-Fazeli, E., Sterflinger, K., 2020. Shotgun proteomics reveals putative polyesters in the secretome of the rock-inhabiting fungus *Knufia chersonesos*. *Sci. Rep.* 10, 9770. <https://doi.org/10.1038/s41598-020-66256-7>.
- Uchida, H., Nakajima-Kambe, T., Shigeno-Akutsu, Y., Nomura, N., Tokiwa, Y., Nakahara, T., 2000. Properties of a bacterium which degrades solid poly(tetramethylene succinate)-co-adipate, a biodegradable plastic. *FEMS Microbiol. Lett.* 189, 25–29. <https://doi.org/10.1111/j.1574-6968.2000.tb09201.x>.
- Valainis, D., Dondl, P., Foehr, P., Burgkart, R., Kalkhof, S., Duda, G.N., van Griensven, M., Poh, P.S.P., 2019. Integrated additive design and manufacturing approach for the bioengineering of bone scaffolds for favorable mechanical and biological properties. *Biomed. Mater.* 14, 065002. <https://doi.org/10.1088/1748-605X/ab386c>.
- Wahdan, S.F.M., Ji, L., Schädler, M., Wu, Y.-T., Sansupa, C., Tanunchai, B., Buscot, F., Purahong, W., 2022. Future climate conditions accelerate wheat straw decomposition alongside altered microbial community composition, assembly patterns, and interaction networks. *ISME J.* 1–14. <https://doi.org/10.1038/s41396-022-01336-2>.
- Wang, H., Liu, S.-R., Wang, J.-X., Shi, Z.-M., Xu, J., Hong, P.-Z., Ming, A.-G., Yu, H.-L., Chen, L., Lu, L.-H., Cai, D.-X., 2016. Differential effects of conifer and broadleaf litter inputs on soil organic carbon chemical composition through altered soil microbial community composition. *Sci. Rep.* 6, 27097. <https://doi.org/10.1038/srep27097>.
- Wang, P., Li, S.-P., Yang, X., Zhou, J., Shu, W., Jiang, L., 2020. Mechanisms of soil bacterial and fungal community assembly differ among and within islands. *Environ. Microbiol.* 22, 1559–1571. <https://doi.org/10.1111/1462-2920.14864>.
- White, T.J., Bruns, T.D., Lee, S., Taylor, J., 1990. Amplification and direct sequencing of fungal ribosomal RNA genes for phylogenetics. In: Innis, M.A., Gelfand, D.H., Sninsky, J.J., White, T.J. (Eds.), *PCR Protocols: A Guide to Methods and Applications*. Academic Press, San Diego, pp. 315–322.
- Wilhelm, R.C., Singh, R., Eltis, L.D., Mohn, W.W., 2019. Bacterial contributions to delignification and lignocellulose degradation in forest soils with metagenomic and quantitative stable isotope probing. *ISME J.* 13, 413–429. <https://doi.org/10.1038/s41396-018-0279-6>.
- Xu, J., Guo, B.-H., 2010. Poly(butylene succinate) and its copolymers: research, development and industrialization. *Biotechnol. J.* 5, 1149–1163. <https://doi.org/10.1002/biot.201000136>.
- Yamamoto-Tamura, K., Hoshino, Y.T., Tsuboi, S., Huang, C., Kishimoto-Mo, A.W., Sameshima-Yamashita, Y., Kitamoto, H., 2020. Fungal community dynamics during degradation of poly(butylene succinate-co-adipate) film in two cultivated soils in Japan. *Biosci. Biotechnol. Biochem.* 84, 1077–1087. <https://doi.org/10.1080/09168451.2020.1713718>.
- Yang, Y., Liu, W., Zhang, Z., Grossart, H.-P., Gadd, G.M., 2020. Microplastics provide new microbial niches in aquatic environments. *Appl. Microbiol. Biotechnol.* 104, 6501–6511. <https://doi.org/10.1007/s00253-020-10704-x>.
- Zang, H., Zhou, J., Marshall, M.R., Chadwick, D.R., Wen, Y., Jones, D.L., 2020. Microplastics in the agroecosystem: are they an emerging threat to the plant-soil system? *Soil Biol. Biochem.* 148, 107926. <https://doi.org/10.1016/j.soilbio.2020.107926>.
- Zhang, S.-J., Zeng, Y.-H., Zhu, J.-M., Cai, Z.-H., Zhou, J., 2022. The structure and assembly mechanisms of plastisphere microbial community in natural marine environment. *J. Hazard. Mater.* 421, 126780. <https://doi.org/10.1016/j.jhazmat.2021.126780>.
- Zhou, J., Ning, D., 2017. Stochastic community assembly: does it matter in microbial ecology? *Microbiol. Mol. Biol. Rev.* 81, e00002-17. <https://doi.org/10.1128/MMBR.00002-17>.
- Zhou, J., Deng, Y., Luo, F., He, Z., Yang, Y., 2011. Phylogenetic molecular ecological network of soil microbial communities in response to elevated CO₂. *mBio* 2, e00122-11. <https://doi.org/10.1128/mBio.00122-11>.

Plastic 1 – Supplementary Information

Fate of a biodegradable plastic in forest soil: Dominant tree species and forest types drive changes in microbial community assembly, influence the composition of plastisphere, and affect poly(butylene succinate-co-adipate) degradation.

Author: Benjawan Tanunchai*, Li Ji*, Olaf Schröder, Susanne Julia Gawol, Andreas Geissler, Sara Fareed Mohamed Wahdan, François Buscot, Stefan Kalkhof, Ernst-Detlef Schulze, Matthias Noll, Witoon Purahong.

*These authors contributed equally to this work.

Status: Published

Publication: Science of The Total Environment

Publisher: Elsevier

Date: 15 May 2023

Science of the Total Environment 873 (2023) 162230

IF (2021) = 10.753

Available online at: <https://doi.org/10.1016/j.scitotenv.2023.162230>

Please see separate attachments



Cite this: *Environ. Sci.: Processes Impacts*, 2022, 24, 233

Received 11th October 2021
Accepted 10th January 2022

DOI: 10.1039/d1em00426c

rscl.li/esp

Nitrogen fixing bacteria facilitate microbial biodegradation of a bio-based and biodegradable plastic in soils under ambient and future climatic conditions†

Benjawan Tanunchai,[†] Stefan Kalkhof,[†] Vusal Guliyev,[†] Sara Fareed Mohamed Wahdan,^{ae} Dennis Krstic,^c Martin Schädler,^{fg} Andreas Geissler,^h Bruno Glaser,ⁱ François Buscot,^{id} Evgenia Blagodatskaya,^{aj} Matthias Noll^{id} and Witoon Purahong^{id}

We discovered a biological mechanism supporting microbial degradation of bio-based poly(butylene succinate-co-adipate) (PBSA) plastic in soils under ambient and future climates. Here, we show that nitrogen-fixing bacteria facilitate the microbial degradation of PBSA by enhancing fungal abundance, accelerating plastic-degrading enzyme activities, and shaping/interacting with plastic-degrading fungal communities.

Introduction

Bio-based and biodegradable plastics offer several advantages over conventional plastics, *e.g.*, saving fossil fuels, improving carbon turnover, and reducing greenhouse gas emissions.^{1–4} Thus, traditional petroleum-based and non-biodegradable plastics are anticipated to be replaced by bio-based and biodegradable plastics in the near future.¹ Some types of bio-based and biodegradable plastics such as poly(butylene adipate terephthalate) (PBAT) and different derivatives of poly(butylene succinate) (PBS) have been tested so far to be more environmentally friendly and less toxic to animals, plants, and soil microorganisms than petroleum-based and non-biodegradable plastics.^{1,3} These bio-based and biodegradable plastics are susceptible to lipolytic enzyme activity produced by microorganisms ubiquitously distributed in natural environments,

Environmental significance

Despite a large part of plastic released in the environment is ending in soils, we know very little on how and by whom plastics, especially bio-based and biodegradable plastics are decomposed under natural field conditions by soil microorganisms. For the first time, we discovered a biological mechanism supporting microbial degradation of a bio-based poly(butylene succinate-co-adipate) (PBSA) plastic in field soils under ambient and future climates. We demonstrate that nitrogen-fixing bacteria facilitate the microbial degradation of PBSA by enhancing fungal abundances, accelerating plastic degrading enzyme activities and shaping/interacting with plastic-degrading fungal communities. The biological mechanism supporting microbial degradation of a bio-based PBSA can be applied to other bio-based and biodegradable plastics owning their similar characteristics as nitrogen poor substrates.

including both terrestrial and aquatic ecosystems.^{2,5} Although a large part of the plastic released in the environment ends in soils, little is known about how and by what kind of soil microorganisms plastics, especially bio-based and biodegradable plastics, are decomposed under natural field conditions.^{1,6} The biological mechanisms behind the microbial degradation of bio-based and biodegradable plastics remain almost unexplored.⁶

The majority of bio-based and biodegradable plastics are characterized by being too nutrient-poor substrates to decay in

^aUFZ-Helmholtz Centre for Environmental Research, Department of Soil Ecology, Theodor-Lieser-Str. 4, D-06120 Halle (Saale), Germany. E-mail: witoon.purahong@ufz.de

^bBayreuth Center of Ecology and Environmental Research (BayCEER), University of Bayreuth, Bayreuth, Germany

^cCoburg University of Applied Sciences and Arts, Institute for Bioanalysis, Friedrich-Streib-Str. 2, D-96450 Coburg, Germany. E-mail: matthias.noll@hs-coburg.de

^dInstitute of Soil Science and Agrochemistry of Azerbaijan National Academy of Sciences, M.Rahim, AZ1073, Baku, Azerbaijan

^eDepartment of Botany, Faculty of Science, Suez Canal University, Ismailia, 41522, Egypt

^fUFZ-Helmholtz Centre for Environmental Research, Department of Community Ecology, Theodor-Lieser-Str. 4, D-06120 Halle (Saale), Germany

^gGerman Centre for Integrative Biodiversity Research (iDiv) Halle-Jena-Leipzig, Deutscher Platz 5e, D-04103 Leipzig, Germany

^hDepartment of Macromolecular Chemistry and Paper Chemistry, Technical University of Darmstadt, Darmstadt D-64287, Germany

ⁱSoil Biogeochemistry, Martin Luther University Halle-Wittenberg, Von-Seckendorff-Platz 3, 06120 Halle, Germany

^jRUDN University, 6 Miklukho-Maklaya St, Moscow, 117198, Russia

† Electronic supplementary information (ESI) available. See DOI: 10.1039/d1em00426c

‡ These authors contributed equally to the manuscript.

nature, because, in contrast to their high carbon (C) content, their nitrogen (N) content is extremely low, resulting in a high C : N ratio.^{6–8} N is among the most important elements for microbial growth, proliferation, and enzymatic activities.⁹ To decompose N-poor substrates, microbes presumably need to establish an N uptake system from the soil or other environments.^{10,11} Knowledge on the decomposition of N-poor substrates such as deadwood^{10,12} and some specific types of leaf litter^{11,13} can help to understand the bio-based and biodegradable plastic decomposition in natural ecosystems.⁶ In such environments, saprotrophic fungi are the main decomposers that produce high biomass and extracellular enzymes to accelerate deadwood and leaf litter decay.^{13,14} However, these fungi are accompanied by bacterial communities, and some recent studies suggest that decomposition of these N-poor substrates is the result of inter-kingdom taxonomic and functional succession.^{13,15} Furthermore, the establishment of an N uptake system and accumulation of N in substrates have also been suggested as the rate-limiting steps of microbial degradation in N-poor substrates.¹¹ While fungi are able to translocate N from soil and other nutrient patches (e.g., soil organic matter and N-rich decomposing plant material) to N-poor substrates,¹⁶ they also commonly obtain N by establishing relationships with microorganisms that are capable of fixing atmospheric N₂.^{12,13,17} The contribution of N-fixing microorganisms to total N accumulation in N-poor substrates may be highly variable in different systems.¹⁰ A recent study found that biological N₂ fixation plays a major role in the increase in wood N content by contributing up to 60% of the total N accumulation in deadwoods.¹⁰

Climate change has been reported to alter microbial interactions in soil,^{18,19} with alterations in biodiversity and ecosystem productivity between ambient and predicted future climatic conditions. Our previous work on the degradation and microbiome of a bio-based and biodegradable plastic packaging and mulching film poly(butylene succinate-co-adipate) (PBSA) under ambient and future predicted climates for the years 2070–2100 showed that the molar and gravimetric masses of PBSA begin to drop at 180 days in soils after the blooming of N-fixing bacteria and of the main PBSA fungal colonizers (*Tetradcladium* spp.) under both climate treatments.⁶ The gravimetric and molar mass of PBSA were substantially reduced (28–33%) after 328 days in both climates.⁶ Consistent with a previous study, we found that fungi were the main decomposers, secreting enzymes to decompose PBSA films.²⁰ However, we also found that bacteria (including known PBS-based plastic decomposing bacteria) increased their abundance and co-dominated in PBSA over time. Interestingly, we often detected diverse taxonomic and functional groups of N-fixing bacteria, including both non-symbiotic N-fixing bacteria (NSNB: aerobic [NSNAB], facultative anaerobic [NSNFB], anaerobic and photosynthetic bacteria [NSNPB]), and symbiotic N-fixing bacteria (SNB). Although the relationships between fungi and N-fixing bacteria were suspected, we did not test them in our previous study.⁶ The relevance of interkingdom succession in PBSA biodegradation turnover and the interplay of fungal enzyme activities and N-fixing bacteria are not understood. In this study, we aimed to (i) provide insights into the taxonomic and

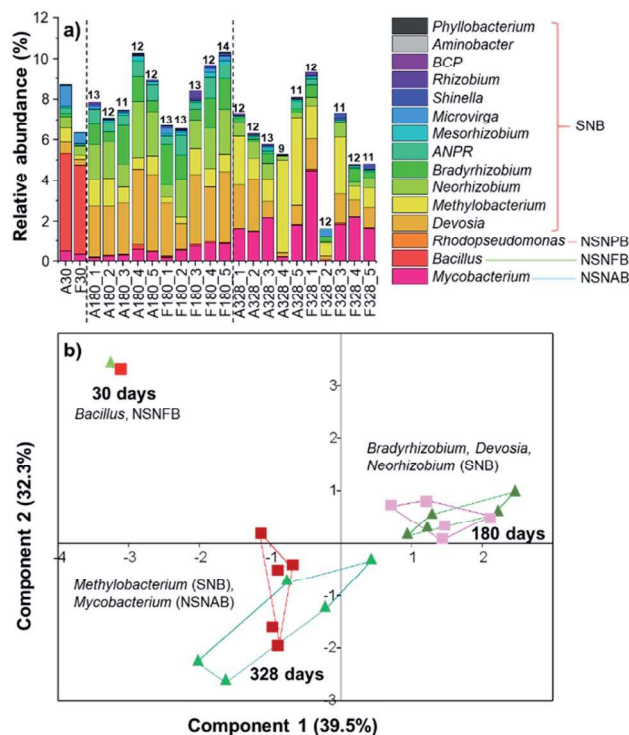


Fig. 1 Nitrogen-fixing bacterial community composition associated with PBSA degradation. (a) Taxonomic richness and relative abundances at the genus level, and (b) temporal shifts in community composition based on principal component analysis. A, present ambient climatic conditions; ANPR, *Allorhizobium*–*Neorhizobium*–*Pararhizobium*–*Rhizobium* complex; BCP, *Burkholderia*–*Caballeronia*–*Paraburkholderia* complex; F, future climatic conditions; NSNAB, non-symbiotic nitrogen-fixing aerobic bacteria; NSNFB, non-symbiotic nitrogen-fixing facultative anaerobic bacteria; NSNPB, non-symbiotic nitrogen-fixing anaerobic and photosynthetic bacteria; SNB, symbiotic nitrogen-fixing bacteria. 30, 180, and 380 indicate days after the beginning of the experiment. Green and red-pink color indicate data point in ambient and future climate plots, respectively.

functional groups of N-fixing bacteria associated with a bio-based and biodegradable plastic PBSA film during the early to intermediate phases of degradation, and (ii) investigate the potential role of N-fixing bacteria in the biodegradation of bio-based and biodegradable plastic PBSA films in soils under ambient and future climatic conditions. Despite the fact that we detected high relative abundances (up to 10% in each PBSA sample) and a wide-ranging diversity of N-fixing bacteria in PBSA samples, their genomic background makes it unlikely that they could degrade PBSA themselves. We therefore hypothesized that N-fixing bacteria may rather facilitate the PBSA degradation process by promoting fungal abundance and interacting with the main PBSA fungal colonizers as well as the entire PBSA-associated fungal community. We expected that the main PBSA fungal colonizers and the PBSA-associated fungal community interacted differently with the different N-fixing bacteria under ambient and future climatic conditions.

Moreover, additional laboratory experiments were carried out to (iii) determine whether N fixation was the rate-limiting step and was directly linked to PBSA degradation processes in

soils. We hypothesized that the dominant functional groups of N-fixing bacteria would differ under field and laboratory conditions. Under field conditions, SNB can be dominant in the presence of plants and light, so that SNB can live symbiotically with plants that provide them with habitats and photosynthates in exchange for a portion of fixed N₂.²¹ To show this unambiguously, we hypothesized that PBSA in soil under laboratory conditions was dominated by free-living N-fixing bacteria, including NSNAB and NSNFB, while SNB disappeared due to the absence of their plant hosts. In soils with N addition, N fixation is no more required/or less important for PBSA degradation; thus, all functional groups of N-fixing bacteria strongly decrease in relative abundances or are even absent from PBSA. As we expected that N fixation were the rate-limiting step in PBSA decomposition processes in soils, we hypothesized that adding the product of N fixation (ammonium, NH₄⁺) to the experimental system would accelerate the PBSA decomposition process by increasing lipase activity in the early phase of PBSA degradation. Lipase has been reported to be an important PBSA degradation enzyme.²²

Methods

Field experiment on PBSA degradation in soil under ambient and future climate conditions

The PBSA degradation experiment was carried out for 328 days in soils at the conventional farming treatment plots (crop rotation: winter rape, winter wheat, and winter barley) of the Global Change Experimental Facility²³ (GCEF), Bad Lauchstädt, Central Germany (51° 22' 60"N, 11° 50' 60"E, 118 m a.s.l.). The basic soil conditions were similar for all experimental plots (classified as Haplic Chernozems, C : N ratio ≈ 10, pH = 7.2). The climate treatment simulates a future climatic projection for Central Germany in the time period 2070–2100 as a mean scenario across several climate models, resulting in reduced summer precipitation by approximately 20%, increased precipitation in spring and autumn by approximately 10%, and increased mean temperature by 0.55 °C.²³ Climate change is known to be one of the most important factors that influence the soil microbiome and their interactions.^{18,19} We set up our PBSA degradation field experiment under both ambient and future climate conditions to investigate the effects of future climate change on the interactions between fungi and N-fixing bacteria. We placed PBSA films (BioPBS FD92, PTT MCC Biochem Company Limited, Thailand; 35% of bio-based carbon derived from corn) in the form of a double-layer thin film with 50 μm thickness on top of the soil in conventional farming plots under both present and future climatic regimes.⁶ Sample setup and sampling were carried out as explained earlier⁶ and are summarized in the ESI.†

Identification and quantification of PBSA-associated bacteria and fungi using high-throughput sequencing and quantitative real-time PCR

We reanalyzed existing datasets on the PBSA microbiome (bacteria and fungi) from our previous PBSA decomposition

study.⁶ The raw bacterial 16S and fungal ITS rRNA gene sequences were deposited in the National Center for Biotechnology Information (NCBI) Sequence Read Archive under the accession number PRJNA595487. Quantitative real-time PCR was used to quantify the fungal abundance (ng DNA per cm² PBSA film). All laboratory procedures have been published elsewhere⁶ and summarized in the ESI.† Potential N-fixing bacteria assignments were carried out from the same bacterial datasets using FAPROTAX and relevant literature,^{24,25} including both N-fixing bacteria associated with cereals (dominant plants in the study plots)²⁶ and legume plants (common plants in this study area).²⁷ All identified N-fixing bacteria are presented in the ESI;† they have been separated into different functional groups: NSNAB, NSNFB, NSNPB, and SNB (Table S1†). In addition, the highly conserved *nifH* gene, which encodes the key iron protein of the nitrogenase complex (nitrogenase reductase) to fix atmospheric N₂,²⁸ was used as an indicator of the abundance of N-fixing bacteria. Their abundance is commonly used to represent potential N fixation.²⁸ The copy number of *nifH* genes was quantified for all PBSA samples collected at 30, 180, and 328 days (same DNA extracts used for Illumina sequencing) by quantitative PCR using the Pol primer set (PolF and PolR) as explained earlier.^{29–31} Various indicators of N-fixing bacteria (richness and relative abundances of specific N-fixing bacterial operational taxonomic units [OTUs] and functional groups, as well as *nifH* gene copy numbers) and fungi (fungal abundance, specific relative abundances of dominant fungal OTUs [relative abundances > 0.5%], and the entire fungal community) were used to test our hypotheses on the role of N-fixing bacteria in facilitating microbial biodegradation of PBSA.

Laboratory experiment on the rate-limiting step in PBSA degradation

To demonstrate that N fixation is the rate-limiting step in PBSA degradation in soil, we set-up a PBSA laboratory decomposition experiment using the soil from the GCEF experimental plot as described in our previous study.³² Briefly, PBSA films were treated with 70% ethanol to sterilize their surfaces and cut into pieces (2–5 mm × 2–5 mm). These pieces (1 g or 6% PBSA, w/w) were buried in sterile glass jars containing 15.7 g dry soil equivalent from one of the two following treatments: (i) soil (PBSA-soil; PS treatment) and (ii) soil with N addition (PBSA-soil-N; PSN treatment), with five independent replicates. In the PSN treatment, the soil was supplemented with the same amount of N (1.4 mL of 1.42 M (NH₄)₂SO₄, equivalent to 0.055 g N per jar or 280 kg N per hectare which is comparable to the highest rate of N fertilisation used in agroecosystems)³² that is usually present in the initial soil without PBSA. Soils without PBSA (with and without N amendment, 16.7 g) were used as controls. We also buried 1 g PBSA in 15.7 g autoclaved soil with similar N supplementation aiming to differentiate between microbial and chemical degradation of PBSA. PBSA-associated microorganisms were analyzed by scanning electron microscopy (SEM) at 0, 30, and 90 days, and gravimetric mass loss of

PBSA as well as microbial community patterns were analyzed after 90 days of incubation using an Illumina MiSeq system with the primer sets described in our previous study (515F/806R for bacteria and fITS7/ITS4 for fungi).³² The raw bacterial 16S and fungal ITS rRNA gene sequences were deposited in the National Center for Biotechnology Information (NCBI) Sequence Read Archive under the accession number PRJNA702448. All laboratory procedures for Illumina sequencing and SEM were done as previously described.^{6,32} Lipase activities in soil were also measured fluorometrically using 4-methylumbelliferone (MUF) at day 90.³³

We set up another PBSA degradation experiment with the same settings (6% PBSA (w/w), five true replicates) as those described earlier, except that the soil and soil-PBSA volumes were increased to 30 g. These samples were incubated in a Respicond V automatic respirometer³⁴ (Nordgren Innovations & Design AB, Hässelby, Sweden) at a constant temperature of 22 °C, in the dark, for 90 days for measuring microbial respiration. After the incubation period, ATR-FTIR spectroscopy was used to investigate the chemical composition of the PBSA samples. Briefly, all samples were washed with phosphate buffered saline and dried at room temperature prior ATR-FTIR analyses using a Nicolet 6700 FTIR equipped with an ATR assembly. Additionally, for a bulk analysis of PBSA, the polymer foils were dissolved in dichloromethane and dried, and the resulting films were investigated. In total, 16 scans within a range of 4000–650 cm⁻¹ were accumulated with a resolution of 4 cm⁻¹. The gravimetric mass loss of PBSA was calculated as explained earlier.^{32,35}

Statistical analysis

The effects of sampling time and climate conditions on N-fixing bacterial community composition at the genus level were visualized and analyzed using principal component analysis (PCA) and two-way permutational multivariate analysis of variance (PERMANOVA). All correlation analyses were conducted using the Spearman's rank correlation. We used Spearman rank correlation between frequently detected PBSA fungal colonisers and N-fixing bacteria to assess the co-occurrence network patterns of the fungal and N-fixing bacterial communities. The co-occurrence network patterns of PBSA fungal colonizers and N-fixing bacterial communities under ambient and future climate conditions were constructed based on the resulting Spearman's rank correlation values (threshold at $\rho \geq 0.65$, $P < 0.05$). The correlation matrix was visualized, and the networks were extracted using Cytoscape v.3.8.0.³⁶ The values of Spearman's rank correlation coefficient were used to determine the thickness of the connection line (edges). The effects of climate, incubation time, and N-fixing bacteria on PBSA-derived fungal community composition under field conditions were tested using non-metric multidimensional scaling (NMDS) based on the Jaccard distance measure and envfit function implemented in the Vegan package in R.³⁷ Comparisons of mean values between different treatments were performed using either a *t*-test or an analysis of variance (ANOVA). All datasets were tested for normality (using a Jarque-Bera test) and homogeneity of

variance (using an *F*-test or Levene's test). Effects of climate treatments and incubation time (180 vs. 328 days) on the N-fixing bacterial richness, relative abundance, and *nifH* gene copy numbers were analyzed using repeated measures ANOVA (after defining climate as between plot factor and time as within plot factor). All statistical analyses were performed using PAST v.2.17³⁸ and IBM SPSS Statistics 22.

Results and discussion

We detected diverse taxonomic and functional groups of potential N-fixing bacteria associated with PBSA under field conditions. These include at least 15 genera of four functional groups: NSNAB (*Mycobacterium*), NSNFB (*Bacillus*), NSNPB (*Rhodopseudomonas*) and SNB (dominated by *Devosia*, *Methylobacterium*, *Neorhizobium*, *Bradyrhizobium*, and the *Allo-rhizobium-Neorhizobium-Pararhizobium-Rhizobium* (ANPR) complex) (Fig. 1), which have been detected over time on PBSA (Table S1†). The relative abundance of N-fixing bacteria mostly ranged between 6% and 10%. SNB had the highest richness at both the genus and OTU levels. Taxonomic and functional shifts of N-fixing bacteria were observed at different incubation times. At 30 days, NSNFB (*Bacillus*) and, at 180 days, SNB (*Devosia*, *Neorhizobium*, and *Bradyrhizobium*) dominated the N-fixing bacterial community, whereas at 328 days, NSNAB (*Mycobacterium*) co-dominated with SNB (*Methylobacterium*) (Fig. 1). *Devosia*, *Neorhizobium*, and *Bradyrhizobium* strongly declined in relative abundance at 328 days. Climate treatments had no significant effect on N-fixing bacterial richness, community composition, and *nifH* gene copy numbers ($P > 0.05$; Fig. 1a, b and S1†).

Nitrogen-fixing bacterial community composition ($F = 7.35$, $P = 0.001$), relative abundance ($F = 6.58$, $P = 0.033$), and *nifH* gene copy numbers ($F = 26.09$, $P < 0.001$) were significantly affected only by incubation time. Incubation time also

Table 1 Spearman's rank correlations (ρ) between fungal abundance and *nifH* gene copy numbers, richness, and relative abundance of specific functional groups of N-fixing bacteria under ambient and future climatic conditions. Numbers in bold indicate values with a strong positive correlation

Pairwise comparison	ρ	<i>P</i> value
Ambient climatic conditions		
Fungal abundance – <i>nifH</i> gene copy numbers	0.80	0.001
Fungal abundance – rel. abundance NSNFB	0.77	0.009
Fungal abundance – rel. abundance SNB	0.72	0.019
Fungal abundance – richness NSNFB	0.74	0.015
Fungal abundance – richness SNB	0.21	0.551
Future climatic conditions		
Fungal abundance – <i>nifH</i> gene copy numbers	0.86	<0.001
Fungal abundance – rel. abundance NSNFB	0.38	0.273
Fungal abundance – rel. abundance SNB	0.94	<0.001
Fungal abundance – richness NSNFB	0.10	0.787
Fungal abundance – richness SNB	0.80	0.006

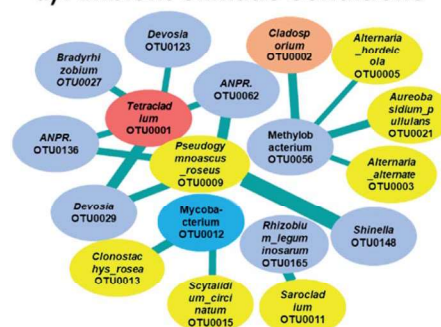
marginally affected the richness of N-fixing bacteria ($F = 4.35$, $P = 0.071$).

The *nifH* gene copy numbers and fungal abundance in both ambient ($\rho = 0.80$, $P = 0.001$) and future climate ($\rho = 0.86$, $P < 0.001$) treatments had a strong positive correlation, indicating that N-fixing bacteria significantly promoted fungal abundance by providing fixed N (Table 1). The relative abundance and richness of N-fixing bacteria also significantly correlated with fungal abundance and community composition (Tables 1 and 2). However, both symbiotic and non-symbiotic N-fixing bacteria significantly correlated with fungal abundance under ambient climate, whereas only symbiotic N-fixing bacteria correlated with fungal abundance under future climatic conditions (Table 1). Likewise, our previous study also showed that the relative abundances of dominant PBSA fungal colonizers (e.g., *Tetracladium* and *Cladosporium*) also highly correlated ($\rho > 0.77$, $P < 0.01$) with both symbiotic and non-symbiotic N-fixing bacteria in ambient climate and only with symbiotic N-fixing bacteria in future climatic conditions.⁶ This is consistent to our hypothesis that in N limiting substrates, N-fixing bacteria can provide fixed N which is benefit to fungi as an additional source of N to promote their growth and reproduction. A study provides evidence that N-fixing bacteria can promote fungal reproduction in N limiting substrates,¹² however up to now, there still no clear evidence on how fungi can promote N-fixing bacteria in such habitats.

Network analyses revealed that the dominant fungal taxa interacted with different N-fixing bacteria under both climatic conditions (Fig. 2). The key microbial hubs under ambient (SNB: *Methylobacterium*; fungi: *Tetracladium* and *Pseudogymnoascus roseus*) and future climate (NSNAB: *Mycobacterium*; fungi: *Cladosporium* and *Pseudogymnoascus roseus*) were different.

Under laboratory conditions, we showed that N fixation was the rate-limiting step in PBSA degradation in soil (Fig. 3 and 4). The addition of $(\text{NH}_4)_2\text{SO}_4$ to the soil system significantly

a) Ambient climatic conditions



b) Future climatic conditions

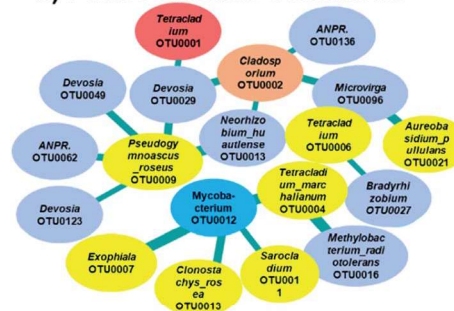


Fig. 2 PBSA fungal colonizers (red, orange and yellow nodes) and N-fixing bacterial (blue nodes) network detected in ambient (a) and future (b) climatic conditions. Line thickness represents the correlation (ρ) values between 0.65–0.91. Sampling time and N-fixing bacteria significantly affected fungal community composition (in terms of richness and relative abundances of NSNB and relative abundances of NSNAB, both globally and as individual OTUs) (Table 2). To sum up, N-fixing bacteria were important for overall fungal abundance, main fungal colonizers, fungal succession, and community composition.

enhanced fungal colonization (Fig. 3g–j). The PSN treatment led to the formation of a network of fungal hyphae, visible to the naked eye, that covered the entire PBSA surface after only a few weeks (Fig. 3g). Compared to the initial PBSA (Fig. 3a and b), the polyester under this hyphal layer had an extremely rough, sponge-like structure due to intensive degradation (Fig. 3h). Under PSN conditions, the material degradation after 30 and 90 days, clearly exceeded the degree of degradation observed in PBSA subjected to the PS treatment at the same sampling times (Fig. 4a and d). In contrast to the PS treatment, where in some cases considerable local differences in colonization and material degradation were observed (Fig. 3c–f), the N amendment resulted in a much more uniform appearance of the samples (Fig. 3g–j). The formation of punctual microhabitats due to the local availability of N and the associated “pitting” obviously played a subordinate role during PSN treatment. The complex PBSA microbiome resulting from the PSN treatment after 90 days (Fig. 3i and j) was found to be similar to that of those without N after 328 days of field-based incubations (data not shown). The PSN treatment also enhanced microbial respiration (Fig. 4a) and lipase activity (Fig. 4b and c). Microbial respiration was activated very early in the PSN treatment (after 7 days) as compared with that in the PS treatment (after 30 days). The degradation rates of PBSA after 90 days were also

Table 2 Effects of climatic conditions, incubation time, and N-fixing bacteria on fungal community composition under field conditions. NMDS = non-metric multidimensional scaling. Numbers in bold and italic indicate values with significant ($P < 0.05$) and marginal significant ($P < 0.1$) correlations

Factors	NMDS1	NMDS2	r^2	P
Climate	1.00	0.02	0.03	0.761
Incubation time	0.86	0.50	0.76	0.001
Richness NSNB	−0.93	0.37	0.01	0.914
Richness SNB	−0.72	−0.69	0.45	0.004
OTU0012 <i>Mycobacterium</i>	1.00	0.09	0.42	0.010
OTU0062 ANPR	−0.93	−0.37	0.48	0.005
OTU0013 <i>Neorhizobium</i>	−0.82	−0.57	0.51	0.007
OTU0136 ANPR	−0.95	−0.31	<i>0.29</i>	<i>0.051</i>
OTU0027 <i>Bradyrhizobium</i>	−0.82	−0.57	<i>0.29</i>	<i>0.051</i>
OTU0029 <i>Devosia</i>	−0.89	−0.46	0.59	0.001
OTU0016 <i>Methylobacterium</i>	0.26	0.96	0.34	0.029
Rel. abundance NSNAB	1.00	0.09	0.42	0.010
Rel. abundance NSNFB	−0.97	0.24	0.12	0.314
Rel. abundance SNB	−0.98	−0.19	0.57	0.006

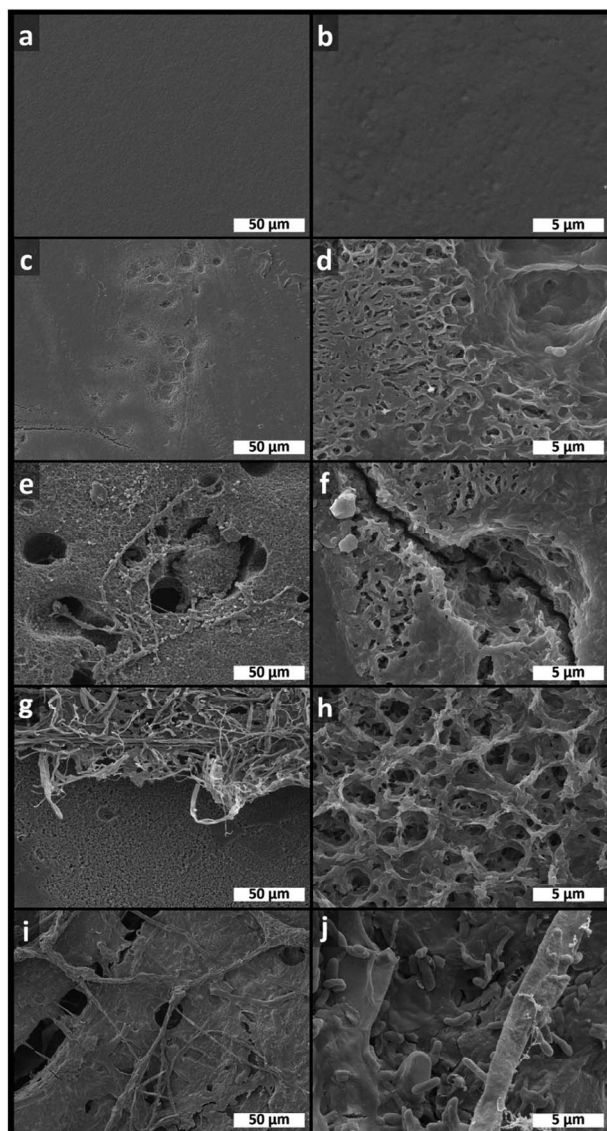


Fig. 3 SEM images of poly(butylene succinate-co-adipate) (PBSA) surfaces at initial state (a and b), after 30 (c and d) and 90 days under PS treatment (e and f), and after 30 (g and h) and 90 days under PSN treatment (i and j). Magnifications in image columns are 1000 \times (left) and 10 000 \times (right).

significantly higher in the PSN treatment ($60.4 \pm 8.5\%$) than in the PS treatment ($12.6 \pm 3.9\%$) (Fig. 4d).

Both the decellularized and cleaned surfaces of PBSA samples incubated in a respirometer as well as the bulk of the remaining PBSA were studied using ATR-FTIR spectroscopy. Under all conditions, a strong band at 1720 cm^{-1} was observed, corresponding to the C=O stretching vibrations of the ester groups (Fig. 4e). Furthermore, a broad peak at 2950 cm^{-1} attributed to C-H stretching vibrations and additional bands in the range of $1300\text{--}1100\text{ cm}^{-1}$ belonging to stretching vibrations of the C-O-C group, which are all characteristic of aliphatic polyesters, were always present (Fig. 4e). Interestingly, in the surface analyses of PBSA under the PSN treatment, additional amide I and II bonds caused by N-H bending vibrations were

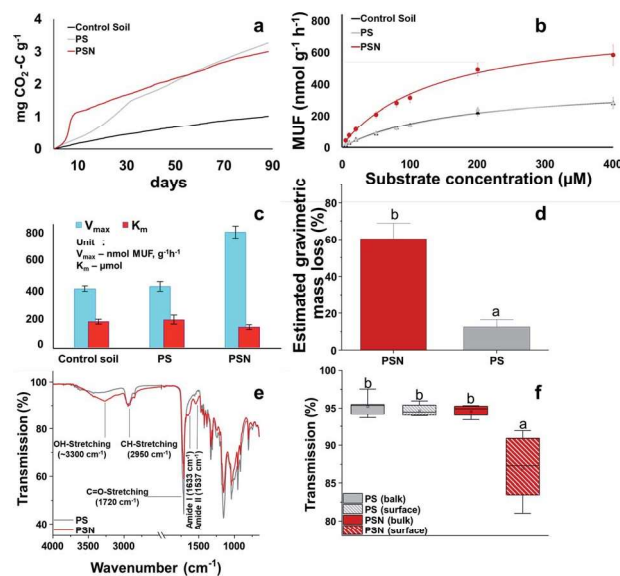


Fig. 4 Acceleration of PBSA decomposition shown by (a) CO₂ emission for 90 days; (b and c) increased lipase activity; (d) increased gravimetric mass loss; and (e and f) ATR-FTIR measurements. By ATR-FTIR, the presence of amide I and II bands as well as an increase of O-H/N-H bending vibrations (e) was observed indicating increased degradation as well as the formation of ester amides at the PBSA surface. (f) ATR-IR transmission of amides from bulk or surface PBSA analyses. Different letters indicate significant differences according to *t*-test or ANOVA ($P < 0.05$).

detected at 1633 and 1537 cm^{-1} (Fig. 4e). These bands may be caused by a degradation process with the formation of polymer amides instead of the sole formation of carbonic acids as degradation hydrolysis products. Furthermore, there is a broad absorption at $\approx 3300\text{ cm}^{-1}$, which is typical for O-H and N-H stretching vibrations. These shifts were comparable to the spectra of amidated poly(ethylene adipate) or poly(ethylene succinate) obtained by Mohamed *et al.*³⁹ Interestingly, these amide bands were not present even after N amendment when the soil was autoclaved (Fig. S2[†]). In summary, only the surface spectra of the samples with N amendment that had not been autoclaved (PSN treatment) and none of the bulk spectra or the surface spectra without N addition (PS treatment) showed bands representative of amides (Fig. 4f). This observation could be explained by the formation of amidated PBSA during degradation due to microbial activity or by the presence of other adducts bound to the surface that are specifically formed under N-fixation conditions when sufficient N is fixed and available on the PBSA surface and surrounding soil. Important data of the surface analyses by ATR-FTIR are summarized in the ESI.[†]

The addition of PBSA or PBSA + N to soils caused significant changes in both the soil and PBSA microbiomes (Fig. 5). Different fungal OTUs were enriched in the PBSA samples of the PS and PSN treatments. *Tetracladium*, *Exophiala*, and *Ilyonectria macrodidyma* dominated the PBSA samples of the PS treatment, but *Fusarium solani* dominated those of the PSN treatment (Fig. 5e). The fungal diversity and richness from the PS treatment were similar to those observed in the early to intermediate

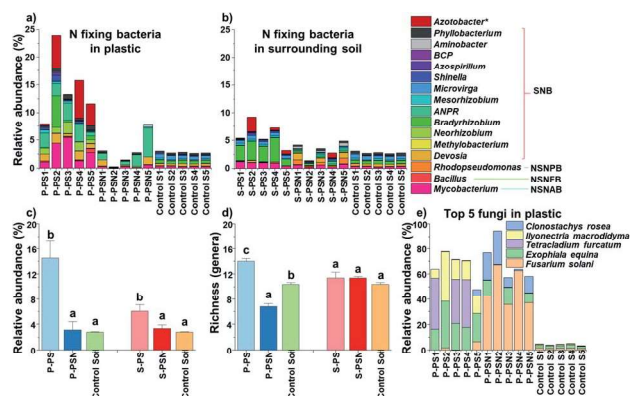


Fig. 5 Microorganisms associated with PBSA. (a) Dominant N-fixing bacterial genera on PBSA under PS (P-PS) and PSN (P-PSN) treatments; (b) dominant N-fixing bacterial genera of the PBSA surrounding soils of the PS (S-PS) and PSN (S-PSN) treatments and control soils. (c) Average relative abundances, (d) richness of N-fixing bacterial genera, and (e) main fungal PBSA colonizers with ability to produce lipase. Different letters indicate significant differences according to ANOVA ($P < 0.05$).

decomposing stages of PBSA under field conditions.⁶ N-fixing bacteria were found to be more dominant in PBSA samples of the PS treatment (the relative abundances of the five dominant genera ranged between 10% and 26%) than in field incubations (with a maximum abundance of ~10%) (Fig. 1a and 5a). In general, N-fixing bacteria were strongly enriched and were more diverse in PBSA than in the surrounding soil, especially in the PS treatment (Fig. 5a and b). Interestingly, we found that SNB (e.g., *ANPR*, *Bradyrhizobium*, *Devosia*, and *Neorhizobium*) together with NSNAB (*Mycobacterium*) and NSNFB (*Bacillus*) co-dominated the N-fixing bacterial communities in PBSA under PS treatment (Fig. 5a and b). Our lab experiment revealed that SNB survived or were even enriched after 90 days in soil without any plant host with the aid of PBSA. In line with this result, we found that all N-fixing bacteria, especially SNB, were almost absent in the control soil without PBSA (Fig. 5a and b).

A recent study has also found that *Bradyrhizobium* (a SNB) may be enriched in soil after PBAT addition under laboratory conditions (without plants, at 30 °C, for 120 days).⁴⁰ In the current study, we showed that higher abundance of SNB was coupled with an increase in *nifH* gene copy numbers ($\rho = 0.51$, $P = 0.018$) (Fig. 1a). Based on metagenomic analyses, Han *et al.*⁴⁰ showed that *Bradyrhizobium* spp. carried PBAT hydrolase genes, and thus they were capable of efficiently degrading PBAT in soils. Although it is quite rare, some studies have shown simultaneous N fixation and growth on hydrocarbons of some N-fixing bacterial taxa.⁴¹ Taken together, we hypothesize that N-fixing bacteria may have two lifestyles: (i) as direct degraders and (ii) facilitators of biodegradable plastics. In contrast to the results from the PS treatment, the relative abundances of all functional groups of N-fixing bacteria on PBSA were strongly reduced or almost absent if N was added to the soil (PSN treatment) (Fig. 5a–c). Although some SNB (e.g., *Azotobacter* and *Bradyrhizobium*) were detected in all N-amended soil samples, they were unable to colonize the respective PBSA samples (Fig. 5a and b, and Table S2†). Furthermore, we only detected

nifH genes in the PBSA of the PS treatment, but not in that of the PSN treatment. This is consistent with our hypothesis that sufficient N supply in the soil caused no increase in N-fixing bacteria. Moreover, the microbial community in N-depleted ecosystems can directly decompose PBSA without delay in finding and employing N-fixing bacteria assisting decomposition processes.

Conclusions

Despite the large amount of bio-based and biodegradable plastics released in the environment ending in soils, little is known about how they are decomposed under natural conditions by soil microbial communities. Our study showed the biological mechanism behind microbial biodegradation of bio-based and biodegradable plastics under field soil conditions with ambient or future climatic conditions. While the establishment of fungal colonizers/decomposers occurred rapidly (within 30 days), they did not function efficiently. The system required assistance from diverse N-fixing bacteria to deliver N for fungal growth, reproduction, and enzyme production. We demonstrated that the establishment of bacterial N fixation in PBSA can take a long time; thus, it can be considered as a rate-limiting step in the microbial biodegradation of bio-based and biodegradable plastics. N amendment alleviated this limitation and accelerated the rate of PBSA degradation by up to five times in the same time frame. We conclude that cross-kingdom relationships between N-fixing bacteria and fungi are important for biodegradation of bio-based and biodegradable plastics under field soil conditions.

Author contributions

Conceptualization: WP, MN, and SK. Field experiment at GCEF: WP, BT, and MS. Laboratory experimental set-up: VG, BT, WP, and EB. Formal analysis: molecular analysis (BT and WP), *nifH* gene quantification (MN), enzyme analysis (VG and EB), CO₂ measurement (VG and EB), mass loss measurement (WP and BT), SEM (AG), and FTIR (SK and DK). Data analysis: WP, BT, SK, DK, and VG. Bioinformatics: SW. Methodology: WP, MN, SK, and EB. Resources: WP, MN, SK, and EB. Supervision: WP, MN, and EB. Visualization: WP, BT, VG, SK, and DK. Writing – original draft: BT, WP, and VG. Writing – review and editing: MN, WP, SK, EB, FB, BG, SW, DK, AG, and MS.

Conflicts of interest

There are no conflicts to declare.

Acknowledgements

The community composition data were computed at the High-Performance Computing (HPC) Cluster EVE, a joint effort of both the Helmholtz Centre for Environmental Research—UFZ and the German Centre for Integrative Biodiversity Research (iDiv) Halle-Jena-Leipzig. The authors thank Anna Heintz-Buschart (Metagenomics Support Unit, German Centre for

Integrative Biodiversity Research (iDiv) Halle-Jena-Leipzig) for bioinformatics support. We thank the Helmholtz Association, the Federal Ministry of Education and Research, the State Ministry of Science and Economy of Saxony-Anhalt, and the State Ministry for Higher Education, Research and the Arts Saxony for funding the Global Change Experimental Facility (GCEF) project. We also thank the staff of the Bad Lauchstädt Experimental Research Station (especially Ines Merbach and Konrad Kirsch) for their work in maintaining the plots and infrastructure of the GCEF, and Dr Stefan Klotz, Dr Harald Auge, and Dr Thomas Reitz for their roles in setting up the GCEF. We thank the Islamic Development Bank for funding Vusal Guliyev. We acknowledge a support of the RUDN University Strategic Academic Leadership Program.

References

- 1 T. P. Haider, C. Völker, J. Kramm, K. Landfester and F. R. Wurm, Plastics of the future? The impact of biodegradable polymers on the environment and on society, *Angew. Chem., Int. Ed. Engl.*, 2019, **58**, 50–62.
- 2 M. Gigli, A. Negroni, M. Soccio, G. Zanaroli, N. Lotti, F. Fava and A. Munari, Influence of chemical and architectural modifications on the enzymatic hydrolysis of poly(butylene succinate), *Green Chem.*, 2012, **14**, 2885–2893.
- 3 T. Iwata, Biodegradable and bio-based polymers: Future prospects of eco-friendly plastics, *Angew. Chem., Int. Ed. Engl.*, 2015, **54**, 3210–3215.
- 4 N. Cheroennet, S. Pongpinyopap, T. Leejarkpai and U. Suwanmanee, A trade-off between carbon and water impacts in bio-based box production chains in Thailand: A case study of PS, PLAS, PLAS/starch, and PBS, *J. Cleaner Prod.*, 2017, **167**, 987–1001.
- 5 A. Biundo, A. Hromic, T. Pavkov-Keller, K. Gruber, F. Quartinello, K. Haernvall, V. Perz, M. S. Arrell, M. Zinn, D. Ribitsch and G. M. Guebitz, Characterization of a poly(butylene adipate-co-terephthalate)-hydrolyzing lipase from *Pelosinus fermentans*, *Appl. Microbiol. Biotechnol.*, 2016, **100**, 1753–1764.
- 6 W. Purahong, S. F. M. Wahdan, D. Heinz, K. Jariyavidyanont, C. Sungkapreecha, B. Tanunchai, C. Sansupa, D. Sadubsarn, R. Alaneed, A. Heintz-Buschart, M. Schädler, A. Geissler, J. Kressler and F. Buscot, Back to the future: Decomposability of a biobased and biodegradable plastic in field soil environments and its microbiome under ambient and future climates, *Environ. Sci. Technol.*, 2021, **55**, 12337–12351.
- 7 S.-H. Pyo, J. H. Park, V. Srebny and R. Hatti-Kaul, A sustainable synthetic route for biobased 6-hydroxyhexanoic acid, adipic acid and ϵ -caprolactone by integrating bio- and chemical catalysis, *Green Chem.*, 2020, **22**, 4450–4455.
- 8 E. S. Stevens, *Green Plastics*, Princeton University Press, 2020.
- 9 L. Prescott, J. Harley and D. Klein, *Microbiology*, McGraw-Hill Higher Education, 1999.
- 10 K. T. Rinne, T. Rajala, K. Peltoniemi, J. Chen, A. Smolander and R. Mäkipää, Accumulation rates and sources of external nitrogen in decaying wood in a Norway spruce dominated forest, *Funct. Ecol.*, 2017, **31**, 530–541.
- 11 T. Osono and H. Takeda, Decomposition of organic chemical components in relation to nitrogen dynamics in leaf litter of 14 tree species in a cool temperate forest, *Ecol. Res.*, 2005, **20**, 41–49.
- 12 B. Hoppe, T. Kahl, P. Karasch, T. Wubet, J. Bauhus, F. Buscot and D. Krüger, Network analysis reveals ecological links between N-fixing bacteria and wood-decaying fungi, *PLoS One*, 2014, **9**, e88141.
- 13 W. Purahong, T. Wubet, G. Lentendu, M. Schloter, M. J. Pecyna, D. Kapturska, M. Hofrichter, D. Krüger and F. Buscot, Life in leaf litter: novel insights into community dynamics of bacteria and fungi during litter decomposition, *Mol. Ecol.*, 2016, **25**, 4059–4074.
- 14 T. Schneider, K. M. Keiblinger, E. Schmid, K. Sterflinger-Gleixner, G. Ellersdorfer, B. Roschitzki, A. Richter, L. Eberl, S. Zechmeister-Boltenstern and K. Riedel, Who is who in litter decomposition? Metaproteomics reveals major microbial players and their biogeochemical functions, *ISME J.*, 2012, **6**, 1749–1762.
- 15 S. R. Johnston, L. Boddy and A. J. Weightman, Bacteria in decomposing wood and their interactions with wood-decay fungi, *FEMS Microbiol. Ecol.*, 2016, **92**, DOI: 10.1093/femsec/fiw179.
- 16 J. B. Boberg, R. D. Finlay, J. Stenlid, A. Ekblad and B. D. Lindahl, Nitrogen and carbon reallocation in fungal mycelia during decomposition of boreal forest litter, *PLoS One*, 2014, **9**, DOI: 10.1371/journal.pone.0092897.
- 17 P. Weißhaupt, W. Pritzkow and M. Noll, Nitrogen metabolism of wood decomposing basidiomycetes and their interaction with diazotrophs as revealed by IRMS, *Int. J. Mass Spectrom.*, 2011, **307**, 225–231.
- 18 S. Wahdan, S. Hossen, B. Tanunchai, C. Sansupa, M. Schädler, M. Noll, Y.-T. Wu, F. Buscot and W. Purahong, Life in the wheat litter: effects of future climate on microbiome and function during the early phase of decomposition, *Microb. Ecol.*, 2021, DOI: 10.1007/s00248-021-01840-6.
- 19 J. E. Kostin, S. Cesarz, A. Lochner, M. Schädler, C. A. Macdonald and N. Eisenhauer, Land-use drives the temporal stability and magnitude of soil microbial functions and modulates climate effects, *Ecol. Appl.*, 2021, e2325.
- 20 K. Yamamoto-Tamura, Y. T. Hoshino, S. Tsuboi, C. Huang, A. W. Kishimoto-Mo, Y. Sameshima-Yamashita and H. Kitamoto, Fungal community dynamics during degradation of poly(butylene succinate-co-adipate) film in two cultivated soils in Japan, *Biosci., Biotechnol., Biochem.*, 2020, **84**, 1077–1087.
- 21 V. C. S. Pankiewicz, T. B. Irving, L. G. S. Maia and J.-M. Ané, Are we there yet? The long walk towards the development of efficient symbiotic associations between nitrogen-fixing bacteria and non-leguminous crops, *BMC Biol.*, 2019, **17**, 99.
- 22 A. Hoshino and Y. Isono, Degradation of aliphatic polyester films by commercially available lipases with special reference to rapid and complete degradation of poly(L-

- lactide) film by lipase PL derived from *Alcaligenes* sp. Biodegradation, *Biodegradation*, 2002, **13**, 141–147.
- 23 M. Schädler, F. Buscot, S. Klotz, T. Reitz, W. Durka, J. Bumberger, I. Merbach, S. G. Michalski, K. Kirsch, P. Remmler, E. Schulz and H. Auge, Investigating the consequences of climate change under different land-use regimes: a novel experimental infrastructure, *Ecosphere*, 2019, **10**, e02635.
- 24 S. C. Wagner, *Biological Nitrogen Fixation*, Nature Education Knowledge, 2011.
- 25 C. Sansupa, S. F. M. Wahdan, S. Hossen, T. Disayathanoowat, T. Wubet and W. Purahong, Can we use Functional Annotation of Prokaryotic Taxa (FAPROTAX) to assign the ecological functions of soil bacteria?, *Appl. Sci.*, 2021, **11**, 688.
- 26 M. Rosenblueth, E. Ormeño-Orrillo, A. López-López, M. A. Rogel, B. J. Reyes-Hernández, J. C. Martínez-Romero, P. M. Reddy and E. Martínez-Romero, Nitrogen fixation in cereals, *Front. Microbiol.*, 2018, **9**, DOI: 10.3389/fmicb.2018.01794.
- 27 E. Velázquez, P. García-Fraile, M.-H. Ramírez-Bahena, R. Rivas and E. Martínez-Molina, Current status of the taxonomy of bacteria able to establish nitrogen-fixing legume symbiosis, in *Microbes for Legume Improvement*, ed. A. Zaidi, M. S. Khan and J. Musarrat, Springer International Publishing, Cham, 2017, pp. 1–43.
- 28 M. R. R. Coelho, I. E. Marriel, S. N. Jenkins, C. V. Lanyon, L. Seldin and A. G. O'Donnell, Molecular detection and quantification of *nifH* gene sequences in the rhizosphere of sorghum (*Sorghum bicolor*) sown with two levels of nitrogen fertilizer, *Appl. Soil Ecol.*, 2009, **42**, 48–53.
- 29 F. Poly, L. J. Monrozier and R. Bally, Improvement in the RFLP procedure for studying the diversity of *nifH* genes in communities of nitrogen fixers in soil, *Res. Microbiol.*, 2001, **152**, 95–103.
- 30 J. C. Gaby and D. H. Buckley, The use of degenerate primers in qPCR analysis of functional genes can cause dramatic quantification bias as revealed by investigation of *nifH* primer performance, *Microb. Ecol.*, 2017, **74**, 701–708.
- 31 W. Purahong, S. Hossen, A. Nawaz, D. Sadubsarn, B. Tanunchai, S. Dommert, M. Noll, L.-A. Ampornpan, P. Werukamkul and T. Wubet, Life on the rocks: first Insights into the microbiota of the threatened aquatic rheophyte *Hanseniella heterophylla*, *Front. Plant Sci.*, 2021, **12**, 634960.
- 32 B. Tanunchai, K. Juncheed, S. F. M. Wahdan, V. Guliyev, M. Udovenko, A.-S. Lehnert, E. G. Alves, B. Glaser, M. Noll, F. Buscot, E. Blagodatskaya and W. Purahong, Analysis of microbial populations in plastic–soil systems after exposure to high poly(butylene succinate-co-adipate) load using high-resolution molecular technique, *Environ. Sci. Eur.*, 2021, **33**, 105.
- 33 X. Ma, B. S. Razavi, M. Holz, E. Blagodatskaya and Y. Kuzyakov, Warming increases hotspot areas of enzyme activity and shortens the duration of hot moments in the root-detritusphere, *Soil Biol. Biochem.*, 2017, **107**, 226–233.
- 34 A. Nordgren, Apparatus for the continuous, long-term monitoring of soil respiration rate in large numbers of samples, *Soil Biol. Biochem.*, 1988, **20**, 955–957.
- 35 E. Delamarque, A. Mattlet, S. Livi, J.-F. Gérard, R. Bayard and V. Massardier, Tailoring biodegradability of poly(butylene succinate)/poly(lactic acid) blends with a deep eutectic solvent, *Front. Mater.*, 2020, **7**, DOI: 10.3389/fmats.2020.00007.
- 36 P. Shannon, A. Markiel, O. Ozier, N. S. Baliga, J. T. Wang, D. Ramage, N. Amin, B. Schwikowski and T. Ideker, Cytoscape: a software environment for integrated models of biomolecular interaction networks, *Genome Res.*, 2003, **13**, 2498–2504.
- 37 J. Oksanen, F. G. Blanche, M. Friendly, R. Kindt, P. Legendre, D. McGlenn, P. R. Minchin, R. B. O'Hara, G. L. Simpson, P. Solymos, M. H. H. Stevens, E. Szoecs and H. Wagner, *Vegan: Community Ecology Package*, 2016.
- 38 Ø. Hammer, D. A. T. Harper and P. D. Ryan, PAST: Paleontological statistics software package for education and data analysis, *Palaeontol. Electron.*, 2001, **4**, 9.
- 39 H. A. Mohamed, Y. Assem, R. Said and A. M. El-Masry, Synthesis of polyesteramides: poly(ethylene adipate amide) and poly(ethylene succinate amide) and their application as corrosion inhibitors in paint formulations, *J. Coat. Technol. Res.*, 2018, **15**, 967–981.
- 40 Y. Han, Y. Teng, X. Wang, W. Ren, X. Wang, Y. Luo, H. Zhang and P. Christie, Soil type driven change in microbial community affects poly(butylene adipate-co-terephthalate) degradation potential, *Environ. Sci. Technol.*, 2021, **55**(8), 4648–4657.
- 41 J. Foght, Nitrogen fixation and hydrocarbon-oxidizing bacteria, in *Handbook of Hydrocarbon and Lipid Microbiology*, ed. K. N. Timmis, Springer, Berlin, Heidelberg, 2010, pp. 1661–1668.

Plastic 2 – Supplementary Information

Nitrogen fixing bacteria facilitate microbial biodegradation of a bio-based and biodegradable plastic in soils under ambient and future climatic conditions.

Author: Benjawan Tanunchai*, Stefan Kalkhof*, Vusal Guliyev*, Sara Fareed Mohamed Wahdan, Dennis Krstic, Martin Schädler, Andreas Geissler, Bruno Glaser, François Buscot, Evgenia Blagodatskaya, Matthias Noll and Witoon Purahong

*These authors contributed equally to this work.

Status: Published

Publication: Environ. Sci.: Processes Impacts

Publisher: Royal Society of Chemistry (RSC); RSC Publishing

Date: 23 Feb 2022

Environ. Sci.: Processes Impacts 24, 233–241.

© Royal Society of Chemistry 2022

Reproduced from Ref. 600097281 with permission from the Royal Society of Chemistry.

Available online at: <https://doi.org/10.1039/D1EM00426C>

Or please see separate attachments



Contents lists available at ScienceDirect

Science of the Total Environment

journal homepage: www.elsevier.com/locate/scitotenv

Short communication

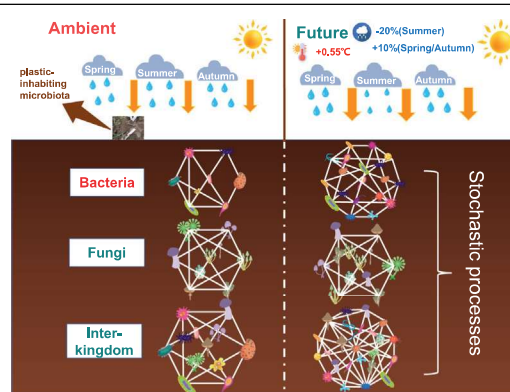
Future climate change enhances the complexity of plastisphere microbial co-occurrence networks, but does not significantly affect the community assembly

Li Ji ^{a,b,*}, Benjawan Tanunchai ^{a,c,1}, Sara Fared Mohamed Wahdan ^{a,d}, Martin Schädler ^{e,f}, Witoon Purahong ^{a,**}^a UFZ-Helmholtz Centre for Environmental Research, Department of Soil Ecology, Theodor-Lieser-Str. 4, 06120 Halle (Saale), Germany^b Key Laboratory of Sustainable Forest Ecosystem Management-Ministry of Education, School of Forestry, Northeast Forestry University, 150040 Harbin, PR China^c Bayreuth Center of Ecology and Environmental Research (BayCEER), University of Bayreuth, Bayreuth, Germany^d Botany Department, Faculty of Science, Suez Canal University, 41522 Ismailia, Egypt^e UFZ-Helmholtz Centre for Environmental Research, Department of Community Ecology, Theodor-Lieser-Str. 4, D-06120 Halle (Saale), Germany^f German Centre for Integrative Biodiversity Research (iDiv) Halle-Jena-Leipzig, Deutscher Platz 5e, D-04103 Leipzig, Germany

HIGHLIGHTS

- Future climate promoted the network complexity and modularity of plastisphere microbiota.
- Future climate altered the potential role of keystone taxa in the plastisphere networks.
- The bacteria and fungi exhibited more competition and cooperation under future climate regime, respectively.
- Neutral-based processes dominated the assembly of the plastisphere microbial community.

GRAPHICAL ABSTRACT



ARTICLE INFO

Editor: Fang Wang

Keywords:

Biodegradable plastic
Plastisphere microbiota
Community assembly
Climate change

ABSTRACT

Biobased and biodegradable plastics have been intensively used in agriculture as mulching films. They provide a distinctive habitat for soil microbes, yet much less is known about the community assembly and interactions of plastisphere microbiota in soils under future climate change. For the first time, we explored the relative importance of ecological processes and the co-occurrence networks of plastic-associated microbes under ambient and future climates. The drift primarily dominated the community assembly of bacteria and fungi after 180D and 328D incubation in both climate regimes. The neutral community model prediction indicated that the migration rate of the plastisphere community in the later decay phase was lower than that in the early decay phase, contributing to the generation of the specific niches. Furthermore, future climate promoted the complexity and modularity of plastic-associated microbial networks: more competition and cooperation were observed in bacteria (or inter-kingdom) and fungi under future climate conditions, respectively. Overall, our findings strengthened the understanding of ecological processes and interplay of plastisphere microbiota during plastic biodegradation in soils under ambient and future climate regimes.

* Correspondence to: L. Ji, UFZ-Helmholtz Centre for Environmental Research, Department of Soil Ecology, Theodor-Lieser-Str. 4, 06120 Halle (Saale), Germany.

** Corresponding author.

E-mail addresses: l.ji@ufz.de (L. Ji), tanunchai.benjawan@ufz.de (B. Tanunchai), Sarah_Wahdan@science.suez.edu.eg (S.F.M. Wahdan), martin.schaedler@ufz.de (M. Schädler), witoon.purahong@ufz.de (W. Purahong).¹ These authors contributed equally to this work.² Current address: School of Forestry, Central South of Forestry and Technology, 410004, Changsha, P.R. China.<http://dx.doi.org/10.1016/j.scitotenv.2022.157016>

Received 5 April 2022; Received in revised form 10 June 2022; Accepted 23 June 2022

Available online 28 June 2022

0048-9697/© 2022 Published by Elsevier B.V.

1. Introduction

Plastic litter has been recognized as a new problem in the list of global threats (Amaral-Zettler et al., 2015; de Souza Machado et al., 2018; Rillig and Lehmann, 2020). The discovery of microplastics in human placentas and feces confirms that humans may no longer be able to live in a plastic-free environment (Ragusa et al., 2021; Zhang et al., 2021a). However, in contrast to the slight decline in total global plastic production, the market for environment-friendly biobased and biodegradable plastics has continuously grown (PlasticsEurope, 2020). Biobased and biodegradable plastics have been intensively used in agriculture for different purposes such as mulching films, agricultural films and food packaging (Tanunchai et al., 2021). Mulching films are considered as the most important source of plastic pollution in terrestrial ecosystems (Serrano-Ruiz et al., 2021; Zhang et al., 2022a). After harvesting, biobased and biodegradable plastic residues may be left in the field despite removal efforts and it is common nowadays that farmers leave the plastic residues on their fields and till them into soils (Koitabashi et al., 2012; Serrano-Ruiz et al., 2021). Thus, biobased and biodegradable plastic can be colonized by diverse soil microorganisms, which will affect the fate of and ecological pollution by plastic (Purahong et al., 2021). Recently, the peculiar microenvironment of the “plastisphere” composed of plastics and their inhabiting microbial communities has received more attention (Amaral-Zettler et al., 2020; Li et al., 2022; Luo et al., 2022; Zettler et al., 2013; Zhou et al., 2021). Although extensive research has been carried out on the composition and diversity of plastisphere microbiota in aquatic ecosystems (Bhagwat et al., 2021; Yang et al., 2020), there is much less information in terrestrial ecosystems, especially for microbial interplay and community assembly in the plastisphere. Given the heterogeneity of the plastisphere and the surrounding environment, microbial communities inhabit the plastic surfaces vary significantly, which may affect environmental safety and sustainability (Agathokleous et al., 2021; Amaral-Zettler et al., 2020; Zang et al., 2020). Thus, disentangling the interaction and community assembly of the plastic-associated microbes is pivotal for evaluating the decay of biobased and biodegradable plastics in soils.

The identification of keystone taxa from co-occurrence networks is crucial for regulating the function and composition of the microbiota (Banerjee et al., 2018). Debroas et al. (2017) revealed the keystone taxa (*Rhodobacteriales*, *Rhizobiales*, *Streptomyetales* and *Cyanobacteria*) from plastic litter in marine ecosystems. Luo et al. (2022) suggested that compared to the surrounding soils, the microbial networks in the plastisphere exhibit more nodes and fewer links. Another central issue about the plastisphere microbiome is unraveling the relative contribution of stochastic and deterministic processes in microbial community assembly (Amaral-Zettler et al., 2020; Li et al., 2022; Zhu et al., 2021). Guo et al. (2018) revealed that global warming enhances microbial community divergence and decreases the stochasticity in microbial community assembly, which implies warming-induced selection (potential deterministic filtering) for microbial communities. Although it has been reported that both determinism and stochasticity govern community assembly in the diverse environment (Costello et al., 2012; Jiao et al., 2020; Schädler et al., 2019), the assembly mechanisms of plastic-associated microbial communities have not been closely examined, especially the importance of basic ecological processes (e.g., dispersal, selection, drift, and diversification). Therefore, evaluation of the relative contribution of both processes in plastisphere microbiota could clarify the potential mechanisms of co-occurring species on biodegradation plastics.

Plastisphere microbiota can adapt to environmental changes by adjusting their community composition, function, and inter/intraspecific interactions (Wang et al., 2022). Given that the biodegradation plastics are generally hydrophobic, the responses of the plastisphere microbiome to temperature and moisture may be more sensitive (Alster et al., 2020; Zhu et al., 2021). Thus, deciphering the mechanisms underlying plastisphere-associated dispersal of microbiota in a scenario of future climate change could provide new insights into the plastisphere microbiota. The Global Change Experimental Facility (GCEF) is used to explore the consequences of future climate change on ecosystem processes in Germany (Schädler et al., 2019). Our previous

findings highlight that the decay of one of the most promising biobased and biodegradable plastics (poly(butylene succinate-co-adipate), PBSA) is enhanced by nitrogen-fixing bacteria which facilitate major fungal decomposers inhabiting the PBSA (Purahong et al., 2021). In the present work, we re-analyzed our previous datasets to explore the community assembly and interaction of PBSA-associated bacteria and fungi. The objective of our study is to illustrate the potential response of bacterial and fungal assemblages and networks to future climate. The findings will generate an important contribution to advance the knowledge of plastic decomposition driven by plastisphere microbiota. Based on a recent study of bacterial community assembly of polyethylene and biodegradable plastic mulches (Ju et al., 2021), we hypothesize that stochastic processes (dominated by dispersal limitation plus ecological drift) play the most important role for PBSA plastisphere microbial community assembly. However, climate change of the next 80 years by increasing temperature and changing precipitation patterns can alter relationships between fungi and bacteria in the plastisphere (Tanunchai et al., 2022). We expect significant changes of microbial community assembly process, co-occurrence networks and their associated keystone microbial taxa in the future climate. Other soil physicochemical properties (i.e. total soil organic carbon (C), total soil nitrogen (N), C: N ratio, and soil pH) of the two climate treatments are not significantly different (Fig. S1), in the optimum range and small gradient. Thus, we expected that these factors do not significantly affect the microbial assembly processes in this experiment. The symbiotic N-fixing bacteria are expected to be keystone taxa in future climate treatment, whereas both non-symbiotic and symbiotic N-fixing bacteria are expected in ambient climate treatment (Tanunchai et al., 2022).

2. Materials and methods

2.1. Study site

Our experiment was conducted in the conventional farming plots of the GCEF, which located at the field research station of the Helmholtz-Centre for Environmental Research in Bad Lauchstadt, Central Germany (51°22'60" N, 11°50'60" E). The site is characterized by a sub-continental climate, as well as an average annual precipitation of 489–525 mm and a mean temperature of 8.9–9.7 °C. The soil type is Haplic Chernozem. The climate treatment simulates the projection of future climate for Central Germany during 2070–2100 (reduced 20 % summer precipitation, increased 10 % precipitation spring and autumn, and increased mean air temperature by 0.55 °C). The air temperature was measured in a height of 5 cm above soil surface by SHT21 I2C Digital Sensor (Sensirion AG, Switzerland). In the GCEF, roofs and western and eastern panels of the plots are automatically closed every day at sunset and opened at sunrise to increase the air temperature by the passive night time warming approach. More details regarding this facility refer to the description of Schädler et al. (2019).

2.2. Experimental design and sampling

In August 2018, the white/transparent PBSA films (double-layer thin film, 21 cm × 30 cm) with 50 μm thickness were set on the soil surface under both ambient and future climate plots. A recent study demonstrated that the color of plastic film alters the inhabited microbial communities and metabolic pathway (Wen et al., 2020). Thus, we used the white/transparent color as it is widely used color for mulching film in agriculture (Liu et al., 2014). The four corners of each film were held down with metal nails to avoid movement and ensure real contact with soil. The PBSA films were buried into the soil (5 cm depth) after 20 days, which attempted to mimic the tillage practice of mulching films into soils and allowed the colonization of soil microbes. After 180 (180D) and 328 days (328D) incubation, the PBSA samples from five replicated plots (16 × 24 m) in both ambient and future climate conditions were collected. The entire PBSA film was collected by clean trowel and gloves at each plot, and the materials located at the direct vicinity of the nailed sample areas were discarded. All PBSA samples were transported on ice to the laboratory immediately and stored

at -20°C . The detailed information about the design is available in the publication of [Purahong et al. \(2021\)](#).

2.3. DNA extraction, Illumina sequencing and data analysis

The PBSA-associated microbial DNA was extracted by the DNeasy PowerSoil Kit (Qiagen, Hilden, Germany). The bacterial 16S rRNA gene V4 region and fungal ITS2 region were sequenced and analyzed as described by [Purahong et al. \(2021\)](#). The functional groups of plastisphere microbiota were annotated using the FAPROTAX, FUNGuild and FungalTraits tools ([Louca et al., 2016](#); [Nguyen et al., 2016](#); [Pölme et al., 2020](#)). The detailed information of data analysis was described in Supplementary materials.

3. Results and discussion

3.1. More complex co-occurrence patterns of plastisphere microbiota under future climate regime

The co-occurrence networks were constructed to illustrate the interaction and niche partitioning of plastic-inhabiting bacterial, fungal and inter-kingdom communities ([Fig. 1](#), [Fig. S2](#)). Although the network patterns of bacteria and fungi were different (i.e. greater modularity in bacteria as compared with fungi), they responded similarly to the future climate change ([Table 1](#)). Specifically, the topological features of networks had greater modularity in the future climate ([Table 1](#), [Fig. 1A–C](#)). Compared with the ambient climate, the number of nodes and links under future

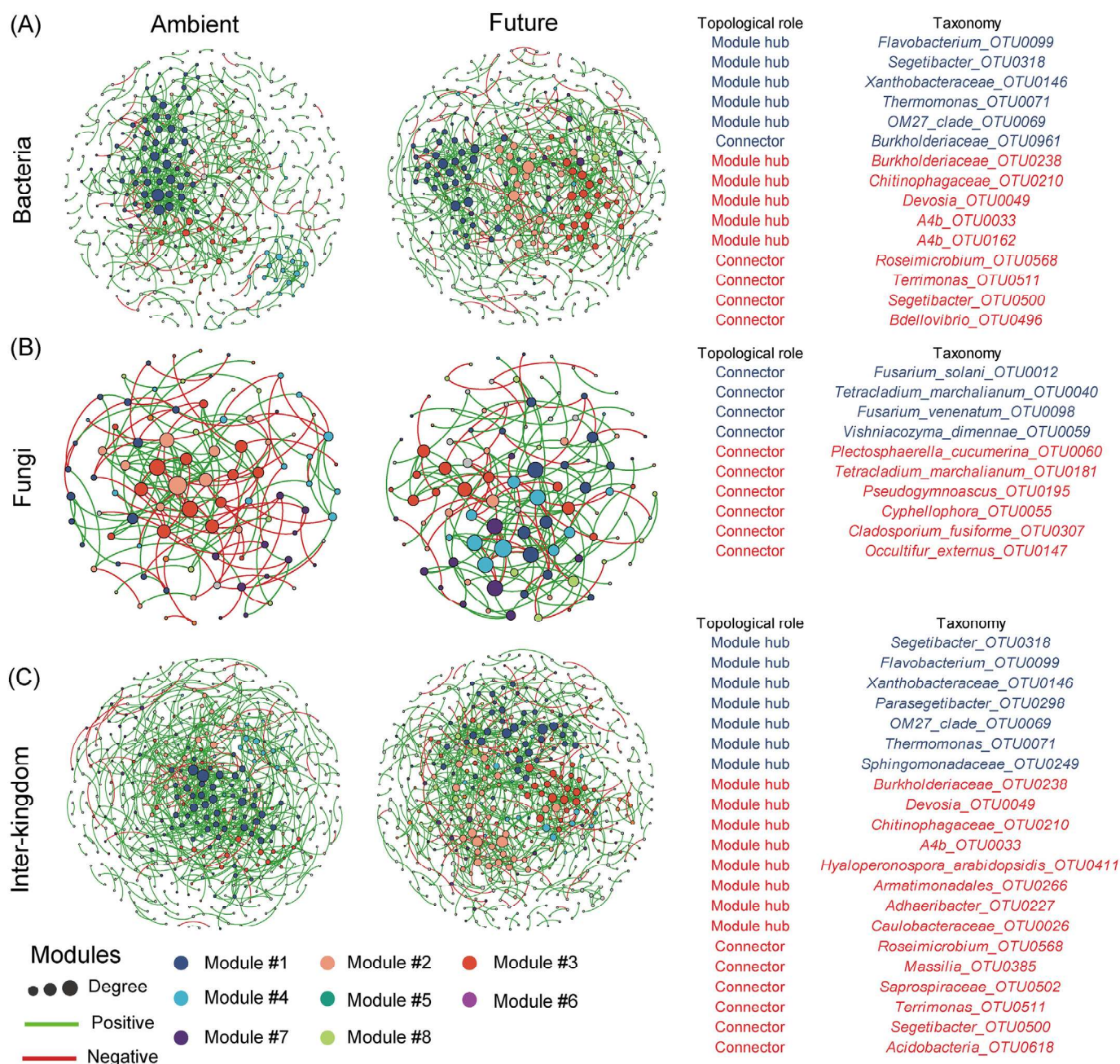


Fig. 1. Modular networks of plastisphere bacteria (A), fungi (B) and inter-kingdom (C) in biodegradable plastic. Node colors represent different modules. The connections denote a strong (Spearman's $\rho > 0.6$) and significant ($P < 0.01$) correlations. The blue and red annotation in bacterial, fungal and inter-kingdom networks represent the keystone taxa under ambient and future climate regimes, respectively.

Table 1
Topological properties of the co-occurrence network in plastisphere microbiota.

Network features		Bacteria		Fungi		Inter-kingdom	
		Ambient	Future	Ambient	Future	Ambient	Future
Empirical network	Number of nodes	404	438	94	105	469	525
	Number of links	692	731	176	183	755	847
	R ² of power-law	0.913	0.871	0.757	0.643	0.935	0.849
	Number of positive correlations	642 (92.8 %)	654 (89.5 %)	104 (59.1 %)	128 (69.9 %)	695 (92.1 %)	748 (88.3 %)
	Number of negative correlations	50 (7.2 %)	77 (10.5 %)	72 (40.9 %)	55 (30.1 %)	60 (7.9 %)	99 (11.7 %)
	Average degree (avgK)	3.426	3.338	3.745	3.486	3.220	3.227
	Average clustering coefficient (avgCC)	0.197	0.200	0.183	0.218	0.188	0.192
	Average path distance (GD)	7.127	7.113	4.645	4.821	7.663	7.393
	Modularity	0.718	0.779	0.583	0.643	0.738	0.783
	Random network	avgCC ± SD	0.014 ± 0.004	0.010 ± 0.004	0.052 ± 0.018	0.040 ± 0.013	0.012 ± 0.003
	GD ± SD	4.367 ± 0.063	4.625 ± 0.058	3.460 ± 0.073	3.677 ± 0.111	4.582 ± 0.058	4.828 ± 0.061
	Modularity ± SD	0.558 ± 0.007	0.576 ± 0.006	0.470 ± 0.013	0.502 ± 0.014	0.588 ± 0.006	0.595 ± 0.005

climate showed a significant increase (Table 1), which indicated the more complex and isolated networks by induced future climate. Yuan et al. (2021) found that climate warming advanced the network complexity and robustness, and confirmed that network stability increases with network complexity as well as modularity. Indeed, the established network structures under future climate change could positively align with the increased temperature, reduced rainfall and other associated changes. Notably, divergent patterns of interactions were found in bacteria and fungi. The bacteria (or inter-kingdom) and fungi exhibited a higher and lower percentage of negative correlations in the scenario of future climate, respectively (Table 1). This result suggested that future climate regime exacerbated the antagonistic relationships among bacterial members as well as the interplay of bacteria and fungi, while promoting the mutualization and niche adaptation among fungal members.

In addition, the keystone taxa from these networks were further identified. The future climate increased the number of keystone species in all networks of kingdoms (Fig. S3A–C, Supplementary appendix). There were 50 %, 50 % and 100 % more keystone species under future climate than under ambient conditions, respectively, which is in line with the finding of Yuan et al. (2021). More importantly, all of the fungal keystone species were detected as the module connectors, and the taxonomic origin of keystone species under future climate was more diverse (Fig. 1, Fig. S3B, Supplementary appendix). In addition, future climate regime improved and decreased the function partitions of plastisphere fungi and bacteria (or inter-kingdom), respectively (Fig. 1). The increasing temperature and decreasing rainfall under future climate leads to the transition of keystone taxa in the network. Our previous study demonstrated that after 3 months of incubation under future climate, the aquatic saprotrophs *Tetracladium* spp. is the dominant taxa and possibly as decomposer to degrade the PBSA (Purahong et al., 2021). *Cladosporium* spp. is found in biodegradable plastics (Kamiya et al., 2007) and is considered as the potential PBSA degraders to efficiently produce lipase (Chinaglia et al., 2014). In this study, the *Tetracladium* spp. was observed as the module connector in both climate regimes, and *Cladosporium* spp. only was found as the connector under future climate (Fig. 1). For the networks of inter-kingdom, we found only bacterial taxa act as the module hubs and connectors, and there had more abundant keystone taxa under future climate conditions. The symbiotic N-fixing bacteria (*Devosia*) was identified as a keystone taxon in future climate treatment, which is consistent to our hypothesis. However, no N-fixing bacteria were found as keystone taxa in ambient climate treatment. This is in line with our previous findings (Tanunchai et al., 2022) that many diverse symbiotic and non-symbiotic N-fixing bacteria play role as facilitators in ambient climate; thus, they may not specifically appear as keystone taxa in this treatment. These results were supported by our previous study (Purahong et al., 2021), that is, N-fixing bacteria can facilitate the decomposition of PBSA by supporting the dominant PBSA-inhabiting fungi. Altogether, in order to promote the cooperation between bacteria and fungi, the niche partitioning was more pronounced under future climate. Our results revealed that the future climate conditions interfered with the

network complexity of plastisphere microbiota, and enhanced the competition between microbial members. The microbial modules with a similar niche will be generated synergistically during the degradation of PBSA.

3.2. Drift primarily dominated the community assembly of plastisphere microbiota

Understanding the relative importance of ecological stochasticity of microbiome is fundamental to decipher the microbial community assembly under future climate regimes (Guo et al., 2018). In both bacterial and fungal communities, the migration rate of neutral community models in 180D was higher than those in 328D (Fig. S4A–H), which suggested species dispersal of plastic-inhabiting microbiota was higher in the early phase. Moreover, the higher explained community variance (R² value) for both bacteria and fungi in two sampling times was observed in the ambient treatment (Fig. S4). This finding revealed that stochasticity played a more crucial role in the microbial community structure in the ambient condition. The role of stochastic processes in the plastisphere was reported in both aquatic (Li et al., 2021; Zhang et al., 2022b) and soil environments (Ju et al., 2021; Zhu et al., 2021). Additionally, the relative contribution of ecological processes was evaluated based on the null model and iCAMP framework. The pNST value was >0.5 in all treatments, and there had no significant difference between different climates and sampling times (Fig. 2A, C; Fig. S5A, S5B), which further indicated the stochastic processes predominately governed the plastisphere microbiota, including both bacteria and fungi. Li et al. (2021) found that the plastisphere bacteria and fungi in two aquatic ecosystems were both controlled by the deterministic processes due to narrow habitat niche breadth of the plastisphere. However, accumulated evidence verifies that stochastic processes are also important for plastisphere in both aquatic (Sun et al., 2021; Zhang et al., 2021b) and terrestrial ecosystems (Ju et al., 2021). Furthermore, for biodegradable mulching films placed in agricultural soil, ecological drift plays the dominant role in bacterial community assembly and its importance increases over times (Ju et al., 2021). We further calculated the specific ecological processes by Raup-Crick metric, and found the drift played the most important role in stochastic processes (Fig. 2B, D). Thus, we propose that the stochastic balance between dead and birth of plastisphere microbiota (ecological drift) in both bacteria and fungi could generate the new community structure and assembly in agricultural soil. Ecological drift has the character with the fluctuation of microbial abundances and the variation of population size (immigration, deaths, and stochastic births) (Ruokolainen et al., 2009).

The proportion of assembly processes from 180D under future climate and 328D under ambient climate was highly similar (Fig. 2B, D), which may be attributed to the future climate accelerated the decomposition of PBSA according to our previous findings (Purahong et al., 2021). More specifically, after 328D incubation, the inappreciable variable selection in both bacterial and fungal communities was observed under future climate (Fig. 2B, D). This result further supports our previous inference, that is the more stable community of plastic-inhabiting microbiota is formed in

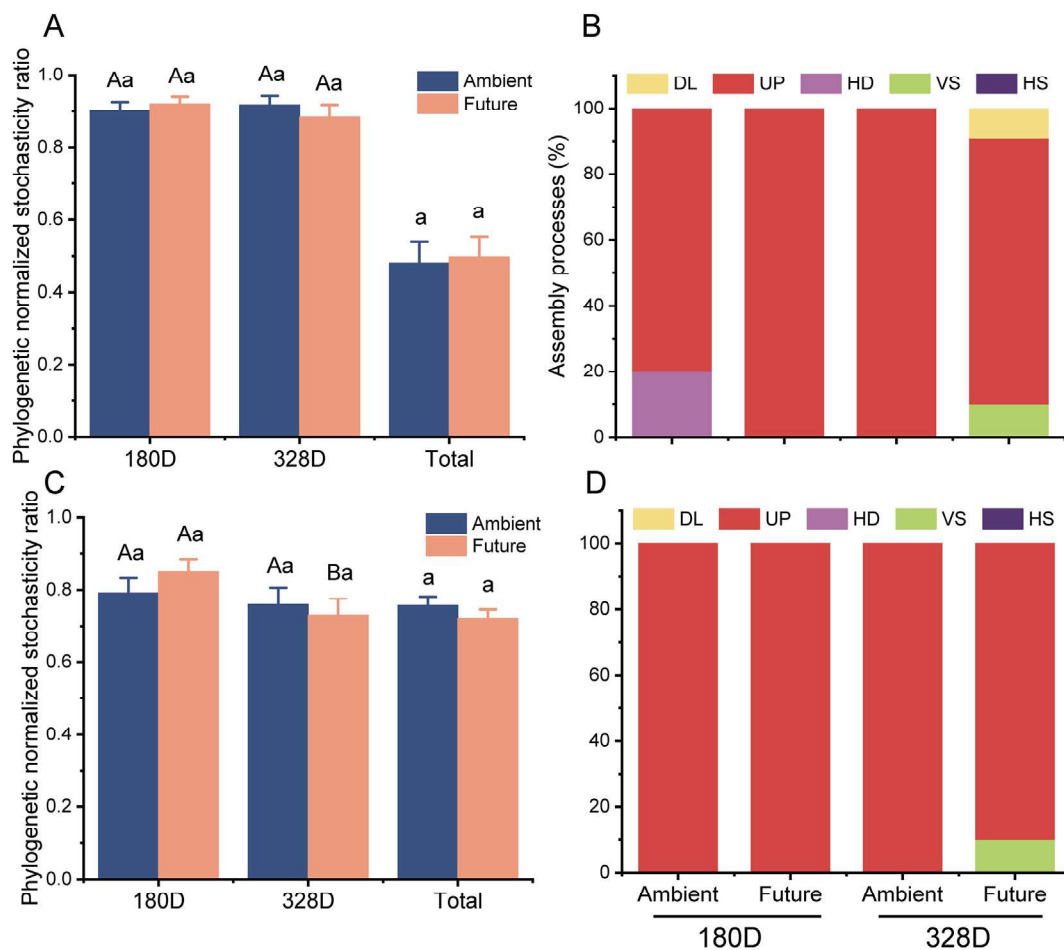


Fig. 2. The ecological stochasticity in the potentially plastisphere bacterial (A) and fungal (C) community assembly estimated by the phylogenetic normalized stochasticity ratio (pNST). The value of 0.5 as the boundary point between more deterministic (<0.5) and more stochastic (>0.5) assembly. Different upper letters indicate the significant difference between 180D and 328D incubation in the same climate regime. Different lower letters indicate the significant difference between ambient and future climate regimes in the same decomposition phase (t -test, $P < 0.05$). The relative contributions (%) of the bacterial (B) and fungal (D) community assembly processes based on pNST. HS, homogeneous selection; VS, variable selection; HD, homogenizing dispersal; UP, undominated process; DL, dispersal limitation.

later phase. Collectively, our results demonstrate that stochasticity dominated the plastisphere microbial community in the scenario of future climate, which formed primarily by drift.

4. Conclusion

In summary, our findings provide novel insights into the community assembly and interaction of plastisphere (biodegradable plastic) microbiota in the scenario of future climate. The networks of plastic-associated bacteria, fungi and inter-kingdom were significantly different under ambient and future climate regimes. Future climate enhanced the network complexity and modularity of plastic-associated microbiota. The bacteria and fungi inhabiting plastic exhibited more competition and mutualism under future climate treatment. For the first time, our work revealed that the trajectory of plastic-associated microbiota was mainly governed by stochastic processes (particularly drift). Further studies are needed to consider the assembly mechanism of the specific microorganisms in plastisphere, which providing a comprehensive picture about plastic biodegradation mechanisms under global change.

CRedit authorship contribution statement

W.P., M.S. and L.J. conceived and designed the study. B.T., S.F.M.W. and W.P. collected the samples and performed the lab work; L.J. and BT wrote the manuscript. L.J., S.F.M.W. and W.P. led the bioinformatics.

All of the authors reviewed and gave comments and suggestions for the manuscript.

Data availability

The raw sequence data are deposited at the National Center for Biotechnology Information (NCBI) database under BioProject ID: PRJNA595487 (<https://www.ncbi.nlm.nih.gov/bioproject/PRJNA595487>).

Declaration of competing interest

The authors declare that they have no known competing financial interests or personal relationships that could have appeared to influence the work reported in this paper.

Acknowledgement

We thank the Helmholtz Association, the Federal Ministry of Education and Research, the State Ministry of Science and Economy of Saxony-Anhalt, and the State Ministry for Higher Education, Research and the Arts Saxony for funding the Global Change Experimental Facility (GCEF) project. Li Ji appreciates the financial support by the China Scholarship Council (No. 201906600038). We also thank the staff of the Bad Lauchstädt Experimental Research Station (especially Ines Merbach and Konrad Kirsch) for their work in maintaining the plots and infrastructure of the GCEF, and Dr. Stefan Klotz,

Prof. Dr. François Buscot, Dr. Harald Auge, and Dr. Thomas Reitz for their roles in setting up the GCEF.

Appendix A. Supplementary data

Supplementary data to this article can be found online at <https://doi.org/10.1016/j.scitotenv.2022.157016>.

References

- Agathokleous, E., Iavicoli, L., Barceló, D., Calabrese, E.J., 2021. Ecological risks in a 'plastic' world: a threat to biological diversity? *J. Hazard. Mater.* 417, 126035.
- Alster, C.J., von Fischer, J.C., Allison, S.D., Treseder, K.K., 2020. Embracing a new paradigm for temperature sensitivity of soil microbes. *Glob. Chang. Biol.* 26, 3221–3229.
- Amaral-Zettler, L.A., Zettler, E.R., Mincer, T.J., 2020. Ecology of the plastisphere. *Nat. Rev. Microbiol.* 18, 139–151.
- Amaral-Zettler, L.A., Zettler, E.R., Slikas, B., Boyd, G.D., Melvin, D.W., Morrall, C.E., Proskurowski, G., Mincer, T.J., 2015. The biogeography of the plastisphere: implications for policy. *Front. Ecol. Environ.* 13, 541–546.
- Banerjee, S., Schlaeppli, K., Der Heijden, M.G.A.V., 2018. Keystone taxa as drivers of microbiome structure and functioning. *Nat. Rev. Microbiol.* 16, 567–576.
- Bhagwat, G., Zhu, Q., O'Connor, W., Subashchandrabose, S., Grainge, I., Knight, R., Palanisami, T., 2021. Exploring the composition and functions of plastic microbiome using whole-genome sequencing. *Environ. Sci. Technol.* 55, 4899–4913.
- Chinaglia, S., Chiarelli, L.R., Maggi, M., Rodolfi, M., Valentini, G., Picco, A.M., 2014. Biochemistry of lipolytic enzymes secreted by *Penicillium solitum* and *Cladosporium cladosporioides*. *Biosci. Biotechnol. Biochem.* 78, 245–254.
- Costello, E.K., Stagaman, K., Dethlefsen, L., Bohannan, B.J., Relman, D.A., 2012. The application of ecological theory toward an understanding of the human microbiome. *Science* 336, 1255–1262.
- de Souza Machado, A.A., Kloas, W., Zarfl, C., Hempel, S., Rillig, M.C., 2018. Microplastics as an emerging threat to terrestrial ecosystems. *Glob. Chang. Biol.* 24, 1405–1416.
- Debroas, D., Mone, A., Ter Halle, A., 2017. Plastics in the North Atlantic garbage patch: a boat-microbe for hitchhikers and plastic degraders. *Sci. Total Environ.* 599, 1222–1232.
- Guo, X., Feng, J.J., Shi, Z., Zhou, X.S., Yuan, M.T., Tao, X.Y., Hale, L., Yuan, T., Wang, J.J., Qin, Y.J., Zhou, A.F., Fu, Y., Wu, L.Y., He, Z.L., Nostrand, J.D.V., Ning, D.L., Liu, X.D., Luo, Y.Q., Tiedje, J.M., Yang, Y.F., Zhou, J.Z., 2018. Climate warming leads to divergent succession of grassland microbial communities. *Nat. Clim. Chang.* 8, 813–818.
- Jiao, S., Yang, Y., Xu, Y., Zhang, J., Lu, Y., 2020. Balance between community assembly processes mediates species coexistence in agricultural soil microbiomes across eastern China. *ISME J.* 14, 202–216.
- Ju, Z., Du, X., Feng, K., Li, S., Gu, S., Jin, D., Deng, Y., 2021. The succession of bacterial community attached on biodegradable plastic mulches during the degradation in soil. *Front. Microbiol.* 12, 785737–785737.
- Kamiya, M., Asakawa, S., Kimura, M., 2007. Molecular analysis of fungal communities of biodegradable plastics in two Japanese soils. *Soil Sci. Plant Nutr.* 53, 568–574.
- Koitaibashi, M., Noguchi, M.T., Sameshima-Yamashita, Y., Hiradate, S., Suzuki, K., Yoshida, S., Watanabe, T., Shinozaki, Y., Tsushima, S., Kitamoto, H.K., 2012. Degradation of biodegradable plastic mulch films in soil environment by phylloplane fungi isolated from gramineous plants. *AMB Express* 2, 1–10.
- Li, C., Wang, L., Ji, S., Chang, M., Wang, L., Gan, Y., Liu, J., 2021. The ecology of the plastisphere: microbial composition, function, assembly, and network in the freshwater and seawater ecosystems. *Water Res.* 202, 117428.
- Li, Y., Yang, R., Guo, L., Gao, W., Su, P., Xu, Z., Xiao, H., Ma, Z., Liu, X., Gao, P., 2022. The composition, biotic network, and assembly of plastisphere protistan taxonomic and functional communities in plastic-mulching croplands. *J. Hazard. Mater.* 128390.
- Liu, E.K., He, W.Q., Yan, C.R., 2014. 'White revolution' to 'white pollution'—agricultural plastic film mulch in China. *Environ. Res. Lett.* 9, 091001. <https://doi.org/10.1088/1748-9326/9/9/091001>.
- Louca, S., Parfrey, L.W., Doebeli, M., 2016. Decoupling function and taxonomy in the global ocean microbiome. *Science* 353, 1272–1277.
- Luo, G., Jin, T., Zhang, H., Peng, J., Zuo, N., Huang, Y., Han, Y., Tian, C., Yang, Y., Peng, K., 2022. Deciphering the diversity and functions of plastisphere bacterial communities in plastic-mulching croplands of subtropical China. *J. Hazard. Mater.* 422, 126865.
- Nguyen, N.H., Song, Z., Bates, S.T., Branco, S., Tedersoo, L., Menke, J., Schilling, J.S., Kennedy, P.G., 2016. FUNGuild: an open annotation tool for parsing fungal community datasets by ecological guild. *Fungal Ecol.* 20, 241–248.
- Pölme, S., Abarenkov, K., Nilsson, R.H., Lindahl, B.D., Clemmensen, K.E., Kausserud, H., Nguyen, N., Kjoller, R., Bates, S.T., Baldrian, P., 2020. FungalTraits: a user-friendly traits database of fungi and fungus-like stramenopiles. *Fungal Divers.* 105, 1–16.
- PlasticsEurope, 2020. *Plastics: The Facts*. PlasticsEurope, Brussels.
- Purahong, W., Wahdan, S.F.M., Heinz, D., Jariyavidyanont, K., Sungkapreecha, C., Tanunchai, B., Sansupa, C., Sadubsarn, D., Alaneer, R., Heintz-Buschart, A., 2021. Back to the future: decomposability of a biobased and biodegradable plastic in field soil environments and its microbiome under ambient and future climates. *Environ. Sci. Technol.* 55, 12337–12351.
- Ragusa, A., Svelato, A., Santacroce, C., Catalano, P., Notarstefano, V., Carnevali, O., Papa, F., Rongioletti, M.C.A., Baiocco, F., Draghi, S., 2021. Plasticenta: first evidence of microplastics in human placenta. *Environ. Int.* 146, 106274.
- Rillig, M.C., Lehmann, A., 2020. Microplastic in terrestrial ecosystems. *Science* 368, 1430–1431.
- Ruokolainen, L., Ranta, E., Kaitala, V., Fowler, M.S., 2009. When can we distinguish between neutral and non-neutral processes in community dynamics under ecological drift? *Ecol. Lett.* 12, 909–919.
- Schädler, M., Buscot, F., Klotz, S., Reitz, T., Durka, W., Bumberger, J., Merbach, I., Michalski, S.G., Kirsch, K., Remmler, P., 2019. Investigating the consequences of climate change under different land-use regimes: a novel experimental infrastructure. *Ecosphere* 10, e02635.
- Serrano-Ruiz, H., Martin-Closas, L., Pelacho, A.M., 2021. Biodegradable plastic mulches: impact on the agricultural biotic environment. *Sci. Total Environ.* 750, 141228.
- Sun, Y., Zhang, M., Duan, C., Cao, N., Jia, W., Zhao, Z., Ding, C., Huang, Y., Wang, J., 2021. Contribution of stochastic processes to the microbial community assembly on field-collected microplastics. *Environ. Microbiol.* 23, 6707–6720.
- Tanunchai, B., Juncheed, K., Wahdan, S.F.M., Guliyev, V., Udovenko, M., Lehnert, A.-S., Alves, E.G., Glaser, B., Noll, M., Buscot, F., 2021. Analysis of microbial populations in plastic-soil systems after exposure to high poly (butylene succinate-co-adipate) load using high-resolution molecular technique. *Environ. Sci. Eur.* 33, 1–17.
- Tanunchai, B., Kalkhof, S., Guliyev, V., Wahdan, S.F.M., Krstic, D., Schädler, M., Geissler, A., Glaser, B., Buscot, F., Blagodatskaya, E., 2022. Nitrogen fixing bacteria facilitate microbial biodegradation of a bio-based and biodegradable plastic in soils under ambient and future climatic conditions. *Environ. Sci. Process Impacts* 24, 233–241.
- Wang, C., Wang, L., Ok, Y.S., Tsang, D.C., Hou, D., 2022. Soil plastisphere: exploration methods, influencing factors, and ecological insights. *J. Hazard. Mater.* 128503.
- Wen, B., Liu, J.-H., Zhang, Y., Zhang, H.-R., Gao, J.-Z., Chen, Z.-Z., 2020. Community structure and functional diversity of the plastisphere in aquaculture waters: does plastic color matter? *Sci. Total Environ.* 740, 140082. <https://doi.org/10.1016/j.scitotenv.2020.140082>.
- Yang, Y., Liu, W., Zhang, Z., Grossart, H.-P., Gadd, G.M., 2020. Microplastics provide new microbial niches in aquatic environments. *Appl. Microbiol. Biotechnol.* 104, 6501–6511.
- Yuan, M.M., Guo, X., Wu, L.W., Zhang, Y., Xiao, N.J., Ning, D.L., Shi, Z., Zhou, X.S., Wu, L.Y., Yang, Y.F., Tiedje, J.M., Zhou, J.Z., 2021. Climate warming enhances microbial network complexity and stability. *Nat. Clim. Chang.* 11, 343–U100.
- Zang, H., Zhou, J., Marshall, M.R., Chadwick, D.R., Wen, Y., Jones, D.L., 2020. Microplastics in the agroecosystem: are they an emerging threat to the plant-soil system? *Soil Biol. Biochem.* 148, 107926.
- Zettler, E.R., Mincer, T.J., Amaral-Zettler, L.A., 2013. Life in the "plastisphere": microbial communities on plastic marine debris. *Environ. Sci. Technol.* 47, 7137–7146.
- Zhang, J., Wang, L., Trasande, L., Kannan, K., 2021a. Occurrence of polyethylene terephthalate and polycarbonate microplastics in infant and adult feces. *Environ. Sci. Technol. Lett.* 8, 989–994.
- Zhang, B., Yang, X., Liu, L.C., Chen, L., Teng, J., Zhu, X.P., Zhao, J.M., Wang, Q., 2021b. Spatial and seasonal variations in biofilm formation on microplastics in coastal waters. *Sci. Total Environ.* 770.
- Zhang, X.-L., Zhao, Y.-Y., Zhang, X.-T., Shi, X.-P., Shi, X.-Y., Li, F.-M., 2022a. Re-used mulching of plastic film is more profitable and environmentally friendly than new mulching. *Soil Tillage Res.* 216, 105256.
- Zhang, S.J., Zeng, Y.H., Zhu, J.M., Cai, Z.H., Zhou, J., 2022b. The structure and assembly mechanisms of plastisphere microbial community in natural marine environment. *J. Hazard. Mater.* 421.
- Zhou, J., Gui, H., Banfield, C.C., Wen, Y., Zang, H., Dippold, M.A., Charlton, A., Jones, D.L., 2021. The microplastisphere: biodegradable microplastics addition alters soil microbial community structure and function. *Soil Biol. Biochem.* 156, 108211.
- Zhu, D., Ma, J., Li, G., Rillig, M.C., Zhu, Y.-G., 2021. Soil plastispheres as hotspots of antibiotic resistance genes and potential pathogens. *ISME J.* 1–12.

Plastic 3 – Supplementary Information

Future climate change enhances the complexity of plastisphere microbial co-occurrence networks, but does not significantly affect the community assembly

Author: Li Ji*, **Benjawan Tanunchai***, Sara Fareed Mohamed Wahdan, Martin Schädler, Witoon Purahong

*These authors contributed equally to this work.

Status: Published

Publication: Science of The Total Environment

Publisher: Elsevier

Date: 20 October 2022

Science of the Total Environment, 157016.

© 2022 Published by Elsevier B.V.

Reprinted with permission from Elsevier.

Available online at: <https://doi.org/10.1016/j.scitotenv.2022.157016>

Or please see separate attachments



Interactions Between High Load of a Bio-based and Biodegradable Plastic and Nitrogen Fertilizer Affect Plant Biomass and Health: A Case Study with *Fusarium solani* and Mung Bean (*Vigna radiata* L.)

Sarah-Maria Scheid^{1,2} · Kantida Juncheed³ · Benjawan Tanunchai^{1,4} · Sara Fareed Mohamed Wahdan^{1,5} · François Buscot^{1,6} · Matthias Noll^{4,7} · Witoon Purahong¹

Accepted: 10 March 2022 / Published online: 30 March 2022
© The Author(s) 2022

Abstract

Bio-based and biodegradable plastics such as mulching films are widely used in agricultural field sites. However, there are limited studies of their impact on plant development and health even though an important soil-borne plant pathogen *F. solani* has been reported to associate with various types of bio-based and biodegradable plastics, especially polybutylene succinate-co-adipate (PBSA). To evaluate the influence of PBSA amendment in soils on plant development and health, *F. solani* and mung bean (*V. radiata*) were used as models in a modified petri-dish test using soil suspensions. Mung bean seeds were incubated in suspensions with two dilutions (high vs. low dilution with low vs. high PBSA amendment) of soils pre-incubated 1 year with PBSA under different treatments (combinations of N fertilizer (ammonium sulfate) and PBSA load) in the modified petri dish test. Plant development and disease incidence were recorded with both microscopic and molecular techniques (specific PCR and Illumina amplicon sequencing). Treatment with PBSA and N fertilizer in non-sterile soil suspensions strongly increased the disease caused by *F. solani* on *V. radiata* at both low and high soil dilution. At high soil dilution, the *F. solani* disease incident was 67.5% while at the low dilution the disease incidence reached 92.5%. In contrast, in treatments PBSA but without N fertilizer, non *F. solani* disease was observed. Apart from *F. solani* infection, other soil fungi can also infect the mung bean seedlings, especially at low soil dilution levels. Nevertheless, based on this short-term study, we found no evidence that PBSA alone can significantly increase the overall disease incidence.

Keywords PBSA · Plant health · Ammonium sulfate fertilization · Mulching film · Plastic accumulation

Sarah-Maria Scheid, Kantida Juncheed, and Benjawan Tanunchai have contributed equally to this work.

Matthias Noll and Witoon Purahong are senior authors.

✉ Witoon Purahong
witoon.purahong@ufz.de

François Buscot
francois.buscot@ufz.de

Matthias Noll
Matthias.noll@hs-coburg.de

¹ Department of Soil Ecology, UFZ-Helmholtz Centre for Environmental Research, Theodor-Lieser-Str. 4, 06120 Halle (Saale), Germany

² Institute for Integrated Natural Sciences, University of Koblenz and Landau, Universitätsstraße 1, 56070 Koblenz, Germany

Introduction

Mulching film has been used globally across agro-ecosystems [1]. It is an integral part of modern agriculture due to the effect of climate change, which caused serious drought

³ Department of Biomedical Sciences and Biomedical Engineering, Faculty of Medicine, Prince of Songkla University, Songkhla 90110, Thailand

⁴ Bayreuth Center of Ecology and Environmental Research (BayCEER), University of Bayreuth, 95440 Bayreuth, Germany

⁵ Botany Department, Faculty of Science, Suez Canal University, Ismailia 41522, Egypt

⁶ German Centre for Integrative Biodiversity Research (iDiv), Halle-Jena-Leipzig, Leipzig, Germany

⁷ Institute of Bioanalysis, Coburg University of Applied Sciences and Arts, 96450 Coburg, Germany

problems [2]. Mulching films preserve water from evaporation and maintain soil moisture [3]. Furthermore, mulching films can also improve the microclimate around the plants, by enhancing the water and dissolved nitrogen (N) ions (i.e. NH_4^+ , NO_3^-) use efficiency and regulating increasing soil temperature, based on a “greenhouse-effect” [4–7]. Consequently, the growth rates (in both root and shoot), biomass and yield production of plants are promoted [8, 9]. Due to the wide advantages of mulching films, their usages in farmlands are increasing annually. Polyethylene (PE) is the material used for decades in the production of mulching films [10]. European agriculture uses about 570,000 tons of PE annually [11]. Unfortunately, PE mulching films are considered as the major source of macro-, micro- and nano-plastics contamination in agricultural soils [12]. Currently, bio-based and biodegradable plastics are becoming an important alternative material for mulching films used in agriculture. The major advantages of bio-based and biodegradable plastics compared with conventional petroleum-based plastics included the use of renewable resources and the reduction of petroleum and energy consumption [13]. Additionally, the bio-based production reduces emission of greenhouse gases [14]. There are many bio-based and biodegradable plastics used as mulching film such as starch-based polymers, polylactic acid (PLA), polybutylene adipate terephthalat (PBAT), polybutylene succinate (PBS), and polybutylene succinate-co-adipate (PBSA) [15–17]. Due to the biodegradability of bio-degradable plastics in soil environments, after cultivation period, farmers may leave residues of mulching films to decompose in their agricultural fields in order to save time and labor costs [18, 19]. In case of PBSA, it can be degraded approximately 30% per year in temperate regions [20]. Thus, the PBSA residues can be accumulated in the soil systems over time [10].

Unfortunately, there is little knowledge about the degradation process of bio-based and biodegradable plastics and their effects on soil microbial activity, especially those obtained by high resolution molecular approaches such as Next Generation Sequencing (NGS) [21]. Furthermore, the impact of bio-based and biodegradable plastics on plant health is still unclear. Thus, we need more experiments that determine whether bio-plastic substances affect soil functions and plant health. Recently, Sforzini et al. (2016) introduced a biotest method to determine the soil ecotoxicity after exposure to high concentration of biodegradable plastics on autotrophic organisms, bacteria, protozoa and invertebrates such as *Daphnia magna* (crustacea) and earthworm *Eisenia andrei* as model organisms [22]. Choices of model organisms were made on the basis of the different trophic levels of which they are representative in food chains of terrestrial and aquatic ecosystems. Corn starch-based plastics and biodegradable polyesters were shown to have no significant effect on plant development and soil (micro-) organisms

[22]. The quality of soils after input at high concentration of starch-based plastic (1%) has been assessed with a large array of biotests based on the same model organisms, and these plastics were classified as not harmful to agricultural utilizations [22]. In contrast, Qi et al. (2018, 2020) showed different negative effects of low-density PE and starch-based biodegradable plastics on wheat growth [23, 24]. In comparison to petroleum-based plastics, they found that bio-based and biodegradable mulch films have potentially a higher negative impact on growth of wheat. Indeed, when macro-plastics (particle size > 5 mm) degrade in water or soil, it breaks up into smaller particles, called micro-plastics (particle size < 1 mm). Micro-plastics revealed stronger negative effects on wheat growth than macro-plastics [23].

Moreover, some studies reported that various plant pathogenic fungi can colonize bio-degradable plastics [20, 21, 25, 26]. Thus, leaving the degraded mulching film in soils, can trigger some problems related to plant health and productivity as many plant fungal pathogens can colonize, grow and reproduce on residue of bio-based and biodegradable plastics. This situation can lead to the promotion of the diseases of various plants, such as cereal crops, vegetables, trees, and ornamental plants. Recently, PBSA has been reported to be colonized by *F. solani* [17, 20]. Furthermore, our earlier study demonstrated that *F. solani* strongly enriched in soil that was highly amended with PBSA and N fertilizer (e.g. ammonium sulfate) [21]. *F. solani* is an important soil-borne plant pathogen, which causes diseases in many agricultural crop species, including e.g. *Cucurbitaceae* and *Fabaceae* [27, 28]. This fungus infects plant roots, seedlings and can cause the soybean sudden death syndrome [29]. It is especially harmful for bean species. Nevertheless, we do not know, if such enrichment of *F. solani* caused by the interactions between PBSA and ammonium sulfate can significantly affect plant biomass and health.

Hence, in the study we aimed to (i) evaluate the effects of high load of PBSA amendment in soils and its interaction with N fertilizer (in the form of ammonium sulfate) to plant biomass (including shoot and root biomass) and health, (ii) to demonstrate that mismanagement of PBSA mulching film (for instance as agricultural waste) can cause negative effects on plant health. We use *F. solani* and mung bean (*V. radiata* L.) as a model for this evaluation. We used suspensions of soils pre-incubated 1 year with PBSA under different treatments encompassing combinations of N fertilizer (ammonium sulfate) and PBSA load to realise a petri dish test on the effect of different experimental treatments on growth and infection of seedling by *F. solani*. We hypothesize that high load of *F. solani* in soil as feedback to addition of PBSA and N fertilizer can significantly increase the *F. solani* disease incident in mung bean. In treatment without addition of N fertilizer, we expect that the *F. solani* disease incident is similar to the one in control soils without PBSA addition. Two

dilution levels of PBSA in soil (1:10 and 1:5) were used, which accounts for 0.6% and 1.2% initial PBSA (wt/wt) in soil suspensions, respectively, as is in line with previously reported plastic contamination in agricultural soils (approx. 1% PBSA in soil) [30, 31]. Nevertheless, in our opinion there is high possibility that the concentrations of bio-based and biodegradable plastics in soil can be even higher than 1%, especially if plastic mulch films are intentionally left in the field after usage. This model experiment enables us to anticipate a potential risk in plant health stemming from the mismanagement of bio-based and biodegradable plastic PBSA in agricultural field.

Materials and Methods

Experimental Design

To evaluate the effects of PBSA amendment in water/soils on the mung bean biomass and development, we did the following 9 treatments: (i) sterile water (SW); (ii) sterile soil (SS); (iii) sterile soil and PBSA (SSP); (iv) sterile soil and N fertilizer (SSN); (v) sterile soil, PBSA and N fertilizer (SSPN); (vi) non-sterilized soil = soil (S); (vii) soil and N fertilizer (SN); (viii) soil and PBSA (SP); and (ix) soil, PBSA and N fertilizer (SPN). The soil used for the 8 treatments was a Haplic Chernozem, C:N ratio ~ 10, pH = 7.16 ± 0.02 (mean \pm SE) from central Germany on which a 1-year PBSA decomposition experiment with 6% (wt/wt, PBSA (BioPBS FD92, percent bio-based carbon = 35%, PTT MCC Biochem Company Limited, Thailand) had been run at 22 °C in darkness by maintaining 17.5% water content) as previously described by Tanunchai et al. [21]. The PBSA film was a double-layer thin film (21 cm \times 30 cm) with 50 μ m thickness used in the 1-year pre-incubation study. High load of ammonium sulfate ($(\text{NH}_4)_2\text{SO}_4$ (equivalent to 280 kg N per hectare) was used as N fertilizer in SSN, SSPN, SN, and SPN treatments. After 1 year of PBSA decomposition, soil pH was significantly lowered in pre-treatments with N fertilizer regardless of PBSA addition (~2 level of pH). We homogenized the soil/PBSA carefully. In PSN, all PBSA were decomposed after 1 year whereas in PS treatment there were > 50% of PBSA remaining. Thus, soil from PSN, SN and control treatments were homogenized the same way by well mixing with sterile spatula and separated into 4 subsamples. For PS treatment, we separated PBSA and soil, mixed each compartment and pooled them based on weight into 4 subsamples. Two subsamples of each treatment were autoclaved for 3 times and used as sterile treatments whereas other two subsamples were used as non-sterile treatment. The soil or soil-PBSA subsamples from each treatment were diluted with sterile distilled water to a 1:10 (high dilution, low concentration, accounting for 0.6% initial PBSA) and

1:5 (low dilution, high concentration, accounting for 1.2% initial PBSA). Initial PBSA content in high and low dilutions were accounting for 0.6 and 1.2%. We previously analyzed fungal communities in all soil treatments using Illumina amplicon sequencing as explained earlier [21]. In this current study, *F. solani* was found enriched in treatment SPN (~33%) as compared with other treatments (~2% or less). PBSA addition or N fertilization alone did not increase the relative abundances of *F. solani* [21].

Modified Petri-dish Assay to Study *Fusarium* Disease Incidence in Mung Bean

Petri-dish assay to study *Fusarium*-based disease incidence of *V. radiata* seeds was modified from Purahong et al. [32]. *V. radiata* seeds (VIG 1631) were ordered from the Leibniz Institute of Plant Genetics and Crop Plant Research (IPK) Gatersleben, Germany. To avoid contamination, the seeds were surface sterilized with a 2% (vol./vol.) NaClO solution for 8 min under a lamina air flow. Later, the seeds were rinsed 6 times with distilled water to remove any chemical residues [32]. After that, the seeds were dried on sterile filter papers for 1 h and kept inside the sterile lamina air flow.

For seed incubation, 8 seeds were placed in an autoclaved glass petri-dish (9 cm in a diameter) on tissue paper supplied with 10 mL sterile water. Incubation of the seeds were carried out under an illuminated air flow to avoid contamination. Additionally, the seeds were disposed in two rows with the seedling embryo turned upwards. We added 1 mL of soil solution (low or high concentration of soil) to each petri dish (125 μ L soil solution per seed). The experiment was run with five independent replicates for each treatment and for each soil dilution concentration. To keep the moisture inside the petri-dishes, all five plates from the same treatment were packed in a clean PE bag with sterilized wet tissue paper and were securely closed with a wire. All plates were incubated in an incubator at 22 °C for six days in the darkness. After two, four and six days of germination, the biomass, the plant development and disease incidence of each seedling were examined, and the numbers of germinated and infected seedlings were counted. The disease incident was calculated in percentage. Within the petri dish, four seedlings were randomly collected from each plate for DNA extraction. Initial mung bean seeds and 1-year soil from SPN treatment were also taken for DNA extraction. The other 4 seedlings for each plate were separated with a scalpel into root and shoot and taken for measurement of biomass. Shoots and roots of seedling were dried in an oven at 105 °C for 24 h. Thereafter dry weight was measured using a five-digit balance (Mewes Wägetechnik, Haldensleben, Germany). Each seedling was optically observed and divided into healthy (seedling have the similar appearance than negative control without any additions) and diseased seedlings (seedling have the similar

appearance than same seedling with addition of *F. solani* (DSMZ 1164) as positive control) from each treatment were separated. The modified petri-dish assay was repeated with three replicates and the results are presented in (Supplementary Material Tables S1, S2, S3).

DNA Extractions and Detection Of *F. solani*

All seedlings were taken from each treatment separately into 50 mL tubes and washed with 50 mL of 0.1% (vol./vol.) sterile tween solution for three times to remove any soil particles. Thereafter the seedlings were washed again four times with double-distilled water to remove tween solution residues. At the end, each tube was filled with 15 mL nuclease and proteinase-free water (AppliChem, Darmstadt, Germany) and incubated for 1 h at 4 °C. After incubation the water solution was discarded. Each washed seedling was homogenized separately by adding liquid N₂ and crushing with a sterile nail. DNA was extracted using QIAGEN DNeasy Plant Mini Kit (Qiagen, Hilden, Germany) according to the manufacturer's protocol. For extraction 100 mg of homogenized seedling was used. The quality of DNA was checked using the nanodrop. The detection of *F. solani* were carried out from healthy and infected seedlings with specific PCR by employing the primer pair 1- TEF-Fs4f [5'-ATC GGCCACGTCGACTCT-3'] and TEF-Fs4r [5'-GGCGTC TGTTGATTGTTAGC-3'] [33]. DNA extract of *F. solani* (DSMZ 1164) was used as positive control. PCR assays were performed in 20 µL reaction mixtures containing 4 µL FIREPol® master mix ready to load (Solis BioDyne, Tartu, Estonia), 1 µL of each forward and reverse primer, 1 µL genomic DNA template and 13 µL nuclease- and proteinase-free water. The PCR products were checked in a 1.5% agarose-gel. The presence of *F. solani* was attested by the presence of the expected band of 658 bp. Fungal community composition in the used 1-year soil with PBSA pre-incubation and seedlings from SPN treatments were analyzed using Illumina amplicon sequencing as described in our previous study [21]. Briefly, DNA extracts from all seedlings of SPN treatment were pooled to get a composite sample. DNA from 1-year soil from SPN treatment was extracted using QIAGEN DNeasy Power Soil Kit (Qiagen, Hilden, Germany) according to manufacturer's instructions. For construction of the fungal amplicon libraries, the fungal ITS2 gene was amplified using the fungal primer pair fITS7 [5'-GTGART CATCGAATCTTTG-3'] [34] and ITS4 primer [5'-TCC TCCGCTTATTGATATGC-3'] [35] with Illumina adapter sequences. Amplifications were performed using 20 µL reaction volumes with 5×HOT FIRE Pol Blend Master Mix (Solis BioDyne). The amplicon products from three technical replicates were then pooled in equimolar concentrations. Paired-end sequencing (2×300 bp) was performed on the pooled amplicon products using a MiSeq Reagent kit v3 on

an Illumina MiSeq system (Illumina Inc., San Diego, CA, United States) at the Department of Soil Ecology, Helmholtz Centre for Environmental Research, Germany. The bioinformatics analyses were carried out using pipeline Dadasnake as described by earlier [36]. Assembled reads fulfilling the following criteria were retained for further analyses: a minimum length of 70 nucleotides, quality scores at least equal to 9 nucleotides with maximum expected error score of 5 nucleotides for forward and reverse sequences and no ambiguous nucleotides. Merging was conducted with 2 nucleotide mismatches allowed and a minimum overlap of 20 nucleotides. Fungal ASVs were classified against the UNITE v7.2 database [37] using the Bayesian classifier as implemented in the mothur classify.seqs command, with a cut-off of 60 nucleotides. The ASV method is used to infer the biological sequences in the sample, as described previously [38]. Rare ASVs (singletons) and chimeras, which potentially represent artificial sequences, were removed. The fungal ecological function of each ASV was determined using FUNGuild as described in our previous study [21].

Statistical Analysis

The data analysis was performed using PAST (version 2.17c) [39]. The disease incidence and plant development and biomass (shoot and root dry weight) were analyzed with a Jarque–Bera test and Shapiro–Wilk W test to determine the distribution of data. A one-way analyses of variance (ANOVA) incorporating the Tukey's pairwise comparisons test was performed. The data were log-transformed when necessary. When Levene's test for homogeneity of variance based on medians was significant either based on non-transformed or log-transformed datasets, the data was analyzed with a Kruskal–Wallis test and followed by a Mann–Whitney pairwise comparison test.

Results

Plant Growth Parameters

At low PBSA concentration, all treatments did not significantly affect plant biomass parameters including both shoot dry weight and root dry weight (Fig. 1). On the other hand, at high PBSA concentrations we detected significant differences in the plant biomass parameters for some treatments. Specifically, shoot dry weight was highest in the SSPN treatment (0.080 ± 0.005 g, mean \pm SE) and lowest in the SN treatment (0.044 ± 0.004 g, mean \pm SE) (Fig. 1b). Root dry weight was also lowest in the SN (0.008 ± 0.002 g, mean \pm SE) but highest in the SPN treatments (0.034 ± 0.011 g, mean \pm SE) (Fig. 1d). In the sterile soil and water control treatments, the effects of PBSA

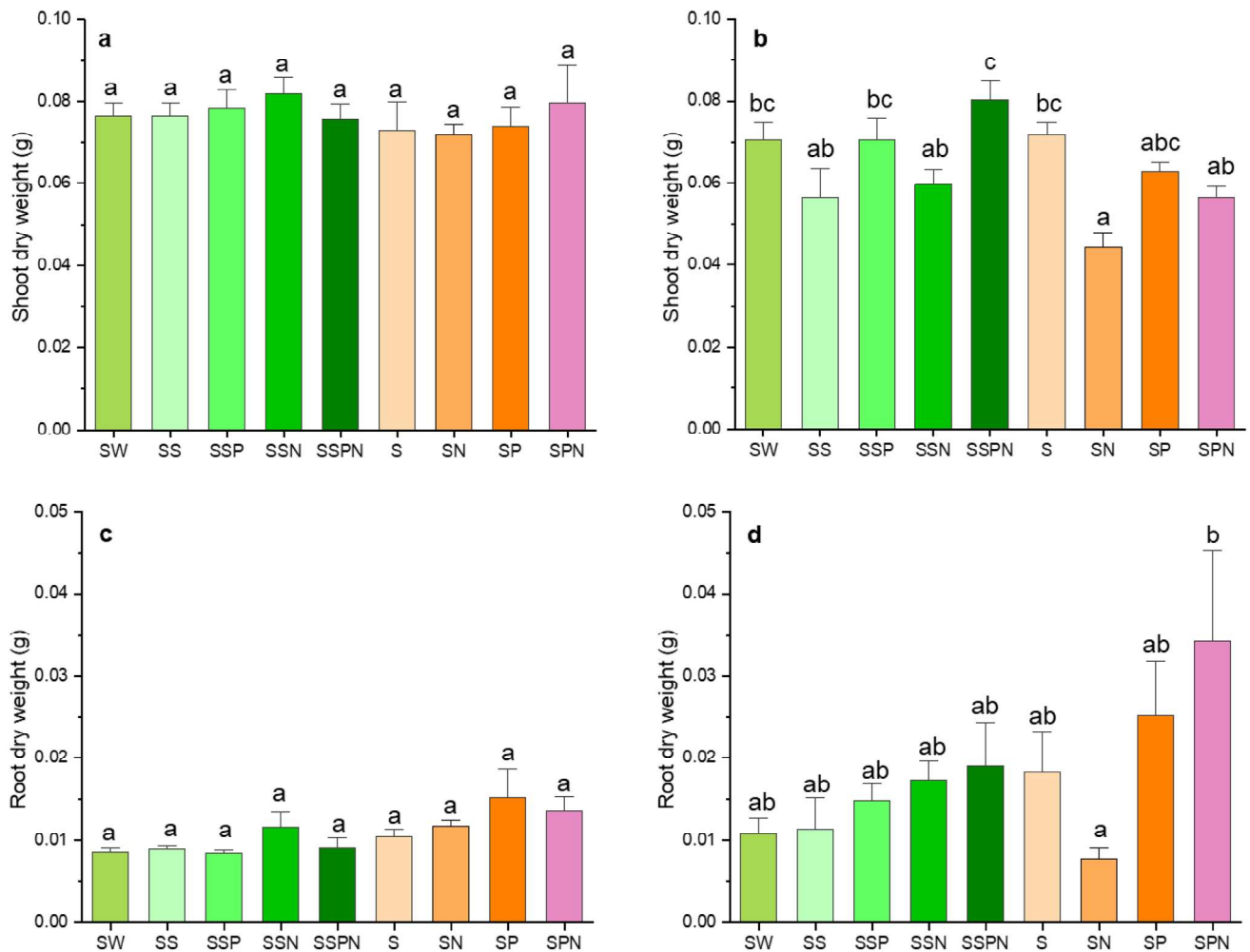


Fig. 1 Shoot and root biomass weight after nine treatments (mean \pm SE, $n=5$) with high (**a, c**) or low (**b, d**) soil dilution concentration. Different letters above the bars indicate significant differences ($P < 0.05$) according to one-way analysis of variance (ANOVA) or Kruskal–Wallis test. Abbreviations are SW, sterile water; SS, sterile

soil; SSP, sterile soil and PBSA amendment; SSN, sterile soil and N fertilizer; SSPN, sterile soil with PBSA amendment and N fertilizer; S, soil; SN, soil and N fertilizer; SP, soil and PBSA amendment; SPN, soil with PBSA amendment and N fertilizer

addition, N fertilization as well as their combined effect on both shoot and root dry weights were almost negligible (Fig. 1). The exception was found for the combined effect of PBSA and N fertilization for the sterile soil (SSPN) treatment (0.080 ± 0.005 g, mean \pm SE) which showed higher shoot dry weight as compared with SSN (0.060 ± 0.004 g, mean \pm SE) and SS (0.056 ± 0.007 g, mean \pm SE) treatments. In contrast, we detected a significant negative effect of N fertilization on shoot and root dry weight in the non-sterile soil treatment (SN).

***F. solani* Disease Incidence**

Either amendment of PBSA (SSP and SP) or N fertilizer (SSN and SN) alone did not increase *F. solani* disease

incidence in both experiments using high or low soil dilution concentrations (Table 1). In contrast, treatment with PBSA amendment and N fertilizer in non-sterile soil (SPN) strongly increased the *F. solani* disease incident. At the high soil dilution concentration, the *F. solani* disease incident was 67.5% while at the low dilution concentration disease incident reached 92.5% (Table 1; Fig. 2, S1). These results were confirmed by specific *F. solani* PCR (Fig. S1).

The independent replication of the experiments showed similar *F. solani* disease incident of 83.3% and 87.5% from low or high dilutions in the soil suspension, respectively (Supplementary Material Table S2). Therefore, a higher concentration of PBSA combined with N fertilizer strongly negatively affected plant development. Nevertheless, also other fungal pathogens infected the mung bean seedlings of the non-sterile treatments (S, SN, SP, and SPN; Table 2

Table 1 *F. solani* disease incident in percent after nine treatments (mean ± SE, n = 5) with low or high soil dilution concentration

Soil dilution concentration	SW	SS	SSP	SSN	SSPN	S	SN	SP	SPN	P value
High	0 ± 0a	0 ± 0a	0 ± 0a	0 ± 0a	0 ± 0a	0 ± 0a	0 ± 0a	0 ± 0a	67.5 ± 6.4b	P < 0.001
Low	0 ± 0a	0 ± 0a	0 ± 0a	0 ± 0a	0 ± 0a	0 ± 0a	0 ± 0a	0 ± 0a	92.5 ± 3.1b	P < 0.001

Different letters indicate significant differences (P < 0.05) according to Kruskal–Wallis test. Abbreviations can be found in legend of Fig. 1

Laboratory experiment

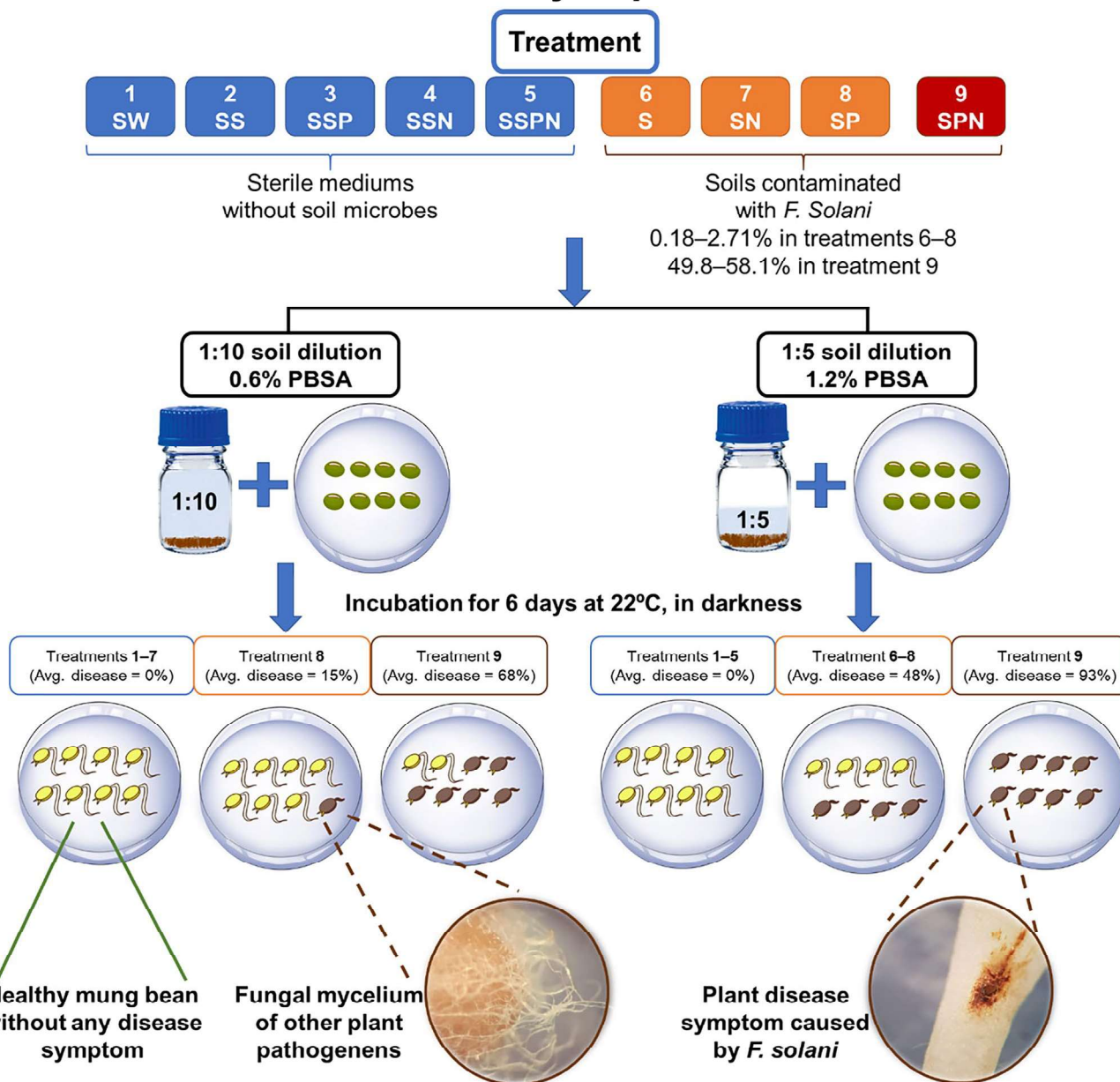


Fig. 2 Microscopic and PCR results of *F. solani* disease incidence after nine treatments and its respective *F. solani* frequency of each seedling and treatment. Abbreviations are SW sterile water; SS sterile soil; SSP sterile soil and PBSA amendment; SSN sterile soil and N fertilizer; SSPN sterile soil with PBSA amendment and N fertilizer; S

soil; SN soil and N fertilizer; SP soil and PBSA amendment; SPN soil with PBSA amendment and N fertilizer. Two soil dilution levels were used: 1:10 (high dilution, low soil or soil/PBSA concentration) and 1:5 (low dilution, high soil or soil/PBSA concentration) (n = 5)

Table 2 Overall disease incident in percent after nine treatments (mean \pm SE, $n=5$) with high or low soil dilution concentrations

Soil dilution concentration	SW	SS	SSP	SSN	SSPN	S	SN	SP	SPN	<i>P</i> value
High	0 \pm 0a	0 \pm 0a	0 \pm 0a	0 \pm 0a	0 \pm 0a	0 \pm 0a	0 \pm 0a	15 \pm 7.3a	67.5 \pm 6.4b	$P < 0.001$
Low	0 \pm 0a	0 \pm 0a	0 \pm 0a	0 \pm 0a	0 \pm 0a	45 \pm 22.6bc	80 \pm 20bc	17.5 \pm 9.4ab	92.5 \pm 3.1c	$P < 0.001$

Different letters indicate significant differences ($P < 0.05$) according to Kruskal–Wallis test. Abbreviations can be found in legend of Fig. 1

and Supplementary Material Table S3). Especially in SN treatment, we found very high disease incident rate of other fungi (80%), which caused strong reductions of both shoot and root weight (Table 2; Fig. 2). Among the non-sterile soil treatments, PBSA amendment treatment (SP) resulted in the lowest overall disease incidents, which was not significantly different from control non-sterile soil (S) as well as all the sterile water and soil treatments (SW, SS). Both SW and SS treatments were completely without any disease incidents of *V. radiata* seedlings. In addition, *F. solani* was not detected in any seedling from these treatments. In contrast, majority of infections in non-sterile soil treatments with PBSA and

N fertilizer (SPN) were caused by *F. solani* (Tables 1 and 2; Fig. 2). We summarized the experimental setup, microscopic results of healthy and infected plants (*F. solani* vs. other fungi) and the overall results in Fig. 2.

Illumina amplicon sequencing of 1 year-soil and mung bean plants in SPN treatment supported these findings as *F. solani* was the most dominant plant pathogen (Table 3 and Supplementary Material Table S4). Top-20 fungal ASVs that had the highest average relative abundances in 1 year-soil and *V. radiata* in SPN treatment are presented in Table 3. The overall relative abundance of *F. solani* was approximately 33% in the soil, while it was highly enriched

Table 3 Top-20 fungal ASVs that had the highest average relative abundances in 1 year-soil and mung bean plants (*V. radiata*) in SPN (soil, PBSA and N fertilizer) treatment, which contributed for 94.9

and 99.7% of the total detected sequences from SPN derived from soil and seedling, respectively

ASV	SPN soil	SPN seedling	Class	Family	Species	Functional group
ASV_000005	6.95	78.41	Sordariomycetes	Nectriaceae	<i>Fusarium solani</i>	Plant Pathogen
ASV_000001	25.31	5.46	Sordariomycetes	Nectriaceae	<i>Fusarium solani</i>	Plant Pathogen
ASV_000002	16.23	0.00	Eurotiomycetes	Herpotrichiellaceae	<i>Exophiala equina</i>	Animal Pathogen-Saprotroph
ASV_000012	14.76	0.84	Leotiomycetes	Pseudeurotiaceae	–	Saprotroph
ASV_000058	6.81	0.03	Leotiomycetes	Myxotrichaceae	<i>Oidiodendron echinulatum</i>	Ericoid Mycorrhizal
ASV_000027	0.00	11.31	Sordariomycetes	Nectriaceae	<i>Fusarium solani</i>	Plant Pathogen
ASV_000065	5.87	0.00	Leotiomycetes	Myxotrichaceae	<i>Oidiodendron echinulatum</i>	Ericoid Mycorrhizal
ASV_000024	3.73	0.00	Sordariomycetes	Nectriaceae	<i>Fusicolla aquaeductuum</i>	Mycoparasite
ASV_000068	2.53	0.00	Leotiomycetes	Pseudeurotiaceae	–	Saprotroph
ASV_000032	0.29	3.59	Sordariomycetes	Nectriaceae	<i>Fusarium</i> sp.	Plant Pathogen
ASV_000083	2.28	0.01	Leotiomycetes	Pseudeurotiaceae	–	Saprotroph
ASV_000132	1.94	0.04	Sordariomycetes	Ophiocordycipitaceae	<i>Purpureocillium lilacinum</i>	Animal parasite
ASV_000029	1.94	0.00	Eurotiomycetes	Herpotrichiellaceae	<i>Exophiala</i> sp.	Animal Pathogen-Saprotroph
ASV_000098	1.50	0.00	Leotiomycetes	Pseudeurotiaceae	–	Saprotroph
ASV_000166	0.96	0.00	Leotiomycetes	Myxotrichaceae	<i>Oidiodendron truncatum</i>	Ericoid Mycorrhizal
ASV_000009	0.90	0.00	Sordariomycetes	Chaetomiaceae	<i>Chaetomium</i> sp.	Saprotroph-Endophyte-Plant pathogen
ASV_000007	0.87	0.00	Sordariomycetes	Nectriaceae	<i>Ilyonectria macrodidyma</i>	Plant Pathogen
ASV_000195	0.75	0.00	Leotiomycetes	–	–	–
ASV_000037	0.71	0.00	Sordariomycetes	Microasceae	<i>Pseudallescheria boydii</i>	Saprotroph
ASV_000214	0.55	0.00	Leotiomycetes	Pseudeurotiaceae	–	Saprotroph

Taxonomic information of all detected fungi can be found Supplementary Table S4

(95% of total sequences) in the seedlings growing in the SPN treatment (Table 3 and Supplementary Material Table S4). Apart *F. solani*, another plant pathogen (*Fusarium oxysporum*) also colonized seedling with low relative abundances (Supplementary Material Table S4).

Discussion

PBSA Alone Does Not Significantly Negatively Impact on Plant Growth and Disease Incidence

Based on a limited number of studies, low concentration of PBSA based plastics have no adverse effects on soil microorganisms (bacteria and fungi) and soil ecosystem functions (including nitrification potential and soil esterase activity) [15, 40]. These results are consistent with those from studies on other bio-based and biodegradable plastics (e.g., PBS and PBAT), where the incorporation of such plastics into soil is generally not harmful to biological soil health, microbial diversity, and soil ecosystem functions, such as nitrification potential, nutrient cycling, and fertility [41, 42]. Nevertheless, a recent study based on high resolution molecular techniques showed that high load of PBSA (6%) caused a significantly decline of archeal, bacterial and fungal richness [21]. The bacterial and fungal community composition also significantly changed after the addition of such high load of PBSA. In addition, another recent study based on high resolution molecular techniques revealed that rhizospheric soil bacterial community composition and their volatile profiles associated with wheat plants were significantly altered by microplastics of starch-based biodegradable plastic mulching film [24].

In this study, we showed that PBSA alone does not significantly negatively impact on plant biomass and *F. solani* disease incidence, even at high PBSA concentrations. Our results on plant biomass are in line with other studies, which focused on similar biotest model ecotoxicity of 1% concentration bio-based and biodegradable plastics degraded under controlled conditions for 6 months on growth of plants (the monocotyledon *Sorghum saccharatum* and the dicotyledon *Lepidium sativum*) [22]. However, these findings were in contradiction to our findings as amendment of 1% low-density PE and a starch-based biodegradable plastic mulching film in soil caused negative effects on wheat growth [23]. Therefore, negative effects of bio-based and biodegradable plastics on plant development may be related to many factors such as types and concentrations of bio-based and biodegradable plastics, plant species and other environmental conditions such as the application of N fertilizer [21, 27]. It is important to examine the impact of bio-based and biodegradable

plastics on plant development from seedlings to maturation stages as well as on soil microbial communities. Bandopadhyay et al. (2020) showed that amendment of biodegradable and bio-based plastics had no significant effect on the soil microbial community composition [43]. Moreover, such microbial compositions were rather mostly affected by microclimate, seasonal and local parameters, which may govern the microbial community composition and hide other effects [43]. Soil health and shifts in microbial community composition may influence plant performance including plant growth, plant mass and plant health [44, 45]. Still, we know very little on bio-based and biodegradable plastic microbiome [20] and their relationships between the degradation processes and its impacts on plant development.

Combination of Amendment of High PBSA Concentration and N Fertilizer Causes Significantly Negative Effect on Plant Health

Some studies have found that bio-based and biodegradable plastics enhanced soil enzyme activity and microbial biomass [41, 46]. High soil quality is linked to higher microbial biomass and enzyme activities compared to those with lower ones [47, 48]. However, increase of microbial biomass and enzyme activity may not necessarily result into a benefit for soil systems or plant development. For example, if the increased microbial biomass and enzyme activities are associated with fungal plant pathogens. Therefore, an effect of plastic derivatives on microbial functional traits requires careful interpretation considering its consequences for soil ecosystem services and plant development.

In our previous study we showed that after amendment of high concentration of PBSA in combination with N fertilizer, the fungal plant pathogen *F. solani* was enriched in soil [21], here we show that such enrichment can affect the health of seedlings. Although the shoot and root biomass of seedlings was not significantly impacted by the SPN treatment, the seedlings were heavily infected with *F. solani*. Such tremendous infections during the developmental stage make the seedlings less competitive and their survival less likely [49, 50]. In view of the dramatic effects observed after high PBSA load and N fertilisation in our petri dish test system with soil water suspension, one can hypothesize that if the experiment would be conducted in the pot experiment or in the field for longer time, the biomass of *V. radiata* in the SPN treatments would be greatly reduced or totally loss.

It has been reported that *F. solani* can colonize various types of biodegradable plastics, especially PBS and its derivatives (PBSA) [26, 51]. Due to their degradability in field soil conditions, PBS and PBSA have been used as mulching films. Meanwhile, farmers may leave such mulching films in the field to reduce the time and labor cost, thus these plastic can

highly accumulate in soil [18, 19, 21]. The PBSA films are described to fragment into smaller pieces (macro plastics), particles (micro- and nano-plastics) or molecules (metabolites and CO₂) [52]. In combination with high load of N fertilizer in the field, *F. solani* can be enriched in both soil and PBSA, which subsequently can increase the disease incident of plant roots and shoots. The usage of high doses of N fertilizer can enrich soil N, which will be taken up by both plant and microbes. It has been shown in our previous study that the same kind of N fertilizer supported *F. solani* to outcompete other fungal PBSA colonizers and become the most dominant fungi in PBSA-soil system [21]. This implies that in conventional agriculture, which involves PBSA based mulching films and high load N fertilizer applications may lead to significant enrichment of *F. solani* in the soil. To prevent such scenario, we suggest ideally to remove the biodegradable mulching films from the field for recycling [21].

Although we successfully demonstrate the clear negative effect of the combination of PBSA load and N fertilizer on plant health, in this treatment we co-manipulated two factors, the plastic addition and the *F. solani* propagule concentration. Thus, what we measured, is the effect of these two factors, and we cannot distinguish whether the effect was due to one factor or the other, or even to the sum of their effects. When only one factor was applied (N fertilization or PBSA addition), we did not detect the negative effect. Clearly, there is a confounding factor (and/or their interactions) and we cannot conclude whether the effect were due to the PBSA load or the *F. solani* propagule quantity. In this regard, our control with sterilized soil helps a little, as it suppressed the propagules, however to fully distinguish the effects of the plastic from the one of the inoculated propagules, we should add another treatment inoculating a known propagule quantity after the sterilization.

Future Study

To avoid potentially negative effects of different types of bio-based and biodegradable plastics on plant development, caused by fungal plant pathogens, it is urgently needed to examine shifts in the soil microbiome during degradation process of bio-based and biodegradable plastics using high-resolution molecular approaches. In addition, the ecotoxicity effects of different types of bio-based and biodegradable plastics on plant developments deserve also more attention by testing against different model plants as well as other economic plants. The effect of different concentrations and types of fertilizers should be tested in presence of PBSA to evaluate its impact on seedling development. Moreover, future studies should also focus on evaluating the effect of bio-based and biodegradable plastics on the long-term effects on soil microbiome, plant development and fitness under various field and weather conditions.

Conclusions

In this work, we raised the concern of the interaction between high load of bio-based and biodegradable plastics (PBSA) and N fertilizer to plant development. Our study suggests that PBSA alone in the soil environment do not significantly negatively impact disease incidence and plant development. However, when N fertilizer and PBSA are simultaneously present in soil, plant pathogen *F. solani* is enriched and thereby plant development was weakened. Thus, it is essential to plan and manage the use of bio-based and biodegradable plastics as mulching films after the agricultural uses.

Supplementary Information The online version contains supplementary material available at <https://doi.org/10.1007/s10924-022-02435-z>.

Acknowledgements The community composition data have been computed at the High-Performance Computing (HPC) Cluster EVE, a joint effort of both the Helmholtz Centre for Environmental Research—UFZ and the German Centre for Integrative Biodiversity Research (iDiv) Halle-Jena-Leipzig. We thank the Helmholtz Association, the Federal Ministry of Education and Research, the State Ministry of Science and Economy of Saxony-Anhalt, and the State Ministry for Higher Education, Research and the Arts Saxony for funding the Global Change Experimental Facility (GCEF) project. We also thank the staff of the Bad Lauchstädt Experimental Research Station (especially Ines Merbach and Konrad Kirsch) for their work in maintaining the plots and infrastructures of the GCEF, and Dr. Stefan Klotz, Dr. Martin Schädler, Dr. Harald Auge, and Dr. Thomas Reitz for their roles in setting up the GCEF. We thank Dr. Turki M. Dawoud for his help for reading and commenting an advanced version of the manuscript.

Author Contributions SS, KJ, BT, MN and WP conceived and designed the study. SS, KJ, BT and WP led the laboratory experimental set-up. WP, FB and MN contributed reagents and laboratory equipment. BT, SS, KJ and WP led the DNA analysis. SW led bioinformatics. WP and SS led the microbial taxonomy and data analyses. SS, KJ, BT and WP wrote the manuscript. MN and WP supervised SS, KJ, BT. MN, SW and FB reviewed and gave comments and suggestions for manuscript. All of the authors gave final approval for manuscript submission.

Funding Open Access funding enabled and organized by Projekt DEAL. This work has been partially funded by the internal research budget to Department of Soil Ecology, UFZ-Helmholtz Centre for Environmental Research.

Data Availability The Illumina sequencing of prokaryotic and fungal datasets are deposited in The National Center for Biotechnology Information (NCBI) database under BioProject ID: PRJNA818504.

Declarations

Conflict of interest The authors declare that they have no competing interests. The authors declare that they have no known competing financial interests or personal relationships that could have appeared to influence the work reported in this paper.

Ethical approval Not applicable.

Consent for publication Not applicable.

Open Access This article is licensed under a Creative Commons Attribution 4.0 International License, which permits use, sharing, adaptation, distribution and reproduction in any medium or format, as long as you give appropriate credit to the original author(s) and the source, provide a link to the Creative Commons licence, and indicate if changes were made. The images or other third party material in this article are included in the article's Creative Commons licence, unless indicated otherwise in a credit line to the material. If material is not included in the article's Creative Commons licence and your intended use is not permitted by statutory regulation or exceeds the permitted use, you will need to obtain permission directly from the copyright holder. To view a copy of this licence, visit <http://creativecommons.org/licenses/by/4.0/>.

References

1. Ngosong C, Okolle JN, Tening AS (2019) Mulching: a sustainable option to improve soil health. In: Panpatte DG, Jhala YK (eds) Soil fertility management for sustainable development. Springer, Singapore, pp 231–249
2. Stringer LC, Dyer JC, Reed MS et al (2009) Adaptations to climate change, drought and desertification: local insights to enhance policy in southern Africa. *Environ Sci Policy* 12:748–765. <https://doi.org/10.1016/j.envsci.2009.04.002>
3. Bu L, Liu J, Zhu L et al (2013) The effects of mulching on maize growth, yield and water use in a semi-arid region. *Agric Water Manag* 123:71–78. <https://doi.org/10.1016/j.agwat.2013.03.015>
4. Mahrer Y (1979) Prediction of soil temperatures of a soil mulched with transparent polyethylene. *J Appl Meteorol Climatol* 18:1263–1267. [https://doi.org/10.1175/1520-0450\(1979\)018%3c1263:POSTOA%3e2.0.CO;2](https://doi.org/10.1175/1520-0450(1979)018%3c1263:POSTOA%3e2.0.CO;2)
5. Wien HC, Minotti PL, Grubinger VP (1993) Polyethylene mulch stimulates early root growth and nutrient uptake of transplanted tomatoes. *J Am Soc Hortic Sci* 118:207–211. <https://doi.org/10.21273/JASHS.118.2.207>
6. Liakatas A, Clark JA, Monteith JL (1986) Measurements of the heat balance under plastic mulches. Part I. Radiation balance and soil heat flux. *Agric For Meteorol* 36:227–239. [https://doi.org/10.1016/0168-1923\(86\)90037-7](https://doi.org/10.1016/0168-1923(86)90037-7)
7. Westhuizen JHVD (1980) The effect of black plastic mulch on growth, production and root development of Chenin blanc vines under dryland conditions. *South Afr J Enol Vitic* 1:1–6. <https://doi.org/10.21548/1-1-2408>
8. Rajablariani HR, Hassankhan F, Rafezi R (2012) Effect of colored plastic mulches on yield of tomato and weed biomass. *IJESD*. <https://doi.org/10.7763/IJESD.2012.V3.291>
9. Zhang F, Zhang W, Li M et al (2017) Is crop biomass and soil carbon storage sustainable with long-term application of full plastic film mulching under future climate change? *Agric Syst* 150:67–77. <https://doi.org/10.1016/j.agsy.2016.10.011>
10. Kasirajan S, Ngouajio M (2012) Polyethylene and biodegradable mulches for agricultural applications: a review. *Agron Sustain Dev* 32:501–529. <https://doi.org/10.1007/s13593-011-0068-3>
11. Hussain I, Hamid H (2003) Plastics in agriculture. In: *Plastics and the environment*. Wiley, New York pp 185–209
12. Piehl S, Leibner A, Löder MGJ et al (2018) Identification and quantification of macro- and microplastics on an agricultural farmland. *Sci Rep* 8:17950. <https://doi.org/10.1038/s41598-018-36172-y>
13. Babu RP, O'Connor K, Seeram R (2013) Current progress on bio-based polymers and their future trends. *Prog Biomater* 2:8. <https://doi.org/10.1186/2194-0517-2-8>
14. Brizga J, Hubacek K, Feng K (2020) The unintended side effects of bioplastics: carbon, land, and water footprints. *One Earth* 3:45–53. <https://doi.org/10.1016/j.oneear.2020.06.016>
15. Haider TP, Völker C, Kramm J et al (2019) Plastics of the future? The impact of biodegradable polymers on the environment and on society. *Angew Chem Int Ed* 58:50–62. <https://doi.org/10.1002/anie.201805766>
16. Niaounakis M (2015) *Biopolymers: processing and products*. Elsevier, Introduction
17. Yamamoto-Tamura K, Hoshino YT, Tsuboi S et al (2020) Fungal community dynamics during degradation of poly(butylene succinate-co-adipate) film in two cultivated soils in Japan. *Biosci Biotechnol Biochem* 84:1077–1087. <https://doi.org/10.1080/09168451.2020.1713718>
18. Serrano-Ruiz H, Martin-Closas L, Pelacho AM (2021) Biodegradable plastic mulches: impact on the agricultural biotic environment. *Sci Total Environ* 750:141228. <https://doi.org/10.1016/j.scitotenv.2020.141228>
19. Koitabashi M, Noguchi MT, Sameshima-Yamashita Y et al (2012) Degradation of biodegradable plastic mulch films in soil environment by phylloplane fungi isolated from gramineous plants. *AMB Express* 2:40. <https://doi.org/10.1186/2191-0855-2-40>
20. Purahong W, Wahdan SFM, Heinz D et al (2021) Back to the future: decomposability of a biodegradable plastic in field soil environments and its microbiome under ambient and future climates. *Environ Sci Technol*. <https://doi.org/10.1021/acs.est.1c02695>
21. Tanunchai B, Juncheed K, Wahdan SFM et al (2021) Analysis of microbial populations in plastic–soil systems after exposure to high poly(butylene succinate-co-adipate) load using high-resolution molecular technique. *Environ Sci Eur*. <https://doi.org/10.1186/s12302-021-00528-5>
22. Sforzini S, Oliveri L, Chinaglia S, Viarengo A (2016) Application of biotests for the determination of soil ecotoxicity after exposure to biodegradable plastics. *Front Environ Sci*. <https://doi.org/10.3389/fenvs.2016.00068>
23. Qi Y, Yang X, Pelaez AM et al (2018) Macro- and micro-plastics in soil-plant system: effects of plastic mulch film residues on wheat (*Triticum aestivum*) growth. *Sci Total Environ* 645:1048–1056. <https://doi.org/10.1016/j.scitotenv.2018.07.229>
24. Qi Y, Ossowicki A, Yang X et al (2020) Effects of plastic mulch film residues on wheat rhizosphere and soil properties. *J Hazard Mater* 387:121711. <https://doi.org/10.1016/j.jhazmat.2019.121711>
25. Abe M, Kobayashi K, Honma N, Nakasaki K (2010) Microbial degradation of poly(butylene succinate) by *Fusarium solani* in soil environments. *Polym Degrad Stab* 95:138–143. <https://doi.org/10.1016/j.polymdegradstab.2009.11.042>
26. Gan Z, Zhang H (2019) PMBD: a comprehensive plastics microbial biodegradation database. *Database*. <https://doi.org/10.1093/database/baz119>
27. Coleman JJ (2016) The *Fusarium solani* species complex: ubiquitous pathogens of agricultural importance. *Mol Plant Pathol* 17:146–158. <https://doi.org/10.1111/mpp.12289>
28. Boughalleb N, El Mahjoub M (2006) In vitro determination of *Fusarium* spp. Infection on watermelon seeds and their localization. *Plant Path J* 5:178–182
29. Abney TS, Richards TL, Roy KW (1993) *Fusarium solani* from ascospores of *Nectria Haematococca* causes sudden death syndrome of soybean. *Mycologia* 85:801–806. <https://doi.org/10.1080/00275514.1993.12026335>
30. Zhang S, Yang X, Gertsen H et al (2018) A simple method for the extraction and identification of light density microplastics from soil. *Sci Total Environ* 616–617:1056–1065. <https://doi.org/10.1016/j.scitotenv.2017.10.213>

31. ZhenMing Z, XueGang L, YouGuo F, Qiang W (2015) Cumulative effects of powders of degraded PE mulching-films on chemical properties of soil. *Environ Sci Technol (China)* 38:115–119
32. Purahong W, Alkadri D, Nipoti P et al (2012) Validation of a modified Petri-dish test to quantify aggressiveness of *Fusarium graminearum* in durum wheat. *Eur J Plant Pathol* 132:381–391. <https://doi.org/10.1007/s10658-011-9883-2>
33. Arif M, Chawla S, Zaidi MW et al (2012) Development of specific primers for genus *Fusarium* and *F. solani* using rDNA sub-unit and transcription elongation factor (TEF-1 α) gene. *Afr J Biotech* 11:444–447. <https://doi.org/10.4314/ajb.v11i2>
34. Ihrmark K, B odeker ITM, Cruz-Martinez K et al (2012) New primers to amplify the fungal ITS2 region—evaluation by 454-sequencing of artificial and natural communities. *FEMS Microbiol Ecol* 82:666–677. <https://doi.org/10.1111/j.1574-6941.2012.01437.x>
35. White TJ, Bruns TD, Lee S, Taylor J (1990) Amplification and direct sequencing of fungal ribosomal RNA genes for phylogenetics. In: Innis MA, Gelfand DH, Sninsky JJ, White TJ (eds) *PCR protocols: a guide to methods and applications*. Academic Press, San Diego, pp 315–322
36. Wei becker C, Schnabel B, Heintz-Buschart A (2020) Dadasnake, a Snakemake implementation of DADA2 to process amplicon sequencing data for microbial ecology. *GigaScience*. <https://doi.org/10.1093/gigascience/giaa135>
37. Nilsson RH, Larsson K-H, Taylor AFS et al (2019) The UNITE database for molecular identification of fungi: handling dark taxa and parallel taxonomic classifications. *Nucleic Acids Res* 47:D259–D264. <https://doi.org/10.1093/nar/gky1022>
38. Callahan BJ, McMurdie PJ, Holmes SP (2017) Exact sequence variants should replace operational taxonomic units in marker-gene data analysis. *ISME J* 11:2639–2643. <https://doi.org/10.1038/ismej.2017.119>
39. Hammer  , Harper DAT, Ryan PD (2001) PAST: paleontological statistics software package for education and data analysis. *Palaeontol Electron* 4:9
40. Yamamoto-Tamura K, Hiradate S, Watanabe T et al (2015) Contribution of soil esterase to biodegradation of aliphatic polyester agricultural mulch film in cultivated soils. *AMB Expr* 5:10. <https://doi.org/10.1186/s13568-014-0088-x>
41. Bandopadhyay S, Martin-Closas L, Pelacho AM, DeBruyn JM (2018) Biodegradable plastic mulch films: impacts on soil microbial communities and ecosystem functions. *Front Microbiol*. <https://doi.org/10.3389/fmicb.2018.00819>
42. Sintim HY, Bandopadhyay S, English ME et al (2019) Impacts of biodegradable plastic mulches on soil health. *Agr Ecosyst Environ* 273:36–49. <https://doi.org/10.1016/j.agee.2018.12.002>
43. Bandopadhyay S, Sintim HY, DeBruyn JM (2020) Effects of biodegradable plastic film mulching on soil microbial communities in two agroecosystems. *PeerJ*. <https://doi.org/10.7717/peerj.9015>
44. M. Tahat M, M. Alananbeh K, A. Othman Y, I. Leskovar D (2020) Soil health and sustainable agriculture. *Sustainability* 12:4859. <https://doi.org/10.3390/su12124859>
45. Wang R, Zhang H, Sun L et al (2017) Microbial community composition is related to soil biological and chemical properties and bacterial wilt outbreak. *Sci Rep* 7:343. <https://doi.org/10.1038/s41598-017-00472-6>
46. Li C, Moore-Kucera J, Miles C et al (2014) Degradation of potentially biodegradable plastic mulch films at three diverse U.S. locations. *Agroecol Sustain Food Syst* 38:861–889. <https://doi.org/10.1080/21683565.2014.884515>
47. Acosta-Martinez V, Tabatabai MA (2000) Enzyme activities in a limed agricultural soil. *Biol Fertil Soils* 31:85–91. <https://doi.org/10.1007/s003740050628>
48. Das S, Varma A (1970) Role of enzymes in maintaining soil health. In: *Soil Biol* pp 25–42
49. Chaparro JM, Badri DV, Vivanco JM (2014) Rhizosphere microbiome assemblage is affected by plant development. *ISME J* 8:790–803. <https://doi.org/10.1038/ismej.2013.196>
50. Hu J, Wei Z, Kowalchuk GA et al (2020) Rhizosphere microbiome functional diversity and pathogen invasion resistance build up during plant development. *Environ Microbiol* 22:5005–5018. <https://doi.org/10.1111/1462-2920.15097>
51. Emadian SM, Onay TT, Demirel B (2017) Biodegradation of bioplastics in natural environments. *Waste Manag* 59:526–536. <https://doi.org/10.1016/j.wasman.2016.10.006>
52. Puchalski M, Szparaga G, Biela T et al (2018) Molecular and supramolecular changes in polybutylene succinate (PBS) and polybutylene succinate adipate (PBSA) copolymer during degradation in various environmental conditions. *Polymers* 10:251. <https://doi.org/10.3390/polym10030251>

Publisher's Note Springer Nature remains neutral with regard to jurisdictional claims in published maps and institutional affiliations.

Plastic 4 – Supplementary Information

Interactions between high load of a bio-based and biodegradable plastic and nitrogen fertilizer affect plant biomass and health: A case study with *Fusarium solani* and mung bean (*Vigna radiata* L.).

Author: Sarah-Maria Scheid*, Kantida Juncheed*, **Benjawan Tanunchai***, Sara Fareed Mohamed Wahdan, François Buscot, Matthias Noll, Witoon Purahong

*These authors contributed equally to this work.

Status: Published

Publication: Journal of Environmental Polymer Degradation

Publisher: Springer Nature

Date: 30 Mar 2022

J Polym Environ.

Copyright © 2022, The Author(s)

Reprinted with permission from Springer Nature.

Available online at: <https://doi.org/10.1007/s10924-022-02435-z>

Or please see separate attachments

4. List of publications in peer-reviewed journals

2023 **Tanunchai, B.***, Ji, L.*, Schröder, O., Wahdan, S. F. M., hongasuk K., et al. (2023). Tree mycorrhizal type regulates leaf and needle microbial communities, affects microbial assembly and co-occurrence network patterns, and influences litter decomposition rates in temperate forest. *Front. Plant Sci.* (In press, IF 2021 = 6.627) *These authors contributed equally to this work.

Tanunchai, B.*, Ji, L.*, Schröder, O., Gawol, S. J., Geissler, A., Wahdan, S. F. M., et al. (2023). Fate of a biodegradable plastic in forest soil: Dominant tree species and forest types drive changes in microbial community assembly, influence the composition of plastisphere, and affect poly(butylene succinate-co-adipate) degradation. *Science of The Total Environment* 873, 162230. doi: 10.1016/j.scitotenv.2023.162230. (IF 2021 = 10.753) *These authors contributed equally to this work.

2022 **Tanunchai, B.***, Ji, L.*, Schroeter, S. A., Wahdan, S. F. M., Larpkern, P., Lehnert, A.-S., et al. (2022a). A poisoned apple: First insights into community assembly and networks of the fungal pathobiome of healthy-looking senescing leaves of temperate trees in mixed forest ecosystem. *Front. Plant Sci.* 13. doi: <https://doi.org/10.3389/fpls.2022.968218>. (IF 2021 = 6.627) *These authors contributed equally to this work.

Tanunchai, B.*, Schroeter, S. A.*, Ji, L., Wahdan, S. F. M., Hossen, S., Lehnert, A.-S., et al. (2022b). More than you can see: Unraveling the ecology and biodiversity of lichenized fungi associated with leaves and needles of 12 temperate tree species using high-throughput sequencing. *Front. Microbiol.* 13. doi: <https://doi.org/10.3389/fmicb.2022.907531>. (IF 2021 = 6.064) *These authors contributed equally to this work.

Juncheed, K.* , **Tanunchai, B.***, Wahdan, S. F. M., Thongsuk, K., Schädler, M., Noll, M., et al. (2022). Dark side of a bio-based and biodegradable plastic? Assessment of pathogenic microbes associated with poly(butylene succinate-co-adipate) under ambient and future climates using next-generation sequencing. *Front. Microbiol.* 13. doi: <https://doi.org/10.3389/fpls.2022.966363>. (IF 2021 = 6.627) *These authors contributed equally to this work.

Wahdan, S. F. M., Ji, L., Schädler, M., Wu, Y.-T., Sansupa, C., **Tanunchai, B.**, et al. (2022). Future climate conditions accelerate wheat straw decomposition alongside altered microbial community composition, assembly patterns, and interaction networks. *ISME J*, 1–14. doi: 10.1038/s41396-022-01336-2. (IF 2021 = 10.302)

Ji, L.* , **Tanunchai, B.***, Wahdan, S. F. M., Schädler, M., and Purahong, W. (2022). Future climate change enhances the complexity of plastisphere microbial co-occurrence networks, but does not significantly affect the community assembly. *Science of the Total Environment*, 157016. doi: 10.1016/j.scitotenv.2022.157016. (IF 2021 = 10.753) *These authors contributed equally to this work.

Tanunchai, B.*, Ji, L.*, Schroeter, S. A., Wahdan, S. F. M., Hossen, S., Delelegn, Y., et al. (2022a). FungalTraits vs. FUNGuild: comparison of ecological functional assignments of leaf- and needle-associated fungi across 12 temperate tree species. *Microb Ecol.* doi: 10.1007/s00248-022-01973-2. (IF 2021: 4.192) *These authors contributed equally to this work.

Tanunchai, B.*, Kalkhof, S.* , Guliyev, V.* , Wahdan, S. F. M., Krstic, D., Schädler, M., et al. (2022b). Nitrogen fixing bacteria facilitate microbial biodegradation of a bio-based and biodegradable plastic in soils under ambient and future climatic conditions. *Environ. Sci.:*

Processes Impacts 24, 233–241. doi: 10.1039/D1EM00426C. (IF 2021: 5.334) *These authors contributed equally to this work.

Purahong, W.*, **Tanunchai, B.***, Muszynski, S.*, Maurer, F., Wahdan, S. F. M., Malter, J., et al. (2022b). Cross-kingdom interactions and functional patterns of active microbiota matter in governing deadwood decay. *Proceedings of the Royal Society B: Biological Sciences* 289, 20220130. doi: 10.1098/rspb.2022.0130. (IF 2021: 5.530) *These authors contributed equally to this work.

Scheid, S.-M.*, Juncheed, K.*, **Tanunchai, B.***, Wahdan, S. F. M., Buscot, F., Noll, M., et al. (2022). Interactions Between high load of a bio-based and biodegradable plastic and nitrogen fertilizer affect plant biomass and health: A case study with *Fusarium solani* and mung bean (*Vigna radiata* L.). *J Polym Environ.* doi: 10.1007/s10924-022-02435-z. (IF 2021: 4.705) *These authors contributed equally to this work.

Guliyev V*, **Tanunchai B***, Noll M, et al (2022) Links among microbial communities, soil properties and functions: Are fungi the sole players in decomposition of bio-based and biodegradable plastic? *Polymers* 14:2801. <https://doi.org/10.3390/polym14142801>. (IF 2021: 4.967) *These authors contributed equally to this work.

Frey, L., **Tanunchai, B.**, and Glaser, B. (2022). Antibiotics residues in pig slurry and manure and its environmental contamination potential. A meta-analysis. *Agron. Sustain. Dev.* 42, 31. doi: 10.1007/s13593-022-00762-y. (IF 2021: 7.832)

Purahong, W., Günther, A., Gminder, A., **Tanunchai, B.**, Gossner, M. M., Buscot, F., et al. (2022a). City life of mycorrhizal and wood-inhabiting macrofungi: Importance of urban areas for maintaining fungal biodiversity. *Landscape and Urban Planning* 221, 104360. doi: 10.1016/j.landurbplan.2022.104360. (IF 2021: 8.119)

Sangiorgio, D., Cellini, A., Donati, I., Ferrari, E., **Tanunchai, B.**, Fareed Mohamed Wahdan, S., et al. (2022). Taxonomical and functional composition of strawberry microbiome is genotype-dependent. *Journal of Advanced Research.* doi: 10.1016/j.jare.2022.02.009. (IF 2021 = 12.822)

2021 Tanunchai, B.; Juncheed, K.; Wahdan, S. F. M.; Guliyev, V.; Udovenko, M.; Lehnert, A.-S.; Alves, E. G.; Glaser, B.; Noll, M.; Buscot, F.; Blagodatskaya, E.; Purahong, W. **2021.** Analysis of microbial populations in plastic–soil systems after exposure to high poly(butylene succinate-co-adipate) load using high-resolution molecular technique. *Environmental Sciences Europe*, 33 (1), 105. <https://doi.org/10.1186/s12302-021-00528-5>. (IF 2021: 5.481)

Purahong, W.; Wahdan, S. F. M.; Heinz, D.; Jariyavidyanont, K.; Sungkapreecha, C.; **Tanunchai, B.**; Sansupa, C.; Sadubsarn, D.; Alaneed, R.; Heintz-Buschart, A.; Schädler, M.; Geissler, A.; Kressler, J.; Buscot, F. **2021.** Back to the future: decomposability of a biobased and biodegradable plastic in field soil environments and its microbiome under ambient and future climates. *Environ. Sci. Technol.*, 55 (18), 12337–12351. <https://doi.org/10.1021/acs.est.1c02695>. (IF 2021: 11.357)

Wahdan, S. F. M.; **Tanunchai, B.**; Wu, Y.-T.; Sansupa, C.; Schädler, M.; Dawoud, T. M.; Buscot, F.; Purahong, W. **2021.** Deciphering *Trifolium Pratense* L. holobiont reveals a microbiome resilient to future climate changes. *MicrobiologyOpen*, 10 (4), e1217. <https://doi.org/10.1002/mbo3.1217>. (IF 2021: 3.904)

Wahdan, S. F. M.; Hossen, S.; **Tanunchai, B.**; Sansupa, C.; Schädler, M.; Noll, M.; Dawoud, T. M.; Wu, Y.-T.; Buscot, F.; Purahong, W. **2021.** Life in the wheat litter: effects of future

climate on microbiome and function during the early phase of decomposition. *Microb Ecol.* <https://doi.org/10.1007/s00248-021-01840-6>. (IF 2021: 4.192)

Purahong, W., Hossen, S., Nawaz, A., Sadubsarn, D., **Tanunchai, B.**, Dommert, S., Ampornpan, L.-A., Werukamkul, P., and Wubet, T. 2021. Life on the rocks: first insights into the microbiota of the threatened aquatic rheophyte *Hanseniella heterophylla*. *Front. Plant Sci.* 12. Frontiers. doi:10.3389/fpls.2021.634960. (IF 2021: 6.627)

Wahdan, S.F.M., Heintz-Buschart, A., Sansupa, C., **Tanunchai, B.**, Wu, Y.-T., Schädler, M., Noll, M., Purahong, W., and Buscot, F. 2021. Targeting the active rhizosphere microbiome of *Trifolium pratense* in grassland evidences a stronger-than-expected belowground biodiversity-ecosystem functioning link. *Front. Microbiol.* 12. Frontiers. doi:10.3389/fmicb.2021.629169. (IF 2021: 6.064)

2020 Fareed Mohamed Wahdan, S., Hossen, S., **Tanunchai, B.**, Schädler, M., Buscot, F., and Purahong, W. 2020. Future climate significantly alters fungal plant pathogen dynamics during the early phase of wheat litter decomposition. *Microorganisms* 8: 908. (IF 2021: 4.926)

Mapook, A., Hyde, K.D., McKenzie, E.H.C., Jones, E.B.G., Bhat, D.J., Jeewon, R., Stadler, M., Samarakoon, M.C., Malaithong, M., **Tanunchai, B.**, Buscot, F., Wubet, T., and Purahong, W. 2020. Taxonomic and phylogenetic contributions to fungi associated with the invasive weed *Chromolaena odorata* (Siam weed). *Fungal Diversity* 101: 1–175. (IF 2021: 24.902)

2019 Purahong, W.*, Sadubsarn, D.*, **Tanunchai, B.***, Wahdan, S.F.M., Sansupa, C., Noll, M., Wu, Y.-T., and Buscot, F. 2019. First insights into the microbiome of a mangrove tree reveal significant differences in taxonomic and functional composition among plant and soil compartments. *Microorganisms* 7: 585. (IF 2021: 4.926) *These authors contributed equally to this work.

Acknowledgements

I would like to thank everyone who supported and motivated me while conducting this PhD dissertation. Special thanks go to my advisor, Dr. Witoon Purahong, for your kind help and support, his constructive suggestions and comments for all the works from my Bachelor to PhD, as well as financial support by his research budget from the Soil Ecology Department of the UFZ-Helmholtz Centre for Environmental Research. I would particularly like to acknowledge my supervisor, Prof. Dr. Matthias Noll, for his kind help and support during my PhD and valuable comments and suggestions for this dissertation. I would like to send special thanks to Prof. Dr. Ernst-Detlef Schulze, the owner of the managed mixed forest of Thuringia, Germany (51°12'N 10°18'E) who allowed us to conduct the largest leaf litter decomposition experiment in Germany. I would like to acknowledge Prof. Dr. Dr. François Buscot, head of the Soil Ecology Department, UFZ-Helmholtz Centre for Environmental Research, for his valuable comments and suggestions. I thank Beatrix Schnabel and Melanie Günther for their help with the Illumina sequencing. I would like to thank the UFZ-Helmholtz Centre for Environmental Research, who made my studies possible with financial support. I would also like to especially thank my friends and colleagues, especially Katalee Jariyavidyanont and Kantida Juncheed, for their support. Finally, I thank Sinekam Tanunchai (my mother) for her support during my studies.

(Eidesstattliche) Versicherungen und Erklärungen

(§ 8 Satz 2 Nr. 3 PromO Fakultät)

Hiermit versichere ich eidesstattlich, dass ich die Arbeit selbstständig verfasst und keine anderen als die von mir angegebenen Quellen und Hilfsmittel benutzt habe (vgl. Art. 64 Abs. 1 Satz 6 BayHSchG).

(§ 8 Satz 2 Nr. 3 PromO Fakultät)

Hiermit erkläre ich, dass ich die Dissertation nicht bereits zur Erlangung eines akademischen Grades eingereicht habe und dass ich nicht bereits diese oder eine gleichartige Doktorprüfung endgültig nicht bestanden habe.

(§ 8 Satz 2 Nr. 4 PromO Fakultät)

Hiermit erkläre ich, dass ich Hilfe von gewerblichen Promotionsberatern bzw. –vermittlern oder ähnlichen Dienstleistern weder bisher in Anspruch genommen habe noch künftig in Anspruch nehmen werde.

(§ 8 Satz 2 Nr. 7 PromO Fakultät)

Hiermit erkläre ich mein Einverständnis, dass die elektronische Fassung der Dissertation unter Wahrung meiner Urheberrechte und des Datenschutzes einer gesonderten Überprüfung unterzogen werden kann.

(§ 8 Satz 2 Nr. 8 PromO Fakultät)

Hiermit erkläre ich mein Einverständnis, dass bei Verdacht wissenschaftlichen Fehlverhaltens Ermittlungen durch universitätsinterne Organe der wissenschaftlichen Selbstkontrolle stattfinden können.

.....

Ort, Datum, Unterschrift